A NEW GENERATION OF UNDERWATER UNMANNED TETHERED VEHICLES CARRYING HEAVY EQUIPMENT AT LARGE DEPTHS

Final Report for the
Doherty Professorship

MITSG 85-30TN

M.S. Triantafyllou, A.M. Amzallag

Sea Grant College Program
Massachusetts Institute of Technology
Cambridge, Massachusetts 02139

December 1984

In 1973, the Henry L. and Grace Doherty Charitable Foundation established the Henry L. Doherty Professorships in Ocean Utilization to encourage non-tenured MIT faculty to focus on contemporary problems in the marine field. The chairs help to attract and support outstanding young teachers and researchers with interdisciplinary backgrounds as they begin work in the emerging marine field.

During their two-year appointments Doherty Professors remain affiliated with their respective academic departments, but conduct their research under the aegis of the MIT Sea Grant Program.

This Sea Grant report is being published as part of the Program's Technical Notes series. The research was conducted by Michael S. Triantafyllou, a Doherty Professor, from 1982-1984 in the MIT Department of Ocean Engineering and Graduate Student A.M. Amzallag.

Copies of this report may be ordered from

Sea Grant Information Center
MIT Sea Grant College Program
Room E38-320
Massachusetts Institute of Technology
77 Massachusetts Ave.
Cambridge, MA 02139

cost: $14.00

FINAL REPORT FOR THE DOHERTY PROFESSORSHIP

"A New Generation of Underwater Unmanned Tethered Vehicles Carrying Heavy Equipment at Large Depths."

by

M.S. Triantafyllou
A.M. Amzallag

December 1984

SUMMARY

This report describes in detail the design, simulation and control system design of a tethered, unmanned submersible capable of carrying heavy loads at large depths.

The need to perform heavy duty tasks underwater is increasing rapidly as the offshore industry and the deep ocean mining companies are installing or plan to operate structures in deep water. This report provides a systematic procedure to design rationally such vehicles and addresses the principal issues of simulation and control. A compilation of data was deemed necessary as the research proceeded as well as the development of new areas such as the dynamics of translating catenaries.

The first, main part of the report describes the overall design and control study (the principal reference is [3]). The second part provides information on the dynamics of travelling cables.

Table of Contents

List of Figures

List of Tables

INTRODUCTION

Underwater vehicles play an important role in the development and maintenance of offshore oil fields. Their use is expected to increase with the realization of the oil industry's deepwater capabilities (depths between 2,000m and 6,000m). For industrial applications, the most useful vehicle will probably need the capacity to carry submerged payloads of up to 4,500 kg. The offshore industry is expected to reach depths between 4,000m and 5,000m over the next decade and consequently such vehicles will be needed.

Offshore activities include oil drilling and production, deepwater pipelaying and harvesting for minerals. These activities involve significant deployment of underwater equipment and machinery, such as subsea completion platforms. We believe that for such depths and tasks an unmanned tethered vehicle will be the most effective.At present, development of submersibles relies on extensive testing and modification of both models and full scale prototypes. This is a costly approach in terms of both time and money. This report presents a method for the preliminary design and control of a submersible. The aim is to reduce design time and cost, as well as provide an estimate of the submersible's performance through the use ofa simulation model and a control system analysis.

The chronology of developments in the offshore industry is as follows: "Rotary drilling started in 1900, offshore drilling in 1947, floating drilling in 1953, use of subsea wells in 1962, drilling in 1,300 ft (400m) water depths was accomplished in 1970 and drilling with dynamically stationed drillships in 1971.". From 1952 to 1970 drilling progressed from water depths of 100 ft

(30m) to 1,400 Ft (430m). From 1970 to 1978 drilling went from water depths of 1,400 ft (430m) to 4,400 ft (1340m). [32] There is a similar trend for production platforms that have progressed from 20 ft (6m) in 1947 to 474 ft (145m) in 1970 and to 1,000 ft (300m) in 1978. [50]

Eighteen rigs with rated water depths of 3,000 ft or more

Name	Type	Rated water depth (ft)	Dynamic positioning	Year built	Status during May
Henry Goodrich	Semi	10,000	Yes	1985	Under con.
Discoverer Seven Seas	Drillship	7,500	Yes	1976	Drilling
Sedco 471	Drillship	6,000	Yes	1978	Upgrading
Sedco 472	Drillship	6,000	Yes	1977	Drilling
Sedco 709	Semi	6,000	Yes	1977	Drilling
Pacnorse I	Drillship	5,000	Yes	1979	Stacked
Sedco 710	Semi	5,000	Yes	1983	Drilling
Ocean Alliance	Semi	4,500	Yes	1986	Under con.
Polly Bristol	Drillship	4,500	Yes	1981	Drilling
Neddrill II	Drillship	4,000	Yes	1977	Drilling
Pelerin	Drillship	3,935	Yes	1976	Stacked
Aleutian Key	Semi	3,000	No	1976	Drilling
Ben Ocean Lancer	Drillship	3,000	Yes	1976	Drilling
Discoverer 534	Drillship	3,000	Yes	1975	Stacked
Dyvi Delta	Semi	3,000	No	1981	Drilling
Penrod 78	Semi	3,000	No	1983	En route
Petrel	Drillship	3,000	Yes	1976	Drilling
Sedco 445	Drillship	3,000	Yes	1977	Drilling

Source: Electronic Rig Stats

Table I: Eighteen rigs with rated water depths of 3,000 ft or more.

Already, the guyed tower developed by Exxon for water depths of 4,000 ft (300m) to 2,000 ft (600m) has been deployed in the gulf of Mexico. [91] The site is in 1,000 ft (300m) of water in the Mississippi Canyon Block 280 where the installation of the guyed tower was started in July 1983. [92] The tension leg platform (TLP) is aimed at depths between 1,000 ft (300m) and 6,000 ft (1,800m). The trend towards deeper water is expected to continue as previously marginal wells are developed. Last year, Sonat's Discoverer Seven Seas drillship topped its own depth record by drilling in 6,448 ft of water

(2,000m) in Shell's Wilmington Canyon Block 587. [80] Later on this year the same drillship is expected to drill in 7,250 ft of water (2,200m) for Shell in Wilmington Canyon Block 372. Table I illustrates present drilling rigs rated at more than 3,000 ft. [80] The next objective in the exploration of the continental rise is for depths ranging between 5,000 ft and 13,000 ft as indicated by D. Hammett of SEDCO Inc.. [32]

Other offshore activities denote the same trend, such as deepwater pipelaying, which in 1980 reached depths of more than 2,000 ft (600m) in the straits of Messina. Similarly, deep ocean mining involved a series of tests in 1969 and 1979 in more than 12,000 ft (3,600m) of water. On the production side there has been the introduction of the guyed tower and the tension leg platform. In the absence of such production means, subsea completion systems are used. In 1981, 42 such systems were installed and in 1982 73 subsea systems were ordered. [81] It is expected that subsea completion systems will dominate, when production will be required beyond water depths of 3,000 ft (900m). [81]

Offshore activities in large water depths will require significant underwater operations to monitor, install and maintain subsea installations. Until now divers were used routinely in depths of 300 ft to 500 ft (90m to 150m). A single 900 ft (270m) dive is reported to cost more than $200,000. [81] The dexterity and overall capacities of divers make them incredibly versatile, however the deepest working dives have been around 1,500 ft (460m) by Comex in the Mediterranean. By 1990 it is expected that the ambient diver will not have progressed much beyond 2,500 ft (760m). Futhermore there is little likelihood that the saturation diver will reach 6,500 ft (2,000m) of depth. [13] Research in remotely operated vehicles is advancing

to solve underwater welding problems which at present are the domain of divers.

In the pipelaying operation in the straits of Messina the need for underwater assistance was demonstrated. In this case a tethered manned vehicle replaced all diving activities beyond 500 ft (150m). [51] Remotely operated vehicles have already begun to supersede divers in activities requiring limited dexterity. In these tasks the ROVs were considerably less expensive than divers and completed their tasks in shorter periods of time. [93] Atmospheric diving suits (ADS) and one-man submersibles provide superior performance to ROVs, but are limited to depths of around 2,000 ft (610m). [59]

Beyond depths of 2,000 ft (610m) only manned and unmanned submersibles can be deployed. Unmanned vehicles are superior to manned vehicles at such depths, in that no lives are endangered. Accidents involving manned vehicles are reported annually. [31, 89, 90] In addition, divers in manned vehicles are protected by heavy spheres with specially designed protective windows. These spheres are the main design item at great depths, along with the life support and power systems. Futhermore, greater risks can be taken with unmanned submersibles, since these can withstand more rugged environments. The only advantage of manned vehicles lies in the adaptability of the human operators and their direct visual supervision. However, this may be offset by more advanced control systems and the use of underwater cameras, sonar and other imaging devices that may be superior to the human eye, especially in waters of low visibility. The position of the operator in the control loop is handled by Sheridan and Verplank. [73] The operator may also have problems visualizing the evolution of the vehicle as he is controlling it.

The development of unmanned vehicles is still at an early stage and most ROVs are relatively light vehicles that operate at moderate depths [14]. In order to install, maintain and repair large subsea structures and equipment, the ROVs will need to carry large payloads and provide great forces. As a result of the high thrust requirements of these vehicles, they will need umbilical cables (tethers) to provide such high power levels. The tethered maintenance vehicle (TMV) by Exxon is an example of such a design.

The aim of this report is to present a design methodology for a submersible required for deepwater applications; to simulate the vehicle's motion with a tether and to design a modern control system for the tethered vehicle. Chapter 1 formulates the design specifications and treats those topics that affect the design, such as materials, buoyancy, cables and so forth. Chapter 2 discusses the hydrodynamic forces that act on the vehicle and the methods for estimating these forces. The ensuing data are later used in the report to derive the simulation model. In chapter 3 our design based on information from chapter 1 is presented, along with its characteristics both loaded and unloaded.

In chapter 4 the simulation model is constructed, which includes a quasi_static simulation model and a model involving perturbations from the desired motion for both the loaded and unloaded cases. The tether model is provided as a transfer function and is added to the vehicle for both simulations. Chapter 5 presents and solves the control problem using Linear Quadratic Gaussian and Loop Transfer Recovery method to design a gain-scheduled controller. The perturbation simulation of chapter 5 is rerun to include the gain-scheduled controller.

Chapter 1

DESIGN FACTORS

Our aim is to design a heavy-lift submersible to operate up to depths of 6,000m. The vehicle is to carry maximum loads of 4,500 kg in water and be used as a general work platform. The latter involves carrying and using tools, as well as deploying various instruments, such as cameras, sonars etc. Furthermore it is desirable to minimize the size, the weight and the power requirements and the cost of the submersible. These requirements may conflict,resulting in a design that is a compromise.

This chapter presents the design problem in detail, as well as the factors affecting the design. These factors include material properties, pressure vessel design, buoyancy systems, cables and cable sizing, propultion motors, thrusters, batteries and other power sources, manipulators and further possible equipment and/or instrumentation. These factors affect the weight, dimensions, cost and power requirements of the submersible and are referenced in the design presented in chapter 4. The discussion of the hydrodynamics involved in the design is delayed until chapter 3.

The principal requirement for the tethered heavy-lift submersible (THLS) is a maximum payload capacity of 4,500 kg in water. Several alternatives may be employed to satisfy this requirement such as the use of thrusters, weight swapping or buoyancy systems. It is assumed that with no payload the vehicle is neutrally buoyant. If thrusters are used, a power loss will cause the submersible and payload to sink together. The use of thrusters reduces the overall submersible weight, but only at the cost of higher power requirements.

Weight swapping is a technique by which the submersible swaps the payload for some equivalent dummy weight. Buoyancy systems can be either active or passive. The active buoyancy system is a self-contained variable buoyancy system within the submersible. The passive buoyancy system is attached to the payload to make it neutrally buoyant. The most flexible system is active buoyancy, although it is not the most reliable. A variable buoyancy system increases the weight and volume of a submersible, setting a minimum size and weight for the vehicle. By using a variable buoyancy system, the submersible is neutrally buoyant with or without the payload.

The vehicle's maximum dimensions are determined by the deployment and maintenance requirements. An important characteristic of this submersible is that it be easily transportable. The requirement that it to fit into standard containers (see table 1-I) is satisfied: Indeed the type 1C (8' by 8' by 20') can be airfreighted. A Boeing 747-200F (freighter) is capable of delivering 90,720 kg of containerized deck cargo over a range of 4,360 nm. A 747-200F can carry up to 29 containers measuring (8' by 8' by 10') or up to 14 type 1C containers. This allows rapid, although costly, deployment of the submersible and associated systems/equipment. For our design the whole system, submersible and associated equipment, are to be fitted into containers that are to occupy a minimum of ship deck space. In our design six containers are necessary for: the submersible (type 1A), the control center (type 1C), the storage of tools (type 1C), the spare parts and spare cables (type 1C), the deck handling equipment and the clump (type 1C) and the last container to house the generators and fuel (type 1C).

The container sets the maximum dimensions and weight of the submersible. Task requirements will affect the vehicle's geometry, although

some flexibility of design is left to the designer. Choice of geometry affects the hydrodynamic drag and added-inertias of the vehicle. The higher the drag and added-inertias become, the greater the required thruster power is in turn, a larger diameter tether cable is required, resulting in an increased drag force. This drag force is felt as a disturbance by the submersible.

Underwater contractors often replace manufacturer-installed thrusters with more powerful thrusters to obtain higher safety margins, as well as increase the vehicle's maneuvrability. This will also increase the tether cable diameter. The tether cable is kept taut in order to avoid entanglement, and this causes such effects as strumming, which in turn induce dynamic disturbances on the vehicle. The control system must eliminate the effects of both the static and dynamic cable disturbances. The support ship motions are decoupled from the tether cable by using an intermediate vehicle known as a clump, cable depressor or garage. The clump is designed to damp out the motions of the support vessel and to provide a relatively motionless point to which the upper end of the tether cable may be fixed.

Further task requirements of the THLS are that it be rugged and survive collisions. It should be able to deploy a wide range of instruments and sensors, as well as an emergency rescue beacon and a cable separator in the case of an extended power failure or a cable entanglement. If such failures occur it is important that there be an emergency power supply. It is desirable that the vehicle be as fast and maneuvrable as possible without sacrificing other characteristics. Finally, for the purpose of this report, the payload is assumed to be a 10 ft (3.048m) long and 5 ft (1.524m) in diameter cylinder that weighs approximately 10,000 kg in air and 4,500 kg in water. These requirements now provide the design guidelines. In the following sections,

specific information is provided to define more clearly these guidelines.

Freight Container	Max Load Capacity	Tare Weight	Outside Dimensions			Inside Dimensions		
			Length	Width	Height	Length	Width	Height
Dry Cargo (1A)	60,260 lbs 27333 kgs	6,400 lbs 2903 kgs	40' 12.192m	8' 2.4384m	8' ---	39'7" 12.065m	7'9" 2.3622m	7'4" 2.2352m
Open Top (1AA) Hi-Cube	60,950 lbs 27646 kgs	6,940 lbs 3148 kgs	40' --	8' --	8'6" 2.5908m	39'6" 12.0396	7'9" --	7'10" 2.3876m
Open Top (1AA)	59,280 lbs 26889 kgs	7,750 lbs 3515 kgs	40' --	8' --	8'6" --	39'6" --	6'8" 2 032m	7'6" 2.286m
Half High Open Top (1A)	45,000 lbs 20412 kgs	6,660 lbs 3021 kgs	40' --	8' --	4'3" 1.2954m	39'6" --	7'9" --	3'4" 1.016m
Dry Cargo (1C)	44,800 lbs 20321 kgs	4,500 lbs 2041 kgs	20' 6.096m	8' --	8' --	19'6" 5.9436m	7'8" 2.3368m	7'4" 2.2352m

For Steel add approximately 600 kgs to Tare Weight.

Table 1-I: Typical Characteristics of aluminum Containers.

1.1 Pressure Vessels

Pressure vessels are used for two purposes in submersibles; either as buoyancy tanks or as pressure housings for equipment and supplies. The choice of material determines the ratio of the weight to buoyancy, also known as the buoyancy factor β of the pressure vessel. Typical buoyancy factors range betwen 0.9 and less than 0.5 for operating depths of 20,000 ft (6,000m) with a safety factor of 1.5, that is a collapse depth of 30,000 ft. [64] The

design cost of the pressure vessel is its weight. Reduction of the safety factor will decrease the pressure vessel's weight. However, this is not recommended since the safety factor allows the design loads to be exceeded and protects from [64]:

- Limitations of the methods of analysis.
- Imperfections in the manufacturing.
- Imperfections in the materials.
- Imperfections in the design.
- Fatigue from residual stresses.
- Degradation from corrosion.

By paying greater attention to these items, the safety factor can be reduced, although the best method is to use more advanced materials when the technology becomes available. The next section deals with the possible materials for use in pressure vessels. For two equal spheres joined by a cylinder the buoyancy factor β is given by [2]

$$\beta = \left(\frac{3p}{\sigma} \right) \left(\frac{\rho_s}{\rho_w} \right) C \tag{1.1}$$

$$C = \frac{R^2(R + d) + (R^2 - d^2)a}{2R^3 + 3R^2d - d^3 + 1.5(R^2 - d^2)a} \tag{1.2}$$

p = pressure at operating depth $\times$ safety factor, psi.
σ = allowable stress, psi.
ρ_s = mass density of the structural material.
ρ_w = mass density of water.
R = radius of the spheres.
a = length of cylindrical shell.
d = distance from sphere center to cylinder wall.

This relation assumes membrane stress as the failure mode as opposed to buckling instability. Spherical shells are more efficient than cylinders in terms of strength to weight ratio, however cylinders are easier to manufacture. Furthermore, differences in internal layout and external size affect the choice of pressure vessel types. The above relation provides the buoyancy factor for several different pressure vessel types. The sphere and cylinder with hemispherical endcaps are the only configurations we will consider. More extensive information on pressure vessels can be obtained from [64, 2, 46, 65, 9, 24, 30].

1.2 Materials

Materials play an important role in the sizing of submersibles. Indeed, higher strength-to-weight ratio materials permit smaller displacements at a given load and operating depth. In addition, the materials chosen must endure the marine environment, repeated dives and collisions. In material selection we must also consider certain other features which are: corrosion resistance, creep, notch-toughness, a high low-cycle fatigue and their joinability or weldability. We will look at materials for the submersible's hull, frame and its pressure vessels or buoyancy tanks. These are the structural materials and in addition we will look at the buoyancy materials and cable materials. At depths of 20,000 ft (6,000m) the problems one encounters with materials differ from those encountered at lesser depths.

Structural materials are stainless and high-strength steels, aluminum alloys, titanium alloys, glass and ceramics, fiber reinforced plastics and plastics. At present only the first three materials are considered for use in the frame.

Material		Aluminium Alloy		Titanium Alloy		Stainless Steel				Ceramic Glass		Glass Reinforced Plastic	Quartz/Resin	Boron/Resin
Specification		7079-T6	5456-H323	Ti6Al4V	TI-155A	HY100	HY150	PH15-7MO	5-CR-MO-V	Pyroceram 9606	Other Glass	143 Glass Fibre & Epoxy Resin	Carbon Coated Quartz & Epoxy	Boron Fibre & P.P.O
Density	Kg/m³	2740	2660	4430	4510	7750	7830	7670	7780	2600	1910	1860	2050	2080
Yield Strength (Tensile)	10³ psi	64-56	36	126	135	100	150	200	240	-	-	58-85	-	-
Yield Strength (Compression)	10³ psi	63-56	34	132	150	100	150	210	260	340 (ult.)	300	58.1	80	140
Ultimate Strength (Tensile)	10³ psi	73-66	48	134	145	-	-	225	280	-	-	85.0	-	-
Modulus of Elasticity		10.3	10.2	16.0	16.0	30	30	29.0	30.0	17.2	-	-	5	22
Elongation	%	6-4	8	10	10	-	-	5	4	-	-	-	-	-
Yield/Ultimate (Tensile)	-	.877 .848	.75	.940	.931	-	-	.889	.857	-	-	.684	-	-
Yield/Density (Compression)	10 in	6.46-5.66	3.75	7.88	6.28	-	-	7.22	7.22	36.2 (compr).	-	-	-	-
Ultimate/Density (Tensile)	10 in	7.37-3.33	5.00	8.38	8.90	-	-	8.12	9.96	3	-	-	-	-
Mod. of Elas./Density (Tensile)	10 in	10.4	10.6	10.0	9.62	-	-	10.5	10.7	18.3	-	-	-	-
Poisson's Ratio	-	.33	.33	-	-	.3	.3	.3	.3	.24	-	-	-	-
Notch Strength		Poor		Fair		Very Good		Good		Poor	-	Good	-	-
Crack Propagation rate		Moderate		Moderate		Slow				Rapid	-	Moderate	Moderate	
Welded Strength Deterioration	-	-	-	Low	Low	Low	Low	Low	Low	-	-	-	-	-
Weldability		Not Suitable		Fair to Good	Good	Excellent		Good	Good	-	-	-	-	-
Other Fabricability Characteristics	-	Fair	-	Good	-	Good	Good	Fair	Fair	Poor	Poor	Fair	-	-
Thermal Expansion Coefficient		13.1	13.3	4.6	5.7	-	-	5	7.1	3.17	-	6.7	-	-
Thermal Conductivity Coefficient	Btu Hr ft °F	74	68	3.8	4	-	-	9	16.6	1.95	-	-	-	-
Low Cycle Fatigue in Marine Environment	-	Fair	Fair	Excellent	-	Good	Good	Good	Good	Fair	-	-	-	-
Corrosion Resistance in Marine Environment		Poor, improved when Anodized & Painted		Excellent	-	Excellent	Excellent	-	-	Excellent	-	-	-	-
Compressive Creep Resistance	-	-	-	Good	-	Excellent	Excellent	Fair to Good		Fair	-	-	-	-
Availability in Heavy Sections	-	Good	Good	Fair	Fair	Good to Fair		Fair	Fair	Fair	-	Poor	Very	Poor
Low Cost/lb Med High		Medium	Medium	High	High	Low	Low	Medium	Medium	Medium	-	Medium	Very	High

Table 1-II: Material Selection Data.

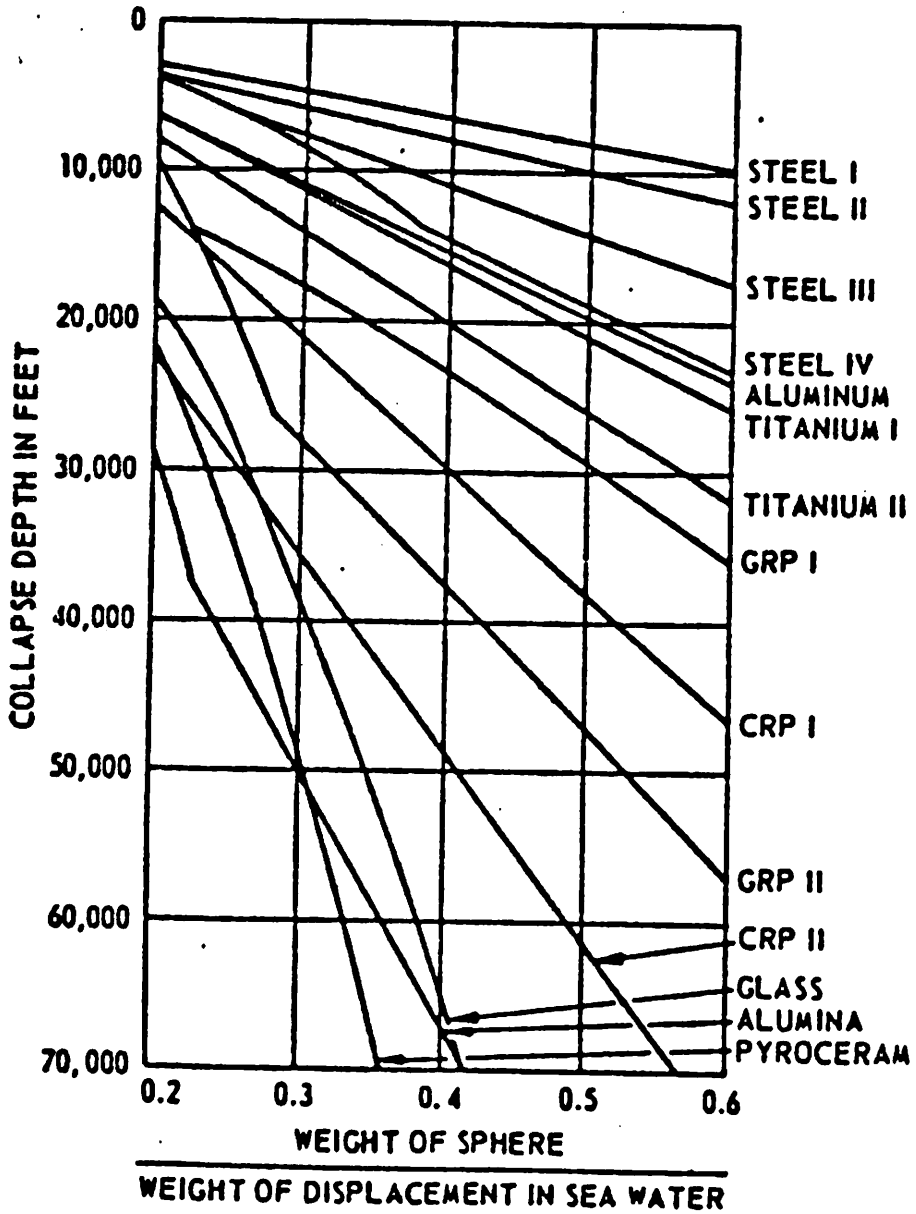

Figure 1-1: Buoyancy Ratio for Spherical Pressure Vessels versus Collapse Depth in feet.

Any of the structural materials may be used for pressure vessels and buoyancy tanks. Figure 1-1 shows the buoyancy ratio for a sphere versus collapse depths for these materials. A general selection guide is given in table 1-II. This section offers a brief treatment of the materials, which is detailed enough, so that weight estimates may be made as a function of material choices. For more specific information refer to the references of the previous section as well as references [55, 42, 56, 45, 54, 44]. It must be noted that the references dated before the early seventies were unduly optimistic about developments in materials.

1.2.1 Steels

Steels have long been familiar materials in the marine industry. The first high-performance pressure hulls were made of steel. There are essentially two types of steel; high strength and high-alloy. High strength steels such as HY-80, HY-100, HY-130 and HY-180 are the results of hull material developments made for US Navy submarines and are primarily low alloy steels. Unfortunately, as their strength increases, their fracture toughness and weldability decrease. However, the fatigue limit increases with strength for smooth specimens. In contrast, a notched specimen has no improvement in the fatigue limit. We note also that increased strength reduces the stress-corrosion cracking resistance and causes the steel to become more susceptible to hydrogen embrittlement. High-alloy steels have had to date limited use due to their high cost, although they offer better ductility and fracture toughness at low temperatures than high strength steels. These high-alloy steels use large percentages of nickel and are also known as maraging steels. They have limited the amounts of impurities such as carbon. As a result, they have yield

strengths up to 300,000 psi, exceptional stress corrosion resistance to seawater and good weldability. In addition, they are relatively easily machined and formed. High-alloy steels are contenders for use in deep diving submersibles, since these vehicles are small and their whole frame can be heat treated.

1.2.2 Aluminum Alloys

At present aluminum alloys are widely used as the main structural frames [14]. In the seventies the Reynolds Metal Company designed and built the Aluminaut [42]. It had a 50 ft cylindrical pressure vessel with an internal diameter of 6.5 ft. The pressure vessel was made of the aluminum alloy 7079-T6 and had a design depth of 15,000 ft (4,500m). Aluminum has long been used to reduce the weight of submersibles and has in general excellent resistance to the marine environment. Unlike steel, aluminum is not susceptible to hydrogen embrittlement, but it requires an inert environment for welding. Its strength to weight ratio is generally higher than that of steel and in terms of cost, aluminum is cheaper than steel over the life of the structure. Its strength is increased as its corrosion resistance drops. However, aluminum is very susceptible to galvanic corrosion. When the Alvin was lost at sea for several months its aluminum frame was severely corroded. The small titanium pressure vessels attached to the frame were the cause of these corrosion attacks.

The fracture toughness of aluminum is considerably lower than that of either steel or titanium alloys. The fact that its Young's modulus is one third that of steel requires the moment of inertia of the frame members to be increased in order to keep its rigidity constant. Aluminum is difficult to weld, but relatively easy to form and machine. Two types of aluminum alloys are

used for marine applications, the 5XXX series and the 7XXX series. The former are alloys whose properties are improved by strain hardening and aging. The series 7XXX are heat treated alloys and are harder to weld than the 5XXX. In general, 5XXX alloys are used in submersible frames. [69]

1.2.3 Titanium Alloys

Titanium alloys are not commonly used in the marine industry due to their cost, as well as difficulties in welding, machining and forming. However, its strength to weight ratio is higher than for steel or aluminum alloys and its marine corrosion resistance is excellent. It has high fracture toughness, although the toughness drops as the strength of the titanium alloy is increased. Titanium has been used to build pressure vessels and buoyancy tanks for deep diving submersibles, such as the Alvin. The titanium alloy most commonly used is Ti6Al4V. Titanium alloys have fatigue properties comparable to steel. However, hydrogen embrittlement can be a problem. If titanium pressure vessels are built to house gases, the oxide layer should provide adequate protection against hydrogen embrittlement. In addition, titanium will resist hot brine solutions and engine exhaust fumes.

1.2.4 Glass & Ceramics

Glass and ceramics are materials that show great promise for use as pressure hull materials. Ceramics include annealed and chemically strengthened glasses, glass ceramics and high-density alumina. Glass has a high compressive strength: Indeed it is capable of withstanding pressures of 3,000,000 psi. [27] In uniaxial compressive loading tests it withstood loads of 500,000 psi. Glass fragility is due to its poor resistance to tensile stresses. This is a result of

crack propagations from surface and interface cracks and can be corrected for by thermochemical strengthening and polishing. Glass pressure vessels become increasingly resistant to mechanical impacts with increases in depth. This is referred to as a depth hardening effect. A borosilicate glass sphere with buoyancy ratios of 0.55 capable of withstanding pressures of 29,500 psi has been tested. This corresponds to 200,000 psi compression stresses in the sphere walls. Glass and ceramics generally have good corrosion resistance, though thermochemically treated glass and ceramics may be affected by the marine environment. The low-cycle fatigue properties of these materials are tied to flaws in the joints and surfaces. Glass and ceramics are moderately priced materials. If their surface imperfections are removed through polishing or thermochemical treatments, they can be used for deep submersible pressure vessels. However, it is necessary to protect them from impacts and any additional loads, especially tensile loads.

1.2.5 Plastics and Fiber Reinforced Plastics

Plastics and Fiber Reinforced Plastics (FRP) have been tested and used both as pressure hulls and protective hulls. It may be equally possible to use composites in the frame's structural members. For deep submersible applications FRPs are the only plastics that can be used in pressure vessels. Acrylic plastics can be used as a transparent hull material where cameras or lights are located under the hull fairing. Acrylic plastics are quite cheap and were used by the US Navy in the pressure hull of manned submersibles capable of depths of 1,000 ft. [78] The Makakai and NEMO were two such vehicles . [79] For the rest of the faired hull FRPs may be used. Fibers used for reinforcing plastics are metals, glass, carbon, boron and Kevlar. Advantages

of FRPs are their high strength to weight ratios, high corrosion resistance and relatively high toughness. Water absorption reduces the "dry strength" of the plastic if external protection is not applied. The compressive strength of these materials is highly dependant on the epoxy resin used in the binding matrix. Cylindrical pressure hulls are much easier to build than spherical hulls due to fiber-winding problems. The cost of the FRPs varies with the fibers chosen, but with increasing development of composite materials the cost of even the better fibers will drop. Abrasion resistance of FRPs may not be sufficient. FRPs offer similar strength to weight ratios to glass and ceramics and will allow for future weight savings in submersibles.

1.2.6 Buoyancy Materials

Buoyancy materials can be gases, liquids or solid i.e. syntactic foams. For gaseous buoyancy systems, pressure resistant buoyancy tanks are required. These are useful as variable buoyancy systems and are discussed in section 2.5. Liquids have been used in bathyscaphs such as the US Navy's TRIESTE and the French's Navy ARCHIMEDE. [44] However, these liquids, usually gasoline or naphta, tend to be flammable or toxic and compressible, losing buoyancy with increased depths. They also require delicate thin shells. Puncture of these shells results in a loss of buoyancy liquids with potentially disastrous results.

The only solid buoyancy materials we will consider are syntactic foams. Syntactic foams are made by mixing glass balloons whose diameters range from 2 to 2,000 microns with thermosetting resins. "The microballoons are the key, according to Lou Watkins, Manager of Flotation Products. 'Control of the microballons gives you control of the physical properties of the foam. We can

make ultralight foams , superstrong foams, even flexible foams for wrapping around cables. No other material gives the engineer so much design freedom in specifying just the right characteristics to do a certain job.'" [58]

Syntactic foams are inexpensive, quite strong and can be molded into any shape. The densities of syntactic foams have dropped to 480 kg/m^3 ($30lb/ft^3$) for use at deep depths. However, at great depths small samples, (one cubic inch), of syntactic foam have absorbed up to 2 % of water. This leads to a slight deterioration in the properties of the syntactic foam. Water absorption is reduced in large blocks of foam, as only the surface layers absorb water. By coating the syntactic foams this problem can be greatly reduced. In table 1-III the properties of syntactic foams are given. Another use of syntactic foams is in sandwich core materials. These are hull materials in which the hull panels are made of syntactic foam covered with either Fiber Reinforced Plastics or metallic skins. [44] The strength to weight advantages of sandwich core materials is high, but as yet little information exists for these promising materials. Tests in the late sixties were not encouraging due to the foams available at that time [46]. It is possible that modern foams will provide better results. More information on syntactic foams exists in references [55, 44, 79, 58, 16, 74].

1.3 Cables

The tether cable links the support ship to the submersible providing both power and a communications link. Tethers must also have good static and dynamic load bearing capabilities, since they must bear the load of the submersible, its payload and the clump if one is used. Cables may be affected

Nominal Density	30 lb/ft^3 480 kg/m^3
Net Buoyancy	34 lb/ft^3 545 kg/m^3
Initial Compressive Strength	
2 % offset yield, psi	> 15,000
Ultimate, psi	> 18,000
Compressive modulus, psi	550,000
Compressive Strength after Hydrostatic Imersion*	
2 % offset yield, psi	14,000
Ultimate, psi	17,000
Compressive modulus, psi	520,000
Water absorption (1 cu. in square at 10,000 psi)	< 2 %
Shear strength, psi	> 6,000
Tensile strength, psi	> 6,000
Tensile modulus, psi	600,000
Bulk modulus, psi	550,000
Impact strength, ft/lbs/in	0.25
Fatigue, (Number of cycles between 14.7 psi and 10,000 psi hydrostatic pressure)	>10,000
Creep	*No permanent deformation after 52 weeks of hydrostatic immersion at pressures of up to 13,500 psi*

* 1,000 x 20 min cycles between 14.7 psi and 10,000 psi hydrostatic pressures.
(Note: Data is mainly from US Naval Applied Science Laboratory.)

Table 1-III: Properties of Syntactic Foams [55, 44, 79].

by torsion loads. In addition, tension fatigue performance is an extremely important characteristic of cables. Cables must also be flexible and preferably have a small diameter to reduce drag. It is possible to vary the buoyancy of certain cables. A tether cable can be broken down into the following parts: power conductors, signal conductors, various electrical insulation layers and structural members.

Power conductors and metallic signal conductors are generally made of copper or aluminum and sometimes coated with other metals such as silver. The other type of signal conductor is the optical fiber which has definite advantages over coaxial signal cables. [21] From reference [79], "A typical 0.12-m- (0.005-in-) diameter optical fiber can provide a usable bandwidth of at least 50 MHZ over a length of more than 7,600m (25,000 ft), which is sufficient to support a sophisticated tethered system operating at abyssal depths. For comparison, a conventional 21.6-mm- (0.9-in-) diameter coaxial cable provides a bandwidth of about 13 MHZ over the same cable length. For certain applications, miniature optomechanical stands can be used as the entire tether cable or can be assembled as a conductor element into larger cables of arbitrary size, capacity and complexity."[1]

Table 1-IV specifies those materials used as insulation, jackets, shielding and strength members as a function of their density. [83] Tables 1-V and 1-VI give the mechanical and electrical characteristics of customed designed oceanographic cables made by the Rochester Corporation. [83] Table 1-VII gives the characteristics of tether cables designed by the Naval Undersea

---

[1]These values are estimates and are only useful in approximating the weights of hydraulic propulsion systems.

Material	Specific Gravity	Use
Metals:		
Steel; rolled and IPS	7.85	Chain, wire rope, EM cable braids
; armour wire	7.80	EM cable armour
Stainless Steel 302, 304, 305, 316; wire	8.02	Wire rope, EM cable braids
Iron; wrought bar	7.77	Chain
Copper; wire	8.92	EM cable conductor
Aluminum; hard drawn wire	2.70	EM cable conductor
Lead; sheathing	11.38	EM cable shield
Synthetic Fibers:		
Kevlar 29	1.44	Line, EM cable strength member
Kevlar 49	1.45	Line, EM cable strength member
Nylon	1.14	Line
Polyester	1.38	Line, EM cable braids
Polypropylene	0.90	Line, EM cable, wire rope core and jacket
Glass E	2.55	EM cable strength member
Glass S	2.50	EM cable strength member
Natural Fibers:		
Manilla	1.38	Line, wire rope core
Jute; dry fillers	0.50	EM cable
; treated fillers	0.63	EM cable
; asphalted serving	1.70	EM cable
Cotton; dry braid	0.60	EM cable
; weatherproof braid	1.40	EM cable
Extruded Plastics:		
Hypalon	1.12-1.28	EM cable jacket, insulation
Nitrile Rubber	0.98-1.10	EM cable jacket
Neoprene	1.23-1.25	EM cable jacket
Nylon	1.07	EM cable jacket
Polyethylene; low density	0.92	EM cable insulation
; high density	0.95	EM cable insulation
Polyurethane	1.06	EM cable, wire rope, and line jackets
PVC	1.2 -1.5	EM cable, insulation
Kynar	1.85	EM cable, insulation
Teflon	2.20	EM cable, insulation
Flexible Foams:		
Urethane; compressible	0.50	EM cable buoyant jackets
; non-compressible	0.58	EM cable buoyant jackets

Table 1-IV: Specific Gravity of the Materials Used in EM Cables, Ropes and Chain.

Stock #	Armor OD In.	Core Dia. Inches	Inner Armor No./In.	Outer Armor No./In.	Armor Jacket Thk/Mtl – Inches	Calc. Armor Ratio	Break Str. Lbs.	Wt. Air Lbs./1000 ft.	Wt. Sea Wtr. Lbs./1000 ft.	Min. Sheave Diam. In.
30300	.300	.186	24/.025 Beryllium	24/.032 Copper	–	2.0	4700	169	141	13
50519	.523	.328	24/.0435	24/.054	–	1.9	19000	397	312	22
60580	.240	.162	15/.039 (3 armored coaxes w/lead fillers)	–	.030 Nyl	–	9200	600	477	24
80302	.302	.189	24/.0245	24/.032	–	1.9	6800	143	114	13
80464	.464	.289	24./0385	24/.049	–	2.0	16000	347	279	20
90347	.347	2.03	18/.037	24/.037	–	1.7	9700	196	159	15
90463	.463	.288	24/.0385	24/.049	–	2.0	16000	350	283	20
90552	.454	.390	36/.032	–	.049 PU	N.A.	5000	276	169	13
90645	.645	.432	24/.0575	35/.049	–	1.17	26800	566	435	23
90653	.653	.440	24/.0575	35/.049	–	1.13	26,400	573	437	23
90667	.667	.489	36/.041	36/.048	–	1.5	21,600	600	460	19
90680	.675	.445	22/.065 Stainless	36/.050 Steel	–	1.05	33000	655	511	26
90688	.688	.425	24/.0575	24/.074	–	1.9	35000	782	633	30
90786	.786	.450	18/.084	24/.084	–	1.7	45000	1034	840	34
90788	.788	.578	22/.077	36/.057	–	1.01	40000	902	707	31
90812	.812	.594	35/.051	35/.0575	–	1.7	33000	1015	809	20
90815	.815	.595	36/.051	36/.059	–	1.7	36000	868	659	24
91378	1.378	1.002	36/.084	36/.104	–	1.4	102000	2408	1810	42

NOTE: All values are nominal

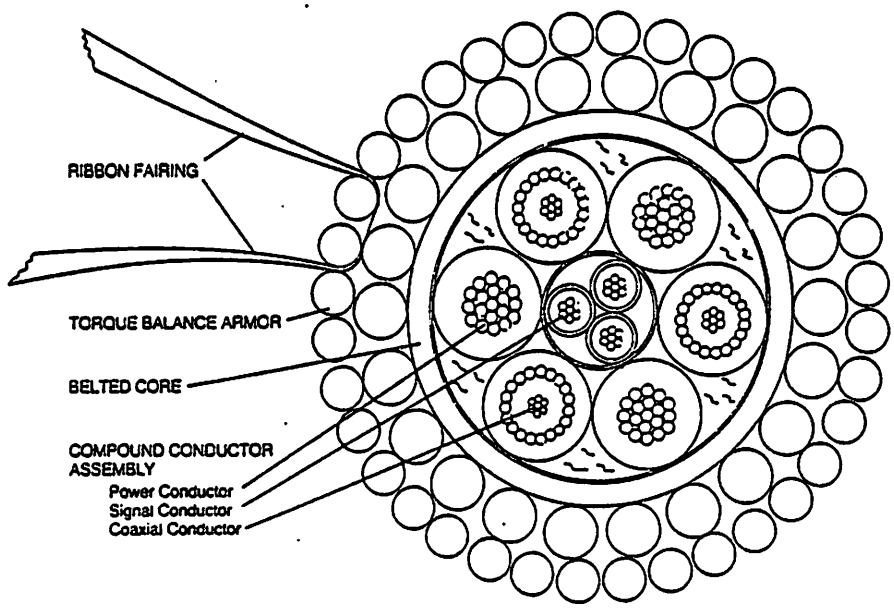

A Typical Compound Cable With Unique Features Stock #90680

From: Electromechanical Oceanographic Cables and Electrical Underwater Connectors, The Rochester Corporation, Culpepper, Virginia, 1975

Table 1-V: Custom Designed Oceanic Cables Mechanical Characteristics.

Total # Conductors	Stock #	OD In.	No. Cdr	Cdr. AWG – Str.	Insul. Thk/Mtl. – In.	Core Belt – In.	DC Res/1000 Cdr. Ohms	DC Res/1000 Shield	Cap. uufd/ft.	Z_0 Ohm	Att. db/1000 Freq. MHz		Special Feature Application
3	30300	.300	3	22-7 Coax	.013 PP	.015	16		58	33			N00-PD-0870
				#38 Br Shd	None	PE	.6						Magnetometer cable
5	50519	.523	2	16-19	.019 PP	.040	4.5		41	–			Faired
			3	22-7 Coax	.011 PP	PU	16.0	7	66	50			Oceanographic
3	60580	.593	3	20-7 Coax	.040 PE	–	10		34	50	4.1	1	Weighted Oceanog.
				24w Serv Shd	.011 PE		1.8				1.2	.1	"Nixie"
8	80302	.302	7	22-7	.014 PP		16	–	39	–			Instrument Tow
			1	18-7	.019 PP		6.6	–	33	–	–	–	
8	80464	.464	2	12-19	.027 PE	–	1.92		75				Transducer Mooring
			6	20-7	.014 PP		10.5		65				
9	90347	.347	8	22-7	.011 PP	.012	16	–	46	–	–	–	Ribbon Fairing
			1	18-7	.020 PP	Ht	6.6	–		–			Antenna Buoy Tow
9	90463	.463	3	18-7 Coax	.020 PP	–	6.6	3.4	57	35	6.1	1	Instrument Tow
			3	22-7	.021 PP	–	16.0	–	39		1.7	1	Side Scan Sonar
11	90552	.552	1	24-19 Coax	.064 PE	.030	27		22	75	2.8	1	TV Camera
			10	18-7	.015 PP	PU	6.5						Pipe Inspection
10	90645	.645	4	24 TSP	.011 PP	.045	28		27		15	1	Deep Tow
			1	22-7	.040 PE	PU	19	–	30		9.4	.5	Seismic
			1	20-7	.027 PP		11	–			5	.1	
13	90653	.653	4	22-7 TSP	.011 PP	.035	16				17	5	Ribbon Faired Tow
			5	20-7	.015 PP	PP	11						Cable
15	90867	.667	6	14-19	.022 PP	.038	2.9		25		.5	.015	Tow Acoustic
			6	20-7	.018 PP	Ht	10		16				Device
			3	18-7	.027 Tz		7						
12	90680	.675	3	14-19	.027 PE	.040	2.9		46				Faired Oceanographic
			3	22-7 Coax	.020 PE	PU	16.0	4.1	46	34	6.1	1	Buoy Mooring
			3	22-7	.011 PE		16.0		26				
9	90688	.688	3	10-19	.026 PP	.030	1.2		60		2.8	1	Ribbon Fairing
			1	22-7 Coax	.035 PP	Ht	16	3.2	31	50	1.7	.1	
			5	20-7	.016 PP		10		32		.5	.01	
35	90786	.786	34	22-7	.011 PP	.040	16.0	.4	55	–	–	–	Sonar Tow Cable
			1	9-19	.024 PVC	PU	.9						
19	90788	.788	1	20-19 Triax	.042 PP		12	11	30	53	4.2	1	Underground
			8	16-19	.028 PP		4.8	5.9			1.6	.1	Geophysical Logging
			4	20-19 Coax	.016 PP		12.8	6.4	57	28	1.2	.01	Cable
22	90812	.812	11	20-7 TSP	.014 Tz	.030	11.0	.6	36	–	–	–	Water Blocked
				20-7 Drain		Tzl							Hi-Temp Geothermal
				A1 Myl Shd									Well Logging
24	90815	.815	3	20-7 Coax	.044 PE	.045	10	2.3	32	50			
			18	20-7	.018 PE	PP	10						
29	91378	1.378	4	12-7	.044 PP		1.7						
			6	20-7	.018 PP		10						
			1	Brd shd	.060 PP			1.2					
			10	#18 TSP	.020 PP		6.6						

NOTE: All values are nominal. Detailed design sheets available on request.

From: Electromechanical Oceanographic Cables and Electrical Underwater Connectors, The Rochester Corporation, Culpepper, Virginia, 1975

Table 1-VI: Custom Designed Oceanic Cables Electrical Characteriatics

Parameter	Primary Cable	Tether Cable
Physical		
- As built diameter (in)	1.213	0.86
- Length (ft)	23,000	850
- Air Weight (lb/1000 ft)	802	254
- Water Weight (lb/1000 ft)	351	-4.5
- Specific Gravity	1.82	1.007*
- Cable Load at First Member Break (lb)	77,000	5200
- Torque Balanced ?	Yes	No
Electrical		
- Resistance (ohm/1000 ft)		
- Core	0.284	----
- Shield	0.191	----
- Loop	0.475	8.97
- Attenuation at 12 Mhz (dB/1000')	2.43	41.6
- Char. Impedance (ohms)	45.8	50.0
- Capacitance (μF/1000 ft)	0.034	0.031
- Corona Onset Level (VRMS, 60 Hz)	7000	7000

* This should be interpreted as a design value only. For example, short sections of the tether cable will float in fresh water; an effect which may be due to end effects or adherent air bubbles.

Table 1-VII: Properties for Primary Tether Cables Designed by the Naval Undersea Center.

Center for use with their submersible RUWS capable of operating in depths of 20,000 ft (6,000m). [85] This reference describes how these cables were designed and tested, especially with respect to the use of Kevlar 49 as the structural member. The following table 1-VIII makes a general comparison between Kevlar, Steel and other plastics as strength members in cables. Kevlar used in cables cost $8.50 /lb, whereas cabling steels cost $1.50 /lb. [78] Thus, Kevlar yarn has an almost identical cost per unit volume as steel wires.

Its only disadvantage with respect to steel is that it has a reduced flexure lifetime. [79] In reference [37], the mechanical and durability characteristics of Kevlar cables and ropes are detailed. Kevlar offers high-strength, high modulus, low elongation, non-conductivity and corrosion resistance. In addition, carefully designed Kevlar cables can have excellent creep and fatigue resistance, and retention of mechanical properties after extensive seawater exposure. Its only problem is abrasion resistance. However, abrasion resistance is not critical, since it is a necessary characteristic of the outer armour of the cable. Due to variations in fiber properties, designing cables with Kevlar strength members is different than with steel; references [37, 86] offer greater detail on this topic.

1.4 Cable Current Ratings

In any particular cable, power is lost in the form of dissipated heat. This generated heat and its dissipation is a function of the current, the materials used and the internal layout of the cable. The maximum temperature the cable conductors may reach and the heat dissipation characteristics jointly determine the maximum current. Figure 1-2 shows the thermal dissipation paths in a standard power cable. The current is obtained as follows [57],

$$I = \left[\frac{\Delta\theta - W_d[\, 0.5T_1 + n(T_2 + T_3)]}{RT_1 + nR(T_2 + T_3)} \right]^{0.5} \tag{1.3}$$

$\Delta\theta$ = conductor temperature rise (°K)

I = current flowing in one conductor.

	T-728 Nylon	T-73 Dacron	Kevlar 29	Kevlar 49	GIPS**
Tenacity, gpd* Nominal	9.8	9.5	21 7	21 7	2 9
psi	143,000	168,000	400,000	400,000	285,000
Modulus, gpd* Nominal	55	115	500	850	200
psi (10^6)	0.8	2.0	12***	19***	29
Specific Modulus, in., 10^8	0.3	0.6	2.3	3.6	1.0
Density (g/cc)	1.14	1.38	1 44	1.44	7.86
Elongation, % Nominal	18.3	12.0	4	2.4	2.0
Loop Tenacity, gpd	7 7	5.8	10.5	10.5	--
Knot Tenacity, gpd	--	--	7.5	7.5	--
Filament Diameter, in	0 0027	0 0024	0 00047	0 00046	0 020

*gpd = grams per denier Denier is the weight in grams of 9000 meters of yarn.
gpd is a specific strength (or modulus) determined by dividing the yarn break load in grams by yarn denier
**Galvanized improved plow steel
***Single filament modulus

Table 1-VIII: Comparison of Properties of Yarn and Steel Wire.

R = a.c. resistance per unit length of conductor at maximum temperature (ohm/m).

W_d = dielectric loss per unit length for the insulation surrounding the conductor (W/m).

T_1 = thermal resistance per unit length between one conductor and the sheath (°Km/W)

T_2 = thermal resistance per unit length of the bedding between sheath and armour (°Km/W).

T_3 = thermal resistance per unit length of external serving of

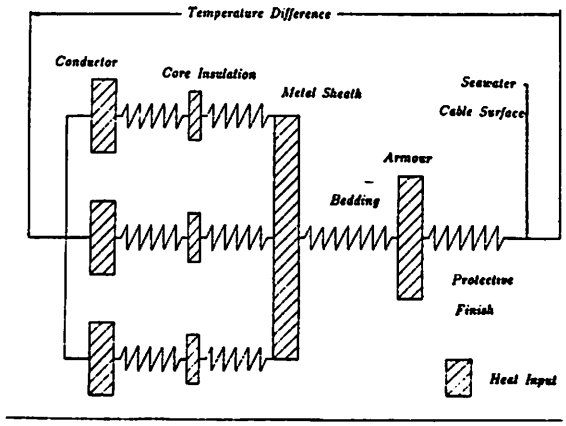

Figure 1-2: Thermal Dissipation Paths in a Cable.

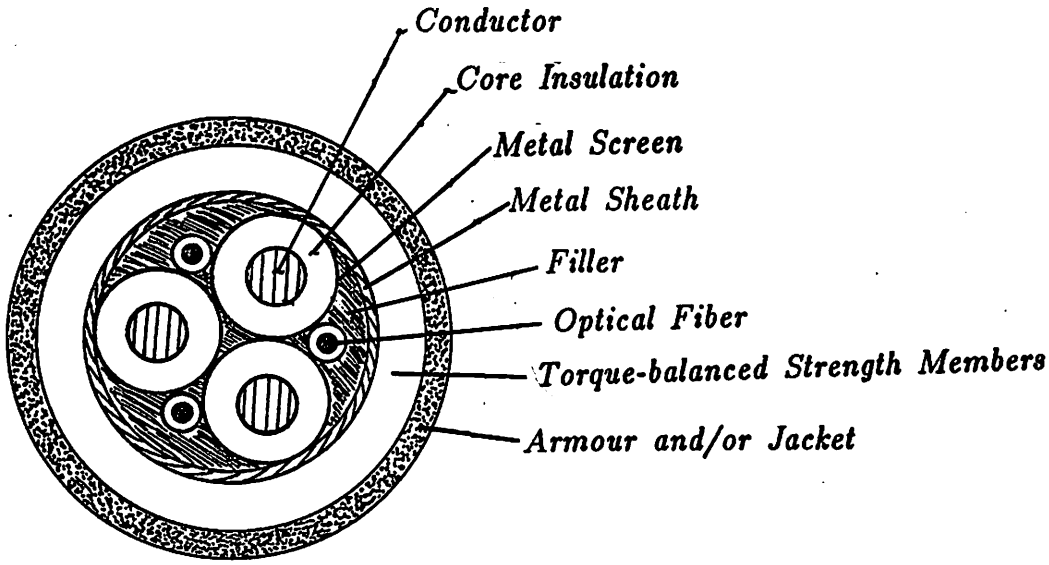

Figure 1-3: Tether Cable Cross-Section.

the cable (°Km/W).

n = number of equal diameter load-carrying conductors.

Figure 1-3 shows the cross-section of the cable we will consider. It is a three-core screened cable (Hochstadter type) with three optical fibers for communications. The screens are all grounded and each core carries an a.c.

phase. As a result the electrical characteristics for each of the three conductors can be treated approximately as individual core cables. [28]

Material	Type	Volume resistivity (min) at 20°C (ohm m)	Permittivity at 50 Hz	Tan δ at 50 Hz
*Thermoplastic**				
polyvinyl chloride	TI 1	2×10^{11}	6–7	0.1
polyvinyl chloride	2	1×10^{12}	4–6	0.08–0.1
polyvinyl chloride	TI 2	2×10^{11}	6–7	0.09–0.1
polyvinyl chloride	4	1×10^{9}	5–6	0.07–0.13
polyvinyl chloride	5	5×10^{11}	6	0.9
polyethylene LD	PE 03	1×10^{16}	2.35	0.0003
polyethylene LD	PE 2	1×10^{16}	2.35	0.0003
polyethylene HD		1×10^{16}	2.35	0.0006
polypropylene		1×10^{16}	2.25	0.0005
Elastomeric†				
general purpose GP rubber	EI 1	2×10^{12}	3–4.5	0.01–0.03
heat resisting GP rubber	GP 1	7×10^{12}	3–4	0.01–0.02
heat resisting GP rubber	GP 2	1×10^{13}	3–4	0.01–0.02
heat resisting MEPR rubber	GP 4	7×10^{12}	3–4	0.01–0.02
flame-retardant rubber	FR 1	5×10^{12}	4.5–5	0.02–0.04
flame-retardant rubber	FR 2	1×10^{13}	4–5	0.015–0.035
OFR rubber	OR 1	1×10^{10}	8–11	0.05–0.10
silicone rubber	EI 2	2×10^{12}	2.9–3.5	0.002–0.02
ethylene vinyl acetate	EI 3	2×10^{12}	2.5–3.5	0.002–0.02
hard ethylene propylene rubber		2×10^{13}	3.2	0.01
crosslinked polyethylene		1×10^{14}	2.3–5.2	0.0004–0.005
Fluorocarbons				
polytetrafluoroethylene		1×10^{16}	2	0.0003

Table 1-IX: Electric Properties of Polymeric Materials.

In the equation several assumptions have been made. First, the losses in the sheath or armour are negligible in multicore cables [56] and second the a.c. resistance of the conductor is given by the d.c. resistance. The reason for the latter is that for conductors with cross-sectional areas below 0.4 in^2 (258mm^2) the skin effects and proximity effects are small. The a.c. resistance is at most 1.04 times the d.c. resistance value. Furthermore, the thermal resistance T_4 is essentially zero since it is the ocean's thermal resistance. The dielectric loss is given by,

Material	Thermal resistivity (K m/W)
Insulation	
Paper (varies with cable type)	5.5–6.5
PE and XLPE	3.5
PVC – up to and including 3 kV	5.0
over 3 kV	6.0
EPR – up to and including 3 kV	3.5
over 3 kV	5.0
Butyl rubber and natural rubber	5.0
Protective coverings	
Compounded jute and fibrous materials	6.0
PCP	5.5
PVC – up to and including 35 kV cables	5.0
over 35 kV cables	6.0
PE	3.5
Materials for ducts	
Concrete	1.0
Fibre	4.8
Asbestos	2.0
Earthenware	1.2
PVC	7.0
PE	3.5

Figure 1-4: Thermal Resistivity of Materials.

$$W_d = \omega\ C\ U_0^2\ \tan\delta \quad (W/m). \tag{1.4}$$

$\omega = 2\pi f$ (1/s) in which f is frequency in (Hz).

U_0 = phase to neutral voltage (V).

$\tan\delta$ = dielectric power factor (see table 1-IX for values of different materials).

C = capacitance (F/m).

$$C = \left(\frac{\epsilon}{18\ \log_e(D_i/d_c)} \right) 10^{-9} \tag{1.5}$$

ϵ = relative permittivity (see table 1-IX for values of different materials).

D_i = external diameter of insulation excluding screen.

d_c = diameter of conductor.

$$T_1 = \frac{\rho_T}{2\pi} G \tag{1.6}$$

$$T_2 = \frac{\rho_T}{2\pi} \log_e \left(1 + \frac{2t_2}{D_s} \right) \tag{1.7}$$

$$T_3 = \frac{\rho_T}{2\pi} \log_e \left(1 + \frac{2t_3}{D} \right) \tag{1.8}$$

G = geometric factor for multicore screened cables [29], see figure 1-5.

ρ_T = thermal resistivity of insulation (°Km/W) see table 1-IX.

t_2 = thickness of bedding (mn).

t_3 = thickness of outer covering (mn).

D_s = external diameter of sheath.

D = external cable diameter.

The resistance of the conductor is given by $R = R_{20}[1 + \alpha_{20}(\theta - 20)]$,where R_{20} is the conductor resistance at T = 20 °C. Table 1-X gives the resistance of different copper and aluminum conductor sizes.

θ = actual temperature of cable (°C)

α_{20} = temperature coefficient per degree C at 20 °C for copper is 0.00393 and for aluminum is 0.00403.

The method outlined in this section determines the maximum tether cable current capacity. The power requirements determine the voltage required. The maximum a.c voltage that can be applied to polyethylene , is around 50 kV/mm thicness of insulation material. If the cable is under pressure then the

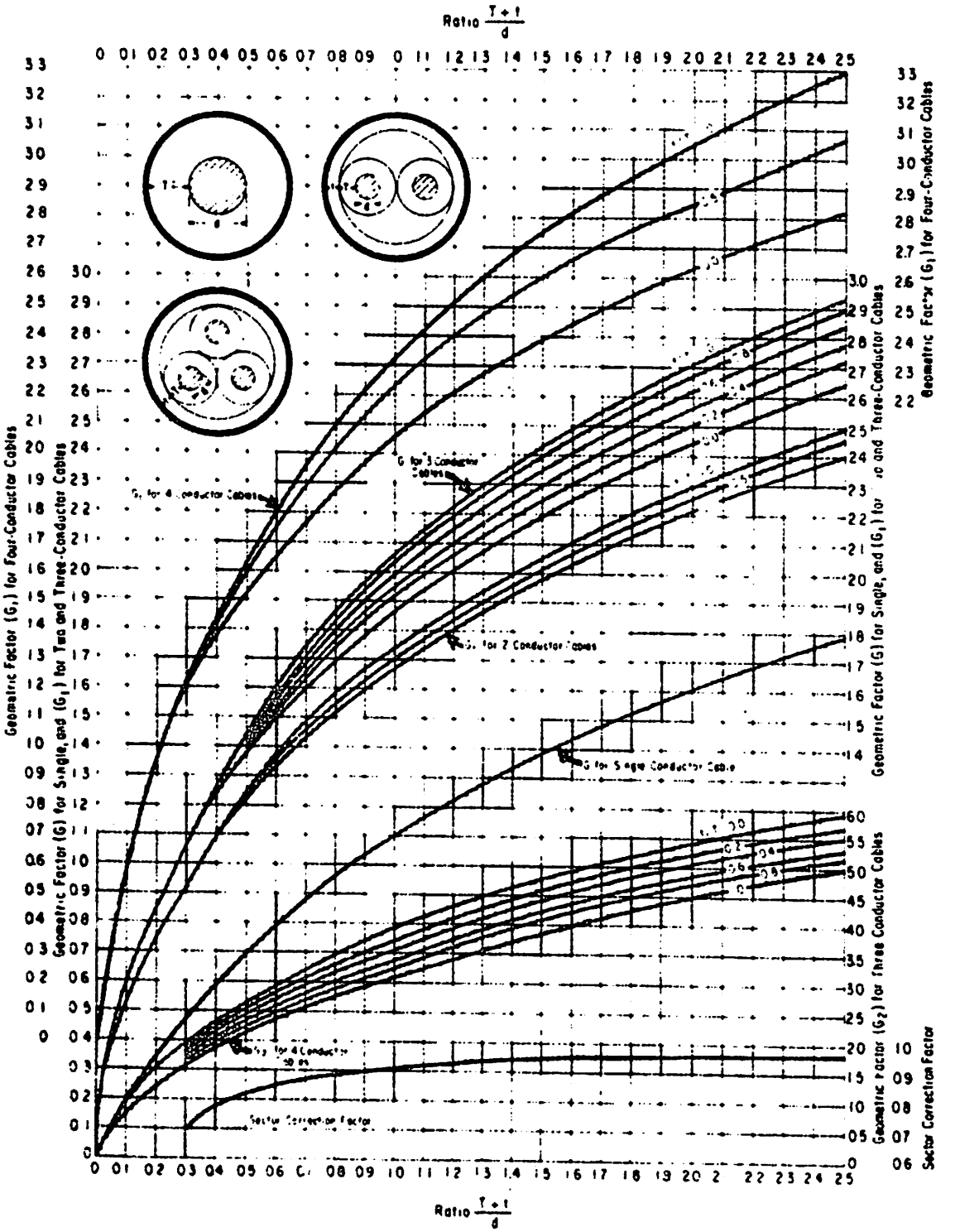

Figure 1-5: Geometric Factors for Cables.

Nominal area (AWG or MCM*)	Equivalent metric area† (mm^2)	Nominal d.c. resistance			Maximum d.c. resistance‡ Single-core cable		Maximum d.c. resistance‡ Multi-core cable	
		Copper (ohm/km)	Coated copper (ohm/km)	Aluminium (ohm/km)	Copper (ohm/km)	Aluminium (ohm/km)	Copper (ohm/km)	Aluminium (ohm/km)
20	0.519	33.9	36.0		34.6		35.3	
18	0.823	21.4	22.7		21.8		22.2	
16	1.31	13.4	14.3		13.7		14.0	
14	2.08	8.45	8.78		8.62		8.79	
13	2.63	6.69	6.96		6.82		6.96	
12	3.31	5.32	5.53	8.71	5.43	8.88	5.54	9.06
11	4.17	4.22	4.39	6.92	4.30	7.06	4.39	7.20
10	5.26	3.34	3.48	5.48	3.41	5.59	3.48	5.70
9	6.63	2.65	2.76	4.35	2.70	4.44	2.75	4.53
8	8.37	2.10	2.19	3.45	2.14	3.52	2.18	3.59
7	10.6	1.67	1.73	2.73	1.70	2.78	1.73	2.84
6	13.3	1.32	1.38	2.17	1.35	2.21	1.38	2.25
5	16.8	1.05	1.09	1.72	1.07	1.75	1.09	1.79
4	21.2	0.832	0.865	1.36	0.849	1.39	0.866	1.42
3	26.7	0.660	0.686	1.08	0.673	1.10	0.686	1.12
2	33.6	0.523	0.544	0.857	0.533	0.874	0.544	0.891
1	42.4	0.415	0.431	0.680	0.423	0.694	0.431	0.708
1/0	53.5	0.329	0.342	0.539	0.336	0.550	0.343	0.561
2/0	67.4	0.261	0.271	0.428	0.266	0.437	0.271	0.446
3/0	85.0	0.207	0.215	0.339	0.211	0.336	0.215	0.343

Table 1-X: USA Stranded Conductor Sizes and Resistances at 20°C for Fixed Wiring.

maximum breakdown voltage increases [56]. In chapter 3 the weight and diameter will be estimated to include the tension members. References [56], [6], [28] offer greater information on tether cable manufacturers.

1.5 Variable Buoyancy Systems

Variable buoyancy systems are not used by all ROV builders, since some believe their cost is excessive. Hamilton Standard has developed a variable buoyancy system that employs mostly off-the-shelf components. [70] The only limitations on using the present system at deeper depths are the pressure

Insulation	Temperature C	Voltage Range
Rubber	60	0 - 2000
	70	0 - 28000
	75	0 - 8000
	80	0 - 28000
	85	0 - 15000
	90	0 - 2000
	125	0 - 5000
EPR	90	0 - 35000
XLPE	90	0 - 69000
PVC	60-75	0 - 600
PE	75	0 - 35000

Table 1-XI: Temperature - Voltage Limits for Insulation.

housings for the control system and the buoyancy tank. [71] The pressure limit on off-the-shelf pressure housings is 4,500 psi. For deepwater applications it is generally recommended that a gas generation system be used to replace the bottled nitrogen gas. [71] Hamilton Standard has also developed a gas generation system based on Hydrazine (N_2H_4). [19] The hydrazine decomposes into ammonia, nitrogen and hydrogen gases through the use of an advanced ruthenium-on-aluminum catalyst. This system has a lift capacity of over 200 lbs/ft^3 (3,200 kg/m^3) of propellant at depths of 24,000 ft (7,300m). The

efficiency of decomposing ammonia into hydrogen and nitrogen gases is 80 %. Furthermore, the hydrazine mixture used with 6 % water or ammonia is a liquid that is neutrally buoyant. The present generation system produced only 25 lbs (11.4 kg) of lift per minute. However, the gas generation rate can be augmented, for example by increasing the exposed area of the catalyst. Data from these systems will be used to design a variable buoyancy system.

1.6 Propulsion

There are two types of motors in use for propulsion; electrical and hydraulic. For tethered vehicles, high voltage three phase a.c. electric motors are used. Franklin Electric makes motors that operate at ambient pressures of up to 13,500 psi in saltwater. These motors range in power between 0.25 hp and 100 hp. Their weights range between 31 lbs to 1094 lbs in air and between 23 lbs to 854 lbs in water at operating speeds of 1725 rpm. [28] For motors with lower operating speeds their weight is higher which is probably due to the use of a gearbox. Figure 1-6 gives the weight versus power for these motors at different operating speeds. Electric propulsion motors are oil-filled and pressure compensated to minimize seawater leakage problems. The efficiency of electric motors is between 70 % and 80 %.[2] However, for deep depths hydraulic motors are used, since they provide the same thrust at lighter system weights and with reduced dimensions.

An electric motor drives the hydraulic pump that provides a pressure differential. This in turn keeps the hydraulic fluid's storage tank pressure

---

[2]Values to be used to estimate power requirements

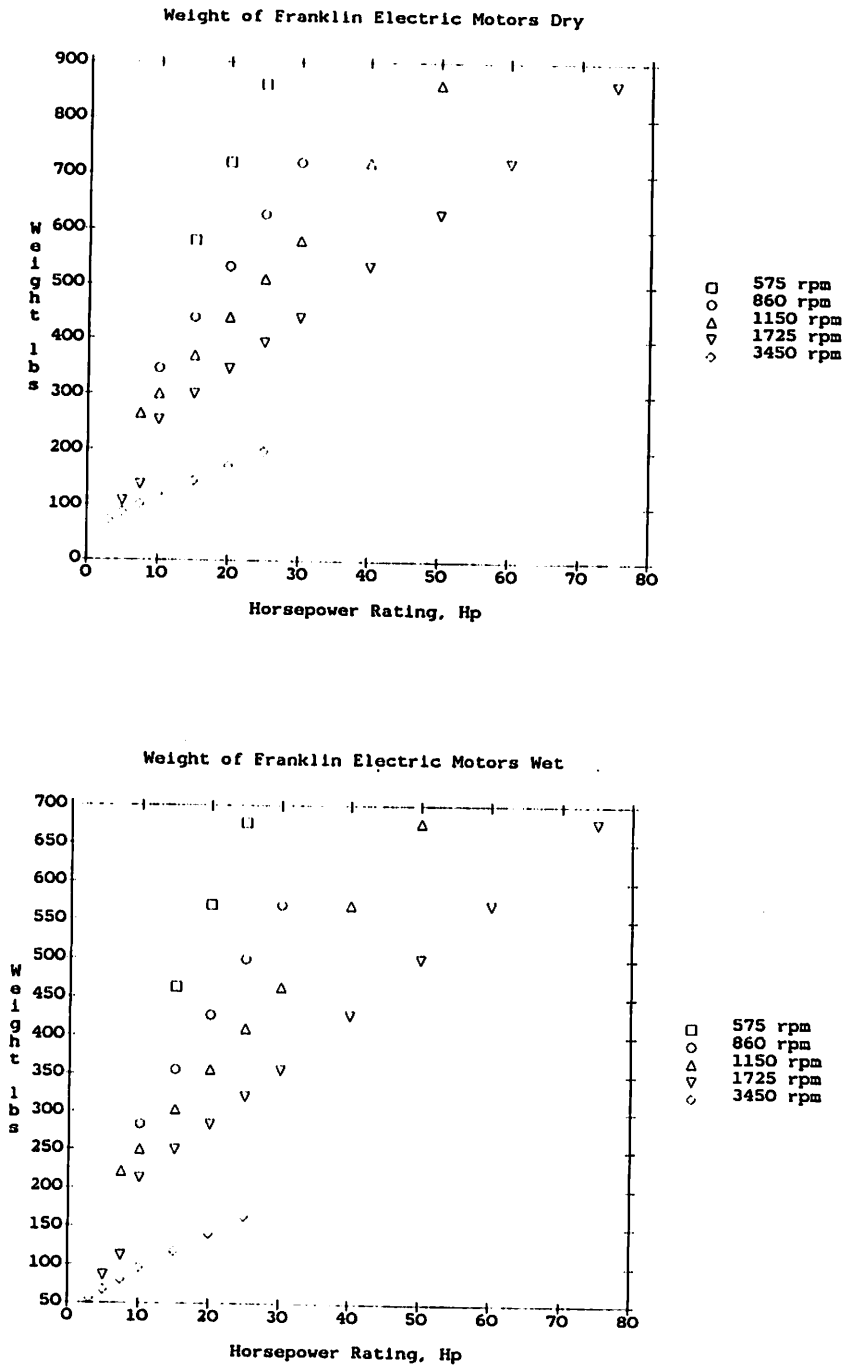

Figure 1-6: Weight versus Power for a.c. Electric Motors.

above ambient. Servovalves control the flow of pressurized fluid to the hydraulic motors. As a result hydraulic propulsion systems are less efficient than electrical systems. The electric motor that runs the pump is operated at a constant load factor and thereby eliminates power surges due to propulsion needs. A general guideline for the weights in air of hydraulic motors is 6 to 15 lbs/hp for motors below 5 hp. For motors between 5 and 10 hp the weights are between 4.5 and 6 lbs/hp and for motors above 10 hp the weights are between 3 to 4.5 lbs/hp.[3] The efficiency of hydraulic pumps is between 80 % and 90 % and for hydraulic motors is between 85 % and 95 %.[4] For more general information on hydraulic pumps and motors see reference [49].

Valves used in hydraulic systems tend to only weigh a few pounds and are not considered in the initial designs. The submersible RCV 150 rated for 600m depths by Hydro Products uses a hydraulic system to power its four thrusters and its manipulator (see reference [10] In figures 1-7 and 1-8 the block diagram for the vehicle's hydraulics and pictorial schematic can be seen. Hydraulic systems involve a great deal of plumbing whose weight is difficult to estimate. For thruster weight determination, it is best to approximate the volume of the thruster and calculate its weight in air and water as a function of the material chosen.

---

[3]These values are estimates and are only useful in approximating the weights of hydraulic propulsion systems.

[4]Values to be used to estimate power requirements.

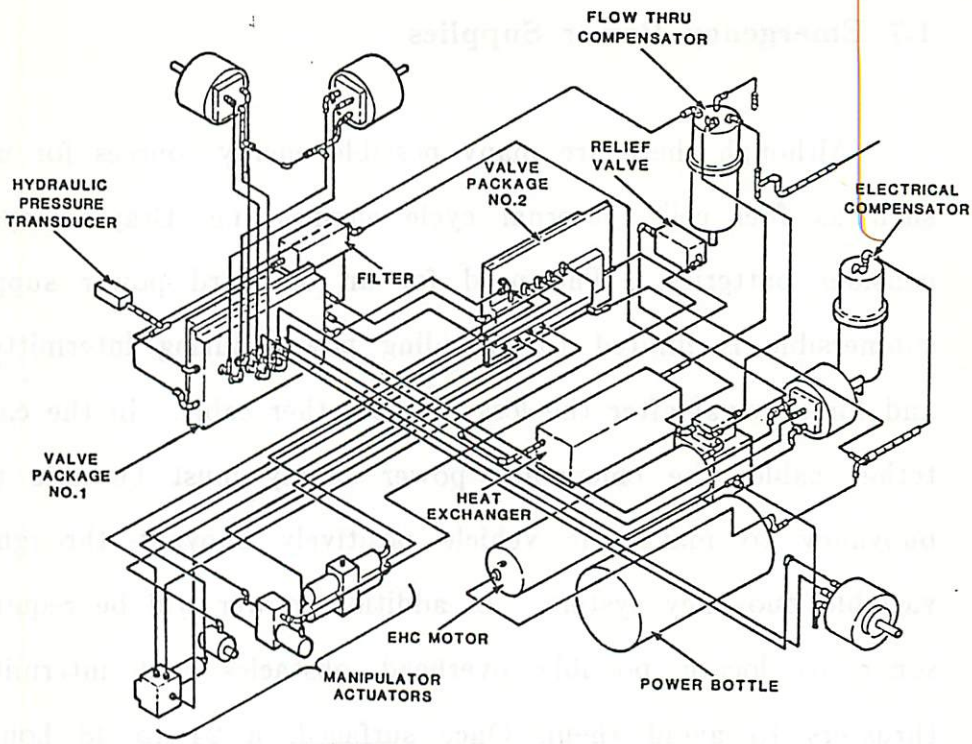

Figure 1-7: RCV-150 Vehicle Hydraulics.

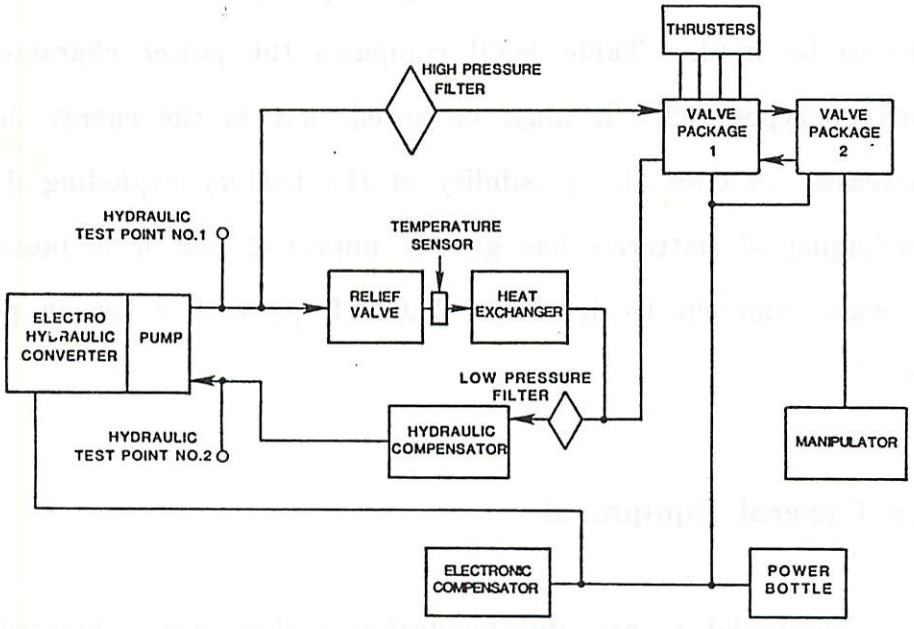

Figure 1-8: Hydraulic System Pictorial Schematic.

1.7 Emergency Power Supplies

Although there are many possible energy sources for use in submersibles such as fuel cells, internal cycle engines (i.e. Brayton cycle), we will only consider batteries. The need for an on-board power supply on a tethered submersible is limited to providing power during intermittent power failures and for survival after the loss of the tether cable. In the case of the loss of a tether cable, the emergency power supply must be able to provide enough buoyancy to make the vehicle positively buoyant through the use of the variable buoyancy system. In addition, power will be required for a scanning sonar to locate possible overhead obstacles and intermittent use of the thrusters to avoid them. Once surfaced, a 24 to 48 hour light and radio beacon must be operated for quick recovery of the vehicle. These requirements determine the storage capacity and rate at which the batteries are to be used. Table 1-XII compares the power characteristics of different battery types. [53] It must be noted that as the energy density of a battery increases, so does the possibility of the battery exploding due to gas releases. Packaging of batteries has greatly improved and it is possible to make them seawater ambient to depths of 20,000 ft [8] with a loss in performance of only 10 %.

1.8 General Equipment

Manipulators provide the dexterity that deep submersibles need for most tasks. They are generally hydraulically powered and have seven degrees of freedom. For moderate depths they typically range in weight between 80 kg

	Leclanche	Alkaline	Mercury	Magnesium	Organic Elect. Li/SO_2-PC-AN/Cl	$Li/SOCl_2$
Negative Electrode	Zn	Zn	Zn	Mg	Li	Li
Positive Electrode	MnO_2	MnO_2	HgO	MnO_2	SO_2/C	$SOCl_2$/C
Electrolyte	NH_4Cl/ H_2O	KOH/ H_2O	KOH/ H_2O	$MgCl_2$/ H_2O	SO_2-PC-AN/ LiBr	$LiAlCl_4$ $SOCl_2$
Energy Density (Wh/kg)	66	77	99	143	330	440 - 550
Energy Density (Wh/cucm)	0.12	0.18	0.43	0 24	0.48	0.91 - 1.5
Open Circuit Voltage (V)	1.5	1.5	1 35	1.7	2.9	3.7
Voltage Stability (0 - 90%)	1 5 - 0.7	1 5 - 0.8	1 3 - 1 1	1.7 - 0 9	2.7 - 2.0	3 6 - 3.2
Power Density (Wh/kg)	55	66	11	88	110	550 - 2200
Power Density (Wh/cucm)	0 09	0 09	0 04	0 18	0.16	0.3 - 2.7
Temperature Range (°C)	-6 - 54	-29 - 71	-6 - 71	5 - 71	-40 - 74	-40 - 100
Operating Voltage (V) at 1 mA/cm^2	1 3	1 3	1 2	1 7	2 7	3 6
Shelf Life (Years) at 21 °C	1	2	> 2	2	> 2	> 2

Table 1-XII: Primary Battery Power Comparisons.

and 250 kg in air and between 50 kg and 150 kg in water. [78], [39], [16], [22] They have a maximum lifting capacity ranging between 30 kg and 120 kg in air and consume around 0.2 to 0.6 kW. The manipulators are generally not used to carry objects.

High resolution medium range sonars packaged for submersibles and currently available, displace $0.35m^3$ and weigh 14 - 23 kg. These sonars provide ranges of 30 - 100m with resolutions of 0.15m - 0.6m. The power consumption of such systems can be estimated to be around 0.3 kW. [22] In addition to acoustic imaging and ranging sensors, there are optical sensors such as cameras, 35mm cameras, television cameras, stereoscopic cameras etc.

These sensors are generally lightweight and have low power requirements. In order to use optical sensors lighting must be provided. The lamps and strobes weigh little and are small, but their power consumption ranges between 300W and 20 kW, depending on the lighting required and the turbidity of the water. [36] Various other sensors will be required and their weight and power requirements will be assumed in the initial design.

Chapter 2

HYDRODYNAMICS

The hydrodynamic forces acting on a body moving in a fluid are a function of the body's geometry and of the body's motion. For example, torpedos are designed to travel at relatively high speeds towards their targets and as a result have slender bodies. This reduces drag in the principal direction of motion. Certain observation submersibles are virtually spherical, since they are required to move in various directions with a specific orientation at low speeds. The tethered heavy lift submersible (THLS) is to be capable of travelling "quickly" from its initial deployed position to the worksite on the seabed and back with or without a payload. In addition, it must have good station-keeping characteristics and be orientable, in order to facilitate the acquisition or delivery of its payload.

The main result is that there are two separate types of operation for the THLS; one being translationary and the other a combination of station keeping and vehicle orientation. These produce conflicting requirements for the hydrodynamic forces involved. There are essentially three types of hydrodynamic forces; added inertia forces, forces due to circulation flows and viscous flow forces. The added inertia terms are important when the vehicle is accelerating or maneuvering. The circulation forces and viscous flow forces occur in situations where the submersible is moving with steady velocities. The Froude-Krylov forces, which are the result of bodies moving in unsteady currents, are neglected. It is assumed that these effects are negligeable and that the control system will compensate for them.

The types of submersible shapes we will consider are spheres, parallelepipeds, torpedo shapes, prolate ellipsoids and ellipsoids. In this Chapter the force derivatives for the added inertias are determined, followed by the derivatives due to circulation and viscous forces. Finally, the generation of control forces through movable surfaces, such as rudders, and with thrusters is dealt with. The combination of the hydrodynamic characteristics and the data from Chapter 2 will allow us to design the submersible in Chapter 4 and then simulate its motion in Chapter 5.

For bluff bodies, the boundary layer separates from the body into a region of separated flow. The assumption of inviscid flows can lead to large errors in the added-mass terms. In such cases it may be necessary to include the region of separated flow in the vehicle's geometry leading to non-linear or time varying added-mass terms. Throughout this section estimates of the added-mass coefficients are made using both potential flow theory and semi-empirical methods. Given the assumptions we have made, certain added mass terms will be inaccurate, where possible this is indicated.

In appendix A it can be seen that if the body is symmetric along one or more planes of symmetry, then the number of coupling added-mass terms is reduced The result is for bodies with spherical or box shapes the added-mass tensor is greatly simplified. The following figure 2-1 defines the body coordinates used in this chapter.

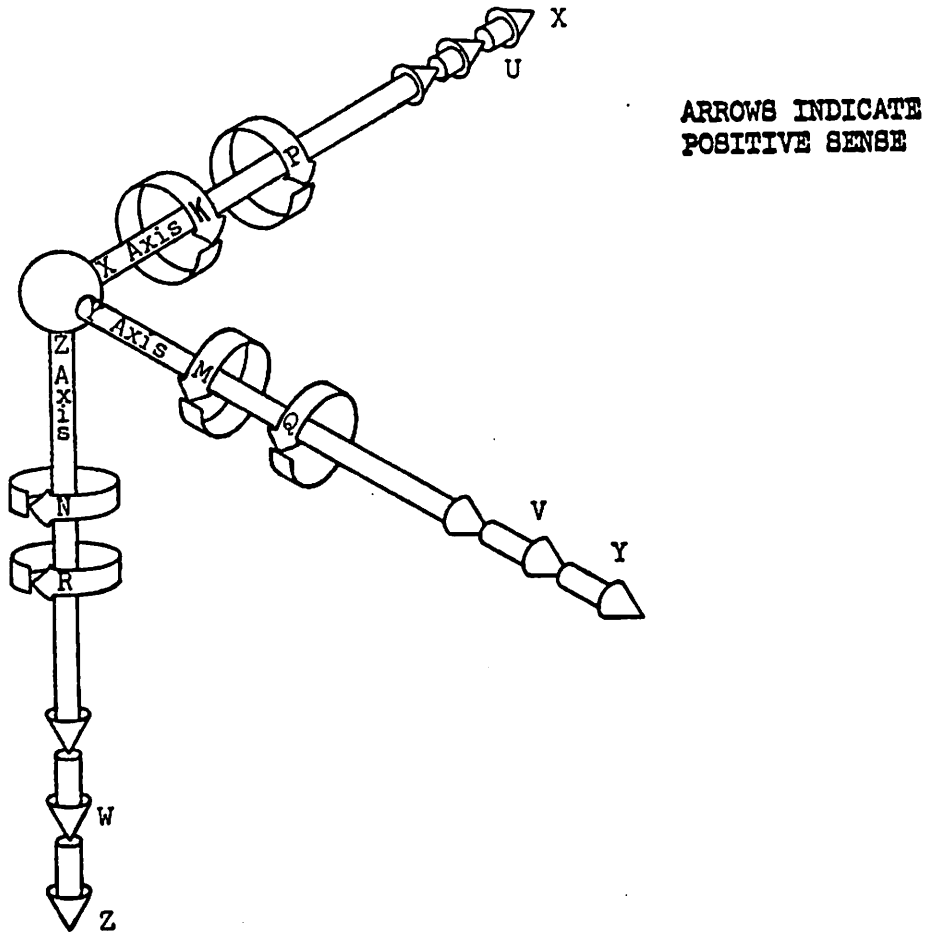

Figure 2-1: Submersible's Body Coordinate System.

2.1 Acceleration Coefficients

The added-mass terms represent the fluid particles surrounding the submerged body that are accelerated with it. These terms appear as acceleration coefficients and are generally lumped together with the submersible's mass and inertia terms. The added-mass is also known as the mass accession term, the apparent mass, the virtual mass and the hydrodynamic mass. In appendix A, the added mass terms are derived from potential theory using Lagrangian dynamics. This is the method derived by H. Lamb [48] and used in reference [38]. The added mass terms are obtained under the following assumptions: the fluid is inviscid, there is no circulation and the body is submerged in an unbounded fluid.

The last assumption is violated at the sea-bottom and at the surface. In reference [25], the proximity of Rankine ovoids to the bottom and surface are examined. The THLS is lowered to deep depths and thus will not be subject to free surface effects. However, as it approaches the sea-bottom it will violate our third assumption. For Rankine ovoids there is no increase in added-mass until they are less than two diameters from the sea-floor. These effects are not treated in this report due to the complexity of accurately determining added-mass of bodies in proximity to a boundary and due to a lack of information.

In the case of faired bodies, the thickness of the boundary layer is small and the flow over more than 80 % of the bodies' surface can be described using potential flow theory. [38] The added-mass coefficients for fins can be seriously affected if they are in the regions of separated flow or in regions where the body's boundary layer is large. The added-mass coefficients are

obtained by determining the first effective aspect-ratio outside of the regions of separated flow. These problems can be greatly simplified by placing the fins outside of these regions. Certain added-mass terms are affected by boundary layers and determination of these terms using model tests require scaling of the Reynold's number.

2.2 For Spherical Vehicles

In the case of spherical vehicles there are three planes of symmetry and the angular acceleration coefficients are zero. This results in three equal translational acceleration coefficients: $X_{\dot{u}}$, $Y_{\dot{v}}$, $Z_{\dot{w}}$. The value of these coefficients is one half the mass of the water displaced by the vehicle.

$$X_{\dot{u}} = Y_{\dot{v}} = Z_{\dot{w}} = \frac{2}{3} \rho \pi r^3 \tag{2.1}$$

ρ = density of sea water (Kg/m^3).
r = radius of spherical body (m).

2.3 For Box-Shaped Vehicles

Box-shaped vehicles are bodies with three planes of symmetry, as with spheres, and have only six acceleration coefficients, three translational and three rotational. The translational coefficients are given by the empirical relation [85],

$$M = \rho \left(\frac{6.3\ a^2 b^2}{(a^2 + b^2)} \right) + 3abc^{\ 0.5} \tag{2.2}$$

M = translational coefficient for the parallelepiped moving perpendicular to the face 2a $\times$ 2b.

2a = width of parallelepiped (m).

2b = height of parallelepiped (m).

2c = length of parallelepiped (m).

ρ = density of seawater (Kg/m^3).

The coefficients $X_{\dot{u}}$, $Y_{\dot{v}}$, $Z_{\dot{w}}$ are obtained as the value M when the appropriate units

are substituted in the above equation in each case. The rotational acceleration coefficients $K_{\dot{p}}$, $M_{\dot{q}}$, $N_{\dot{r}}$ are obtained using strip theory. [61] The flow at each section of the vehicle is assumed to be locally two dimensional. The added-mass and inertia coefficients for two-dimensional rectangles are given in figures 2-2 and 2-3 [83]. We assume the submersible's longest dimension to be its length. Integrating the added-inertia of a rectangle along the vehicle's length yields $K_{\dot{p}}$, where

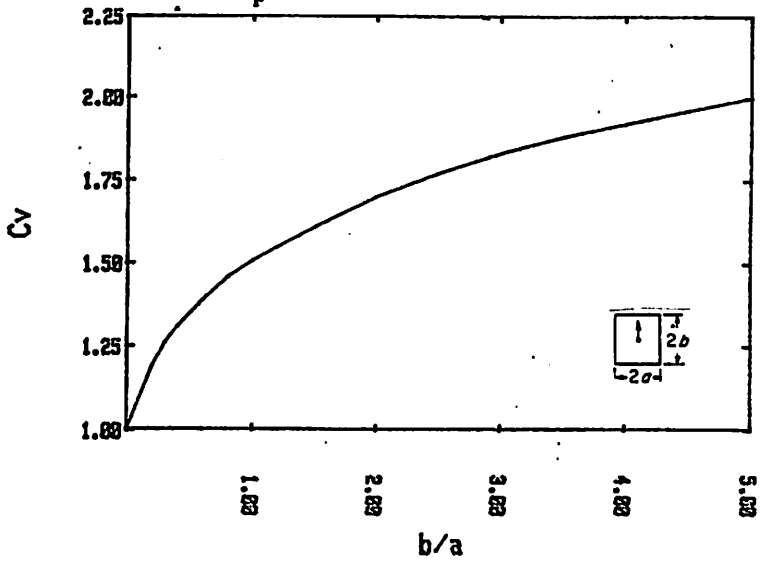

Figure 2-2: Added-mass Coefficient for 2-D Rectangular Sections.

$$K_{\dot{p}} = \frac{1}{4} C_R \pi \rho a^4 c \qquad (2.3)$$

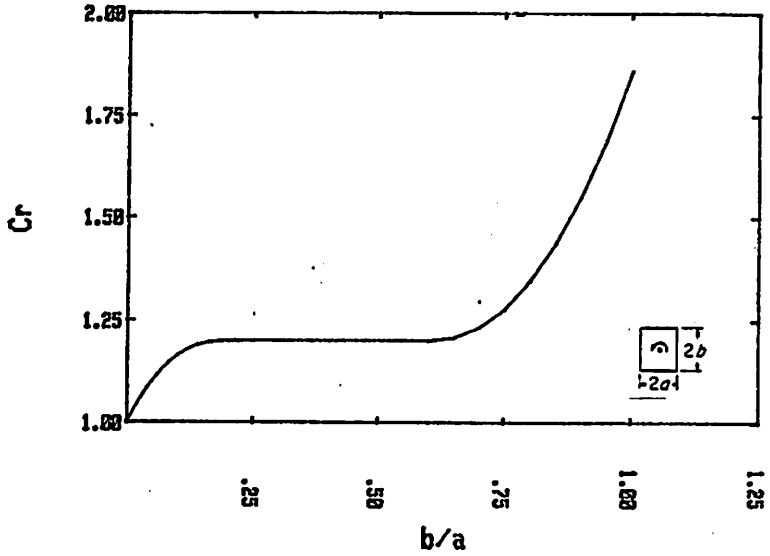

Figure 2-3: Added-inertia Coefficient for 2-D Rectangular Sections.

Strip theory produces accurate results for bodies with length-to-diameter ratios above 10. In general, the bodies we will deal with will have length-to-diameter ratios of around 2 to 6. In order to compensate we will use a correction factor f_c.

$$f_c = 1 - e^{-0.3x} \quad \text{where } x = \text{length-to-diameter ratio.} \tag{2.4}$$

$$\text{and} \quad K_p^{\bullet} = \frac{1}{4} f_c \, C_R \, \pi \, \rho \, a^4 \, c \tag{2.5}$$

This is a crude estimate based on the added-inertia of a flat plate rotated about the axis normal to its face, being zero and by assuming that the error for bodies with length-to-diameter ratios of 10 is about 5 %. The resulting rotational acceleration coefficient is not accurate, but the resulting approximation should be reasonable. Only experimental data can remedy this problem. The two other acceleration coefficients can be determined similarly.

2.4 For Cylindrical and Ellipsoidal Bodies

This group includes three different types of bodies; torpedo-shaped bodies, prolate ellipsoids and general ellipsoids. These bodies are unstable and are fitted with vertical and horizontal tail fins for stability. Bowplanes can be added to improve the vehicle's stability and maneuvrability. An exact theoretical method exists for prolate ellipsoids and is obtained from Lamb. [48] For torpedo-shaped bodies the previous method yields reasonably accurate results. [38] For general ellipsoids the method for prolate ellipsoids will be adapted to provide reasonable estimates. Exact methods exist for general ellipsoids, see references [48, 87, 60, 63] ,but these are computationally long and involve the use of mathematical tables to calculate elliptic integrals. In appendix B, the coefficients for a general ellipsoid are graphed and obtained from reference [63]. For these bodies it is assumed that they have *xz* as a plane of symmetry, that is port-starboard symmetry. This leaves us with the following acceleration coefficients:

Added Inertia Terms
$X_{\dot{u}}$, $Y_{\dot{v}}$, $Z_{\dot{w}}$, $K_{\dot{p}}$, $M_{\dot{q}}$, $N_{\dot{r}}$

Added Inertia Coupling Terms
$X_{\dot{q}}$, $Y_{\dot{p}}$, $Y_{\dot{r}}$, $Z_{\dot{q}}$, $K_{\dot{v}}$, $M_{\dot{w}}$, $M_{\dot{u}}$, $N_{\dot{v}}$

Remaining Terms
$X_{\dot{w}}$, $Z_{\dot{u}}$, $K_{\dot{r}}$, $N_{\dot{p}}$

2.4.1 Longitudinal Coefficients

2.4.1.1 $X_u^{\cdot}$

For the prolate ellipsoid,

$$X_u^{\cdot} = k_1 \, m_{df} \tag{2.6}$$

$$k_1 = \frac{\alpha_o}{2 - \alpha_o} \tag{2.7}$$

$$\alpha_0 = \frac{2(1 - e^2)}{e^3} \left(0.5 \ln \left[\frac{1 + e}{1 - e} \right] - e \right) \tag{2.8}$$

$$e = \frac{2}{l} \left(\frac{l^2}{4} - \frac{s_b}{\pi} \right)^{0.5} \tag{2.9}$$

e = eccentricity of the rotated ellipse.
l = length of body.
s_b = maximum cross-sectional area of the body.
k_1 = Lamb's Inertia coefficient for axial motion.

In figure 2-4, Lamb's Inertia coefficients are plotted for axial, lateral and rotational motion. For the general ellipsoid,

$$X_u^{\cdot} = C_1 \, k_1 \, m_{df} \tag{2.10}$$

where $C_1 = -0.52\varsigma^2 + 1.51\varsigma$ and ς = height-to-width ratio.

The correction factor C_1 is a reasonable approximation for general ellipsoids and comparison with figure B-1 shows the approximation is good to $\pm$ 2.5 %.

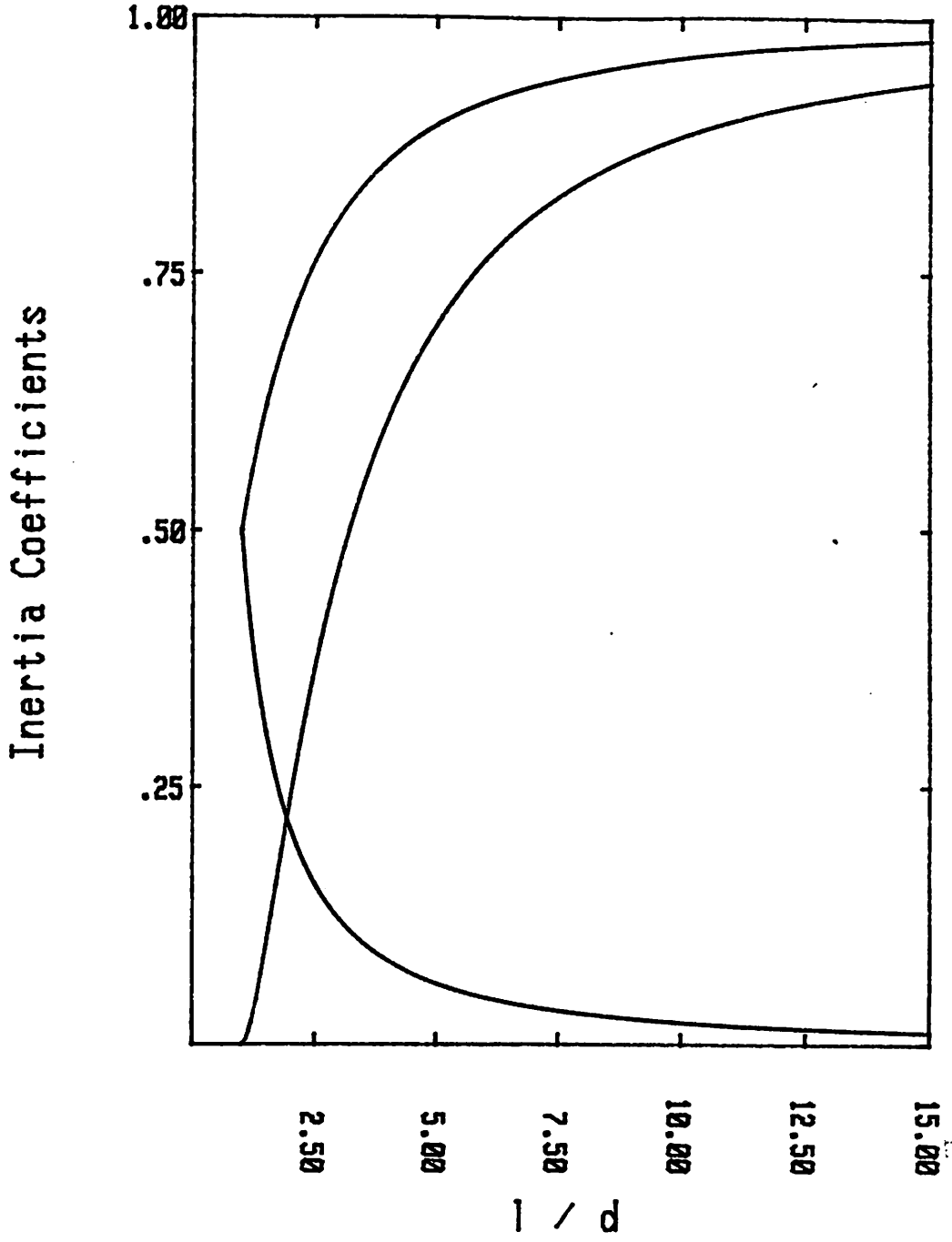

Figure 2-4: Lamb's Inertia Coefficients k_1, k_2 and k' plotted as a function of vehicle l/d.

2.4.1.2 $Z_{\dot{u}}$

The acceleration coefficient $Z_{\dot{u}}$ is generally set to zero and neglected (see reference [38]).

2.4.1.3 $M_{\dot{u}}$

This term is usually insignificant and is set to zero.

2.4.1.4 $X_{\dot{w}}$

For most underwater vehicles $X_{\dot{w}}$ is set to zero. [38]

2.4.1.5 $Z_{\dot{w}}$

For the prolate ellipsoid,

$$Z_{\dot{w}_b} = k_2 \, m_{df} \tag{2.11}$$

$$\text{where } k_2 = \frac{\beta_o}{2 - \beta_o} \tag{2.12}$$

$$\text{and } \beta_o = \frac{1}{e^2} - \frac{1 - e^2}{2e^3} \ln \frac{1 + e}{1 - e} \tag{2.13}$$

For general ellipsoids, $Z_{\dot{w}_b}$ is given by the value of a prolate ellipsoid whose maximum diameter is the width of the general ellipsoid. (Note: the mass of displaced fluid, m_{df}, is the value of the equivalent prolate ellipsoid in this case). Justification for this can be found in reference [62] where the added mass of circular section and elliptical section are identical along a given axis for equivalent width.

In addition to the body contribution, the horizontal surfaces such as fins, bowplane or possibly shroud contribute to this acceleration coefficient. The

added mass, m_a, for the translation of a plate of span b is given by,

$$m_a = \frac{1}{4} k\rho\pi c^2 b \tag{2.14}$$

c = effective chord or mean chord $\frac{s}{b} = \frac{b}{AR}$

$$k = \frac{1}{(1 + 1/AR)^{0.5}} \tag{2.15}$$

Approximation by *Pastor* and *Abkowitz* where k is the correction coefficient for the aspect ratio of the surface and is given in figure 2-5.

AR = aspect ratio of surface = b^2/s
s = planform area of surface.

$$Z^{\cdot}_{w_t} = \frac{1}{4} k\rho\pi c^2 b \tag{2.16}$$

Similarly for a single bowplane, $Z^{\cdot}_{w_{bp}} = \frac{1}{4} k\rho\pi c^2 b$.

For a shroud the contribution to $Z^{\cdot}_w$ is determined by projecting it onto an equivalent flat plate. Thus,

$$Z^{\cdot}_{w_s} = \frac{1}{2} k\rho\pi c^2 r \tag{2.17}$$

c = chord of shroud.
r = shroud's radius.

The coefficient $Z^{\cdot}_w$ represents the sum of all the contributing terms i.e.,

$$Z^{\cdot}_w = Z^{\cdot}_{w_b} + 2Z^{\cdot}_{w_t} + 2Z^{\cdot}_{w_{bp}} + Z^{\cdot}_{w_s} \tag{2.18}$$

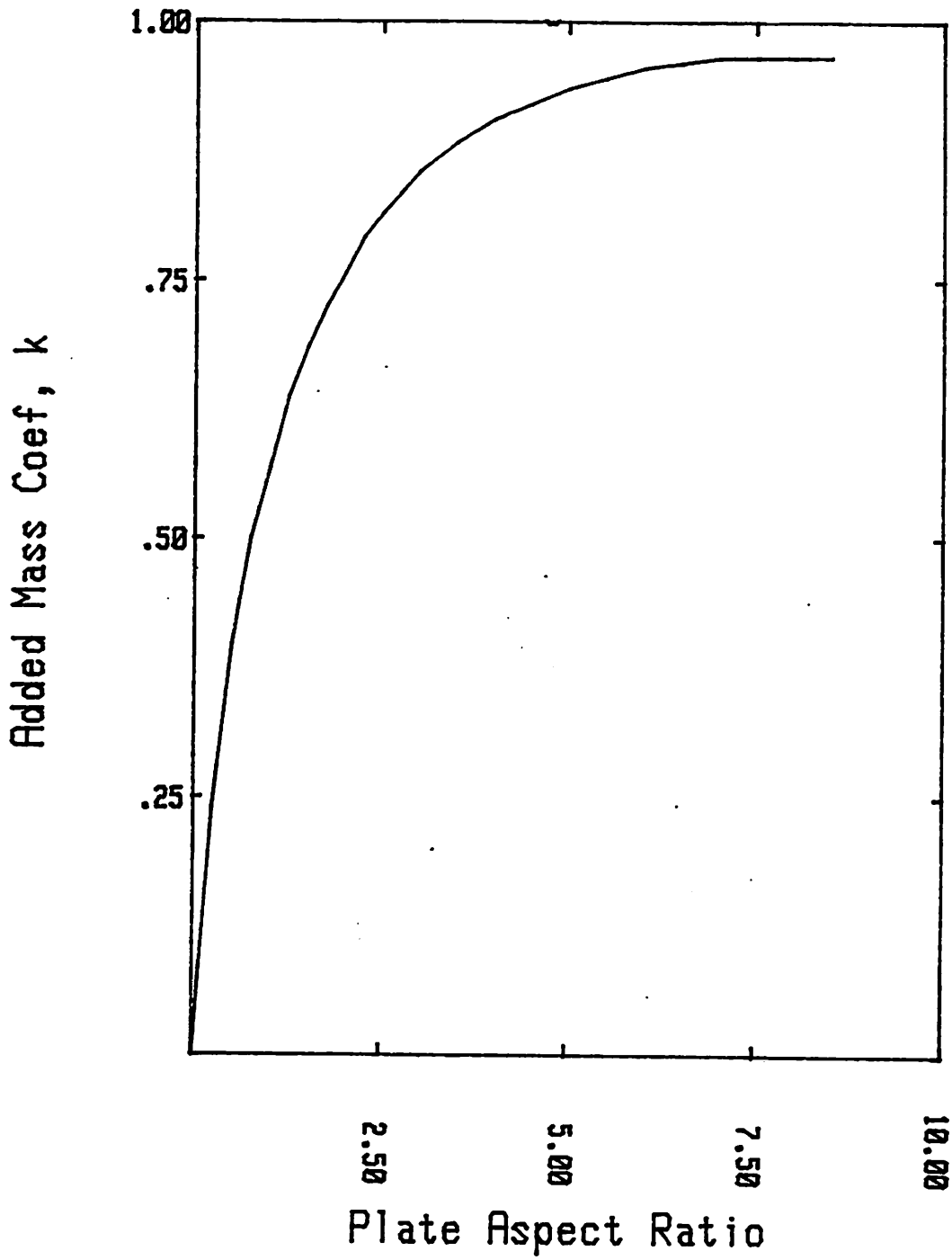

Figure 2-5: Coefficients of Added Mass for Rectangular Plates.

2.4.1.6 $M_w^{\cdot}$

This term represents the pitching moment caused by a vertical acceleration. This is significant in vehicles with large horizontal planforms. The x-moment arm from the vehicle's center of buoyancy to the points of action of the $Z_w^{\cdot}$ components produce the $M_w^{\cdot}$ components. For example,

$$M_{w_t}^{\cdot} = Z_{w_t}^{\cdot} x_{ht} \tag{2.19}$$

x_{ht} = x-distance between center of buoyancy and centroid of the horizontal surface.

The term $M_w^{\cdot}$ represents the sum of all these terms, as follows

$$M_w^{\cdot} = 2M_{w_t}^{\cdot} + 2M_{w_{b_p}}^{\cdot} + M_{w_s}^{\cdot} \tag{2.20}$$

2.4.1.7 $X_q^{\cdot}$

This term is usually insignificant and is set to zero.

2.4.1.8 $Z_q^{\cdot}$

This term is the same as $M_w^{\cdot}$, i.e. $Z_q^{\cdot} = M_w^{\cdot}$

2.4.1.9 $M_q^{\cdot}$

For a prolate ellipsoid,

$$M_{q_b}^{\cdot} = - k_b' I_{y_{df}} \tag{2.21}$$

$$k_b' = \frac{e^4(\beta_0 - \alpha_0)}{(2 - e^2)[2e^2 - (2 - e^2)(\beta_0 - \alpha_0)]} \tag{2.22}$$

k'_b = Lamb's coefficient for added moment of inertia.
$I_{y_{df}}$ = moment of inertia about the y-axis of the mass of fluid displaced by the body.

For a general ellipsoid, an equivalent prolate ellipsoid with a maximum diameter equal to the ellipsoid's maximum width is used. The previous arguments are then applied. For the case of the horizontal tailplane, their contribution to the acceleration coefficient is given by $M^{\bullet}_{q_{ht}}$. (This includes both port and starboard surfaces.)

$$M^{\bullet}_{q_{ht}} = - \frac{k'_p \rho \pi b^2 c^3}{48} + 2Z^{\bullet}_{w_{ht}} x^2_{ht} \tag{2.23}$$

where k'_p is the coefficient of added moment of inertia for a flat plate and is given in figure 2-6. A curve fitted approximation yields,

$$k'_p = \left(\frac{AR}{9} \right)^{0.36} \tag{2.24}$$

For the case, where there are endplates on the surface then there are no edge effects that reduce the added inertia contribution. In this case, $M^{\bullet}_{q_{ht}}$ is determined as follows,

$$M^{\bullet}_{q_{ht}} = - \frac{2\rho \pi b c^4}{8} + 2Z^{\bullet}_{w_{ht}} x^2_{ht} \tag{2.25}$$

The bowplanes and shroud are treated similarly to the tailplane. Thus, the complete acceleration coeficient $M^{\bullet}_q$ becomes

$$M^{\bullet}_q = M^{\bullet}_{q_b} + M^{\bullet}_{q_{ht}} + M^{\bullet}_{q_{bp}} + M^{\bullet}_{q_{sh}} \tag{2.26}$$

2.4.2 Lateral Coefficients

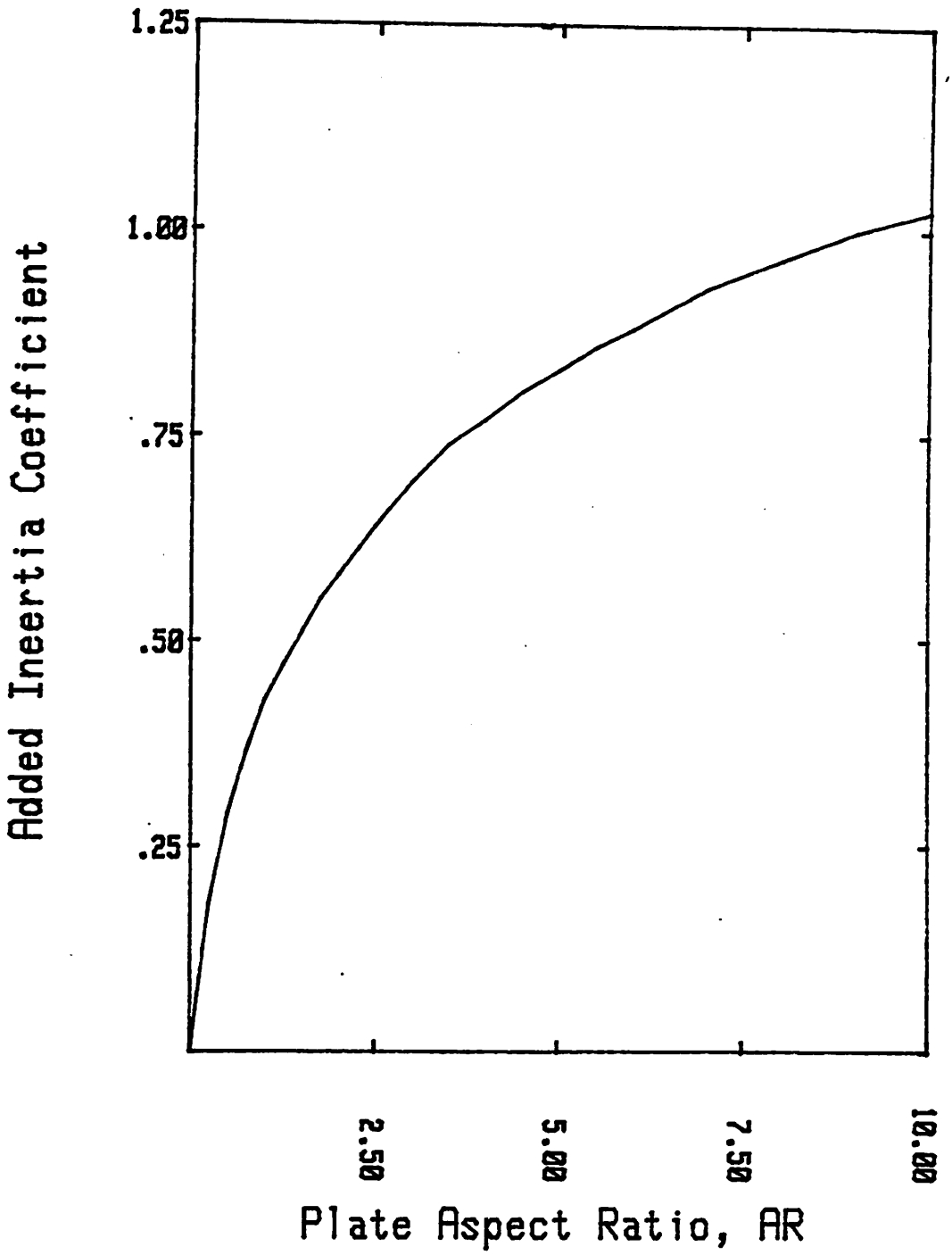

Figure 2-6: Coefficients of Added Inertia for Rectangular Plates.

2.4.2.1 $Y_v^{\cdot}$

For axisymmetric bodies $Y_{v_b}^{\cdot} = Z_{w_b}^{\cdot}$. For the case of general ellipsoids, the procedure used to find $Z_{w_b}^{\cdot}$ for prolate ellipsoids can be used. However, the maximum diameter of the equivalent prolate ellipsoid is given by the maximum height of the general ellipsoid. Using the relations for a flat plate from $Z_w^{\cdot}$, the contributions of vertical surfaces can be determined. The complete expression for $Y_v^{\cdot}$ becomes,

$$Y_v^{\cdot} = Y_{v_b}^{\cdot} + Y_{v_{uvt}}^{\cdot} + Y_{v_{lvt}}^{\cdot} + Y_{v_{sh}}^{\cdot} \tag{2.27}$$

where, $Y_{v_{uvt}}^{\cdot}$ = contribution from the upper vertical tail.

$Y_{v_{lvt}}^{\cdot}$ = contribution from the lower vertical tail.

$Y_{v_{sh}}^{\cdot}$ = contribution from the shroud.

2.4.2.2 $Y_p^{\cdot}$

The acceleration coefficient $Y_p^{\cdot}$ is equal to $K_v^{\cdot}$.

2.4.2.3 $Y_r^{\cdot}$

The acceleration coefficient $Y_r^{\cdot}$ is equal to $N_v^{\cdot}$.

2.4.2.4 $K_v^{\cdot}$

This term is made up of the vertical tail surface contribution $K_{v_{uvt}}^{\cdot}$ and $K_{v_{lvt}}^{\cdot}$. It is assumed that the upper and lower vertical tailfins are not necessarily the same size or located the same distance from the x-axis. Thus, for tailfins that are vertical,

$$K_v^{\cdot} = -(Y_{v_{uvt}}^{\cdot} z_{uct} + Y_{v_{lvt}}^{\cdot} z_{lct}) \tag{2.28}$$

$$K_v^{\bullet} = K_{v_{uvt}}^{\bullet} + K_{v_{lvt}}^{\bullet} \tag{2.29}$$

z_{uct} = distance from the x-axis to the upper vertical tail's centroid.

z_{lct} = distance from the x-axis to the lower vertical tail's centroid.

2.4.2.5 $K_p^{\bullet}$

For general ellipsoids the body contribution is,

$$K_{p_b}^{\bullet} = m_{44} \tag{2.30}$$

Where m_{44} is obtained from figure B-4. To this we add the contribution from the vertical tailfins. For the upper vertical tailfin,

$$K_{p_{uvt}}^{\bullet} = I_{x_a} = - \frac{\pi \rho}{48} D_{\lambda} D_{\Gamma} k_p' c^2 b^3 \tag{2.31}$$

D_{λ} = taper correction factor, see figure 2-7.

D_{Γ} = dihedral correction factor, see figure 2-8.

These can be approximated by,

$$D_{\lambda} = 1 - 0.195 \left(\frac{c_r}{c_t} - 1 \right)^{0.472} \qquad \text{(error is } \pm 4 \text{ \%)} \tag{2.32}$$

c_r = chord at the root of the surface.

c_t = chord at the tip of the surface.

$D_{\Gamma} = -0.00373\ \Gamma^{2.2} + 1$ (error is $\pm$ 2 %)

Γ = dihedral angle in degrees.

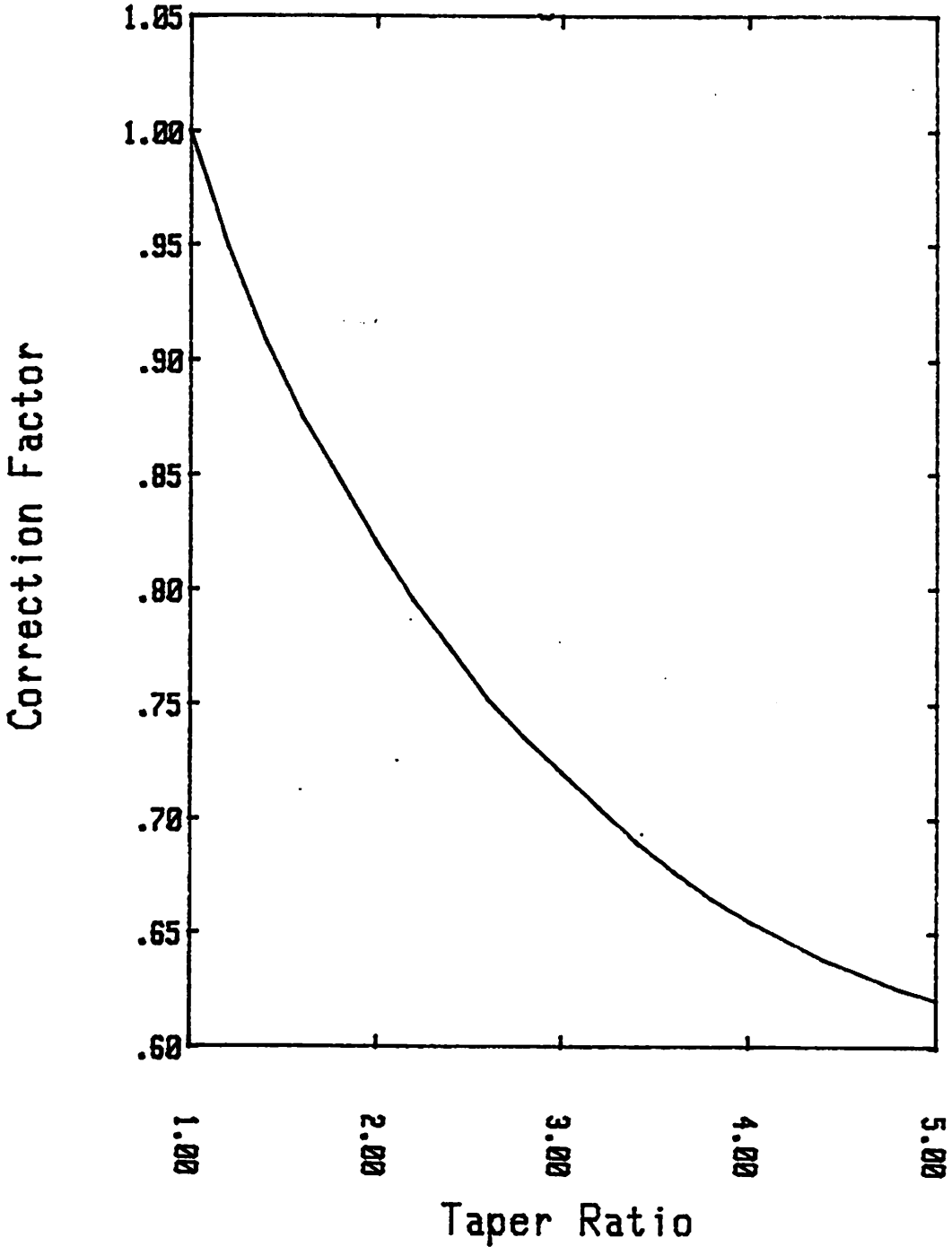

Figure 2-7: Dependence of the Added Moment of Inertia on Taper Ratio.

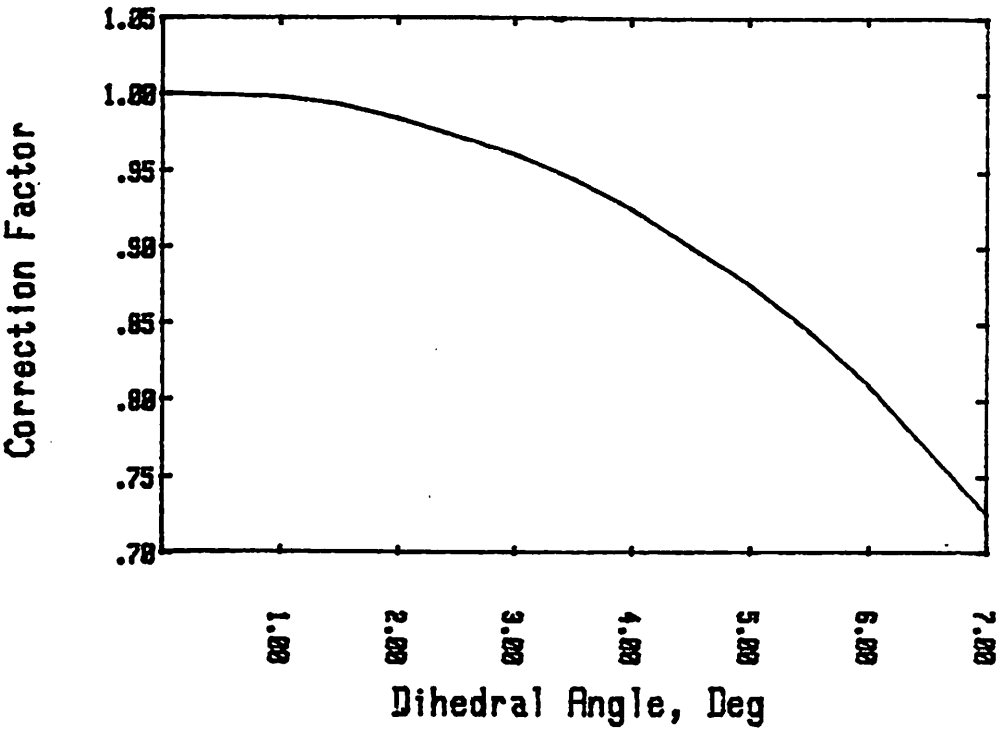

Figure 2-8: Variation of the Added Moment of Inertia of a Single Plate with Dihedral Angle

The complete expression for this term becomes,

$$K'_p = K'_{p_b} + K'_{p_{uvt}} + K'_{p_{lvt}} \tag{2.33}$$

2.4.2.6 K'_r

This term is mainly due to the vertical surfaces being different to the vertical surfaces, being different in size and/or location.

$$K'_r = K'_{v_{uvt}} x_{uvt} + K'_{v_{lvt}} x_{lvt} \tag{2.34}$$

x_{uvt} = distance to upper vertical tail surface centroid from c.b. (+ve aft.)

x_{lvt} = distance to lower vertical tail surface centroid from c.b. (+ve aft.)

2.4.2.7 N'_v

As for K'_r, the term N'_v is due to the vertical surfaces.

$$N'_v = N'_{v_t} = - Y'_{v_{uvt}} x_{uct} - Y'_{v_{lvt}} x_{lct} \tag{2.35}$$

2.4.2.8 N_p

$N'_p = K'_r$ (see appendix A)

2.4.2.9 N'_r

The body contribution to this term is,

$$N'_{r_b} = -k'_b I_{Z_{df}} \tag{2.36}$$

$I_{Z_{df}} = I_{Y_{df}}$ for axisymmetric bodies.

For general ellipsoids, $I_{Z_{df}}$ can be determined from an equivalent prolate ellipsoid whose maximum diameter is the general ellipsoid's maximum height. For the upper vertical tail,

$$N'_{r_{uvt}} = \left(\frac{k'_p \rho \pi b^2 c^3}{48} \right) + Y'_{v_{uvt}} x^2_{uvt} \tag{2.37}$$

The complete expression for the term N'_r is given as,

$$N'_r = N'_{r_b} + N'_{r_{uvt}} + N'_{r_{lvt}} \tag{2.38}$$

2.5 Forces Due to Steady Flows

There are two types of forces that are generated by steady flows: Lift and drag forces. Drag forces are the result of viscous and separated flows. Viscous flows are limited to the boundary layer which is a thin region that envelopes the vehicle's surface. In this region there are two types of flows: laminar and turbulent. [62, 34] For Reynolds numbers (Re) above 5×10^5 the smooth laminar flows become turbulent. Where,

$$\mathrm{Re} = \frac{UL}{\nu} \tag{2.39}$$

U = velocity of flow.

L = length of body.

ν = viscosity of fluid.

In the boundary layer a drag force known as friction drag is produced. The frictional drag coefficient,

$$C_F = 1.328\ \mathrm{Re}^{-0.5}\ ,\ \mathrm{Re} \leq 5 \times 10^5 \tag{2.40}$$

$$C_F = \frac{0.075}{(\log_{10} \mathrm{Re} - 2)^2}\ ,\ \mathrm{Re} \geq 5 \times 10^5 \tag{2.41}$$

Separation of the flow occurs at the tail end of the body either because it tapers down or because the body ends abruptly. This is known as base pressure or form drag and is characterised by the coefficient C_P. The drag coefficient C_D is given by $C_D = C_F + C_P$. The resulting drag force acts in the opposite direction to the direction of motion and D is given by,

$$D = 0.5\rho U^2 S C_D \tag{2.42}$$

S = wetted surface area of body (area of body in unseparated flow).

For further information on drag forces see references [62, 34, 18, 11].

The lift force is the result of circulation and is generally proportional to the angle of incidence between the body and the flow. For certain bodies , especially slender bodies of revolution, crossflow drag contributes to the lift force at higher angles of attack. This generally produces a lift coefficient C_L of the following form,

$$C_L = C_{L_C}\alpha + C_{L_D}\alpha^2 \tag{2.43}$$

α = angle of incidence between body and flow.

C_{L_C} = lift due to circulation.

C_{L_D} = lift due to cross-flow drag.

The drag force generally acts in through the vehicle's center of geometry and produces no moments. Lift forces act through a center of pressure and create moments. In an aircraft, the pitching moment created by the wing is neutralized by a moment produced by the tailplane. In faired submersibles, the body produces a pitching (or yawing) moment that the tail surfaces neutralize. Lift forces are small for bluff bodies, but destabilizing and are not adequately predicted by lift theory.

It must be noted that lift and drag forces are not linear. Although in practice, the hydrodynamics and aerodynamics of vehicles are broken down into a longitudinal and a lateral problem for translating bodies, this is not accurate. The sum of the longitudinal and lateral forces will differ to varying degrees with the actual values. These force problems are broken down into two-dimensional problems for the sake of simplicity. In general, reasonably

accurate results are obtained for angles of incidence and yaw below 12°.

2.6 For Spherical Vehicles.

Vehicles with spherical shapes have no lift force, only a drag force. This force is determined by calculating the Reynolds number,

$$\mathrm{Re} = \frac{Ud}{\nu} \tag{2.44}$$

and then from figure 2-9 finding the corresponding drag coefficient C_D. The drag force D is then,

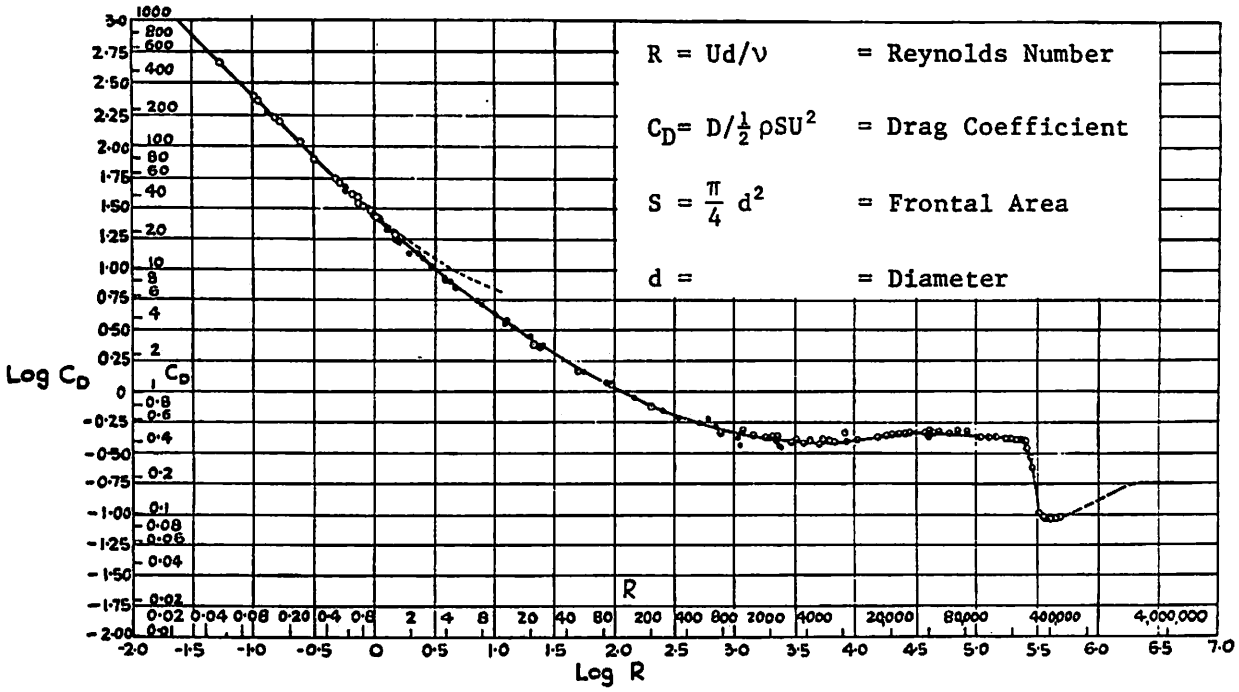

Figure 2-9: Drag Coefficient of a Sphere.

$$D = 0.5\rho S U^2 C_D \tag{2.45}$$

$S = \frac{\pi}{4} d^2$ where d = diameter of sphere.

For a spherical vehicle rotating in a fluid, the drag can be assumed to be equivalent to the flat plate frictional drag for a plate whose area is πd^2 and length is πd. The Reynolds number is given by,

$$Re = \frac{\dot{\theta} d^2}{\nu} \tag{2.46}$$

where $\dot{\theta}$ is the rotational speed. Using the previous relations for C_F, the damping moment due to drag M_D is,

$$M_D = 0.5\rho S \{\dot{\theta} d\}^2 C_F \frac{d}{2} \tag{2.47}$$

$S = \pi d^2$

Although this is an approximation it should provide reasonable values.

2.7 For Box-Shaped Vehicles.

Box-shaped vehicles are bluff bodies. Flows around these bodies are not adequately described by theory. Few references exist on three dimensional bluff bodies and the main reference used is Nakaguchi. [61] In refernce [61], the results of tests of box-shaped bodies with square cross-sections are presented for lift, drag and pitching moment as a function of angle of incidence. These results were obtained at Reynolds number of 1.7×10^5. In order to use the drag data (C_{D_T}), the frictional drag coefficient has to be corrected for. Given,

$$C_{D_T} = C_P + C_F(Re = 1.7 \times 10^5) \tag{2.48}$$

then for a given vehicle the drag C_{D_V} is expressed as,

$$C_{D_V} = C_{D_T} - C_F(Re=1.7 \times 10^5) + C_F(\textit{Reynolds number of vehicle}) \tag{2.49}$$

The lift, drag and pitching moment coefficients are given in appendix . These coefficients can be curve fitted such that,

$$\begin{aligned} C_D &= C_{D_0} + C_{D_1}\alpha^2 + C_{D_2}\alpha^4 \\ C_L &= C_{L_0}\alpha + C_{L_1}\alpha^3 \\ C_M &= C_{M_0}\alpha + C_{M_1}\alpha^3 \end{aligned} \tag{2.50}$$

These results can be assumed to be correct for vehicles with cross-sections that are approximately square. This is applicable to most box-shaped submersibles. The transversal drag force and rotational damping moment can be determined using strip theory. The drag for a two-dimensional rectangular section is given in figure 2-10. The correction factors for translation and rotation of three-dimensional bodies can be borrowed from the section on acceleration coefficients. The friction drag must be added to the pressure drag in order to obtain the complete value for the purely translational drag force and purely rotational damping moment.

2.8 For Cylindrical and Ellipsoidal Bodies.

The configurations that we consider are streamlined body shapes (either cylindrical or ellipsoidal) with control surfaces. There are two possible tailplane configurations, we consider the single vertical fin with a horizontal

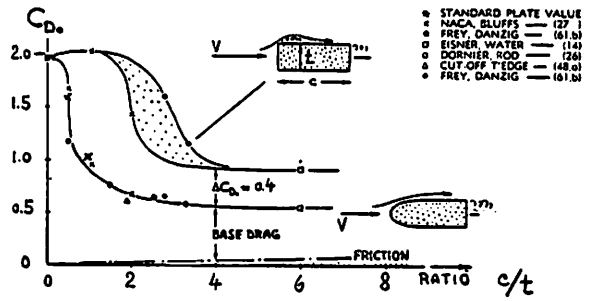

Drag coefficient of "rectangular" sections (tested between walls) with blunt leading edge (upper part) and with rounded shape (lower part), against length ratio.

Figure 2-10: Rectangular Section Drag [33].

tailplane and a horizontal tailplane with vertical fins at each end. In addition, the possibility of adding a bowplane is also considered. The methods for obtaining the drag force, the lift induced drag force, the lift and pitching as well as the lateral forces and moments.

2.8.1 Drag

For streamlined body, the drag coefficient, based on cross-sectional areas is given by [33],

$$C_{D_o} = C_f \{ 3(l/d) + 4.5(d/l)^{0.5} + 21(d/l)^2 \} \quad (2.51)$$

where,

C_f = coefficient of frictional drag.

l = length of body.

d = minimum diameter of maximum cross-sectional area.

For wings and stabilizers the sectional drag coefficient C_{D_s} is given by,

$$C_{D_s} = 2C_f \{ 1 + 2(t/c) + 60(t/c)^4 \}$$

$$D = q_\infty \, S \, C_{D_s} \tag{2.52}$$

where,

C_f = flat plate frictional drag.
t = thickness of surface section.
c = chord of surface section.
S = surface area of section.
q_∞ = dynamic pressure.

In addition to the section drag of the stabilizers, there is interference drag in the corners, where the tail meets the body, and at the tip of the stabilizer. When a wing adjoins a wall or an end plate there is interference drag, ΔD, due to corners. This is given by [34],

$$C_{D_C} = \frac{\Delta D}{q_\infty \, c^2} = 0.85 \left(\frac{t}{c} \right)^3 - 0.0003 \tag{2.53}$$

The wing-tip drag at the tip of a single surface is given by [34],

$$C_{D_C} = \frac{\Delta D}{q_\infty \, c^2} = 0.075 \left(\frac{t}{c} \right)^2 \tag{2.54}$$

To complete the determination of the drag coefficient for the submersible in forward motion, the drag due to the lateral (or vertical) tunnel thruster duct openings must be included. For carefully faired duct openings, the average drag coefficient is $C_D = 0.07$ [43] where,

$$D_{duct} = C_D \, q_\infty \, A \tag{2.55}$$

A = duct cross-sectional area.

D_{duct} = drag added by duct opening.

The drag for both transversal and rotational maneuvers can be estimated by using strip theory where the drag for a two-dimensional ellipse is given by,

$$C_{D_o} = 2\, C_{f_{lam}} (1 + c/t) + 1.1(t/c) \quad \text{(laminar flow)}$$
$$C_{D_o} = 2\, C_{f_{turb}} (4 + 2\, c/t) + 120(t/c)^2) \quad \text{(turbulent flow)} \tag{2.56}$$

The correction factors (Lamb's inertia coefficients) k_2 and k' can be used to correct for three-dimensional effects.

The drag due to the surfaces can be calculated as the drag due to flow normal to a flat plate. For the case of a surface attached to a body its width to height ratio is taken as a surface with twice its given height. The drag coefficient $C_{D_{FP}}$ for flow normal to a flat plate is given by,

$$C_{D_{FP}} = 1.18 + e^{-15.72(h/w + 0.0127)} \tag{2.57}$$

h = height of plate.

w = width of plate.

The payload's section drag in steady motion can be estimated as C_D = 0.7 to 0.85 . In addition, an interference drag section coefficient of 0.3 must be added. This interference drag corresponds to the case of a bomb suspended below a fuselage.

$$D_P = q_\infty \{ C_D + 0.3 \} A_p = \text{drag of payload.}$$
$$A_P = \text{cross-sectional area of payload.} \tag{2.58}$$

2.8.2 Induced Drag

This is the drag force that acts on the body as a function of the lift and sideforces. The corresponding lift coefficients are given in the next section. The induced drag of the body, $D_{b\alpha}\alpha^2 + D_{b\beta}\beta^2$,is given as,

$$D_{b\alpha} = 0.5\rho\ U^2\ l^2\ C_{l\alpha}^2\ /\ \pi\ a_b$$
$$D_{b\beta} = 0.5\rho\ U^2\ l^2\ C_{l\beta}^2\ /\ \pi\ a_b \qquad (2.59)$$

The induced drag for the stabilizers is given as,

$$D_t = 0.5\rho\ U^2\ l^2\ \frac{(FA_tG)^2}{\pi a_t}$$
$$D_t = 0.5\rho U^2 l^2\ \frac{(FA_tG)^2}{\pi a_t} \qquad (2.60)$$

Note : The previous drag components are the linear drag components. There are also non-linear higher order terms due to crossflow drag that we are neglecting.

2.8.3 Stability Derivatives.

These are the forces and moments that act on the vehicle when it is at an angle of incidence with respect to the velocity of its center of gravity. In this section, the longitudinal stability derivatives X_u, X_w, Z_w, Z_q, M_w and M_q are determined as well as the lateral stability derivatives Y_v, Y_r, N_v, N_r, K_v and Y_p. Note that the stability derivatives X_q and M_u are generally small enough to be neglected. The three-dimensional problem of lift and sideslip, forces and moments is divided into two-dimensional problems: longitudinal and lateral. As mentioned previously, this approach is not strictly accurate, but

yields acceptable results for angles of attack and yaw below 12 °. Stabilizers and wing surfaces stall at angles of attack of around 15 °.

2.8.3.1 X_u

This is the derivative that depends uniquely on the drag coefficient, such that,

$$X_u = - \rho |U| S C_D \tag{2.61}$$

2.8.3.2 X_w

This is the derivative that depends on the lift coefficientand also the induced drag coefficient. This is the increase in drag that the vehicle is subject to when traveling at an angle of attack.

$$X_w = - 0.5 \rho |U| S \{ C_L - C_{D_\alpha} \} \tag{2.62}$$

2.8.3.3 Z_w

This is the static normal-force derivative and is given by,

$$Z_w = Z_{wo} + Z_{wt} \tag{2.63}$$

Z_{w_o} = static-normal force derivative due to body.

Z_{w_t} = static-normal force derivative due to vertical tail surfaces.

from references [75, 39] , $Z'_{w_o} = -(0.234m'^{0.79} + D')$ (2.64)

$Z_{w_o} = Z'_{w_o}\ 0.5\ \rho\ U^2\ l^2$

l = length of vehicle.

U = resultant velocity of vehicle in steady motion.

$$C_{L_\alpha} = \frac{\partial C_L}{\partial \alpha} = \text{lift-slope.}$$

$$C_{L_\alpha} = L'_w = 0.234m'^{0.79}$$

see references [6, 4, 39].

$$m' = \frac{m}{0.5\rho l^3} = 2\frac{\nabla}{l^3} \tag{2.65}$$

∇ = volume of displaced fluid.

m = mass of displaced fluid.

This method is primarily applicable to bodies of revolution. For the general ellipsoid the value of ∇ is calculated for an equivalent prolate ellipsoid with maximum diameter equal to the vehicle's maximum width [70]. The tail contribution is,

$$Z'_{w_t} = - F A_t G$$

$$F = \frac{2\pi \varsigma_1 \varsigma_2}{1 + 2/a_t} \tag{2.66}$$

F = tail surface lift factor, see references [62, 39]

A_t = effective area of tail surface = $4 b_t^2 / a_t$

G = downwash factor for rectilinear motion.

ς_1 = Weinig's correction factor

$$= \frac{(1 + a/2)\tanh(2/a)}{1 + \tanh(2/a)} \tag{2.67}$$

ς_2 = wake factor

$$= 0.9 \left(1 - \frac{0.6d}{Hb_0} \right) \sqrt{(H^2 - 1)(H + 3)\lambda C_s C_t} \tag{2.68}$$

a_t = effective aspect ratio of tail surface

$$= (a + 2) \left(1 - \frac{R^2}{b^2} \right) - 2 \tag{2.69}$$

a = geometric aspect ratio of tail surface, including intersected portion of body.

b_t = effective span of tail surface.

$$= b \left(1 - \frac{R^2}{b^2} \right) \tag{2.70}$$

b = geometric span of tail surface, including intersected portion of body.

Note, that in the case of a horizontal surface with endplates the flow is assumed to be two-dimensional. This would give the surface an infinite aspect ratio, the wing span is not a meaningful quantity so long as the surface's actual area is known. This also simplifies the relations such as the lift factors. For example, F becomes simply $2\pi \varsigma_1 \varsigma_2$.

R = radius of body.

b = actual semi-span of tail surface.

d = 2R

H = boundary layer shape parameter $\simeq$1.6 (on average)

b_0 = distance from tail surface tip to body.

λ = length to diameter ratio of body.

C_s = surface area coefficient of body alone = $\frac{S}{\ell^2}$

s = surface area of body.

C_t = drag coefficient of body alone.

$$G = 1 - \frac{1}{\pi} \gamma \lambda^2 L_{w_o} \tag{2.71}$$

γ = ratio of downwash angle at tail surface to the downwash angle at the center of body lift.

In Hoerner [35], the value of γ is given as 1.6 for elliptical sections. In general γ must be determined from experimental tests to determine the effect of the body [39] and forward surfaces (i.e. bowplane). Since little information is available for the determination of γ we will assume $\gamma = 1.6$.

If the vehicle is fitted with bowplanes, then G for the tailplane becomes,

$$-Z'_{w_{bp}} = L'_{w_{bp}} = \frac{2\pi\varsigma_1 A_{bp}}{1 + 2/a_{bp}} \tag{2.72}$$

for the following bowplane dimensions.

$\lambda_{bp} = 1 / a_{bp}$

a_{bp} = effective aspect ratio of bowplane (see a_t)

A_{bp} = effective area of bowplane (see A_t)

For the case without bowplanes, $Z'_w = Z'_{w_o} - FA_tG$

For the case with bowplanes, $Z'_w = Z'_{w_o} - FA_tG + Z'_{w_{bp}}$

(This assumes that the downwash due to the bowplanes is negligeable).

It must be noted that since the bowplanes are placed at the front of the vehicle, they are not affected by the vehicle's wake (i.e. $\varsigma = 1$) and there is no significant downwash to affect them.

2.8.3.4 M_w

The static moment derivative, M_w is equal to,

$$M_w = M'_w \; 0.5 \; \rho U^2 \; \ell^3 \tag{2.73}$$

$$M'_w = M'_{w_o} - x_t F A_t G_t + x_{bp} Z'_{w_{bp}} \tag{2.74}$$

x_t = distance from c.g. to tail's c.p.

x_{bp} = distance from c.g. to bowplane's c.p.

$M'_w = M'_{w_o} - x_t F A_t G$ (vehicle has no bowplanes.)

M'_{w_o} = static-moment derivative of body.

$M'_{w_o} = 0.87 \; k \; m'$

$k = k_2 - k_1$ = Munk Moment.

k_2 , k_1 are Lamb's inertia coefficients.

For the general ellipsoid k is given in figure 2-11 [70], the Munk Moment may be approximated by k*.

$k^* = c^* \; k$
c^* = correction factor for general ellipsoid.

In this instance let 2a = length of ellipsoid.
2b = width of ellipsoid.
2c = height of ellipsoid.

then for $2 \geq b/c > 1$, $c^* = (-0.69 \; b/c + 0.715)c/a + b/c$

and for $0.2 \leq b/c < 1$, $c^* = (-0.153 \; b/c + 0.176)c/a + b/c$

These results are accurate to $\pm$ 3 %.

2.8.3.5 Z_q

The rotary normal force derivative Z_q for a vehicle with only a tailplane is given as,

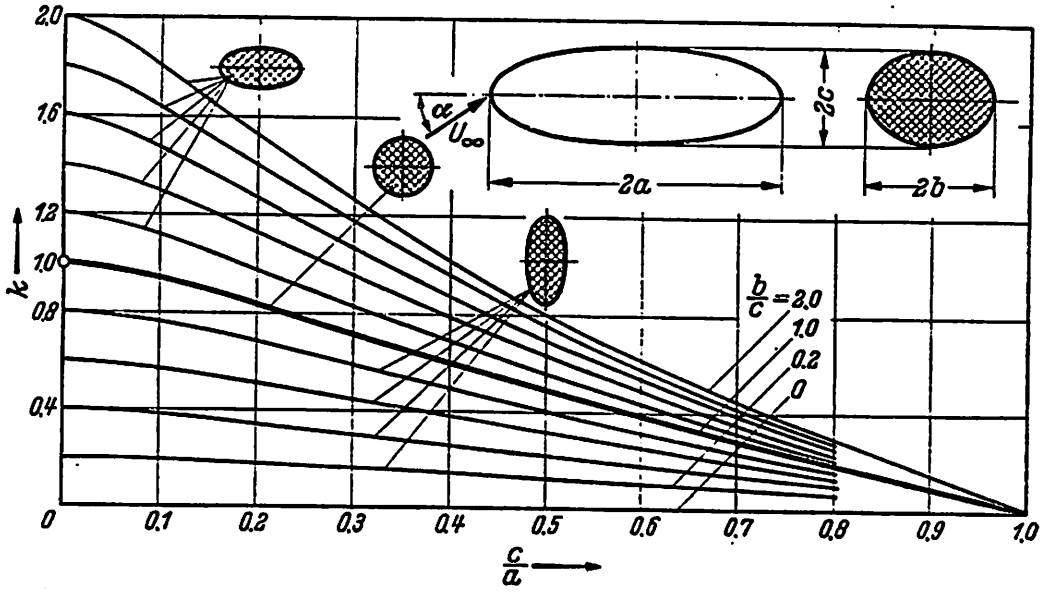

Figure 2-11: Munk Moment k for a General Ellipsoid.

$$Z_q = Z'_q \; 0.5 \; \rho \; l^3 \; U$$

$$Z'_q = Z'_{qo} + Z'_{qt} \qquad (2.75)$$

$$Z'_{qo} = \text{body's contribution} = -(0.10 - k_1) \; m'$$

$$Z'_{qt} = - \; FA_t K$$

$$K = x_t - \frac{0.10}{\pi} \gamma \lambda^2 \; m' \text{ (downwash factor for rotary motion)}$$

For the case of a vehicle with a tailplane and a bowplane,

$$Z_q = Z'_{qo} + Z'_{q_{tb}} + Z'_{q_{bp}}$$

$$Z'_{q_{bp}} = x_{bp} \; Z'_{w_{bp}} \qquad (2.76)$$

$$Z'_{q_{tb}} = - \; FA_t K$$

2.8.3.6 M_q

The rotary moment derivative M_q is given as,

$$M_q = M'_q \, 0.5 \, \rho \, l^4 \, U$$

$$M_q = M'_{qo} + M'_{q_t} + M'_{q_{bp}}$$

$$M'_{qo} = - \, 0.045 \, m' \text{ (body's contribution)} \qquad (2.77)$$

$$M'_{qt} = - \, x_t \, FA_t K \text{ (tailplane contribution)}$$

$$M'_{q_{bp}} = x_{bp} \, Z'_{w_{bp}}$$

The main reference for these derivatives is [39].

For the lateral derivatives Y_v, Y_r, N_v and N_r these are equivalent to Z_w, Z_q, M_w, and M_q respectively. These lateral derivatives can be determined as for the longitudinal derivatives by using the appropriate dimensions and angles. If the center of pressure of the vertical tailfins is not located on the x-axis then there are two additional stability derivatives to consider : K_v and Y_p.

2.8.3.7 K_v

The static roll moment derivative in sideslip K_v, is given as,

$$K_v = K'_v \, 0.5 \, \rho \, l^3 \, U^2$$

$$K_v = y_t \, Y_{v_t} \qquad (2.78)$$

2.8.3.8 Y_p

The static side force derivative due to a roll, Y_p, is given as,

$$Y_p = Y'_p \, 0.5 \, \rho \, l^3 \, U$$

$$Y'_p = K'_v \qquad (2.79)$$

2.9 Thrusters

For submersibles two types of thrusters are considered: tunnel or ducted thrusters and kort nozzles. The use of open propellers is not recommended since they can easily be damaged or become entangled in a tether. The kort nozzle which is a flow-accelerating duct, has a higher overall efficiency than an open propeller, especially for low-speed and high-thrust power requirements. For more specific and detailed information on kort nozzles refer to [43, 68, 19]. Tunnel thrusters are less efficient than kort nozzles due to the viscous losses as well as inlet and diffusion losses. More references for tunnel thrusters can be found in [43]. From reference [43], the thrust to shaft horsepower is given by,

$$\frac{T}{P} = \left(\frac{C^2}{\rho} \frac{A}{P} \right)^{\frac{1}{3}} \tag{2.80}$$

T = thrust in lbs.

P = shaft horsepower.

P/A = Power/Duct area (Hp/ft^2)

ρ = density of water.

C = Static Merit Coefficient.

The static merit coefficient, C, and other necessary data for the determination of thrust as a function of shaft horsepower are given in figure 2-12. Tunnel thrusters are used for maneuvering at low speeds. When the submersible is in motion the jets of lateral or vertical thrusters are deflected and lose their efficiency. In addition, interference between the lateral thrusters and horizontal thrusters is hard to determine and may produce undesirable

characteristics. In the DSRV the aft thruster produced the inverse of the desired side force at certain forward speeds.

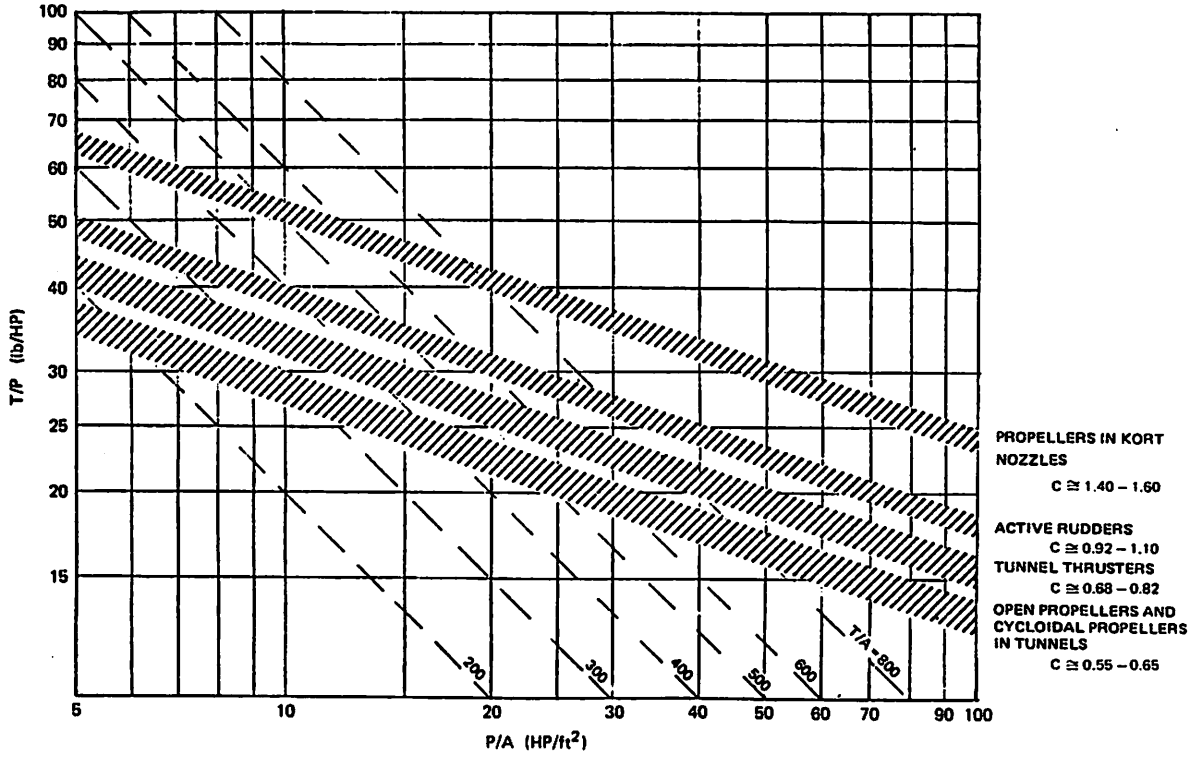

Figure 2-12: Curves of Thrust/Power Ratio versus Power/Area Ratio with Contours of Static Merit Coefficient C .

In figure 2-13, the dimensions of the Innerspace Corporation's thruster models 1001 and 1002 are given. The shaft power requirements are determined from the shaft speed in figure 2-15. The shaft speed is determined from figure 2-16 as a function of thrust. Thus, the power requirements for the thrusters can be determined. In addition Innerspace manufactures automatic tilting screens that increase the thrust by 5 % by generating a fine turbulence in the incoming flow. These screens are used to protect the thruster from any debris.

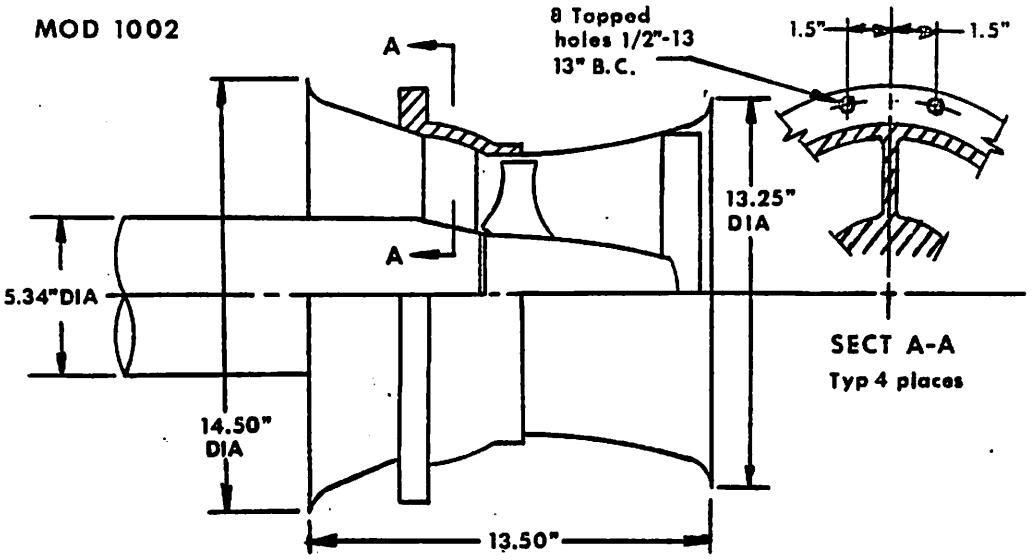

Figure 2-13: Dimensions of Innerspace Co. Thruster models 1001 and 1002.

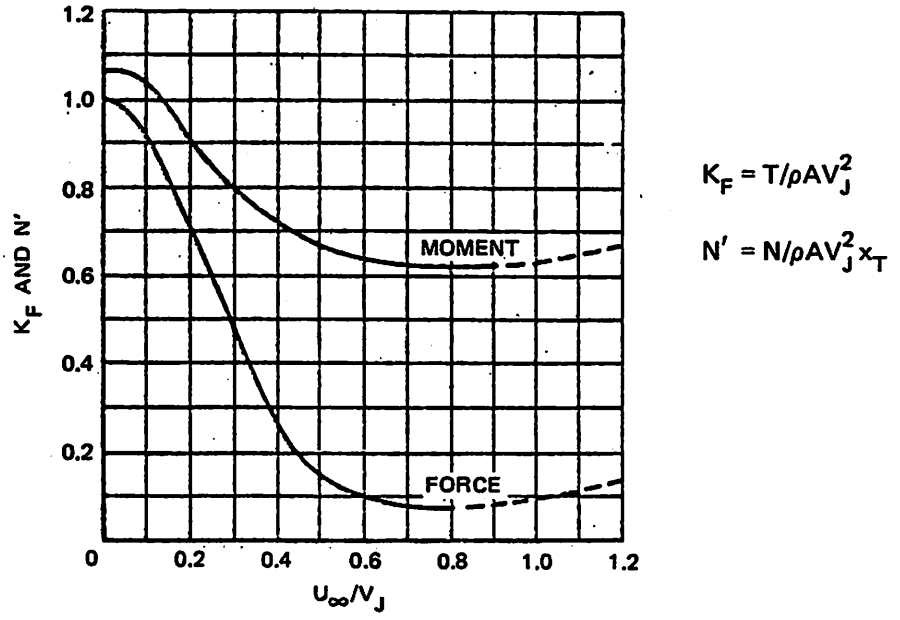

Figure 2-14: DSRV Lateral Thruster Performance as a Function of Forward Velocity.

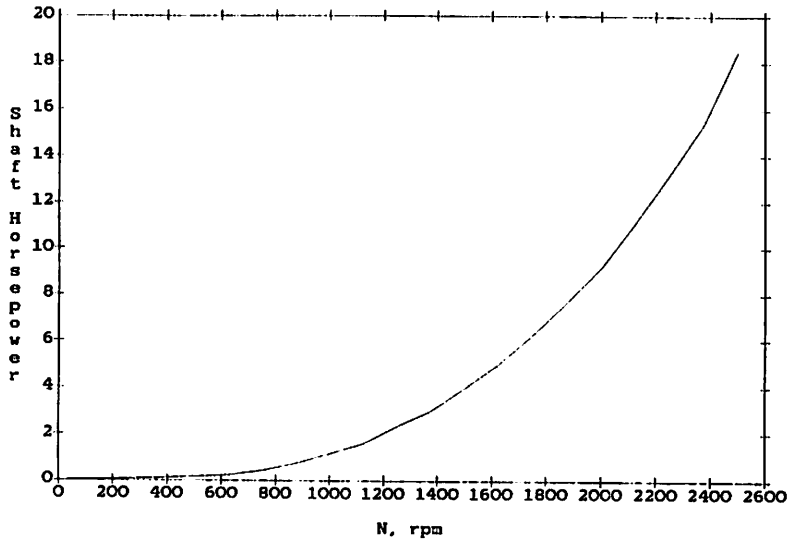

Figure 2-15: Shaft Speed vs. Shaft Power for models 1001 and 1002.

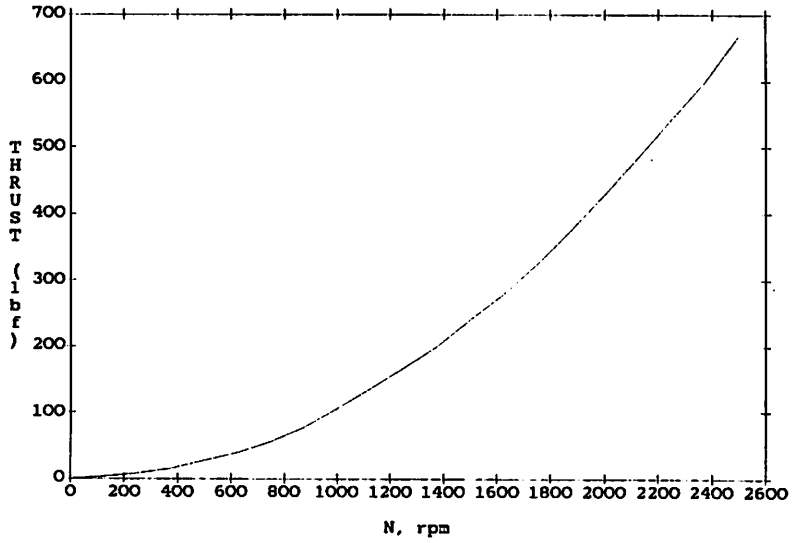

Figure 2-16: Shaft Speed versus Thrust for models 1001 and 1002.

2.10 Control Surfaces

The bowplane vertical and horizontal tail surfaces are used to produce control forces. They are fitted with control flaps to produce these forces. The lift coefficient, C_L, for a wing fitted with control surface is given as, reference [70],

$$C_L = C_{L_\alpha} \alpha + \frac{\partial C_L}{\partial \eta_f} \eta_f \qquad (2.81)$$

η_f = control-surface angle.

$\lambda_f = c_f/c$ = control surface chord ratio.

$$\frac{\partial C_L}{\partial \eta_f} = C_{L_\alpha} \frac{\partial \alpha}{\partial \eta_f} \qquad (2.82)$$

$$\frac{\partial \alpha}{\partial \eta_f} = - \frac{2}{\pi} \left(\sqrt{\lambda_f (1 - \lambda_f)} + \arcsin \sqrt{\lambda_f} \right) \qquad (2.83)$$

Note the theoretical value of $\frac{\partial \alpha}{\partial \eta_f}$ is about 5 % greater in magnitude than the measured values.

2.11 Drag on Unfaired Cables

The normal coefficient C_D of cables over a range of Reynold's Number is given in table 2-I. The effects of strumming can increase the effective drag coefficient by up to 2.5 times. The frictional drag coefficient for cables, C_t, is given in figure 2-17 as a function of Reynold's number. It can be seen that the frictional drag coefficient is much lower than the normal drag coefficient.

Cable (1)	REYNOLDS NUMBER RANGE 10^3-10^4 Minimum (2)	Average (3)	Maximum (4)	Number of tests (5)	10^4-10^5 Minimum (6)	Average (7)	Maximum (8)	Number of tests (9)
Unjacketed stranded steel cable	0.98	1.54	2.47	65	0.30	1.29	3.60	115
Smooth jacketed steel cables	1.16	1.50	1.64	11	0.72	1.14	1.78	24
Synthetic line:								
Braided	1.11	1.14	1.15	3	1.11	1.14	1.16	5
Plaited	0.79	1.17	1.64	15	0.88	0.99	1.15	78

Table 2-I: Normal Drag Coefficients For Cables.

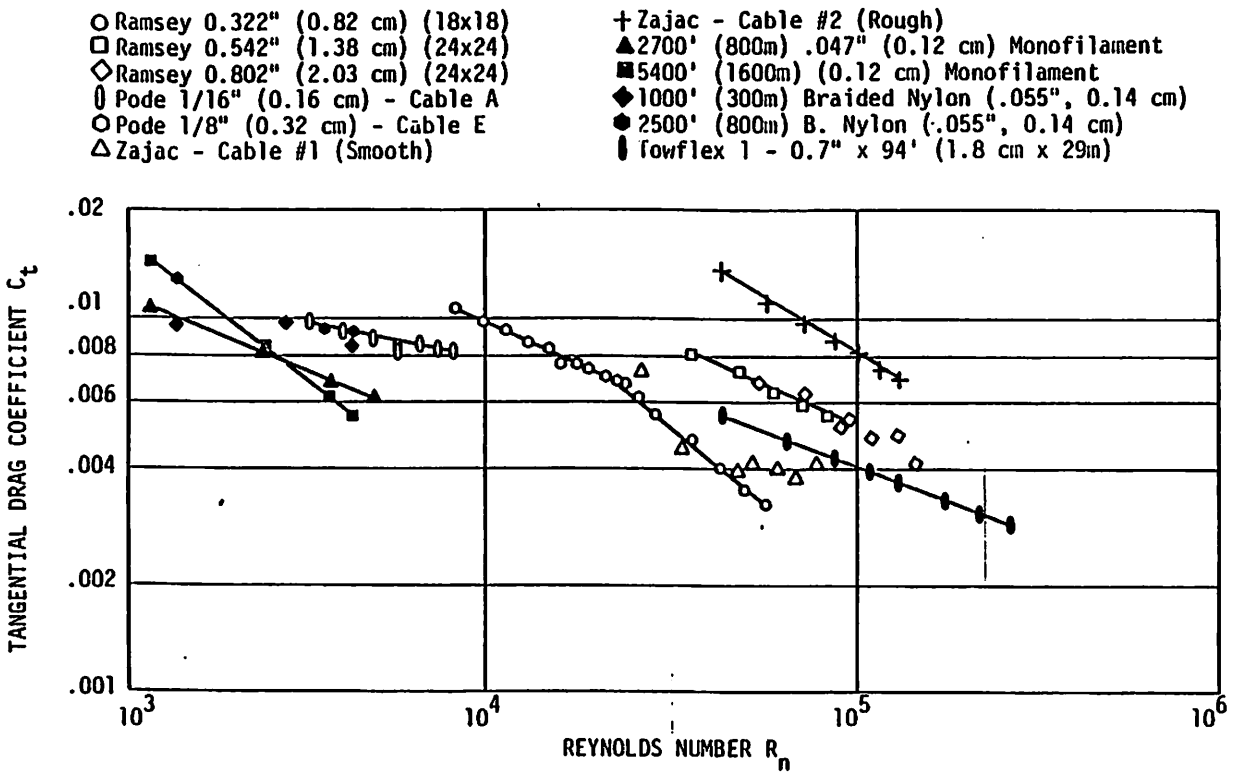

Figure 2-17: Frictional Drag Coefficient vs. Reynolds Number for Various Cable Types.

Chapter 3

The Design Of The Tethered Heavy Lift Submersible.

In this chapter the design for the THLS is presented and discussed. The vehicle's size, configuration and power requirements are determined. In addition, the hydrodynamic characteristics of the THLS are determined with and without payload. The strength of the tether cable is an input. The tether cable size is determined from its required strength, the peak power requirement of the THLS and the density of the tether. Finally, the clump design is presented.

3.1 Submersible Design

The mission requirements of the THLS are rapid deployment and a high maneuvrability, with or without payload. Minimization of the power requirements is an important factor since vehicle size, weight, reliability and tether size are adversely affected by greater power requirements. In order for the THLS to be rapidly deployable, it must be capable of operating in ocean currents. The Gulf stream has surface currents that reach 5 knots ($2.5ms^{-1}$) and these persist to depths of several hundred meters [35]. In addition, there is a deeper counter current that reaches speeds of 0.3 knots ($0.15ms^{-1}$). At great depths, currents reach 0.5 knots ($0.25ms^{-1}$), but have generally much lower velocities. There are areas where, at great depths, the current reaches velocities of 5 knots ($2.5ms^{-1}$), but these are due to the outflows of large rivers such as the Amazon. Thus, it may be important for a THLS to be able to

move at velocities above 5 knots ($2.5ms^{-1}$).

Faired vehicles have much lower drag coefficients (on the order of 0.1 to 0.2) than vehicles with bluff body shapes. The drag coefficient for the latter varies between 0.5 and 2.0. The main advantage of fairing (or streamlining) a vehicle is the reduction in the power requirements. In addition, the hull fairing provides protection for the instrumentation and on-board equipment from collisions . The likelihood of damaging the structural frame in a faired vehicle during a collision is lower.

In open unfaired submersibles, the layout of the instrumentation is extremely flexible. In the present design, four areas have been left empty to provide flexibility in the accommodation of the instrumentation. These are flooded compartement bays, two of which are located at the tips of the nose and tail cone. The other two are located below the submersible's centerline and just after the vertical thruster units. The hull fairing for these compartements is made of acrylic plastic so that cameras and lights may be placed under the fairing. The internal space frame that envelopes the buoyancy and propellant tanks has four attachment points on the submersible's lower hull for the payload. Connecting rods extend from these attachment points and are connected to the payload. The manipulator arms are used to attach or remove the rods from the payload. There is a single mating support on the THLS's upper hull with which it can be lifted. This support is used by the clump to structurally anchor the two vehicles together. These features are shown in figures 3-2, and 3-4.

The minimum size of a THLS is determined from the weight of the flooded variable buoyancy system and the syntactic foam required to keep the

vehicle neutrally buoyant. The material chosen for the spherical buoyancy tanks is titanium and the buoyancy ratio β is 0.57 (See figure 2.1) for a maximum operating depth of 6,000 m (about 20,000 ft). This corresponds to a safety factor of 1.5 or a collapse depth of 30,000 ft. The internal displacement of the variable buoyancy system is equivalent to 4,600 kg of water/1025.9 kg m^{-3} (density of water at 20 °C) or 4.484 m^3. For a titanium buoyancy sphere, the external radius, r_o, is 1.0473 times the internal radius, r_i. The outside diameter of the spherical buoyancy tanks versus the number of buoyancy tanks for an internal displacement of 4.484 m^3 is given in figure 3-1. The maximum internal width of a container is 2.3m and this results in a minimum of eight buoyancy tanks. The buoyancy tanks are evenly distributed around the center of buoyancy as in figure 3-4. Each buoyancy tank has an outside diameter of 1.071 m (or 3.514 ft).

Since the submersible fits into a type 1A container, its maximum weight dry is 24,430 kg. The hydrazine propellant is stored in two spherical buoyancy tanks, each with an internal volume of 0.75 m^3. The internal radius of the hydrazine propellant tanks is 0.564 m and the outside radius is 0.590 m. This corresponds to 1,539 kg of hydrazine propellant. The mass of the two spherical titanium propellant tanks is 1006 kg. The stored propellant can produce up to 4,800 kg of lift, providing a 200 kg lift safety margin. The vehicle's displacement, ∇_t , is broken down as follows,

$$\nabla_t = \nabla_{bt} + \nabla_{sf} + \nabla_{st} + \nabla_{pt} + \nabla_{sw} + \nabla_x \qquad (3.1)$$

∇_{bt} = displacement of the buoyancy tanks.

= 4.484 m^3 × $(1.0473)^3$ = 5.151 m^3

∇_{sf} = displacement of the syntactic foam.

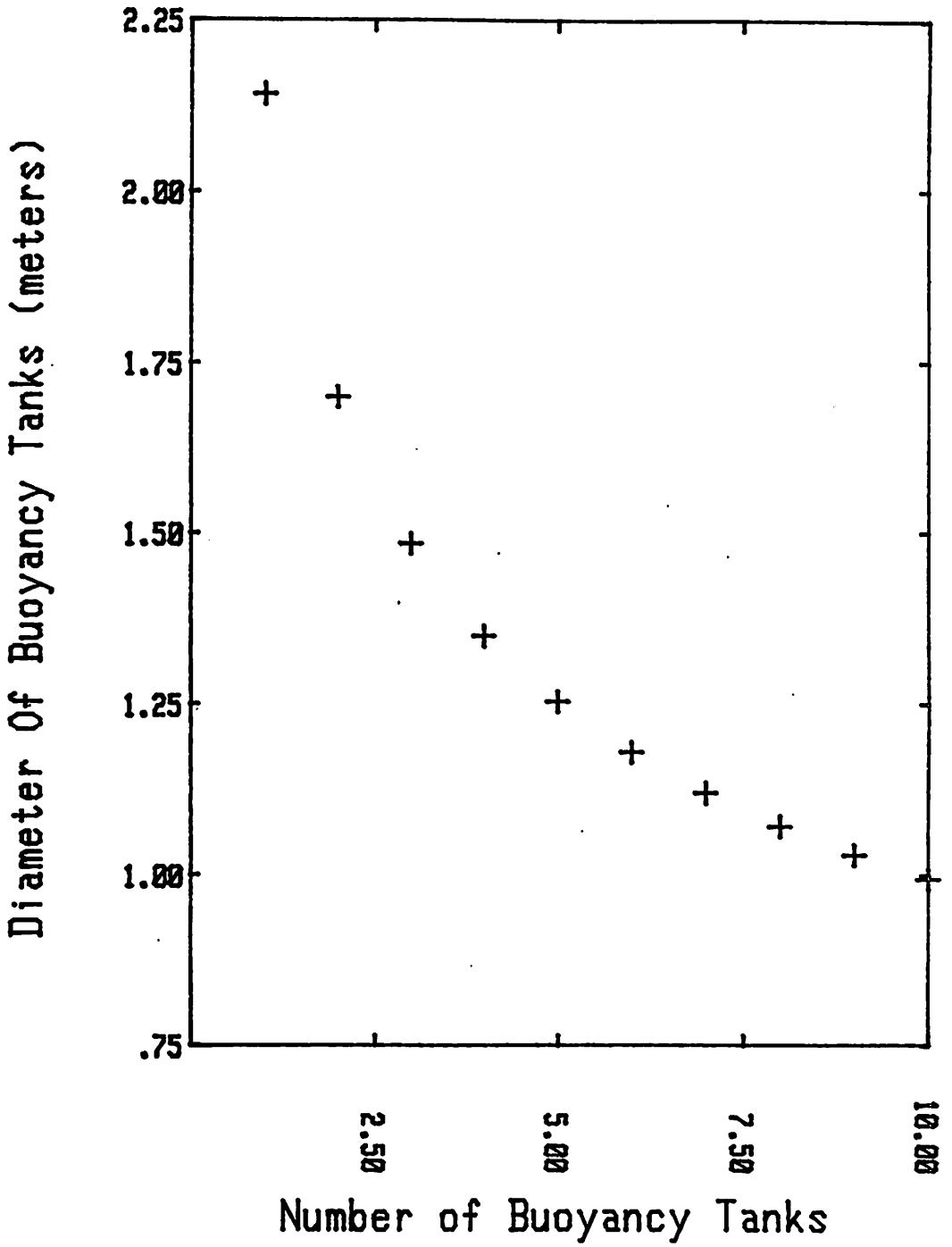

Figure 3-1: Number of Spherical Titanium Buoyancy Tanks versus their Outside Diameter for an Internal Displacement of 4.484 m^3.

∇_{st} = displacement of structure and hull.

= 0.08 ∇_t (estimate).

∇_{pt} = displacement of hydrazine propellant tanks.

= 1.723 m^3

∇_{sw} = displacement of seawater that floods the hull.

= 0.10 ∇_t (estimate).

∇_x = displacement of equipment, thrusters (initial estimate).

= 2.0 m^3

The mass of the vehicle, m_t, is given as,

$$m_t = m_{bt} + m_{wbt} + m_{sf} + m_{st} + m_{pt} + m_{hy} + m_{sw} + m_x \qquad (3.2)$$

m_{bt} = mass of the buoyancy tanks.

= 4510 kg m^{-3} × (5.151 m^3 - 4.484 m^3)

= 3,010 kg.

m_{wbt} = mass of water in the buoyancy tanks.

= 4,600 kg.

m_{sf} = mass of syntactic foam.

= 480 kg m^{-3} × ∇_{sf}

m_{st} = mass of structure and hull.

= 0.15 m_t

m_{hy} = mass of hydrazine propellant.

= 1,539 kg

m_{pt} = mass of the hydrazine propellant tanks.

= 4510 kg m^{-3} × (1.723 m^3 - 1.5 m^3)

= 1,006 kg.

m_{sw} = mass of seawater that floods the hull.

= 0.10 m_t

m_x = mass of equipment, thrusters etc. (initial estimate)

= 4,000 kg.

The equipment is assumed to occupy approximately 2.0 m^3 and have a mass of 4,000 kg. This allows us to make a first estimate of the vehicle's mass and displacement. This involves determining the quantity of syntactic foam required. Equation (3.2) becomes,

$$0.75m_t = m_{sf} + m_{bt} + m_{wbt} + m_{pt} + m_{hy} + m_x \quad (3.3)$$

$$0.75m_t = m_{sf} + 14{,}155 \text{ kg}$$

Equation (3.1) becomes,

$$0.82\nabla_t = \nabla_{sf} + \nabla_{bt} + \nabla_{pt} + \nabla_x \quad (3.4)$$

$$0.82\nabla_t = \nabla_{sf} + 8.874 \text{ m}^3$$

Given $m_t = 1025.9 \text{ kg m}^{-3} \times \nabla_t$ and $m_{sf} = 480 \text{ kg m}^{-3} \times \nabla_{sf}$

This gives $m_{sf} = 6104$ kg.

$\nabla_{sf} = 12.717 \text{ m}^3$.

$m_t = 27{,}012$ kg

$\nabla_t = 26.33 \text{ m}^3$

Clearly these numbers, and the accompanying results in the following chapters represent the final results of what has been an iterative process. The iterative process is illustrated in block diagram form in figure 3-3. Initially the equipment mass and volume are guessed, since they are not known. The

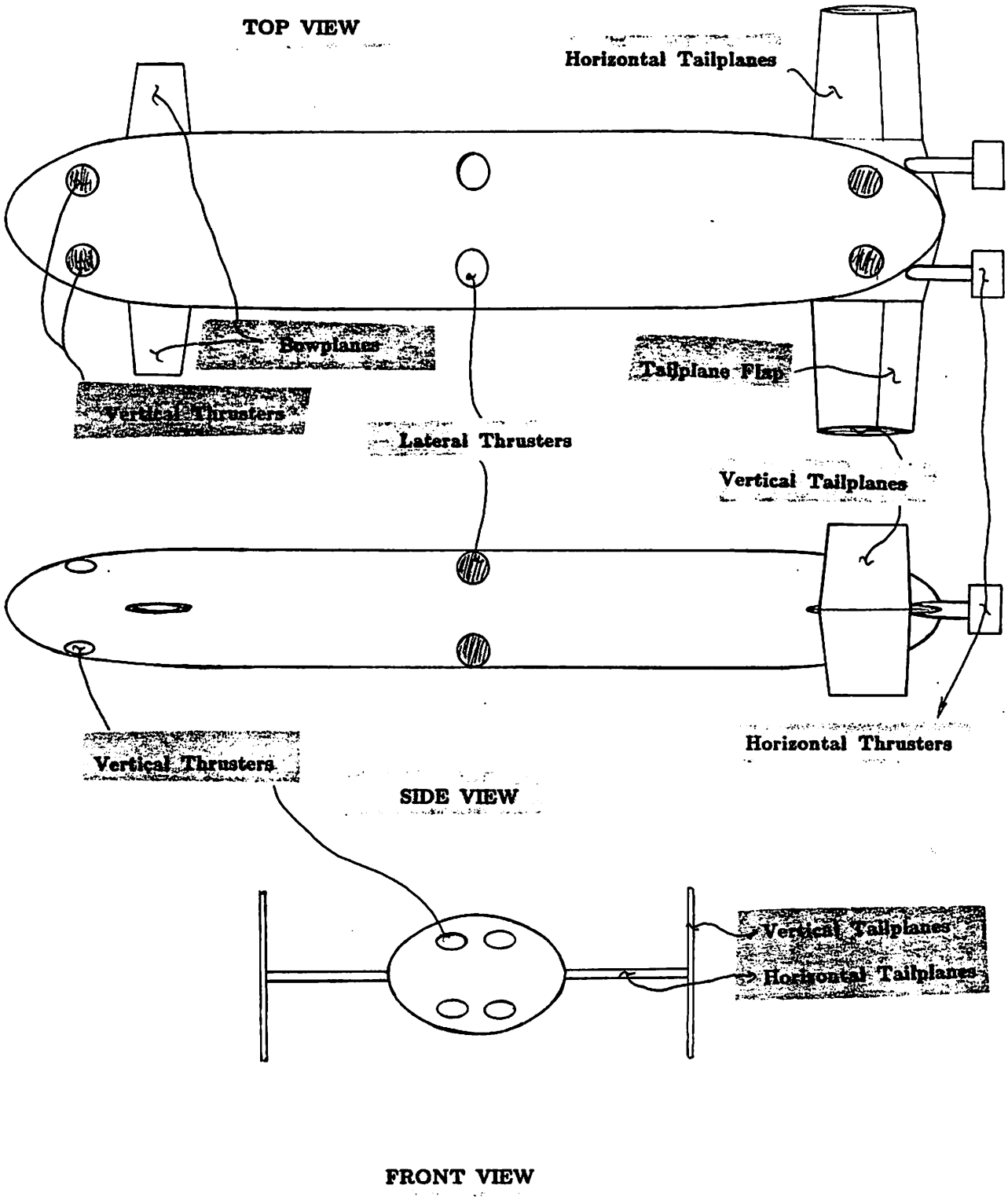

Figure 3-2: Plan views of the THLS design.

mass and volume of syntactic foam required to keep the vehicle neutrally buoyant are determined (see equations (3.3) and (3.4)). The overall vehicle mass and volume is then determined. The vehicle's geometry is defined (for example to fit into a container) and then the thruster requirements are determined. This in turn determines the weight of the main equipment and the amount of additional miscellaneous equipment that it can carry. If this value is not satisfactory then the initial "guess" can now be revised and the whole procedure is repeated. It must be noted that the initial conditions set in equations (3.1) and (3.2) are design specific. They are the result of specific configuration and material choices. Varying these initial conditions will ,of course, modify the final outcome of the design process. Each step of the design process was carried out in, however only the final iteration for each case is presented.

The configuration of the THLS is shown in figures 3-2 and 3-4. The vehicle's dimensions are 7.5 ft (2.286 m) wide, 5 ft (1.524 m) high and 39.226ft (11.956 m) long. The body chosen is fairly streamlined with equally sized ellipsoidal nose and tail cones and a short central cylindrical section . The nose and tail cones are each 11.483 ft (3.5 m) long and the central section is 16.26 ft (4.956 m) long. The vehicle has an elliptical cross-section everywhere. The submersible has a bowplane and a horizontal tailplane with the vertical tailfins at each tip. These surfaces provide forces and moments that allow us to make the vehicle heave, pitch, yaw and roll, as well as stabilize the vehicle. The bowplanes and tailfins are used to provide the control forces during forward motion of the vehicle. The lateral and vertical thrusters are ineffective during forward motion due to the deflection of their jets. For maneuvering the vehicle, there are eight thrusters as shown in figure 3-2. The

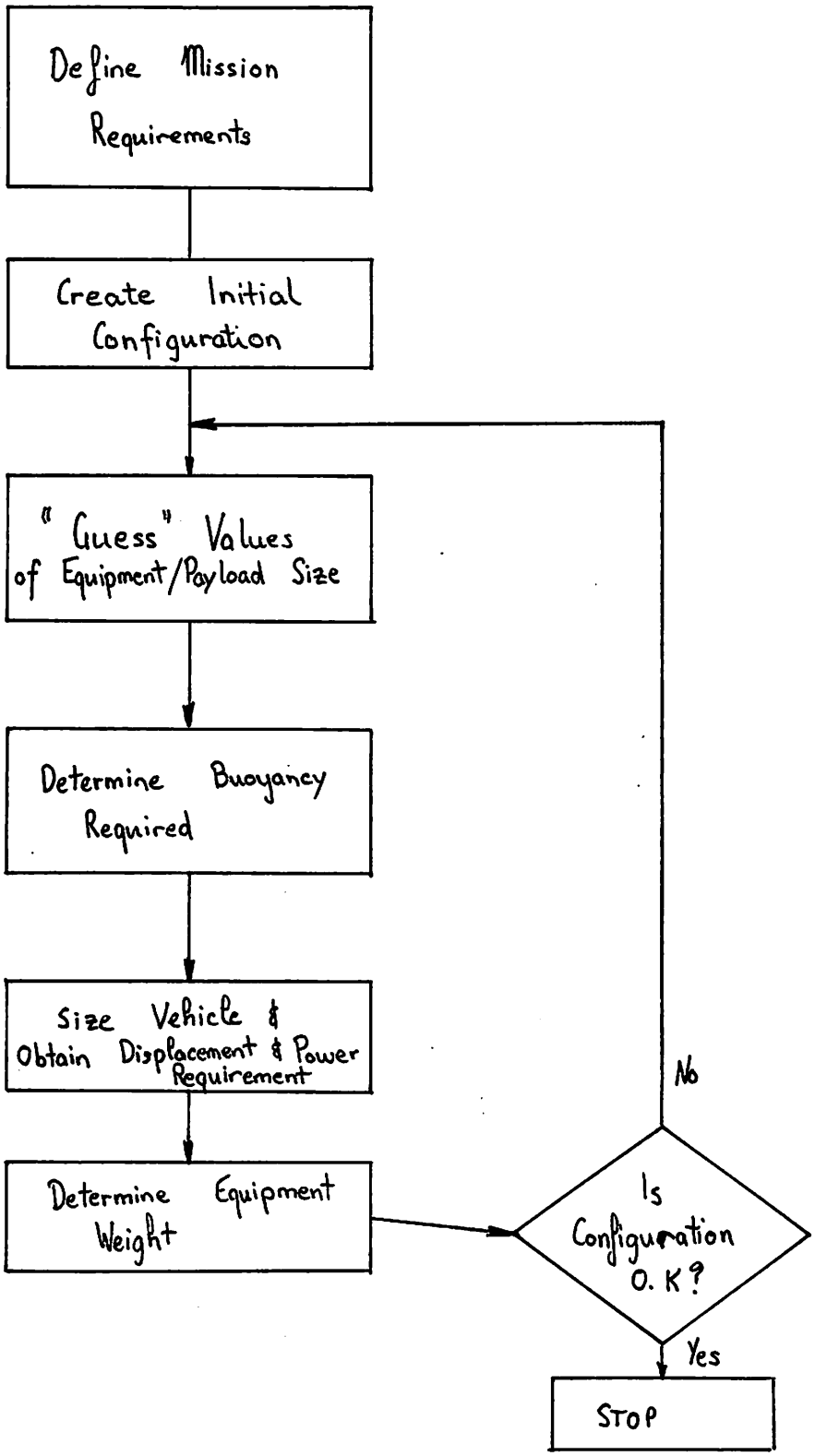

Figure 3-3: Block Diagram of the design process.

two thrusters at the stern provide thrust in the x direction and are used for the translational motion. They can also provide a yawing moment. The two lateral thrusters at amidships can provide a sway force and a small rolling moment. The four vertical thrusters (two at the bow and two at the stern) can provide a heave force and a pitching moment large enough to keep the vehicle and its payload vertical. The two main thrusters (at the stern) are kort nozzles and reduce the vehicle's drag. This is achieved by a suction flow created at the tail cone which delays separation and reduces the vehicle's wake area. This corresponds to a reduction in pressure drag.

If the vehicle's top speed is to be 6 knots (or 3 ms^{-1}) with its payload, then the minimum thrust of the stern thruster can be determined. The vehicle's section drag coefficient at 6 knots is 0.05 . The section drag for our payload is 0.85 . The interference section drag due to the payload suspended under the body is 0.3 (taken from reference [33] for a bomb suspended under a fuselage). The drag force, D, at zero incidence is,

$$\begin{aligned} D &= 0.5\rho V^2 \left(C_{d_v} S_v + (C_{d_p} + C_{d_x}) S_p\right) \\ &= 0.5(1025.9)(3^2)(0.055(\pi 1.143 \times 0.762) + (0.85 + 0.3)(\pi \times 0.762^2)) \\ &= 10{,}379 \text{ N} \end{aligned} \tag{3.5}$$

If the thrusters are oversized by a factor of over 1.7 then each of the stern thrusters is to provide a maximum of 8,822.15 N thrust. Using figure 3-12, the shaft horsepower for kort nozzles are determined. With a static merit coefficient of 1.5 and a power to area ratio of 15 Hp/ft^2, the thrust requirement is 45.65 SHP. The shaft efficiency is 0.99, the hydraulic motor efficiency is 0.9 and the hydraulic pump's efficiency is 0.9. The maximum power required for a horizontal thruster is 55 Hp.

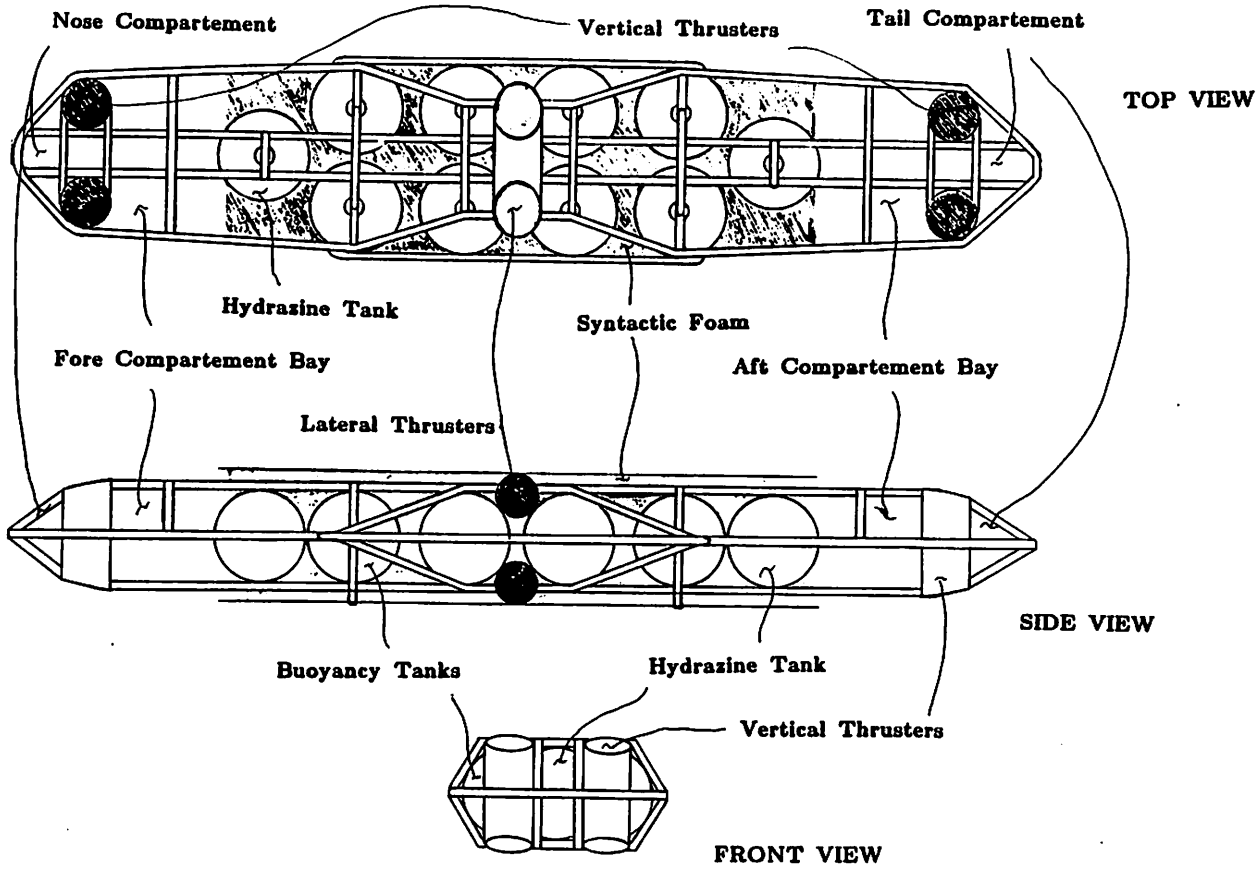

Figure 3-4: Plan views of the THLS internal layout.

The main case of high thrust power requirements is for the four vertical thrusters at the bow and stern. These provide a pitching moment that keeps the vehicle and payload vertical (i.e. the vehicle's horizontal plane is at the vertical). This assumes that the vehicle's center of gravity is set at 0.1 meter below the center of buoyancy and that the payload's center of gravity is at its centroid. Then the thrust required by each vertical thruster, T_v , is given by,

$$4 T_v x_{vt} = g\,(m_t\, y_{cg} + m_p\, y_p) \qquad (3.6)$$

x_{vt} = distance from the center of buoyancy to the center of a vertical thruster.
= 5.0 m.

m_t = total mass of vehicle (buoyancy tanks empty)
= 22,412 kg.

m_p = total payload mass = 4600 kg.

g = acceleration due to gravity = 9.81 ms^{-1}

y_{cg} = distance from c.g. to c.b. = 0.1 meters.

y_p = distance from c.b. to c.g. = 1.9812 meters.

Therefore, T_v = 5,569.5 N.

The vertical thrusters have a maximum thrust requirement of 5,569.5 N, but these must be oversized to allow the vehicle to maneuver in moderate currents while maintaining a vertical attitude. Oversizing the thruster by a factor of 1.2 gives a maximum thrust requirement of 6,683.4 N . The corresponding maximum shaft horsepower provided by each vertical thruster is 57.8 SHP. The vertical thrusters have a minimum diameter of 0.58 m (1.9 ft) and a power to area ratio of 20 Hp/ft^2. The vertical thrusters operating at their maximum thrust require the a.c electric motors that drive the hydraulic pumps to provide 285 Hp. Thus, three 100 Hp a.c electric motors provide sufficient power for the vehicle to maintain a vertical attitude, as well as to position itself in the presence of moderate currents. In addition to the power required by the thrusters, power is constantly required by the equipment and lights. The complete itemization of the vehicle's components, their weight and power requirements is given in table 3-I.

	No	Mass (kgs)	Volume (m^3)	Power Cons. kW
100 Hp A.c. Electric Motors	3	1,489	0.318	223.7
100 Hp Hydraulic Pumps	3	544	0.116	223.7
Horizontal Thrusters (60 Hp)	2	218	0.046	89.5
Vertical Thrusters (60 Hp)	4	435	0.093	179.0
Lateral Thrusters (60 Hp)	2	218	0.046	89.5
Manipulator Arms	2	400	0.156	1.2
High Resolution Sonars	2	46	0.700	0.6
Emergency Power Supply (100 kWh)	1	182	0.050	-------
Additionnal Equipment	--	486	0.475	20
Totals	--	4,000	2.000	244.3

Table 3-I: Main Components of the THLS.

The initial estimates allow for 468 kg of additional unspecified equipment with a displacement of 0.475 m^3. Equipment that has not been specified in terms of weight and displacement includes :

- electrical power conditioning system.
- remainder of the hydraulic power system (such as the valves, the power bottle, the filters, and the interconnecting tubing).
- electronic instrumentation and the associated containment vessels.

- sensors (imaging, inertial, etc ...)
- lights
- emergency radio and light beacons.

This represents the preliminary design of the THLS. The next steps would be to design the components of the submersible and to determine more precisely their mass, displacement and power requirements. The design procedure to determine the overall vehicle mass, displacement and power requirements is then repeated. This is an iterative process that converges on a design solution when the detailed component designs are completed.

3.2 Cable Design

The cable is to transmit up to 245 KW at 44,000 V at 60 Hz as well as survive emergency loads of 10,000 lbs (or 44,480 N). Note that the high voltage requirement is a result of the low current capacity and the high power requirement. It is assumed that in practice the 2.3mm cross-linked polyethylene dielectric provides adequate protection against high voltage breakdown. This is based on the high a.c. voltage breakdown capacity of the polyetylene which is approximately 50 kV/mm. The effect of constant cable flexure may adversely affect this value, but this effect has not been assessed due to a lack of information. Furthermore, the effect of the sea environment on the cable may alter these characteristics. Thus, the method presented to obtain a cable design should provide a reasonable estimate, but should not be taken as a final design.

In addition, the tether has three optical fibers for data transmission. The present cable design provides a good insulation between the power

conductors. The power and signal conductors are protected from the environment by the outer cable layers in which the Kevlar tension members are located. This cable layout provides the best way of shielding the power and signal lines, but not necessarily the best protection of the tension members. The main operational requirements for the tether cable are,

- Positive buoyancy at 6,000 m to avoid entanglement with the submersible or seafloor.
- A minimum diameter to reduce hydrodynamic drag.
- High flexibility to reduce bending loads at winch.
- Ultimate strength of 10,000 lbs (or 44,480 N) for emergencies. (Usual loads are 1125 lbs or 5000 N)

The reason for choosing a *slightly* buoyant tether cable is that it forms virtually a straight line between the submersible and clump in the absence of a current. This reduces the amount of cable that is required as well as the amount that could get tangled up. The major sources of loads on the cable are due to the cureents and to the cable tension maintained by the clump. The summary of the dimensions of the cable components are given in table 3-II. The calculation of the current capacity, using equation (1.3), gives a maximum current rating of 5.63 amperes at 60 Hz for the cable (using data from chapter 2). The ambient seawater temperature is taken as 20°C. The resulting cable characteristics are listed in table 3-III.

The location of the cable on the submersible is chosen so as to minimize two different factors; cable entanglement and the cable disturbance force on the vehicle. The location chosen for the THLS is directly above the vehicle's centers of buoyancy and gravity. The closer the tether cable connection is to

	Material	Specific Gravity	Outer Diameter(in.)	Cross Section Area (sq. ins.)
Power Conductors				
- Wires *(7 AWG)*	Aluminum	2.70	0.145	0.049539
- Insulating Jacket	XLPE	0.92	0.328	0.203950
- Metal Screen	Aluminum	2.70	0.348	0.031856
Optical Fibers				
- Core	Glass	2.55	0.005	0.000150
- Jacket	TPR 2000	0.89	0.015	0.000471
General Cable Void Filler	PE Grease	0.85	-------	0.155912
Cable Sheath	Aluminum	2.70	0.760	0.011860
Sheath Binding Tape	Polyester	1.375	0.762	0.002391
Cable Bedding	Syntactic Foam	0.58	0.900	0.180136
Binding Tape	Polyester	1.375	0.902	0.002831
Load Bearing Members				
- Tension Members (24)	Kevlar49	1.45	0.958	0.059112
- Void Filler	PE Grease	0.85	-------	0.022695
- Binding Tape	Polyester	1.375	0.960	0.003013
Cable Jacket 1	Syntactic Foam	0.58	1.032	0.112645
Cable Jacket 2	TPR 2000	0.89	1.100	0.113864

Table 3-II: Dimensions of the Tether Cable Components.

its center of the body coordinate system the smaller the pitching moment it will create. The disturbance forces on the THLS due to the cable are a function of the cable's tension. The cable tension is required to keep the cable from coiling and getting entangled.

Parameter	Tether Cable
Physical	
- Diameter (m)	0.02794
- Length (m)	1,200
- Mass in Air (kgs/1000 m)	619.37
- Mass in Water (kgs/1000 m)	9.626
- Specific Gravity	1.0102
- Cable Load at First Member Break (lbs)	10,640
Electrical	
- Resistance (ohm/1000 m)	
- Core	1.214
- Shield	1.346
- Loop	2.560
- Capacitance (pF/1000 m)	204.2
- Maximum Current (amps)	5.634
- Operating Voltage (kV)	44
Communications	
- Bandwidth (MHz)	150

Table 3-III: Properties of the Tether Cable design.

3.3 Clump Design

The clump is an intermediate vehicle that is lowered to a depth of a few hundred meters above the sea-floor. The vehicle contains a winch drum which has a diameter of 1 m with a maximum diameter of 1.45 meters and a width of 1.5 m. The overall clump layout is shown in figure 3-5. In addition, the

vehicle contains a winch motor, the tether cable, pressure housings for the electronics, a cable guidepath and a mating clamp. The weight and buoyancy of these different components are given in table 3-IV. The mating clamp is a device through which the tether cable passes. The mating clamp is used to connect the submersible to the clump and is the only structural link between the two. The clump is sized to fit into a container and is to be used in conjunction with a motion compensating handling systems, see reference [85]. This ensures that the clump remains relatively fixed and does not transmit ship motions to the submersible's tether.

The clump is not neutrally buoyant, and on the contrary it is a heavy vehicle even when submerged. This minimizes the horizontal distance the clump drifts as a result of drag forces on the main cable and also due to the tension on the tether cable. The greater the clump's weight, the less significant these effects are. In addition, by using a steel armoured cable, the main cable can carry much heavier loads. In addition it will hang more closely to the vertical.

	Mass (kgs)	Volume (m^3)
Structural Frame	375	0.083
100 Hp A.c. Electric Motor	500	0.106
Winch Drum	450	0.100
Mating Clamp	50	0.011
Additionnal Equipment	500	0.500
Totals	1,875	0.990

Table 3-IV: Main Components of the THLS Clump.

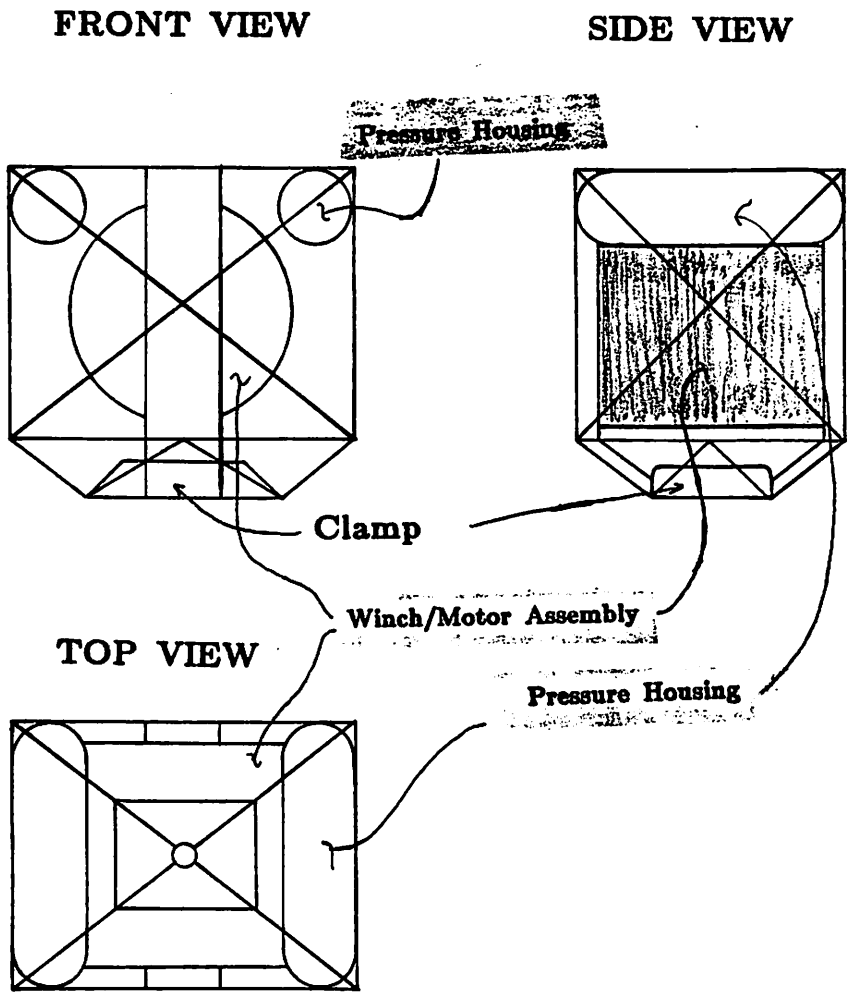

Figure 3-5: Plan views of the THLS Clump design.

Chapter 4

Simulation

In order to assess the performance of the THLS, its motion must be simulated with and without its payload. The simulation of the submersible's motion in three dimensions is extremely complex. In addition to the vehicle's motion, the motion of the tether cable must be considered. The simulation that is carried out in this chapter is the motion of the submersible with and without its payload, from the clump's deployment position to the work site. The trip to and from the work site are simulated in two dimensions, in the presence of ocean currents. In this phase of the submersible's deployment, the cable is constantly being reeled in or out. During this phase the effects of the tether cable on the submersible are determined. At the end of this chapter, perturbations are added to the vehicle's motion and the resulting dynamics are presented. In the next chapter, a controller for the vehicle is designed and the simulation, including perturbations, is carried out with the controller. The controller is designed using singular values and gain scheduling. It is designed to eliminate steady disturbance forces , such as the tether cable forces, as well as to make the vehicle insensitive to high frequency dynamic disturbances. First the vehicle's inertial and hydrodynamic coefficients need to be determined.

4.1 Vehicle's Coefficients.

The vehicle's size, in terms of mass and dimensions, has been determined in the previous chapter. The resulting coefficients are presented in table 4-I. These are the coefficients for the case were there is no payload. The vehicle's coefficients are re-calculated to include the effects of the payload. This is done by assuming that the vehicle's height is the combination of its actual height and that of the payload. This method of calculating the coefficients is only a crude approximation to give an idea of the resulting coefficients. In order to obtain more precise values more experimental and/or theoretical information of the effects of a payload on a body are required. The drag coefficient at zero incidence is taken from the previous chapter. The coefficients for the THLS together with its payload are given in the previous chapter. These coefficients are to be used in the simulation that is now derived.

4.2 Motion Simulation

The present simulation of the THLS's motion is limited to the vehicle going between a target worksite and its clump. This simulation is to be carried out in two-dimensions and does not include a simulation of the acquisition or final deployment phase of a payload. The vehicle's motion is simulated as it goes to and from the worksite with and without a payload. The clump is around 300 m off the sea floor and around 800 m down current from the worksite. The chosen ocean conditions include ocean currents and of course the effects of the tether cable. The current profile is a 1 knot current

Submersible Coefficients	Unloaded	Loaded
Added Mass		
A (Kg)	1159.6	1628.1
C (Kg)	66725.8	66725.8
F_z (Kg)	24077.8	24077.8
Q (Kg m)	443314.	451062.
C_{D_o}		
Body	0.2520	0.9853
Bowplane	0.0154	0.0154
Tailplane	0.0127	0.0127
C_{L_α}		
Body	0.9286	0.9286
Bowplane	2.3768	2.3768
Tailplane	3.5544	3.5544
C_{m_α}		
Body	0.7178	0.7178
Bowplane	2.3768	2.3768
Tailplane	3.5544	3.5544

Table 4-I: Coefficient's of THLS with and without payload.

to a depth of 1,000 meters that reduces to a 0.3 knot current in the opposite direction at a depth of 1,200 meters. The reverse current of 0.3 knots persists to a depth of 5,800 meters. It tapers down to a zero velocity at 6,000 meters which is the sea-bottom, see figure 4-1. The main co-ordinate system is located at the clump as in figure 4-2. The location of the clump, worksite and vehicle are defined with respect to this co-ordinate system, as well as the current velocities. The vehicle's motion is defined in a body co-ordinate system and must be transformed to the main co-ordinate system.

The path chosen for the descent and ascent of the THLS is shown in figure 4-2. The path represents a glide slope that the vehicle follows to reach its worksite after having left its clump. The clump is not neutrally buoyant and hangs on its cable. The clump's position in the water is affected by the

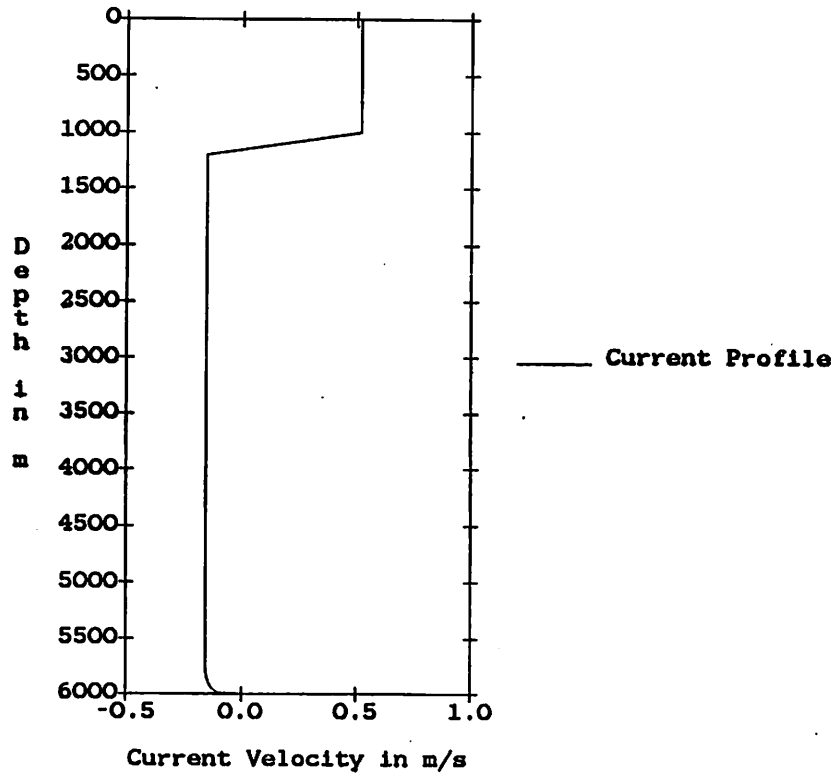

Figure 4-1: The Current Profile Chosen For The Simulations.

currents present. This means that although the support ship may be over the worksite the clump may not. The result is that the THLS is required to compensate for these alignment problems by moving to the worksite. The equations of motion for the THLS, using the body normal co-ordinate system, are derived in the next section. The THLS's horizontal, vertical and pitching velocities are determined through a modified Milne predictor-corrector, known as the Hamming's method. The initial values for this system are determined using a fourth order Runge-Kutta method. These are then converted to the main co-ordinate system and integrated once more to provide the vehicle's location. The results of the simulations are presented in the following figures.

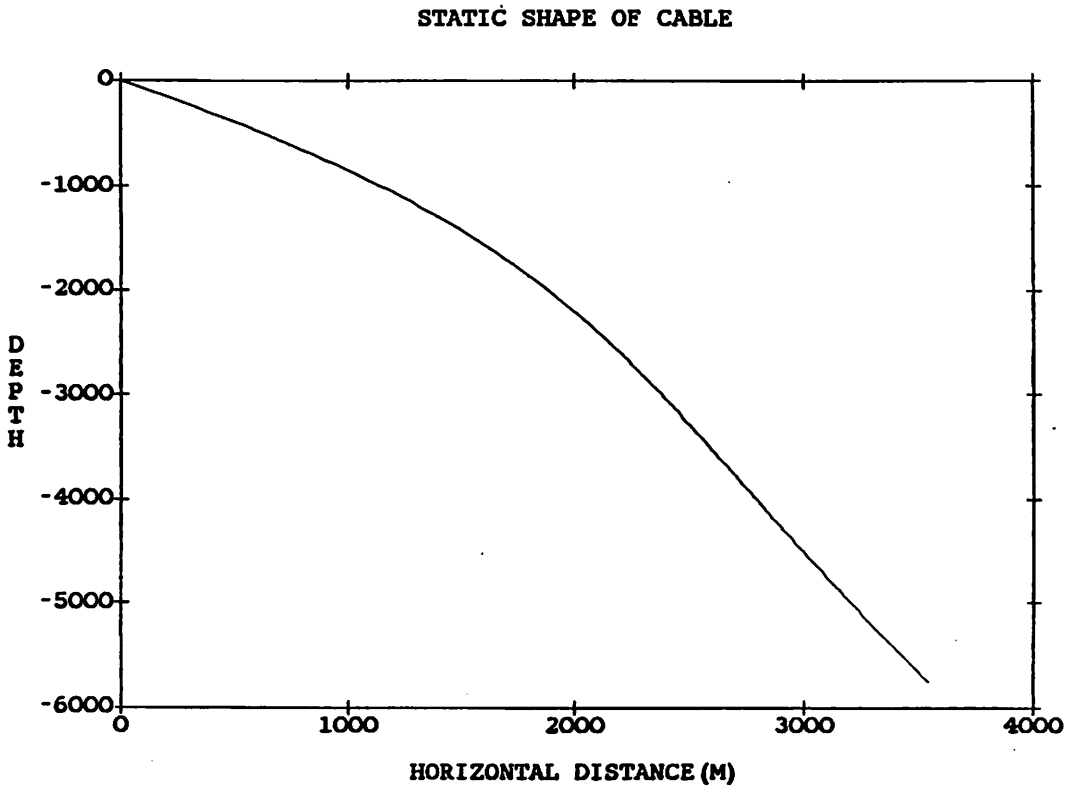

Figure 4-2: Static Shape of the Main Cable Connecting the Clump to the Surface. (*Courtesy of Hyunkyong Shin*)

4.3 The Equations of Motion in the Vertical Plane.

The equations of motion in the vertical plane are represented by two force equations and one moment equation. These equations are composed of the inertial forces, the hydrodynamic acceleration forces, the viscous/circulation forces, the control forces, the cable forces and the gravitational forces. Since the simulation is in the vertical plane, all the out of plane angles, distances, velocites and accelerations are zero. The inertial forces are a function of the vehicle's actual velocity, whereas the hydrodynamic forces are a function of the vehicle's relative velocity in a current. The inertial forces are,

$$X_I = m \left[\dot{u} + qw_i - x_G q^2 + z_G \dot{q} \right]$$

$$Z_I = m [\dot{w} - qu_i - z_G q^2 - x_G \dot{q}] \tag{4.1}$$

$$M_I = I_y \dot{q} + m [z_G(\dot{u} + qw_i) - x_G(\dot{w} - qu_i)]$$

The acceleration forces are (from Appendix A),

$$X_A = X_{\dot{u}}\dot{u} + X_{\dot{w}}(\dot{w} + qu) + X_{\dot{q}}\dot{q} + X_{qw}qw + X_{qq}qq$$

$$Z_A = Z_{\dot{w}}\dot{w} + Z_{\dot{u}}(\dot{u} + qw) + Z_{\dot{q}}\dot{q} + Z_{qu}qu + Z_{qq}qq \tag{4.2}$$

$$M_A = M_{\dot{q}}\dot{q} + M_{\dot{u}}\dot{u} + M_{\dot{w}}\dot{w} + M_{uu}uu + M_{uw}uw$$
$$+ M_{ww}ww + M_{uq}uq + M_{wq}wq$$

where $u = u_i + u_c$, $w = w_i + w_c$, $q = q_i$
u_i, v_i, q_i are the inertial velocities
u_c, w_c are the current velocities in body co-ordinate system (see appendix D)

The viscous/circulation forces are,

$$X_V = X_u u + X_w w + X_q q$$

$$Z_V = Z_u u + Z_w w + Z_q q \tag{4.3}$$

$$M_V = M_u u + M_w w + M_q q$$

The only gravitational term is M_G (see Appendix D for details).
The static cable forces are X_C, Z_C, M_C (see Appendix D for details).

The control forces are,

$$X_{CF} = X_\eta \eta + X_\delta \delta + X_T T$$

$$Z_{CF} = Z_\eta \eta + Z_\delta \delta + Z_T T \tag{4.4}$$

$$M_{CF} = M_\eta \eta + M_\delta \delta + M_T T$$

η = effective angle of attack of bowplanes.
δ = angle of deflection of tailfin flaps.
T = thrust from horizontal thrusters.

The complete equations of motion are,

$$X_I = X_A + X_V + X_{CF} + X_G$$

$$Z_I = Z_A + Z_V + Z_{CF} + Z_G \qquad (4.5)$$

$$M_I = M_A + M_V + M_{CF} + M_C + M_G$$

These become,

$$(m - X_{\dot{u}})\dot{u} - X_{\dot{w}}\dot{w} + (mz_G - X_{\dot{q}})\dot{q} = - mqw_i + X_{qw}qw + X_{\dot{w}}qu$$
$$+ (mx_G + X_{qq})qq + X_u u + X_w w + X_q q + X_\eta \eta + X_\delta \delta + X_T T + X_C$$

$$- Z_{\dot{u}}\dot{u} + (m - Z_{\dot{w}})\dot{w} - (mx_G + Z_{\dot{q}})\dot{q} = - mqu_i + Z_{qu}qu + Z_{\dot{u}}qw$$
$$+ (mz_G + Z_{qq})qq + Z_u u + Z_w w + Z_q q + Z_\eta \eta + Z_\delta \delta + Z_T T + Z_C$$

$$(mz_G - M_{\dot{u}})\dot{u} - (mx_G + M_{\dot{w}})\dot{w} + (I_y - M_{\dot{q}})\dot{q} = - mz_G w_i q - M_{wq}wq$$
$$- mx_G u_i q - M_{uq}uq + M_{uu}u^2 + M_{uw}uw + M_{ww}w^2 + M_u u + M_w w$$
$$+ M_q q + M_\eta \eta + M_\delta \delta + M_T T + M_C + M_G \qquad (4.6)$$

These are re-written dropping all known zero value terms,

$$(m - X_{\dot{u}})\dot{u} + mz_G\dot{q} = - mqw_i + X_{qw}qw + X_{qq}qq + X_u u + X_w w$$
$$+ X_\eta \eta + X_\delta \delta + X_T T + X_C$$

$$(m - Z_{\dot{w}})\dot{w} - Z_{\dot{q}}\dot{q} = - mqu_i - Z_{qu}qu + mz_G qq + Z_u u + Z_w w + Z_q q$$

$$+ Z_\eta \eta + Z_\delta \delta + Z_T T + Z_C$$

$$mz_G \dot{u} - M_{\dot{w}} \dot{w} + (I_y - M_{\dot{q}}) \dot{q} = - mz_G w_i q - M_{uq} uq + M_{uw} uw$$
$$+ M_w w + M_q q + M_\eta \eta + M_\delta \delta + M_T T + M_C + M_G \qquad (4.7)$$

These equations are re-written in the form,

$$\dot{u} = f \{ u_i, w_i, u, w, q, \eta, \delta, T \} + \textit{(cable \& gravitational forces)}$$
$$\dot{w} = f \{ u_i, w_i, u, w, q, \eta, \delta, T \} + \textit{(cable \& gravitational forces)} \qquad (4.8)$$
$$\dot{q} = f \{ u_i, w_i, u, w, q, \eta, \delta, T \} + \textit{(cable \& gravitational forces)}$$

to obtain the values of u, w, and q with the modified predictor corector numerical integration method. These velocities in body normal co-ordinate system are translated to the main co-ordinate system, and a further integration yields the vehicle's position and attitude.

In both of the previous simulations, the control settings for the simulation ,such as the thrust, were calculated at different set points and the values were ramped between these points. The vertical thruster was introduced into the model in order to compensate for the cable tension when the vehicle evolves at low speeds. The model used for the vertical thruster is a simple piece-wise linearization of the DSRV lateral thrusters. The vertical thrust remains constant till a certain forward speed is reached. Then they drop with increasing forward speed until a limiting value for the vertical thrust is reached. This limiting value is the minimum vertical thrust that the thruster will produce. The moment performance of the vertical thrusters has the same characteristics.

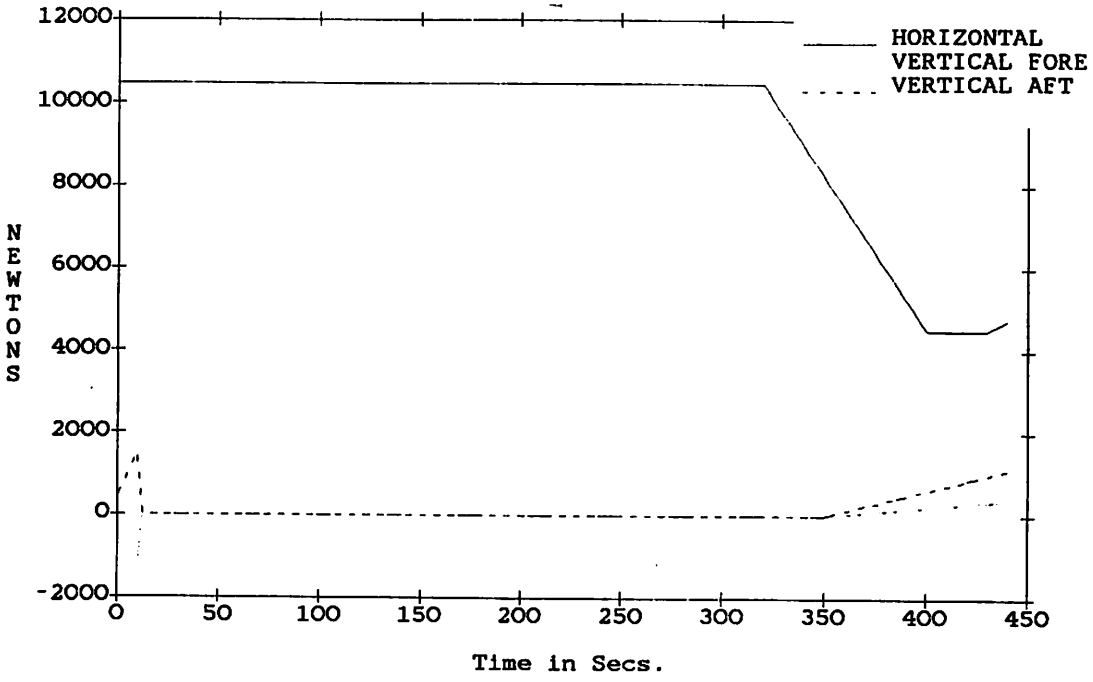

Figure 4-3: Thruster Time History for THLS.

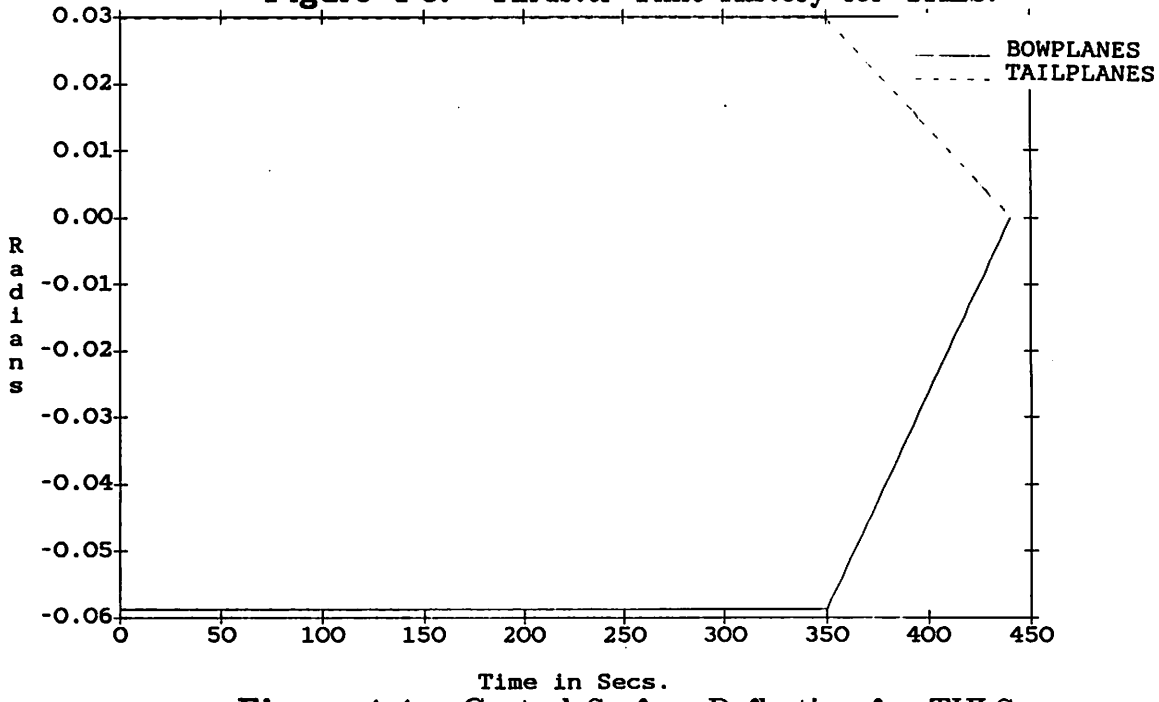

Figure 4-4: Control Surface Deflection for THLS.

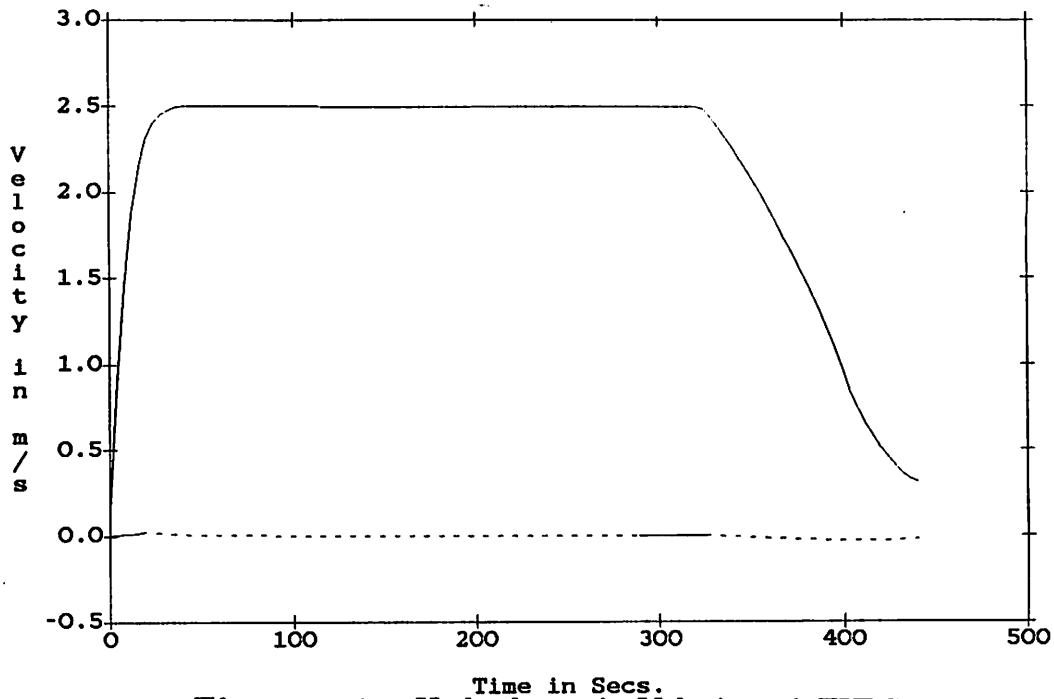

Figure 4-5: Hydrodynamic Velocity of THLS.

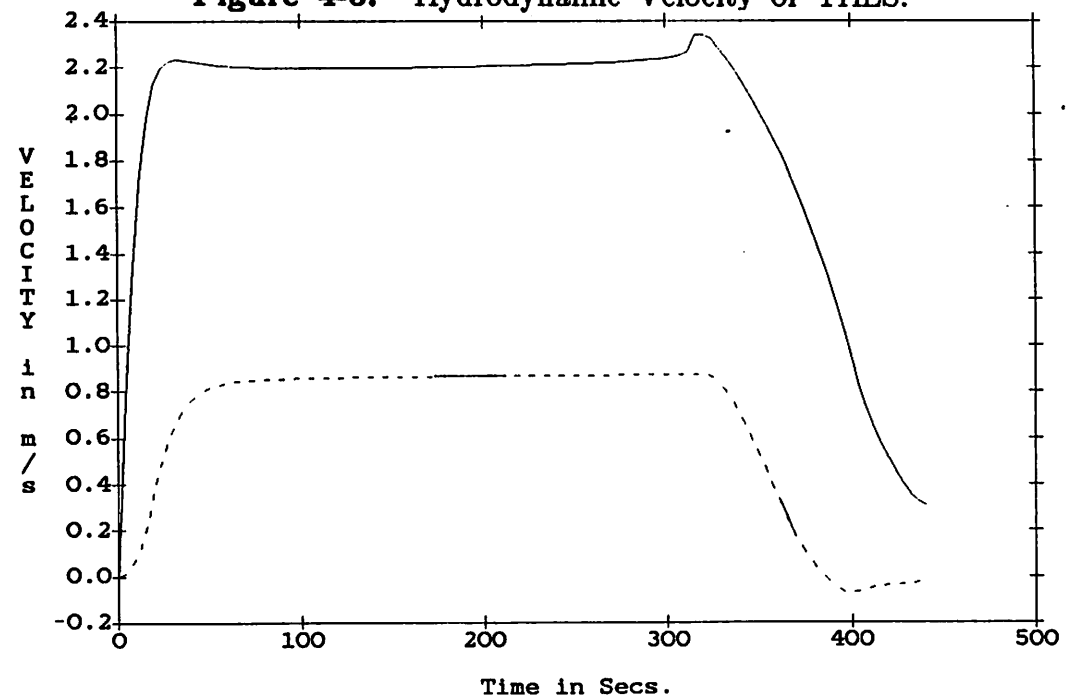

Figure 4-6: Inertial Velocity of THLS.

——— FORWARD
- - - - - DOWNWARD

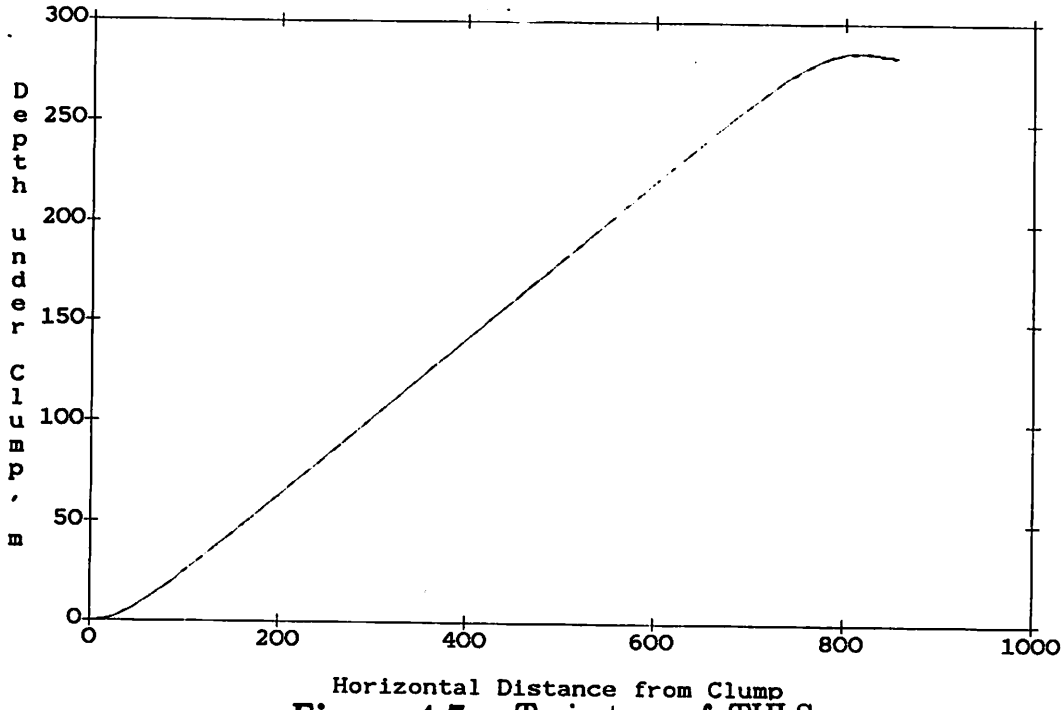

Figure 4-7: Trajectory of THLS.

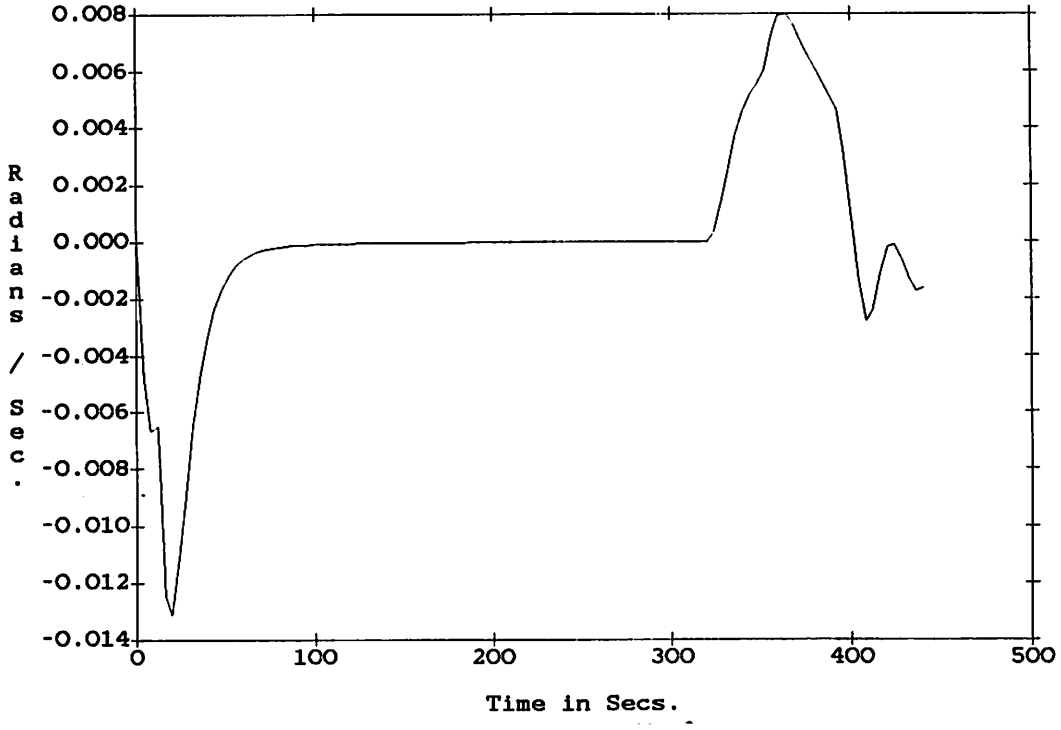

Figure 4-8: Pitch Rate of THLS.

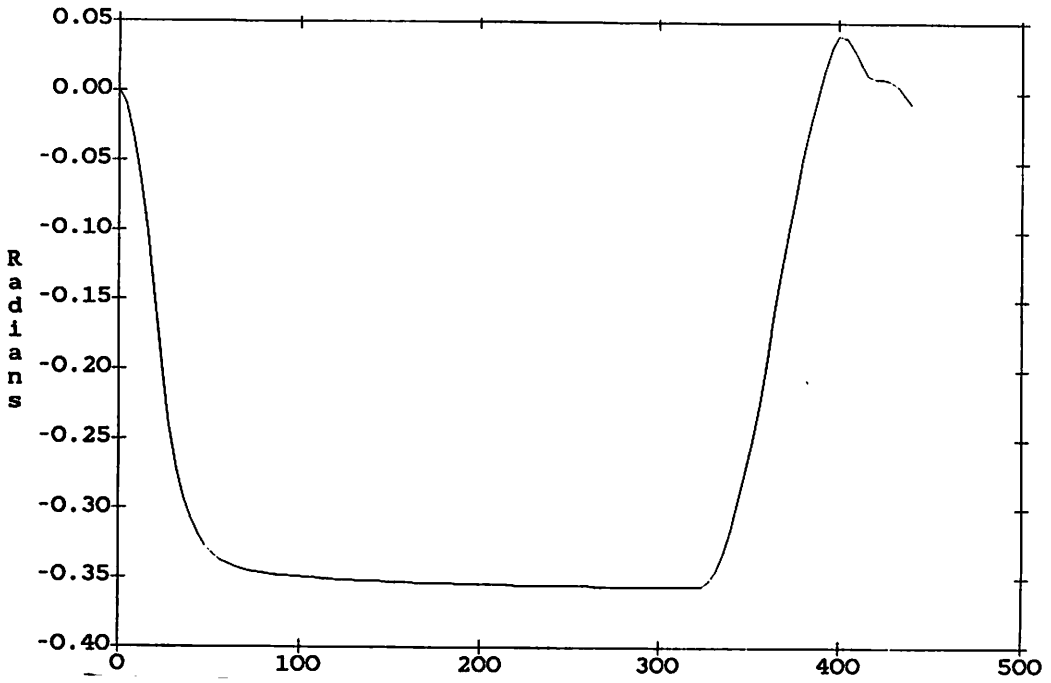

Figure 4-9: Pitch Angle of THLS.

The loaded THLS requires a higher thrust than the submersible alone. This is due to the drag produced by the payload. In addition, the payload drag produces a negative pitching moment on the vehicle and this more than offsets the positive pitching moment due to the cable tension. The loaded THLS does not require vertical thrusters at the start of the dive. Finally, as one would expect the loaded THLS is more sluggish and decelerates faster than the empty submersible. Its pitch response is lower than the unloaded case, but it oscilates more and this is due to the higher effective inertias of the loaded vehicle.

4.4 Simulation with Perturbations

In order to assess the effect of dynamic disturbances on the vehicle, small sinusoidal perturbations are added to the horizontal, vertical and angular velocity components. These perturbations are used to derive state equations.

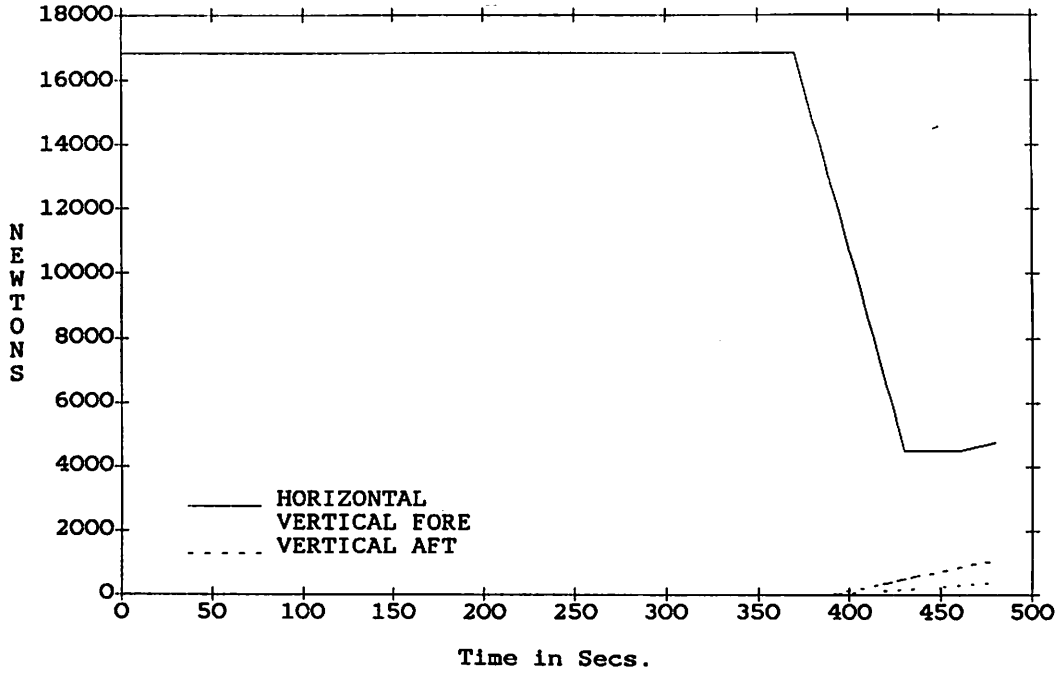

Figure 4-10: Thruster Time History for THLS and PAYLOAD.

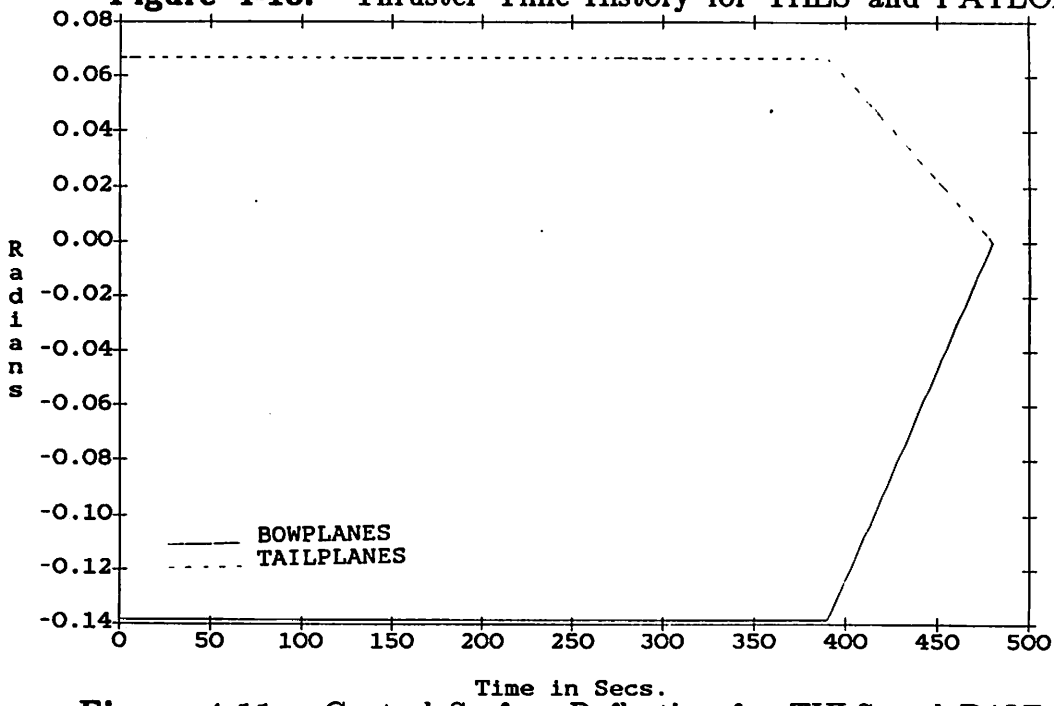

Figure 4-11: Control Surface Deflection for THLS and PAYLOAD.

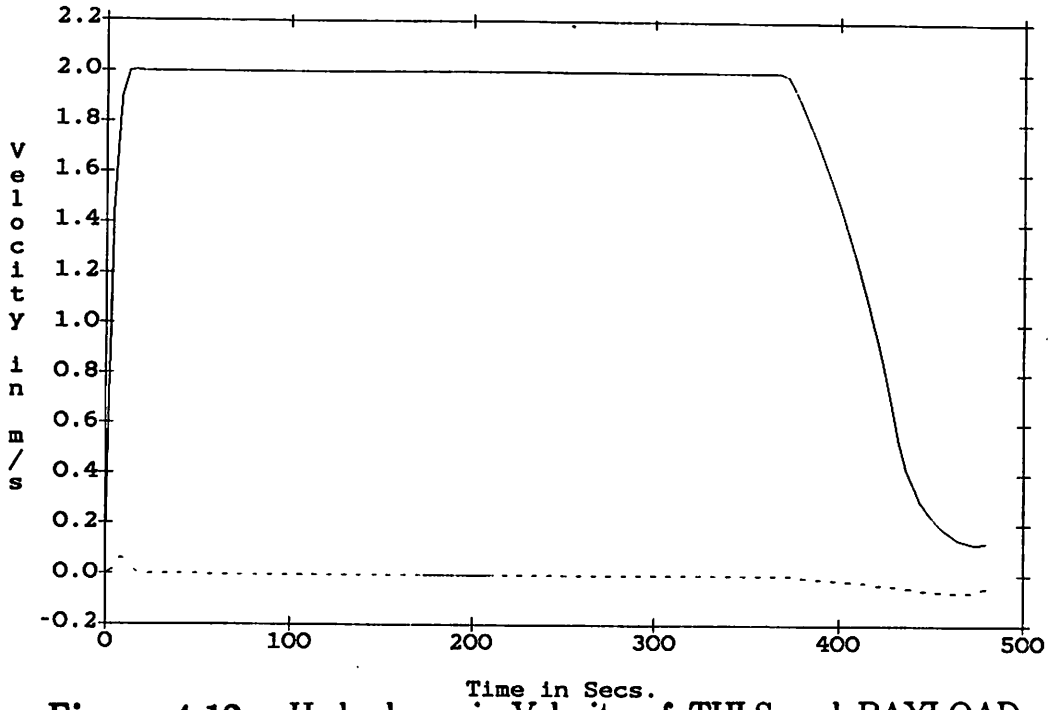

Figure 4-12: Hydrodynamic Velocity of THLS and PAYLOAD.

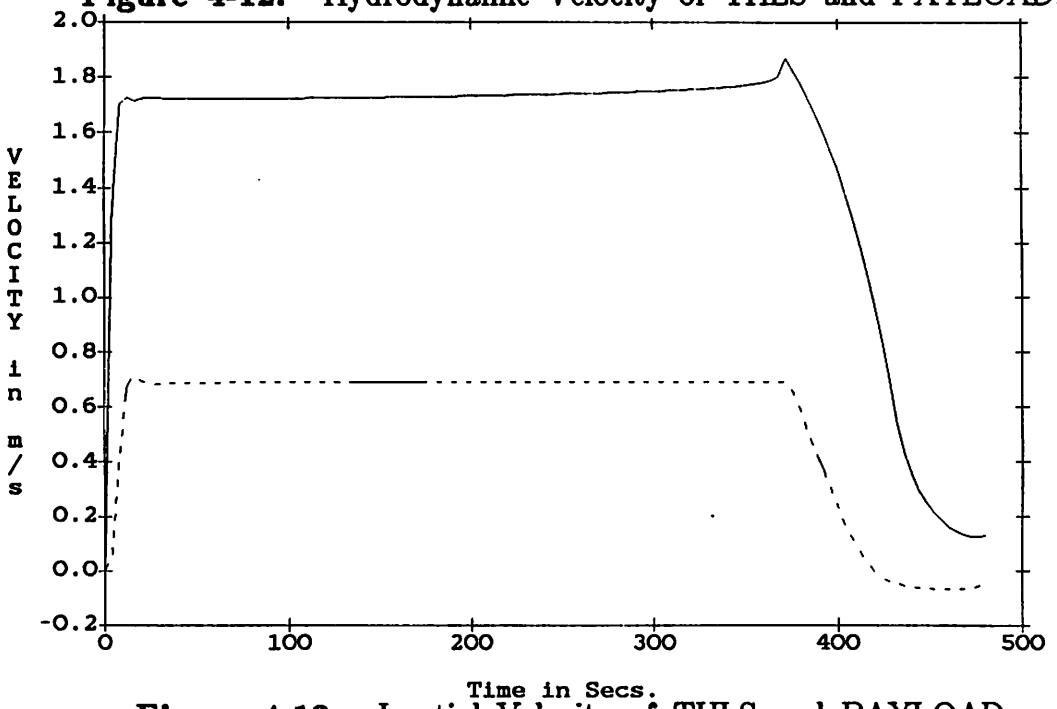

Figure 4-13: Inertial Velocity of THLS and PAYLOAD.

——— FORWARD
- - - - - DOWNWARD

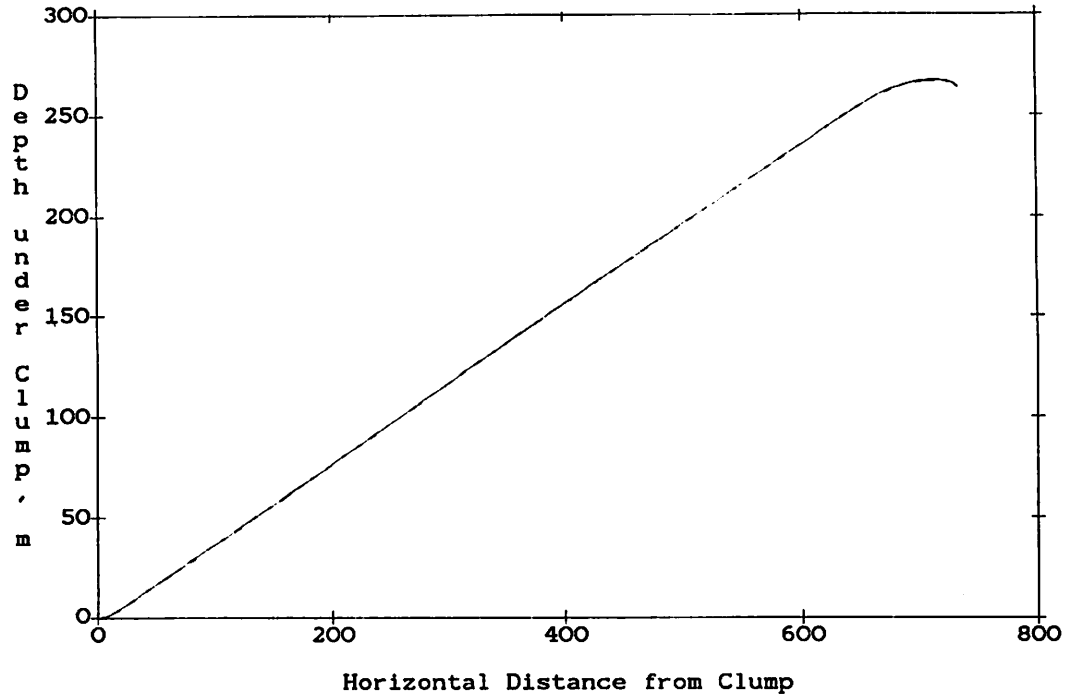

Figure 4-14: Trajectory of THLS and PAYLOAD.

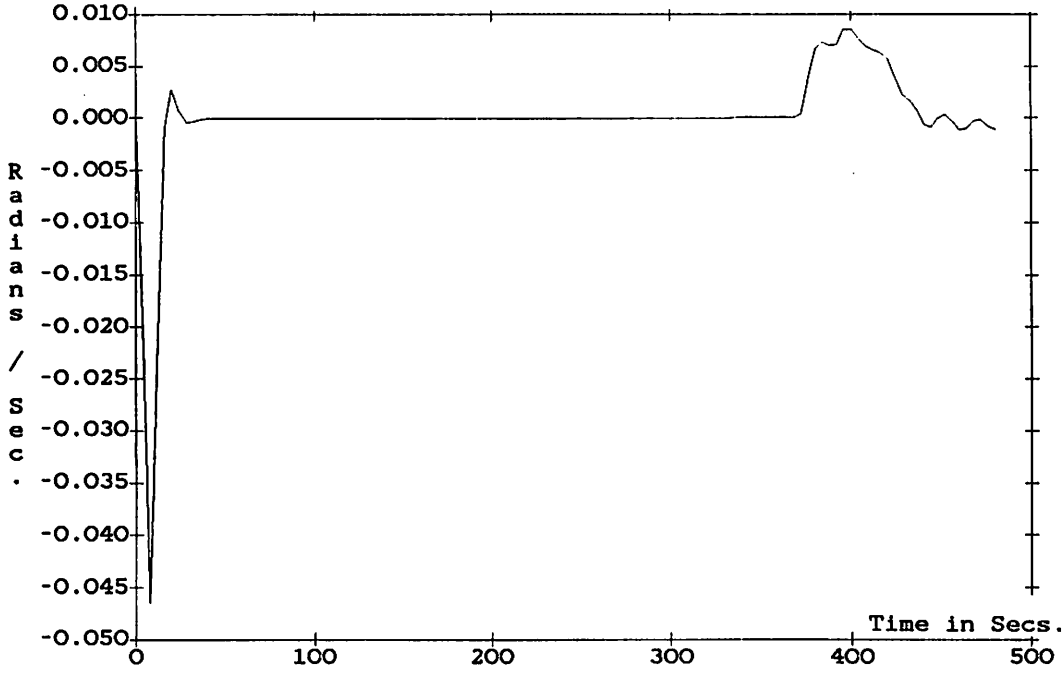

Figure 4-15: Pitch Rate of THLS and PAYLOAD.

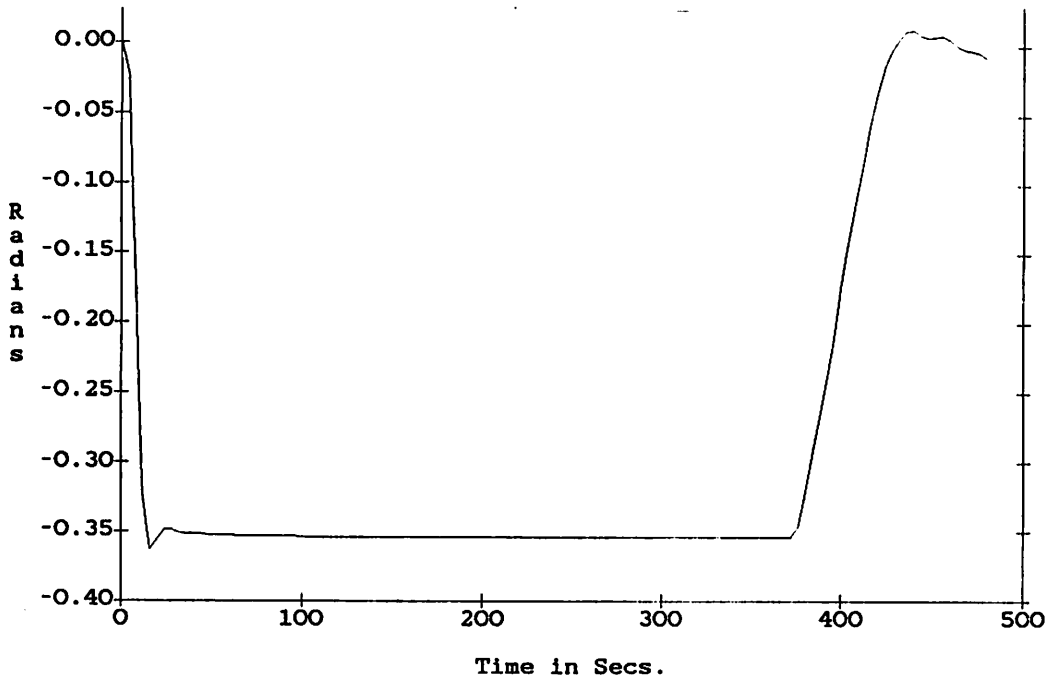

Figure 4-16: Pitch Angle of THLS and PAYLOAD.

The vehicle's velocity terms are expressed as,

$$u = u_o + \tilde{u} \ , \ w = w_o + \tilde{w} \ , \ q = q_o + \tilde{q}$$

$$\dot{u} = \dot{u}_o + \dot{\tilde{u}} \ , \ \dot{w} = \dot{w}_o + \dot{\tilde{w}} \ , \ \dot{q} = \dot{q}_o + \dot{\tilde{q}}$$

$$\theta = \theta_o + \tilde{\theta} \qquad (4.9)$$

The perturbation components are $\tilde{u}$, $\tilde{w}$, $\tilde{q}$, $\dot{\tilde{u}}$, $\dot{\tilde{w}}$, $\dot{\tilde{q}}$, and $\tilde{\theta}$. The steady state components are u_o, w_o, q_o, $\dot{u}_o$, $\dot{w}_o$, $\dot{q}_o$ and θ_o. First the perturbation components of the inertial forces are derived, but note that for the inertial terms the steady state velocities are u_i and w_i.

$$X_I = m\,[(\dot{u}_o + \dot{\tilde{u}}) + (q_o + \tilde{q})(w_i + \tilde{w}) - x_G(q_o + \tilde{q})^2 + z_G(\dot{q}_o + \dot{\tilde{q}})]$$

$$X_I = X_{I_o} + \tilde{X}_I$$

$$\tilde{X}_I = m\,[\,\dot{\tilde{u}} + q_o\tilde{w} + w_i\tilde{q} - x_G(2q_o\tilde{q}) + z_G\dot{\tilde{q}}\,] + \textit{H.O.T.}$$

$$\tilde{Z}_I = m\ [\ \dot{\tilde{w}} - q_o\tilde{u} - u_i\tilde{q} - z_G(2q_o\tilde{q}) - x_G\dot{\tilde{q}}\ ]$$

$$\tilde{M}_I = I_y\dot{\tilde{q}} + m\ [\ z_G(\dot{\tilde{u}} + q_o\tilde{w} + w_i\tilde{q}) - x_G(\dot{\tilde{w}} - q_o\tilde{u} - u_i\tilde{q})\ ] \qquad (4.10)$$

The hydrodynamic acceleration forces are,

$$\tilde{X}_A = X_{\dot{u}}\dot{\tilde{u}} + X_{\dot{w}}(\dot{\tilde{w}} + q_o\tilde{u} + u_o\tilde{q}) + X_{\dot{q}}\dot{\tilde{q}} + X_{qw}(q_o\tilde{w} + w_o\tilde{q}) + X_{qq}(2q_o\tilde{q})$$

$$\tilde{Z}_A = Z_{\dot{w}}\dot{\tilde{w}} + Z_{\dot{u}}(\dot{\tilde{u}} + q_o\tilde{w} + w_o\tilde{q}) + Z_{\dot{q}}\dot{\tilde{q}} + Z_{qu}(q_o\tilde{u} + u_o\tilde{q}) + Z_{qq}(2q_o\tilde{q})$$

$$\tilde{M}_A = M_{\dot{q}}\dot{\tilde{q}} + M_{\dot{u}}\dot{\tilde{u}} + M_{\dot{w}}\dot{\tilde{w}} + M_{uw}(u_o\tilde{w} + w_o\tilde{u}) + M_{uu}(2u_o\tilde{u}) + M_{ww}(2w_o\tilde{w}) + M_{uq}(u_o\tilde{q} + q_o\tilde{u}) + M_{wq}(w_o\tilde{q} + q_o\tilde{w}) \qquad (4.11)$$

The viscous/circulation forces are (see appendix D),

$$\tilde{X}_V = X_{\tilde{u}}\tilde{u} + X_{\tilde{w}}\tilde{w} + X_{\tilde{q}}\tilde{q}$$

$$\tilde{Z}_V = Z_{\tilde{u}}\tilde{u} + Z_{\tilde{w}}\tilde{w} + Z_{\tilde{q}}\tilde{q} \qquad (4.12)$$

$$\tilde{M}_V = M_{\tilde{u}}\tilde{u} + M_{\tilde{w}}\tilde{w} + M_{\tilde{q}}\tilde{q}$$

The only gravitational term is M_G (see Appendix D for details). At certain frequencies, the tether cable's resonant frequencies may be excited. This can produce high dynamic loads on the vehicle and make the system as a whole unstable if these loads are high enough.

The minimum resonant frequency of the tether is increased as the square root of the increase in tension in the tether. The case where the vehicle has

a very long tether (approximately 7,000 m) was checked in the current profile chosen for the simulation and resulted in a minimum resonant frequency at 0.035 radians/sec. This was the first symmetric mode, which does not exist when the cable is inelastic. For the case of an inelastic tether cable the minimum resonant frequency was at .073 radians/sec. This is the first antisymmetric mode and the minimum resonant frequency was still too low. Raising the cable tension would have raised this frequency, but the cable tension was set at 5,000 N which was already high. The minimum resonant frequency for the maximum tether length of 1,000m is 0.259 radians/sec. This length corresponds maximum distance between the clump and the submersible. A distance chosen in order to minimise both entanglements and the submersible's trajectory. The frequency response of the cable is given in the figures in appendix E for both the undamped and the damped cases. It can be seen that the cable is heavily overdamped and does not limit the bandwidth we may wish to assign to the controller. As a result, our previous concern that the tether may constrain the bandwidth of our system no longer holds.

The control forces are,

$$\begin{aligned} \tilde{X}_{CF} &= X_\eta \tilde{\eta} + X_\delta \tilde{\delta} + X_T \tilde{T} \\ \tilde{Z}_{CF} &= Z_\eta \tilde{\eta} + Z_\delta \tilde{\delta} + Z_T \tilde{T} \\ \tilde{M}_{CF} &= M_\eta \tilde{\eta} + M_\delta \tilde{\delta} + M_T \tilde{T} \end{aligned} \tag{4.13}$$

The complete equations of motion are,

$$\tilde{X}_I = \tilde{X}_A + \tilde{X}_V + \tilde{X}_{CF}$$

$$\tilde{Z}_I = \tilde{Z}_A + \tilde{Z}_V + \tilde{Z}_{CF} \tag{4.14}$$

$$\tilde{M}_I = \tilde{M}_A + \tilde{M}_V + \tilde{M}_{CF} + \tilde{M}_G$$

These are re-written in a state equation form as,

$$\underline{M}' \dot{\underline{x}}(t) = \underline{P}\, \underline{x}(t) + \underline{Q}\underline{u}(t) \tag{4.15}$$

$$\underline{y}(t) = \underline{C}\, \underline{x}(t)$$

where,

$$\underline{x}(t) = \begin{bmatrix} \tilde{\theta} \\ \tilde{u} \\ \tilde{w} \\ \tilde{q} \end{bmatrix} \quad \& \quad \underline{u}(t) = \begin{bmatrix} \tilde{\eta} \\ \tilde{\delta} \\ \tilde{T} \end{bmatrix} \tag{4.16}$$

and these yield the standard state equation form,

$$\dot{\underline{x}}(t) = \underline{A}\, \underline{x}(t) + \underline{B}\, \underline{u}(t) \tag{4.17}$$

$$\underline{y}(t) = \underline{C}\, \underline{x}(t)$$

where $\underline{A} = \underline{M}^{-1}\underline{P}$ and $\underline{B} = \underline{M}^{-1}\underline{Q}$

and $y_1(t) = \tilde{\theta}$
$y_2(t) = \tilde{u}$
$y_3(t) = \tilde{w}$

The response of the vehicle to white noise disturbance forces is small and acceptable in that the perturbations terms are small. It can be seen that the pitch response of the loaded vehicle is better than that of the unloaded vehicle

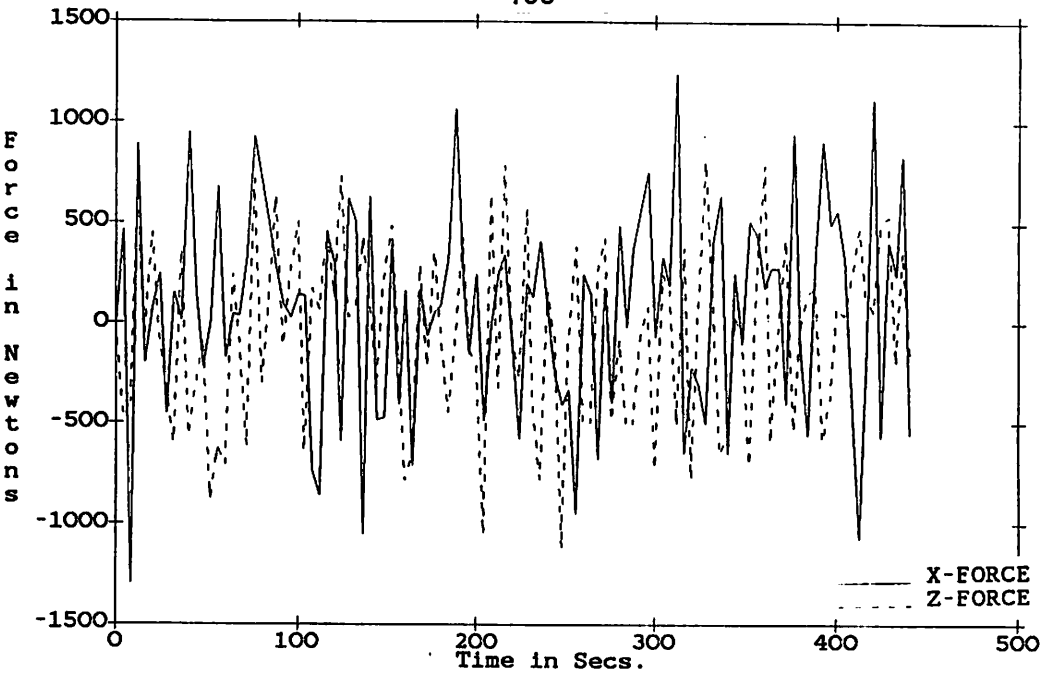

Figure 4-17: Disturbance Forces on the THLS.

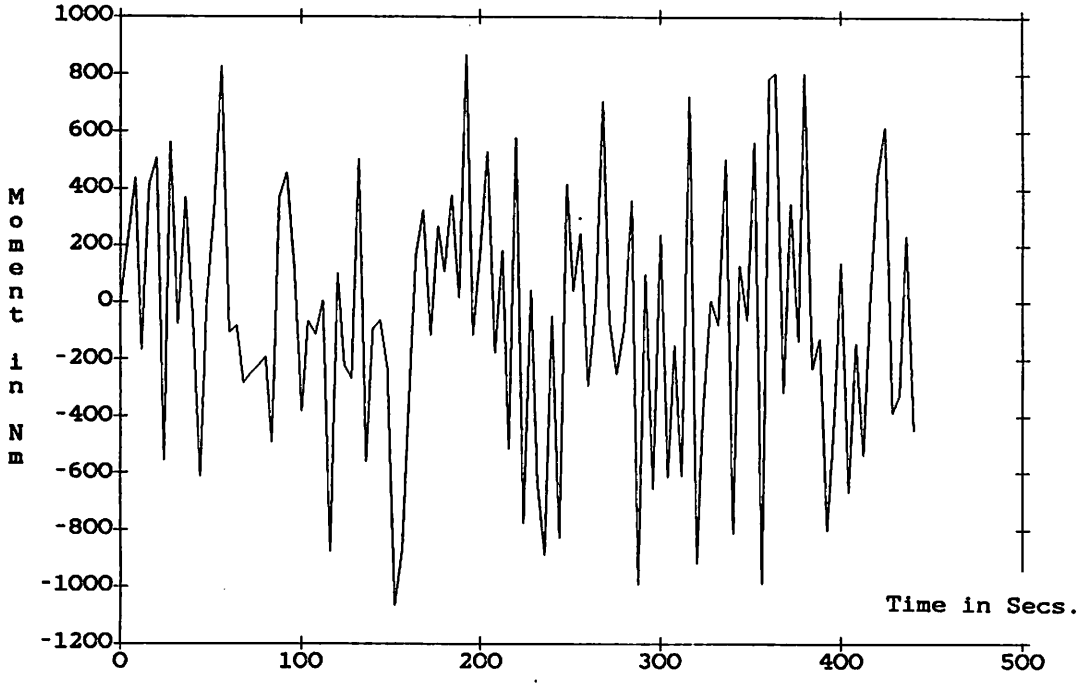

Figure 4-18: Disturbance Moment on the THLS.

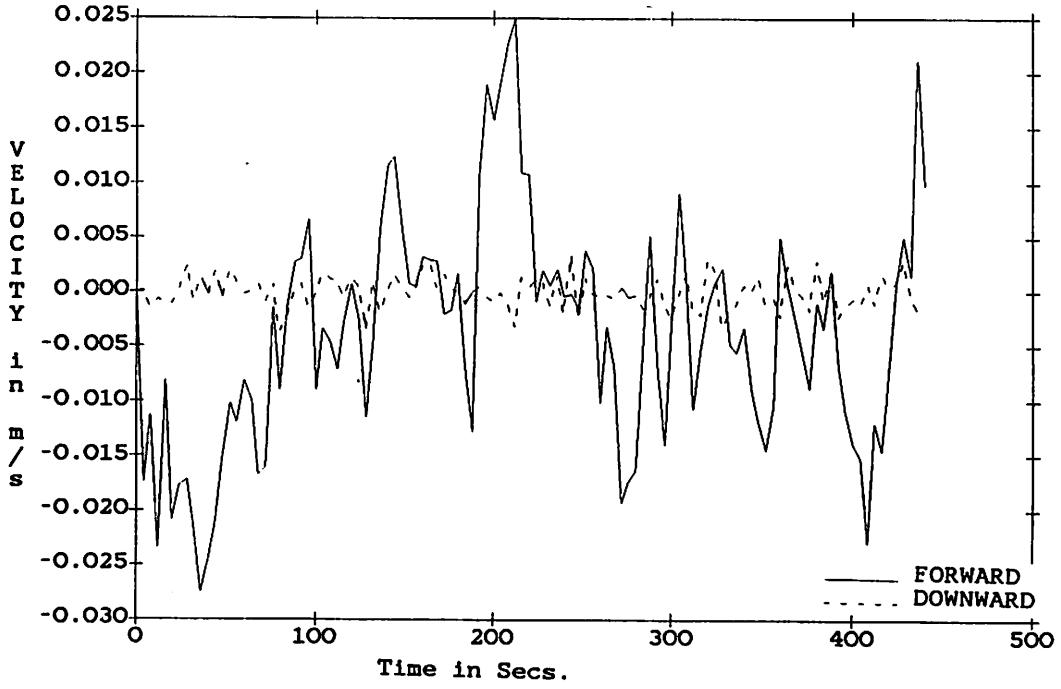

Figure 4-19: Perturbation Velocity of THLS.

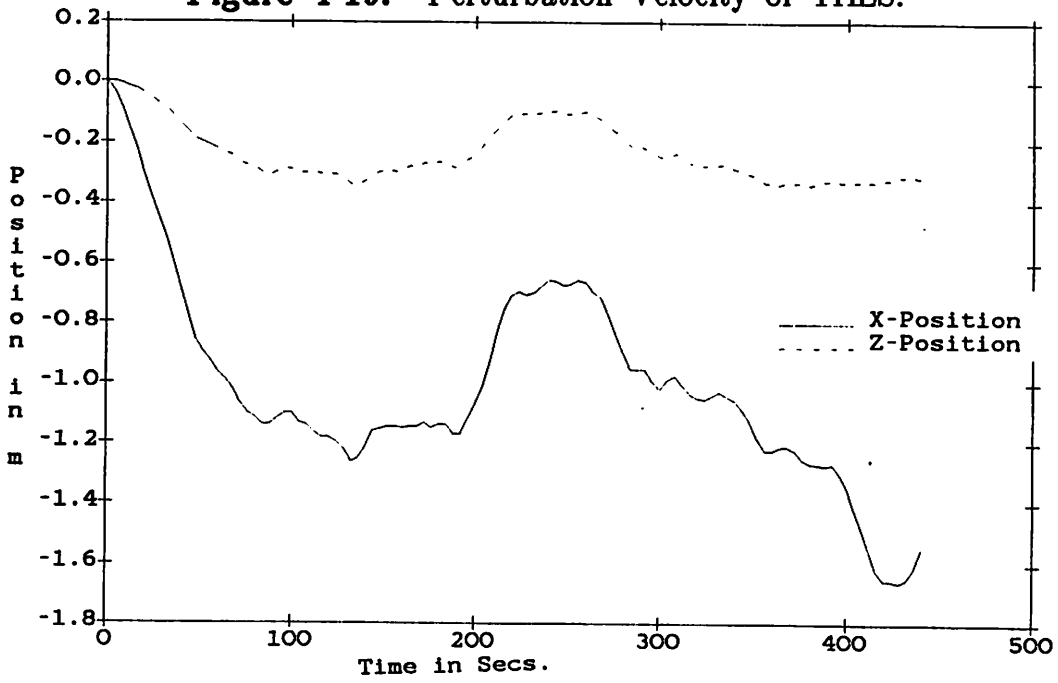

Figure 4-20: Perturbation Trajectory of THLS.

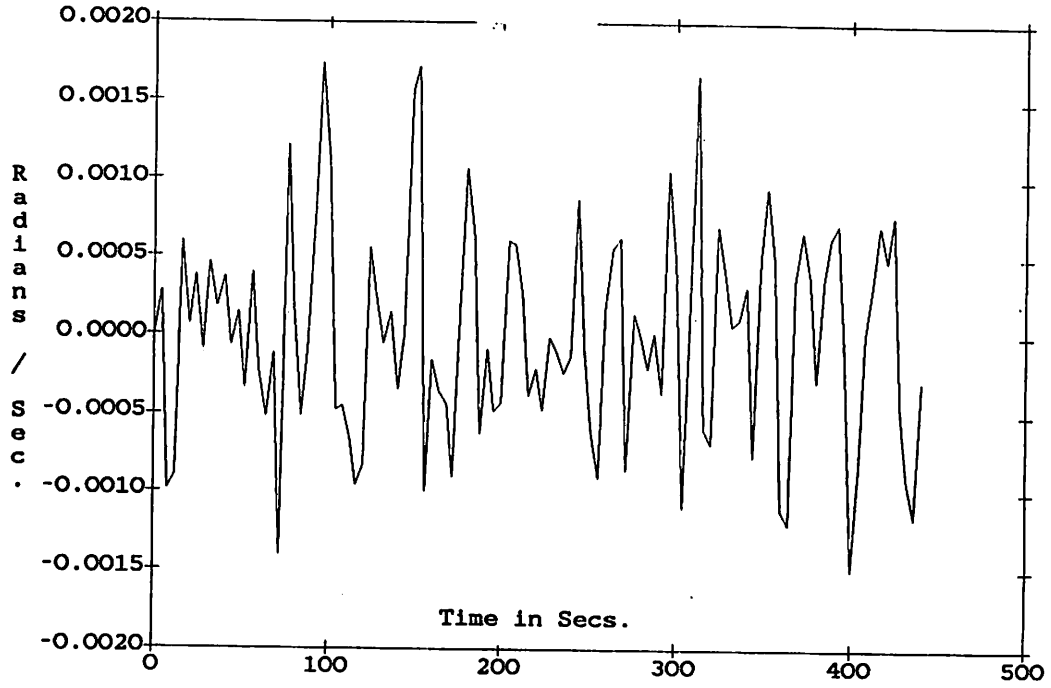

Figure 4-21: Perturbation Pitch Rate of THLS.

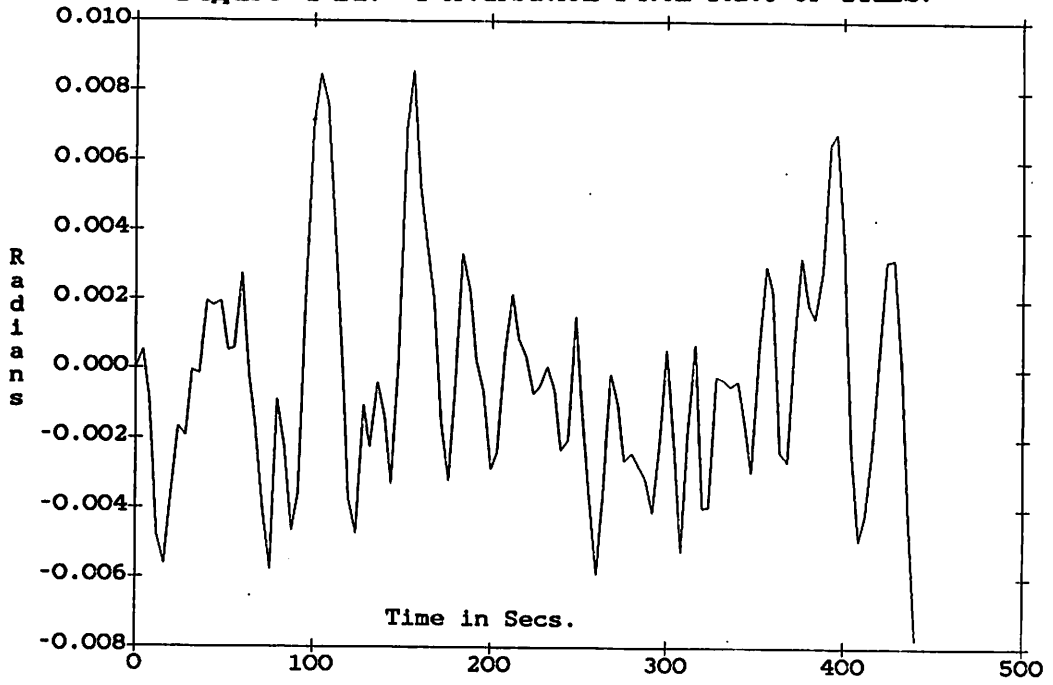

Figure 4-22: Perturbation Pitch Angle of THLS.

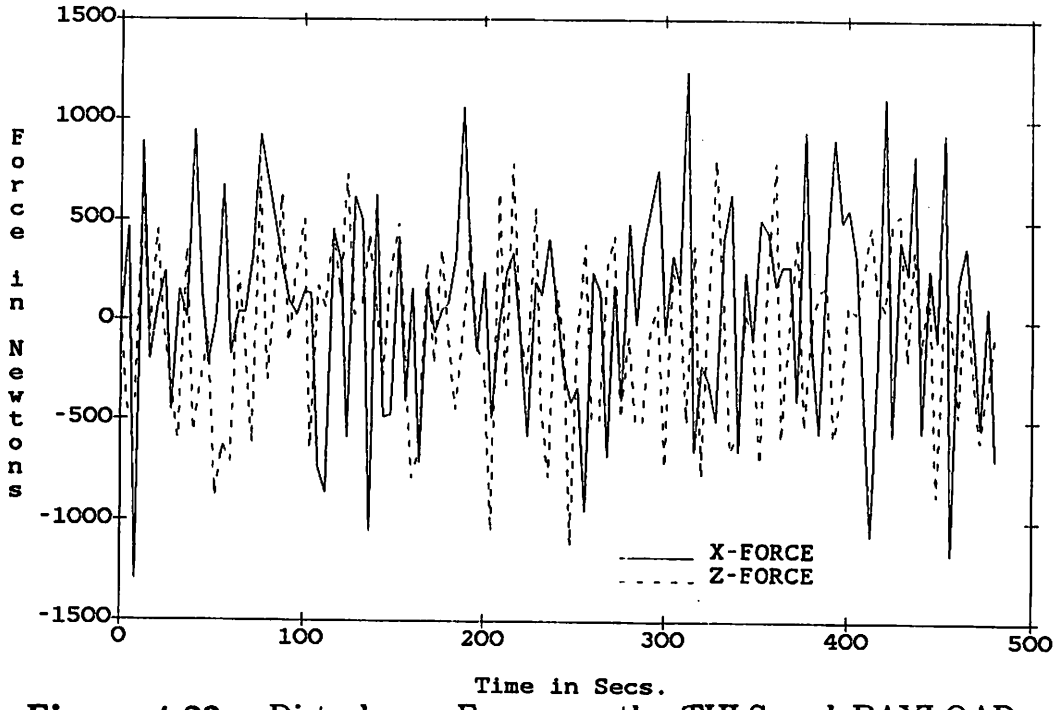

Figure 4-23: Disturbance Forces on the THLS and PAYLOAD.

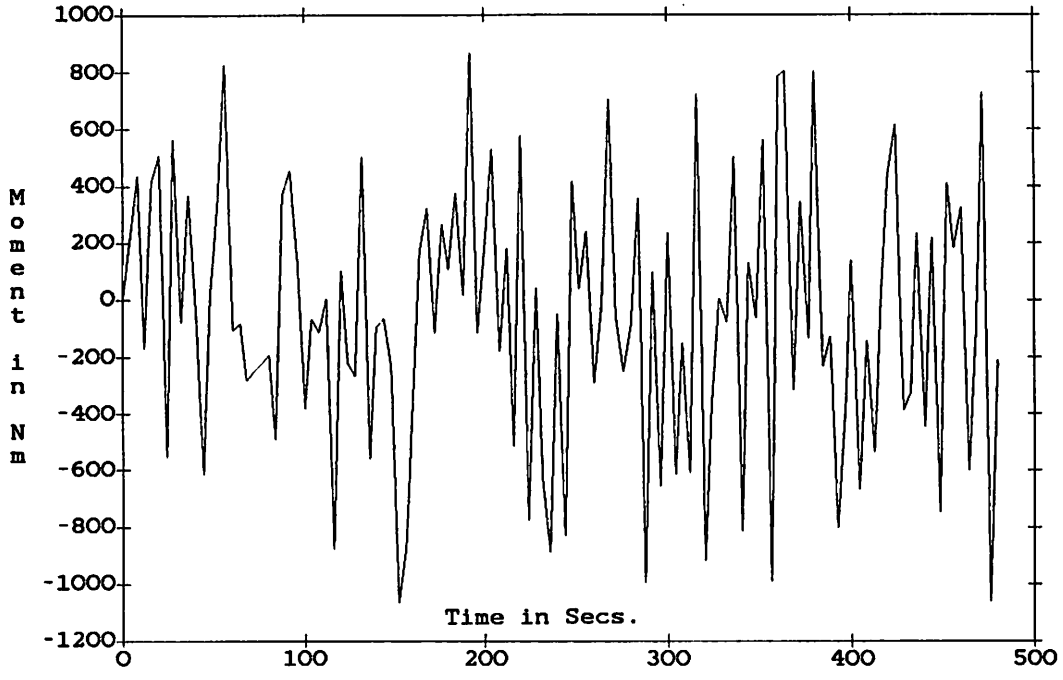

Figure 4-24: Disturbance Moment on the THLS and PAYLOAD.

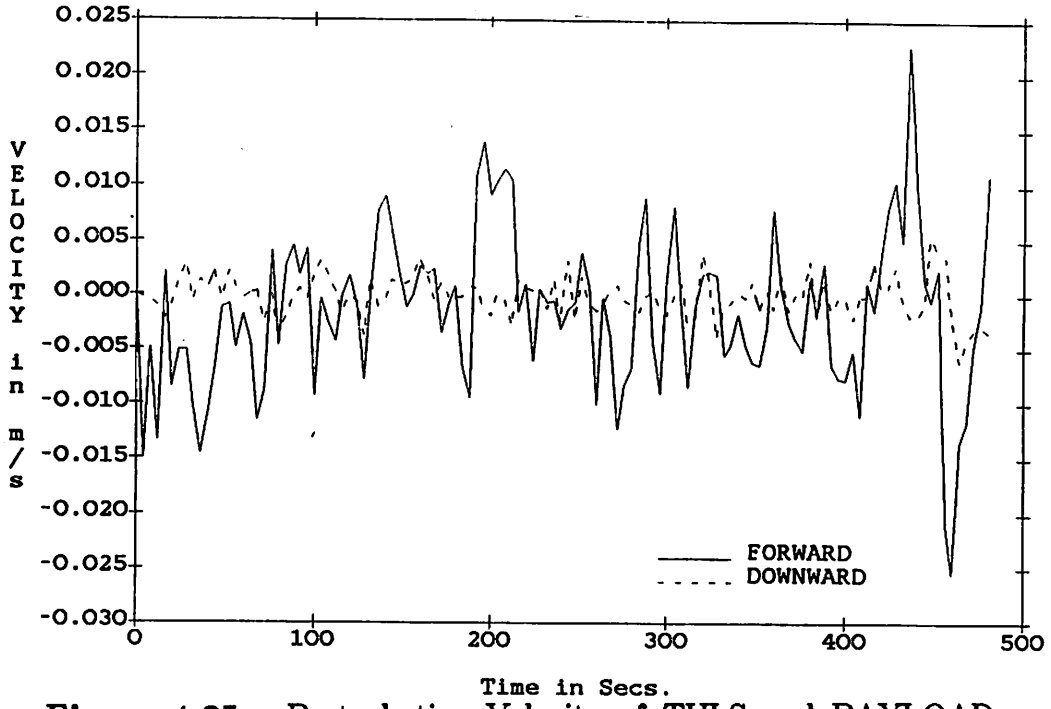

Figure 4-25: Perturbation Velocity of THLS and PAYLOAD.

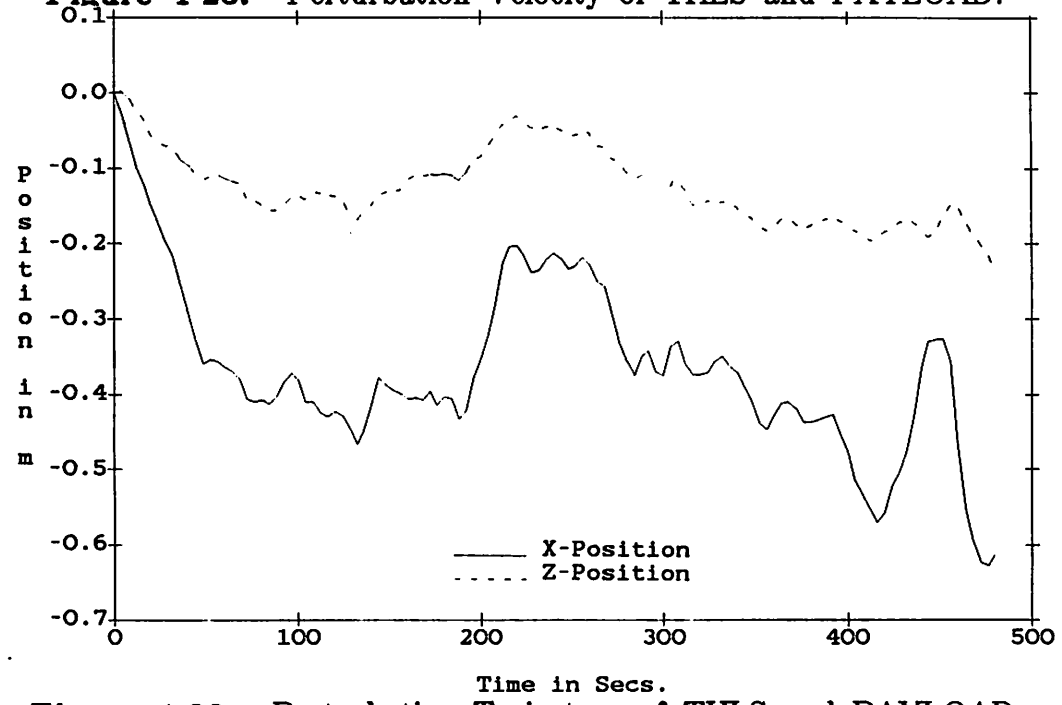

Figure 4-26: Perturbation Trajectory of THLS and PAYLOAD.

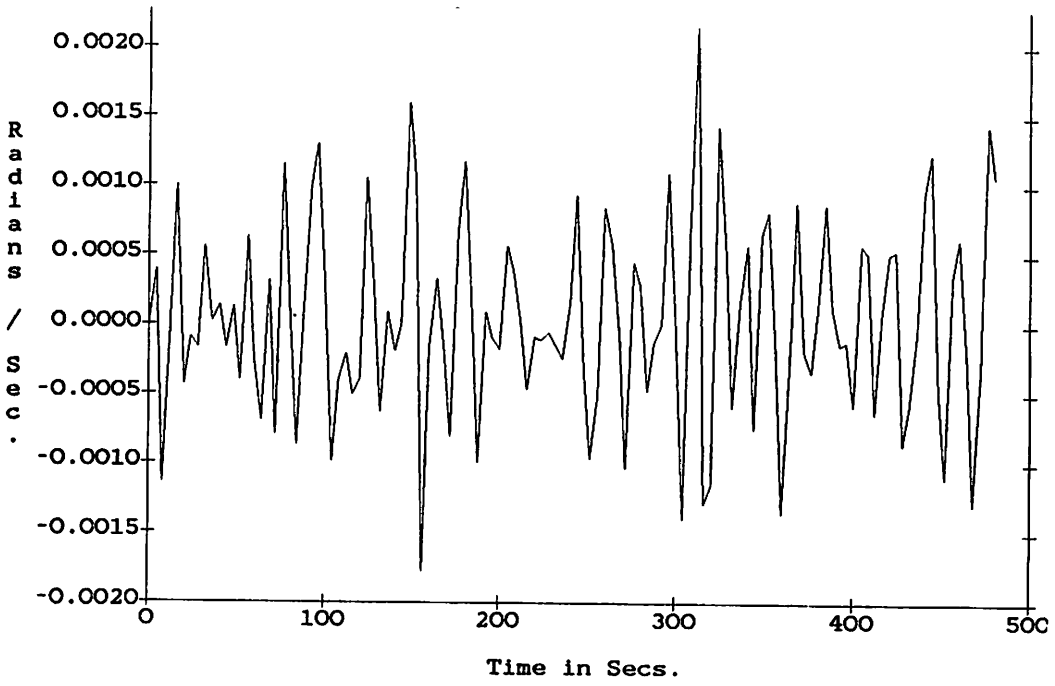

Figure 4-27: Perturbation Pitch Rate of THLS and PAYLOAD.

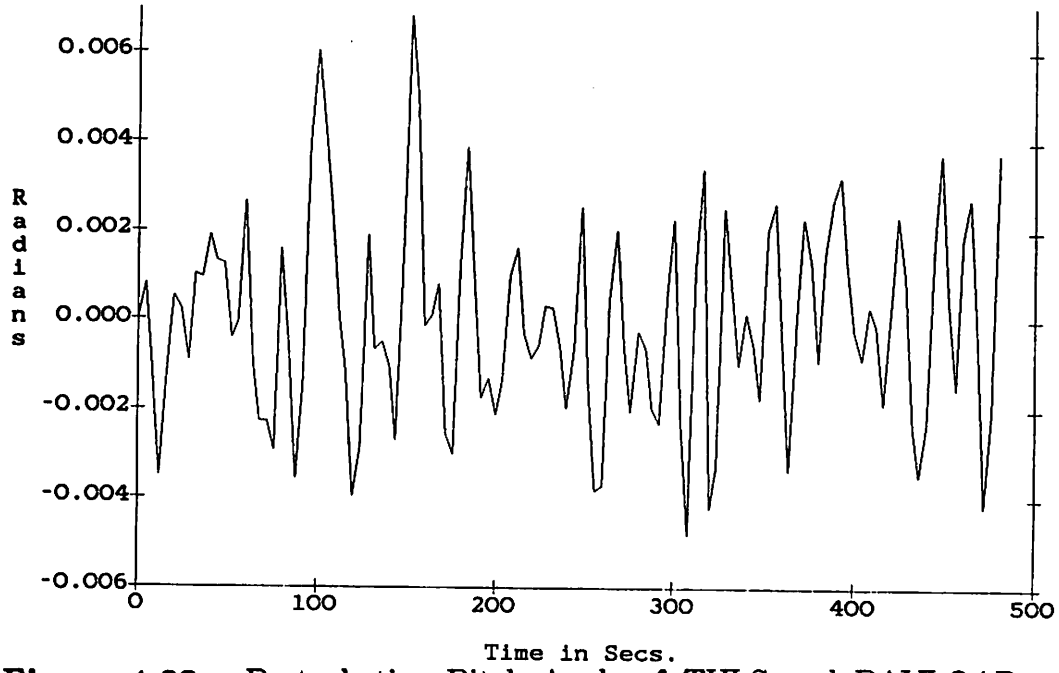

Figure 4-28: Perturbation Pitch Angle of THLS and PAYLOAD.

and that this may again be attributed to the higher effective inertia of the loaded vehicle. (In pitch, the vehicle behaves like a damped spring-mass system and increasing mass increases the spring constant.)

Chapter 5

Multivariable Controller Design

In this chapter the methodology used to create a linear time invariant compensator for a multivariable system is presented. This method uses the concepts of singular values to guarantie that the resulting system is stable. The controller design method is known as the linear quadratic gaussian with loop transfer recovery(LQG/LTR). For the case of a non-linear system, if it is well-behaved, the gain and filter matrices of the compensator can be curve fitted. A well-behaved system is defined as one that changes progressively.

5.1 Linear MIMO Controller Design

In the previous section, the perturbation model for the submersible was derived resulting in the state equations. These state equations (time-varying) are the basis for our controller design. This controller design procedure we will use is known as the multivariable LQG/LTR design methodology.

The model of the submersible that has been derived is assumed to be valid at low-frequencies where command following and disturbance rejection are the main characteristics. There is a certain amount of uncertainty in the model, such as includes unmodeled dynamics, sensor noise, actuator dynamics and the cable dynamics. Unmodeled dynamics in this case can be broken down into non-linear hydrodynamic effects and structural dynamics, as well as possible errors in the hydrodynamic or inertial coefficients. This uncertainty in the model sets a high frequency barrier before which the design must have its

maximum allowable crossover frequency.

In this design the cable is not included in the model and sets the maximum crossover frequency below its first resonance modes. The lowest resonance frequencies or the tether cable occur at its maximum length and the corresponding impedance is shown in appendix E.

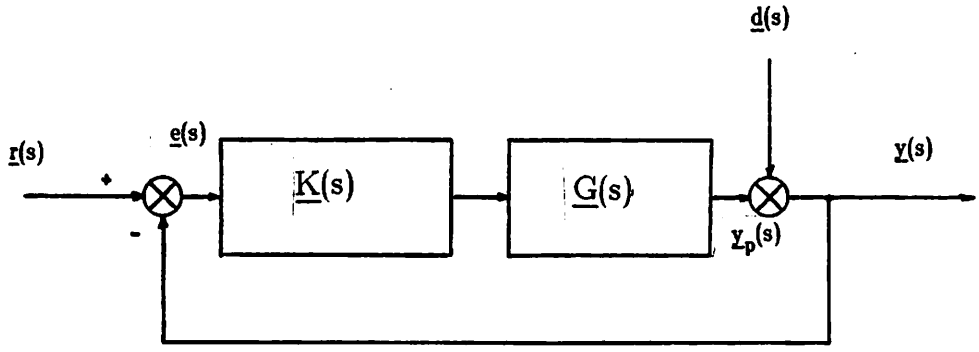

Figure 5-1: Block Diagram of MIMO Compensated Plant

First the low-frequency requirements must be clearly defined. The block diagram for the compensated system is shown in figure 5-1. The transfer function $\underline{G}(s)$ contains the low-frequency model of the submersible $\underline{G}_p(s)$ plus the vehicle's augmented dynamics $\underline{G}_a(s)$. Thus $\underline{G}(s) = \underline{G}_p(s)\underline{G}_a(s)$ and is the nominal design model. The following procedure will help us design the compensator $\underline{K}(s)$. The closed-loop transfer function is,

$$\underline{y}(s) = [\ \underline{I} + \underline{G}(s)\underline{K}(s)\ ]^{-1}\underline{d}(s) + [\ \underline{I} + \underline{G}(s)\underline{K}(s)\ ]^{-1}[\ \underline{G}(s)\underline{K}(s)\ ]^{-1}\underline{r}(s)$$

In order to have good command following (i.e. $\underline{y}(s) \approx \underline{r}(s)$) and good

disturbance rejection at low frequencies ($s = j\omega$ is small) , then the matrix product $\underline{G}(s)\underline{K}(s)$ must be much larger than unity for frequencies below the crossover frequency. At high frequencies, it is desirable for the response to be minimized and this can be achieved by keeping $\underline{G}(s)\underline{K}(s)$ small. These place high and low frequency barriers on the singular value plots and are shown in figure 5-2. Singular values are an extension of the SISO bode analysis and the references on these are [76], [75], [4], [46], [21], [66], [40], and [14]. The main reference is [51].

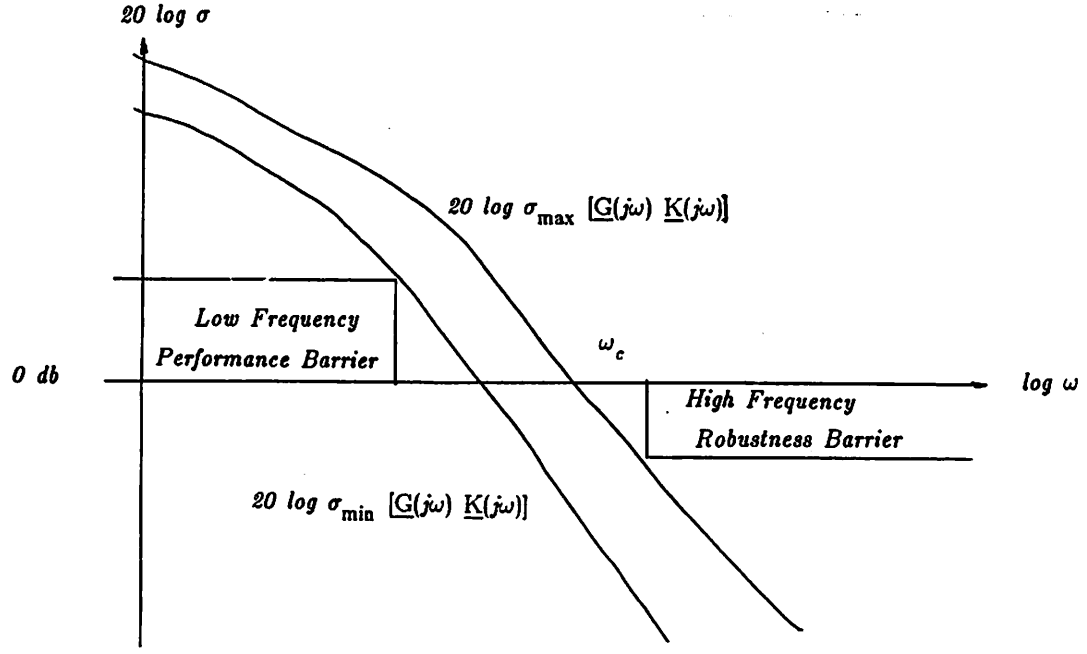

Figure 5-2: Singular Value Barriers at High and Low Frequencies.

5.2 Augmented Dynamics

The dynamics of the plant are augmented with integrators. This improves the step response as well as the steady state error characteristics of the closed loop control system. It is possible to augment the system dynamics with first or higher order systems rather than just integrators. The figure for

the nominal plant that includes the integrator augmented dynamics is shown in figure 5-3. The analogy for the augmented dynamics is in SISO systems where lag, lead, lag-lead compensators are used to obtain the desired bode loop shape. Augmenting system dynamics is a similar process and the augmented dynamics become a part of the model based compensator.

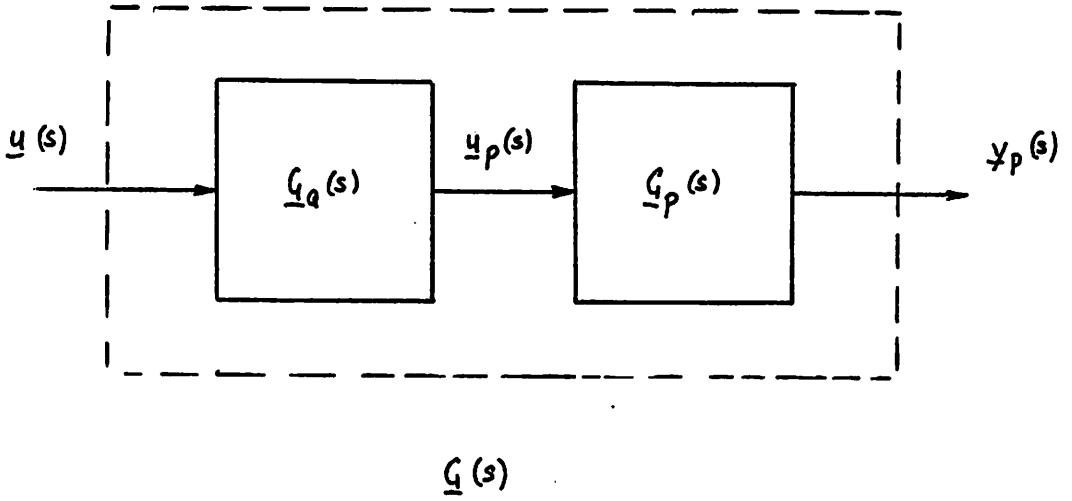

Figure 5-3: Block Diagram for Augmented Plant.

5.3 LQG/LTR Methodology

The LQG/LTR methodology is used to design a model based compensator $\underline{K}_{MBC}(s)$ that satisfies the preceding value requirements. The block diagram for the compensator is shown in figure 5-4. Specifically the LQG/LTR methodology involves finding the values of the Kalman Filter gain matrix H and then finding the corresponding Control Gain matrix G. The following method is valid if the design plant has no non-minimum phase zeros.

The Kalman Filter theory is used to reconstruct an estimate of the state

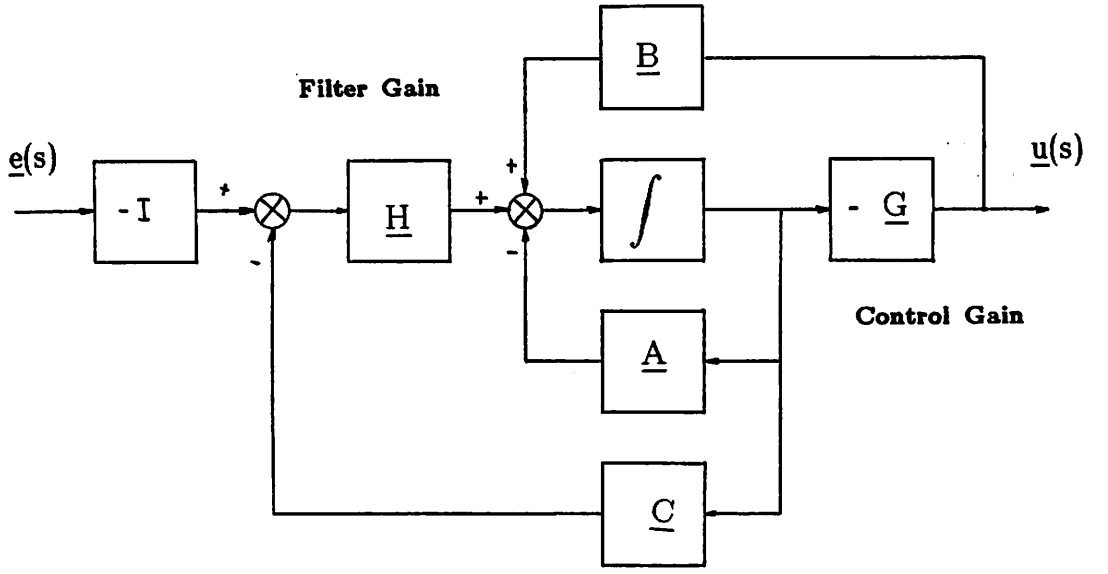

Figure 5-4: Block Diagram of MIMO Compensator $\underline{K}_{MBC}(s)$

vector. First, the Kalman Filter problem must be solved. This is the dual of the LQG control problem. The Kalman Filter state representation is derived from the model's state equation and is given as,

$$\dot{\underline{x}}(t) = \underline{A}\ \underline{x}(t) + \underline{L}\ \underline{\xi}(t)$$

$$\underline{y}(t) = \underline{C}\ \underline{x}(t) + \underline{\theta}(t)$$

where $\underline{\xi}(t)$ is the process or plant white noise and $\underline{\theta}(t)$ is the error due to sensor white noise. The plant noise and sensor noise are assumed to be independent. The covariance for the plant and sensor noise is given as,

$$E\left\{ \underline{x}(t)\ \underline{x}'(t) \right\} = \underline{\Xi}\ \delta(t - \tau)$$

$$E\left\{ \underline{q}(t)\ \underline{q}'(t) \right\} = \underline{\Theta}\ \delta(t - \tau)$$

Where $\underline{\Xi}$ and $\underline{\Theta}$ are the noise intensity matrices. The accurate filter problem involves shaping the Kalman Filter transfer function $\underline{K}_{MBC}(s)$. The block diagram for this loop is given in figure 5-5, where

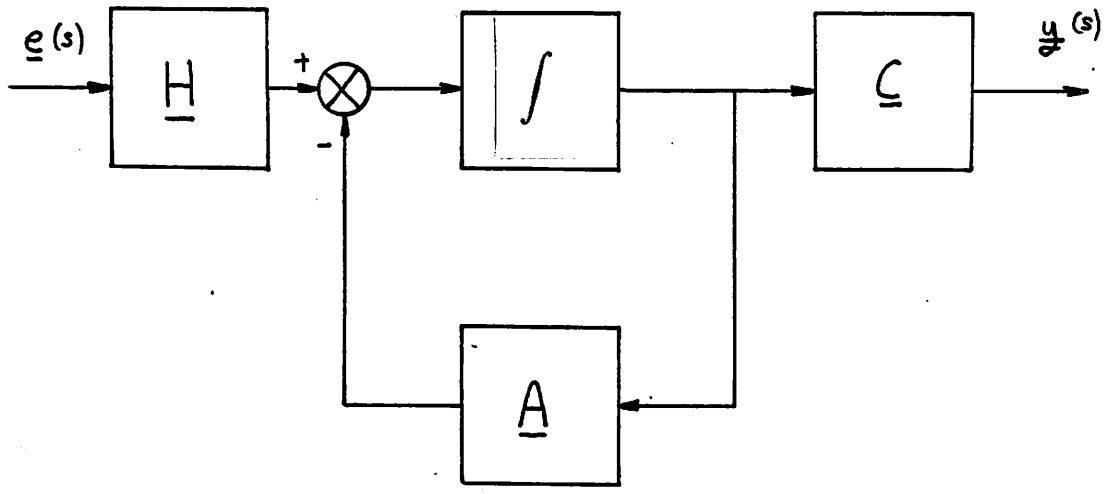

Figure 5-5: Block Diagram of Kalman Filter Loop $\underline{K}_{MBC}(s)$

$$\underline{K}_{MBC}(s) = \underline{C}\,(s\underline{I} - \underline{A})^{-1}\,\underline{H}$$

The noise intensity matrices are set to $\underline{\Xi} = \underline{I}$ and $\underline{\Theta} = \mu\underline{I}$. Appropriate choice of μ and $\underline{L}$ produce the desired Filter loop shape and the corresponding filter gain matrix $\underline{H}$. This is done by finding the symmetric matrix $\underline{S}$ that satisfies the Filter Algebraic Riccatti Equation (FARE),

$$\underline{0} = \underline{A}\,\underline{\Sigma} + \underline{\Sigma}\,\underline{A}' + \underline{L}\,\underline{L}' - \frac{1}{\mu}\,\underline{\Sigma}\,\underline{C}'\,\underline{C}\,\underline{\Sigma}$$

This yields the filter gain matrix $\underline{H} = (1/\sqrt{\mu})\,\underline{\Sigma}\,\underline{C}'$ that satisfies the desired filter loop hape. The singular values of the Kalman Filter transfer function $\underline{G}_{KF}(s)$ can be approximated, in the low-frequency range at least, by the open-loop filter transfer function $\underline{G}_{FOL}(s)$ for a parameter $\mu \ll 1$. The advantages of this approximation will become apparent in section 5.4. The approximation is given as (ref [51]),

$$\sigma_i \left[\underline{G}_{KF}(j\omega) \right] \approx \frac{1}{\sqrt{\mu}}\,\sigma_i \left[\underline{G}_{FOL}(j\omega) \right] \quad \text{for } \mu \ll 1.$$

where $\underline{G}_{FOL}(s) = \underline{C}\,(s\underline{I} - \underline{A})^{-1}\,\underline{L}$

If [$\underline{A}$, $\underline{L}$] is stabilizable and [$\underline{A}$, $\underline{C}$] is detectable then the preceding method yields the following guaranteed properties for $\underline{G}_{KF}(s)$: The system has a gain margin that is between -0.5 and ∞ and a phase margin of $\pm$ 60°. The system is closed loop stable and satisfies the following robustness criterion,

$$\sigma_{min} \left[\underline{I} + \underline{G}_{KF}(s) \right] \geq 1$$

$$\sigma_{min} \left[\underline{I} + \underline{G}_{KF}^{-1}(s) \right] \geq 0.5$$

Now that the filter gain matrix has been obtained the control gain matrix must be found in order to complete the design of the compensator. This final step is known as the loop transfer recovery and consists of the recovery of the $\underline{G}_{KF}(s)$ loop shapes in the $\underline{G}(s)\,\underline{K}(s)$ transfer function. The control gain matrix $\underline{G}$ is given by,

$$\underline{G} = \mu \underline{B}' \underline{K} \qquad \text{where } \underline{K} = \underline{K}' \geq 0$$

The matrix $\underline{K}$ is the solution of the Control Algebraic Equation (CARE) for the design parameter choice q. The CARE is given as,

$$\underline{0} = - \underline{K}\,\underline{A} - \underline{A}'\,\underline{K} - q\underline{C}'\underline{C} + \frac{1}{\mu}\,\underline{K}\,\underline{B}\,\underline{B}'\,\underline{K}$$

This solution is valid if [$\underline{A}$, $\underline{B}$] is stabilizable and [$\underline{A}$, $\underline{C}$] is detectable. The state space description for the compensator in figure 5-4 is given by,

$$\dot{\underline{z}}(t) = (\underline{A} - \underline{B}\,\underline{G} - \underline{H}\,\underline{C})\,\underline{z}(t) - \underline{H}\,\underline{e}(t)$$

$$\underline{u}(t) = - \underline{G}\,\underline{z}(t)$$

In reference [4] it can be shown that as $q \rightarrow \infty$ the values of $\underline{G}(s)\underline{K}(s)$ converge onto those of $\underline{G}_{KF}(s)$. In addition, above the crossover frequencies the roll-off is increased by 20 dB/decade as a result of the LTR method. Thus the resulting compensator has the desired performance.

5.4 Kalman Filter Design

In the previous section the method was presented to determine the Kalman Filter gain matrix. It was stated that the singular values of $\underline{G}_{KF}(j\omega)$ can be approximated by those of $1/\sqrt{\mu}\ \underline{G}_{FOL}(j\omega)$ if $\mu \ll 1$. In this section, $\underline{G}_{FOL}(j\omega)$ is determined by choosing $\underline{L}$ appropriately. This is applicable only to a plant that is augmented with integrators as is discussed in section 5.2.

The nominal design model $\underline{G}(s) = \underline{C}\ (s\underline{I} - \underline{A})^{-1}\ \underline{B}$ has the following $\underline{A}$

and $\underline{C}$ matrices.

$$\underline{A} = \begin{bmatrix} \underline{0} & \underline{0} \\ \underline{B}_p & \underline{A}_p \end{bmatrix}$$

$$\underline{C} = [\, \underline{0} \quad \underline{C}_p \,]$$

The value of $\underline{G}_{FOL}(s)$ is first determined in terms of the plant matrix values.

$$\underline{G}_{FOL}(s) = \underline{C}\,(s\underline{I} - \underline{A})^{-1}\,\underline{L}$$

$$= [\, \underline{0} \quad \underline{C}_p \,] \begin{bmatrix} \underline{I}/s & \underline{0} \\ (s\underline{I}-\underline{A}_p)^{-1}\underline{B}_p/s & (s\underline{I}-\underline{A}_p)^{-1} \end{bmatrix} \begin{bmatrix} \underline{L}_1 \\ \underline{L}_2 \end{bmatrix}$$

$$\underline{G}_{FOL}(s) = \underline{C}_p\,(s\underline{I} - \underline{A}_p)^{-1}\,(\,\underline{B}_p\underline{L}_1/s + \underline{L}_2\,)$$

This form of $\underline{G}_{FOL}(s)$ allows us to define the loop shapes both at high and low frequencies. At both, high and low frequencies the aim is to bring the loop shapes together. For $s = j\omega \rightarrow 0$,

$$\underline{G}_{FOL}(s) \approx -\,\underline{C}_p\,\underline{A}_p^{-1}\,(\,\underline{B}_p\underline{L}_1/s + \underline{L}_2\,)$$

Since the $\underline{L}_1$ term is much larger at low frequencies than the $\underline{L}_2$ term, the contribution of the latter can be neglected. Since at low frequencies $\underline{G}_{FOL}(s)$ is $\underline{I}/s$, the value of $\underline{L}_1$ can be found as follows,

$$\underline{G}_{FOL}(s) \approx - \underline{C}_p \underline{A}_p^{-1} \underline{B}_p \underline{L}_1 / s$$

$$\underline{L}_1 = - (\underline{C}_p \underline{A}_p^{-1} \underline{B}_p)^{-1}$$

For $s = j\omega \rightarrow \infty$ (high frequencies),

$$\underline{G}_{FOL}(s) = \underline{C}_p \underline{I}/s (\underline{B}_p \underline{L}_1 / s + \underline{L}_2)$$

At high frequencies the $\underline{L}_2$ term dominates the $\underline{L}_1$ term and the desired value of $\underline{G}_{FOL}(s)$ is $\underline{I}/s$. The value of $\underline{L}_2$ is,

$$\underline{L}_2 = \underline{C}_p' (\underline{C}_p \underline{C}_p')^{-1}$$

The value for $\underline{L}_2$ is the pseudo-inverse (or penrose inverse) of $\underline{C}_p$.

If the singular values at crossover are separated, then they can be brought closer together by scaling the corresponding components of the $\underline{C}_p$ matrix. Once the choice of the $\underline{L}$ matrix has been made, it is necessary only to change μ until the desired crossover frequency is reached. The LQG/LTR design is completed by varying the design parameter q until the Kalman Filter loop shapes are recovered.

It must be noted that the Kalman Filter presented here tracks all the states adequately except for the state that corresponds to the pitch rate. That state is not tracked by the kalman filter. This is a structural problem of the plant since the pseudoinverse of $\underline{C}_p$ is a 4*3 matrix whose upper 3*3 block is an identity matrix. The most haphazard method of correcting this, is to enter a value in the $\underline{L}\underline{L}'$ matrix that removes the zero weighting of the pitch rate state. The more accurate method is to determine this value as a

dual to the Stochastic Linear Optimal Regulator problem (see reference [46] pg 259-263), where a method for determining the additional states is presented in the form of an extension to the Filter Algebraic Riccati Equation. It allows for improvements in the Kalman Filter without affecting the state feedback control loop.

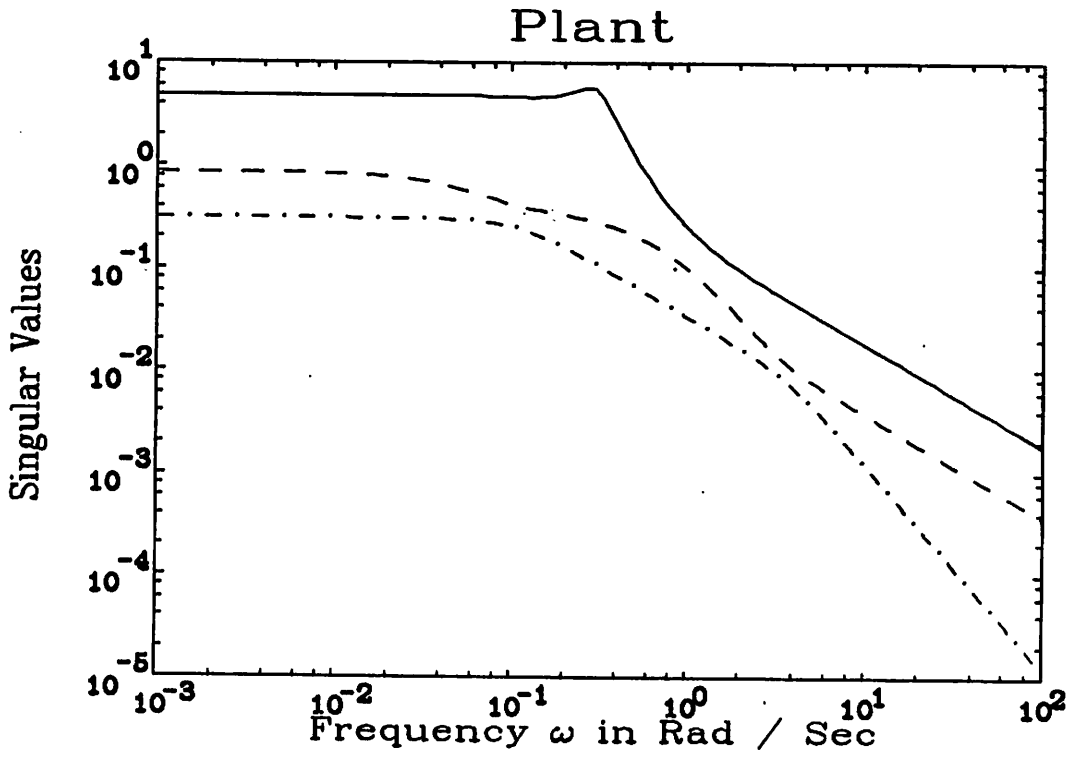

Figure 5-6: Singular Values for the Plant

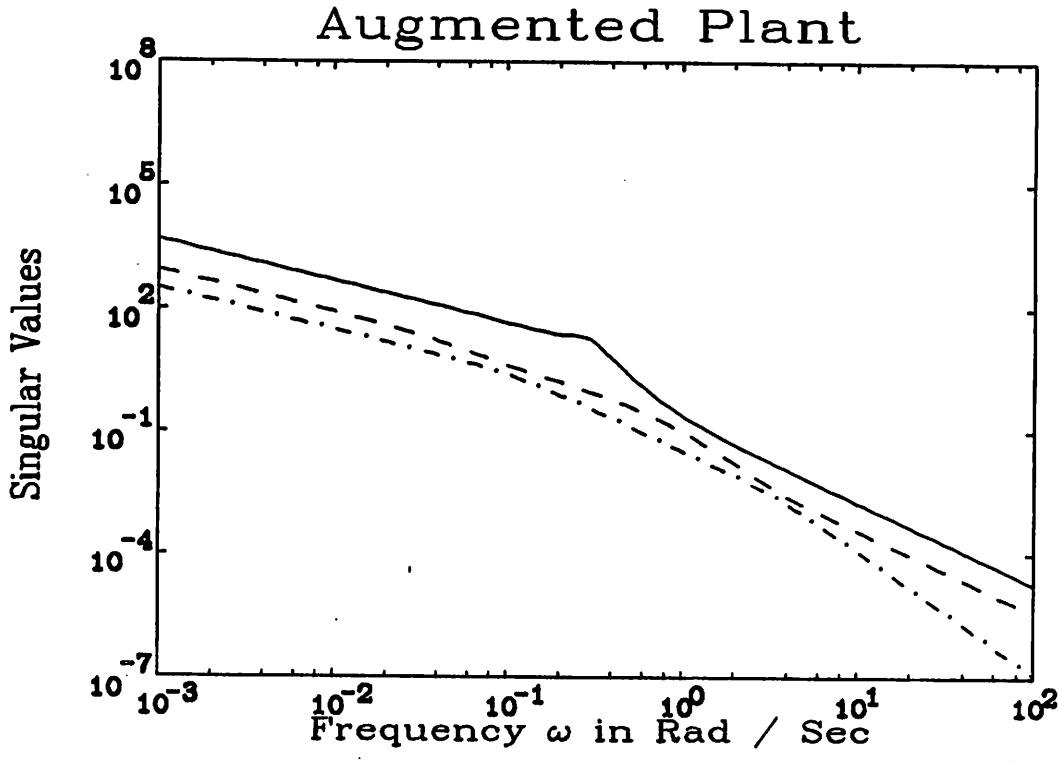

Figure 5-7: Singular Values for the Augmented Plant

5.5 The Closed Loop System

The state space description that corresponds to the closed loop system of figure 5-1 is given as,

$$\begin{bmatrix} \dot{\underline{x}}(t) \\ \dot{\underline{z}}(t) \end{bmatrix} = \begin{bmatrix} \underline{A} & -\underline{BG} \\ \underline{HC} & \underline{A}-\underline{BG}-\underline{HC} \end{bmatrix} \begin{bmatrix} \underline{x}(t) \\ \underline{z}(t) \end{bmatrix} + \begin{bmatrix} \underline{0} \\ -\underline{HC} \end{bmatrix} \underline{r}(t)$$

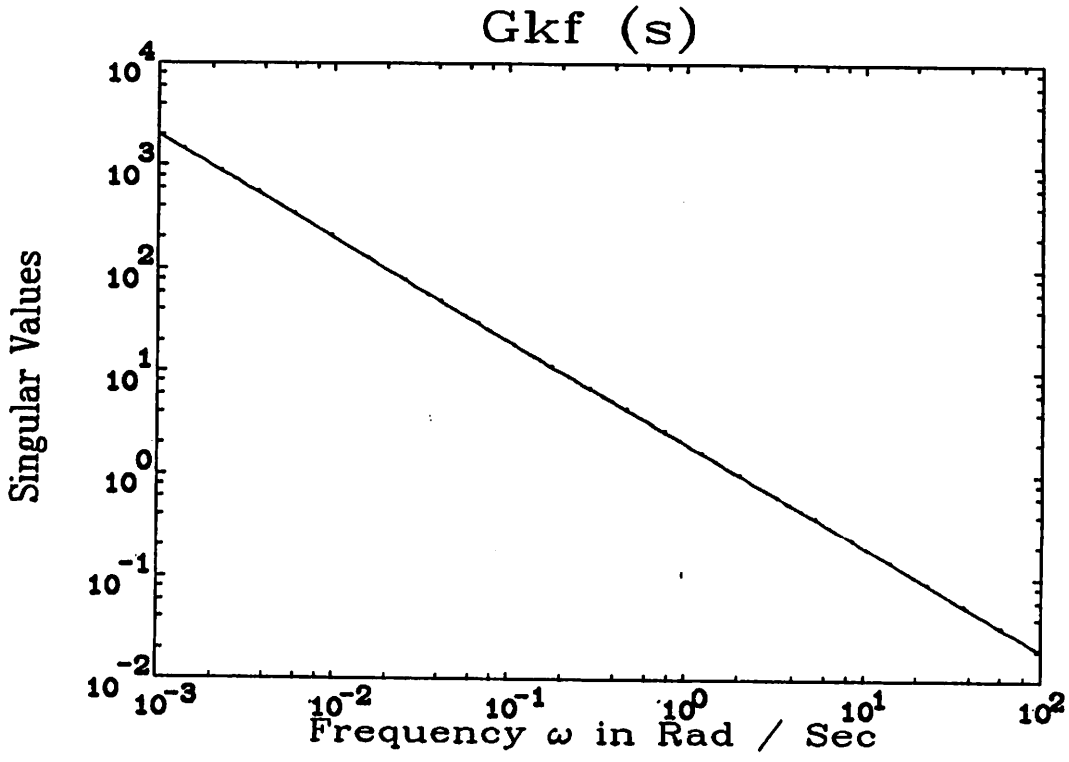

Figure 5-8: Singular Values for the Kalman Filter Loop

$$\underline{y}(t) = \begin{bmatrix} \underline{C} & \underline{0} \end{bmatrix} \begin{bmatrix} \underline{x}(t) \\ \\ \underline{z}(t) \end{bmatrix}$$

The method used to find the poles and zeros for the closed loop system is the same as for the plant. The theory for this problem is well discussed in the following references [14] and [40]. The closed loop system should now possess the characteristics designed into the Kalman Filter loop. The next step is to produce the nonlinear controller and test the controller's performance in carrying out the nonlinear simulation of the previous chapter.

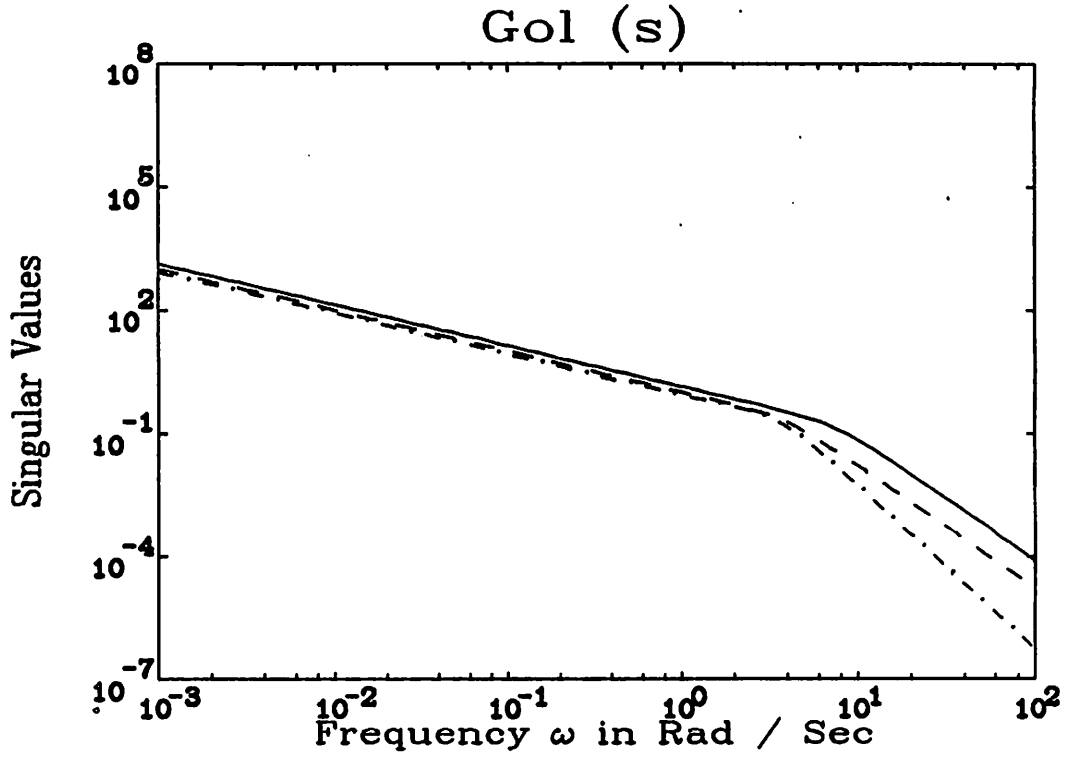

Figure 5-9: Singular Values for the Open Loop System

5.6 Non-linear MIMO Controller Design

In the previous sections, the method for finding the Filter and Control gain matrices for a linear time invariant model based compensator was presented. In the non-linear MIMO design problem, the state space description of the model is time varying. The model that was derived in the previous chapter varies as a function of its forward speed U and as a function of its angle of attack with the incident flow.

The gain-scheduling method involves curve fitting the Filter and Control

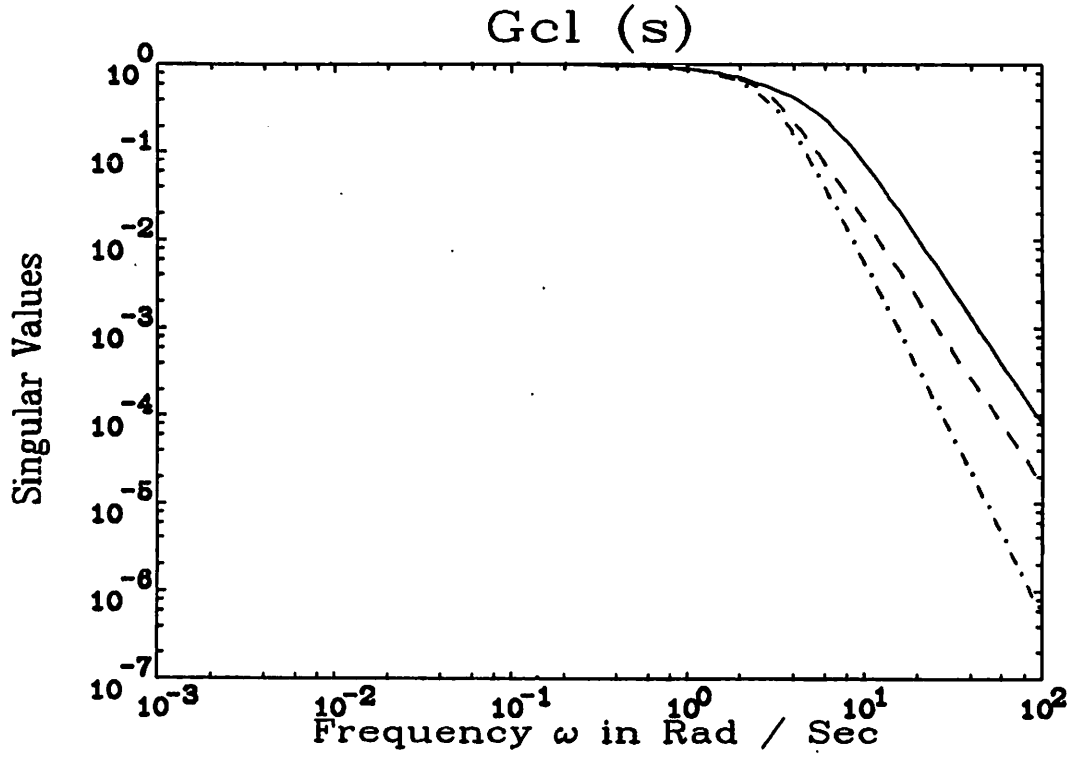

Figure 5-10: Singular Values for the Closed Loop System

gain obtained at different values of forward speed and angle of incidence. In reference [51], K. Liveley fits the Filter and Control gain matrices to a second order polynomial using a least squares method. He finds that a second-order fit provided the greatest correlation for the number of calculations involved. In this thesis, it was not possible to curve fit the gain matrices. As a result a linear interpolation is performed to determine the gain matrices as functions of both forward velocity and angle of attack. Furthermore, this involves interpolating between four gain matrices to obtain the desired scheduled gain matrices. The control gain matrices are determined at six different velocities 0.5 ms^{-1}, 1.0 ms^{-1}, 1.5 ms^{-1}, 2.0 ms^{-1}, 2.5 ms^{-1},and 3.0 ms^{-1} ,as well as at

seven different angles of attack -7.5 degr.,-5.0 degr.,-2.5 degr.,0.0 degr.,2.5 degr.,5.0 degr.,and 7.5 degr. This represents a total of 42 control problems that are solved.

5.7 Simulation with Non-linear MIMO Controller

The simulations of the previous chapter are repeated with the Non-linear controller in the loop in order to determine the controller's performance. The steady state simulation remains unchanged and the same disturbances are used as in the previous case. It can be quickly seen from the following figures that this controller reduces the effects of the disturbances by several orders of magnitude. This is true for both the loaded and unloaded cases. Note that the control surface deflections increase rapidly towards the end of the simulation. This is due to the fact that as the vehicle's velocity decreases the effective force produced by these surfaces decreases as the square of the velocity. It can be seen that the envelope of the controller's deflections is roughly parabolic and coresponds to the inverse of the square of the velocity. This is due to the fact that the disturbances are constant throughout the simulation and do not drop off as the vehicle's velocity does. This is a slight inadequacy in the simulation which happens to illustrate the non-linear performance of the controller.

The results of the simulation are excellent in the sense that the controller virtually eliminates the effects of the disturbances. However a word of caution is required. It was assumed that the bandwidth of the control force actuators and thrusters was higher than the bandwidth of the vehicle dynamics and that their dynamics did not affect the system performance.

This may not necessarily be true. It is dependent on the choice of actuators and cost is a predominant factor. Furthermore, the effects of a rapidly varying current were included in the disturbances, and this is a simplification of the actual problem. Finally, the problem of sensor noise and the selection process for sensors was not addressed. This can be included in the simulation to assess the performance of different sensors by injecting sensor noise at the appropriate point of the loop. Consideration of this problem would determine how well a given controller design can perform with a specific set of sensors, and whether it can be improved or if more expensive sensors are required. There are important considerations that become significant in the final design phases.

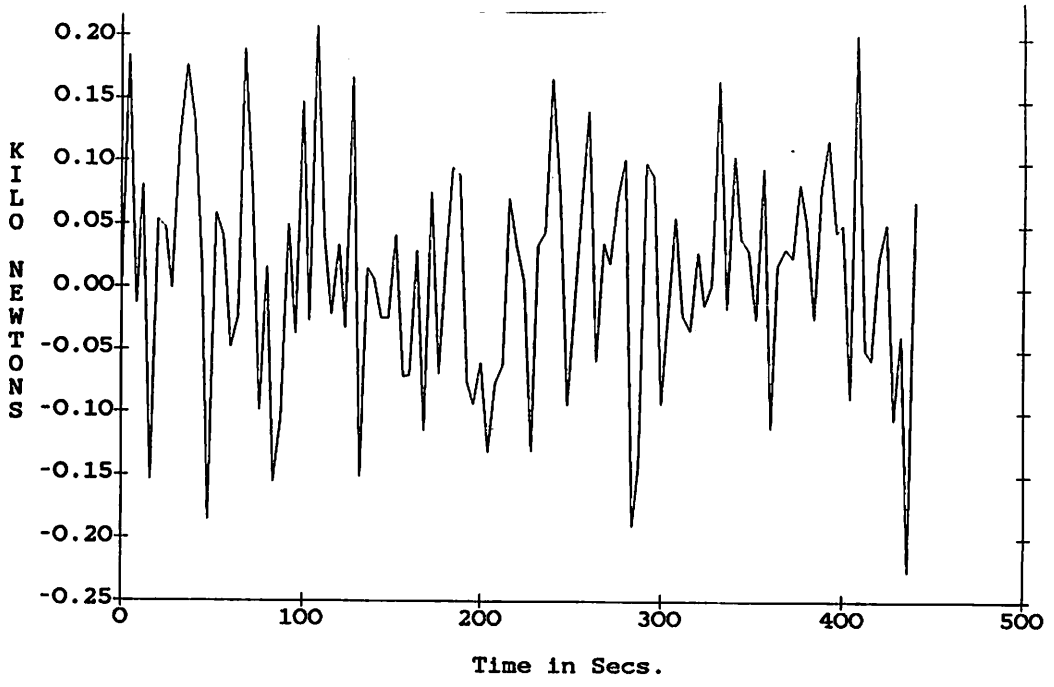

Figure 5-11: Thruster Time History due to Controller for the THLS.

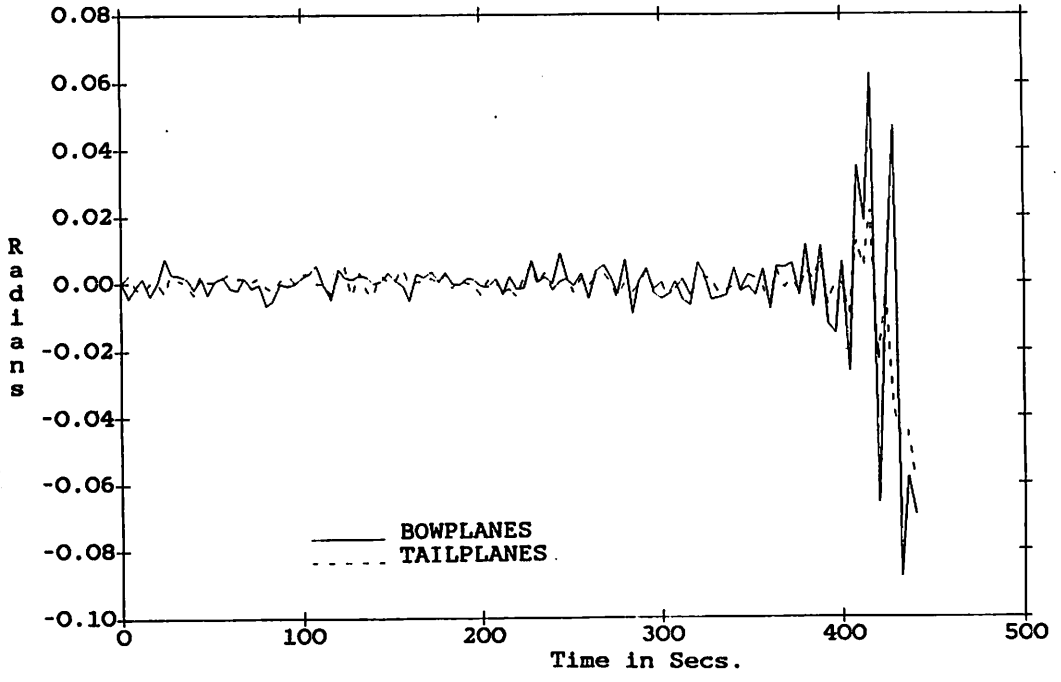

Figure 5-12: Control Deflections due to the Controller for the THLS.

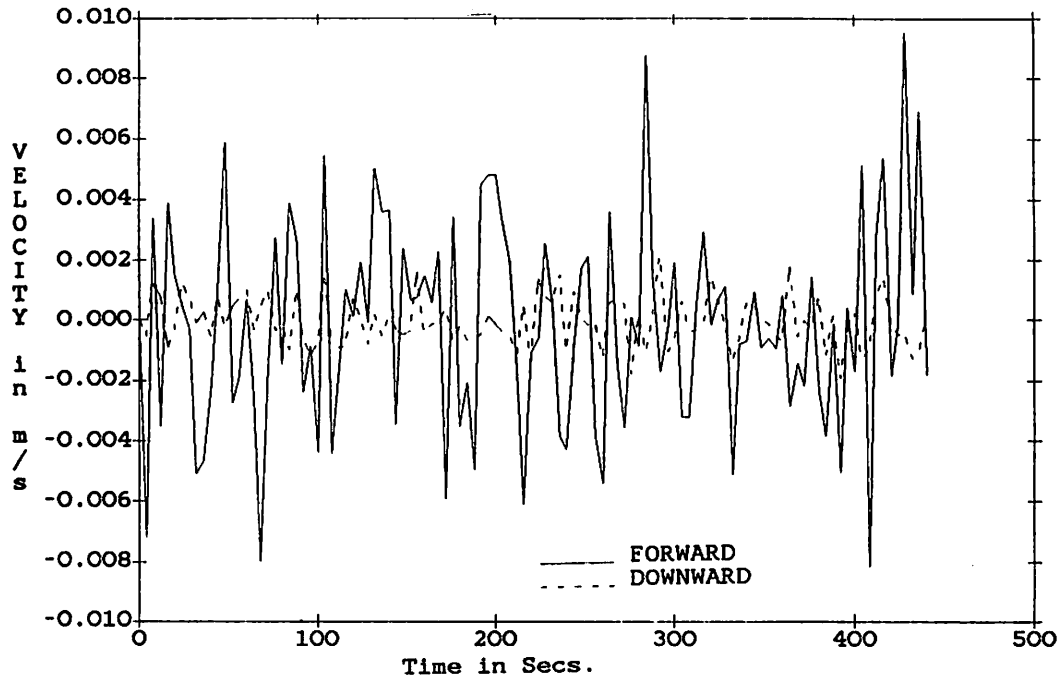

Figure 5-13: Perturbation Velocity of THLS.

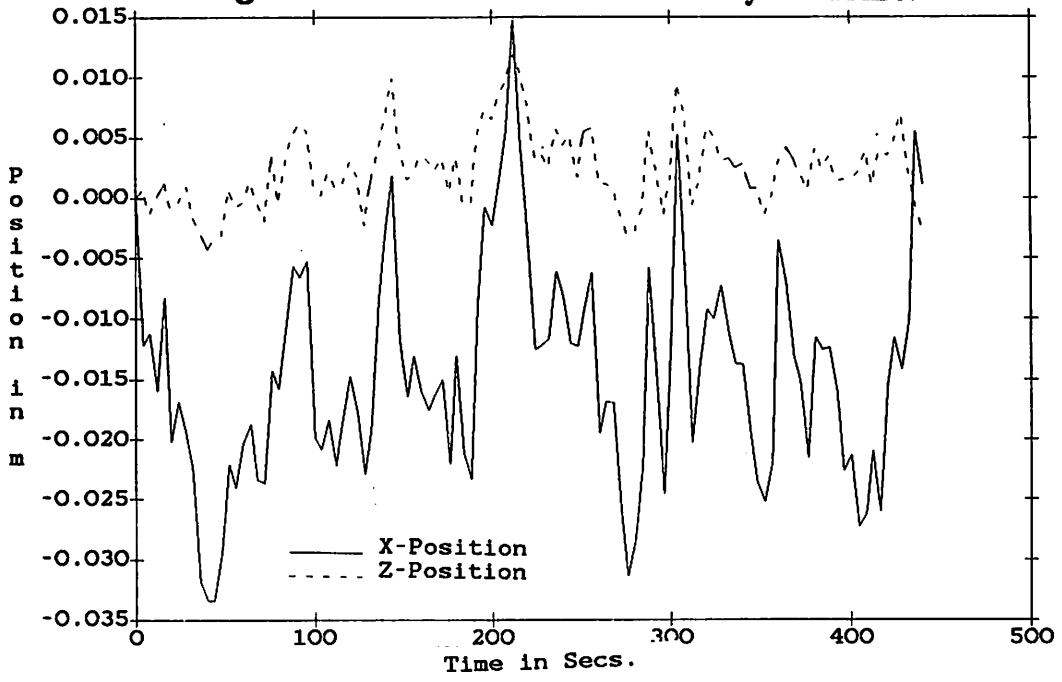

Figure 5-14: Perturbation Trajectory of THLS.

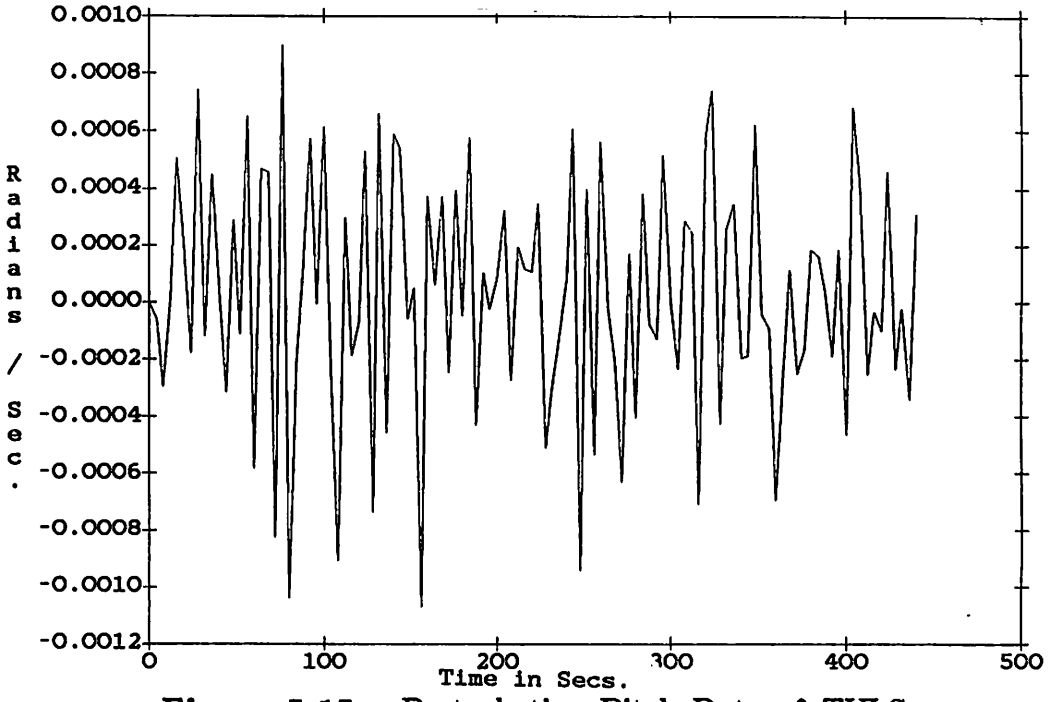

Figure 5-15: Perturbation Pitch Rate of THLS.

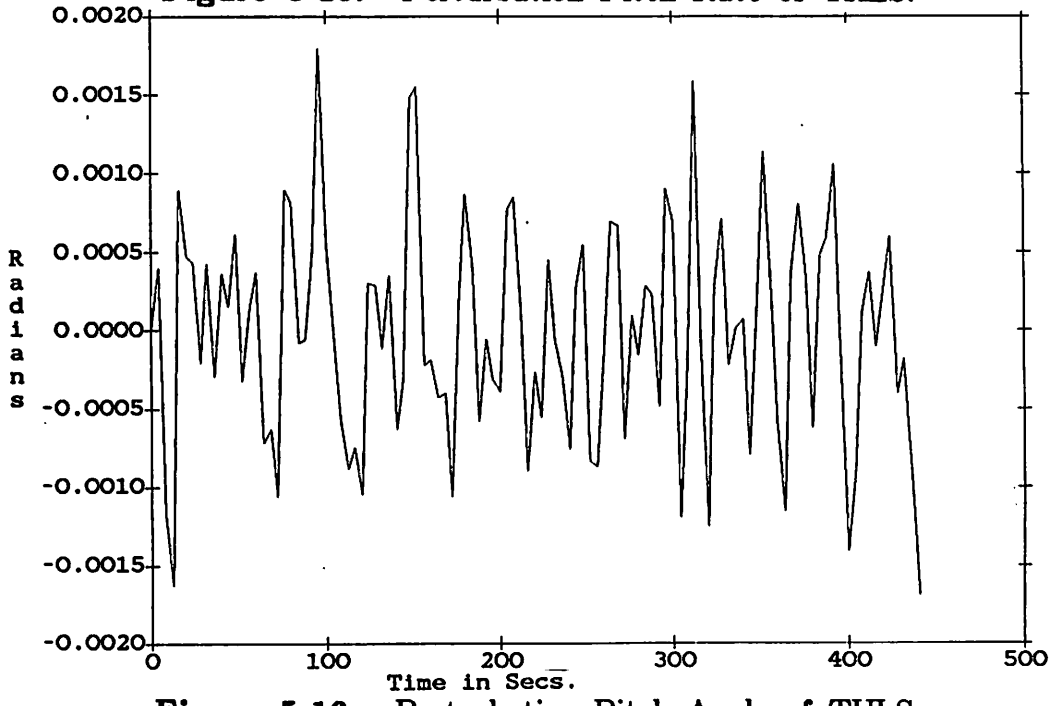

Figure 5-16: Perturbation Pitch Angle of THLS.

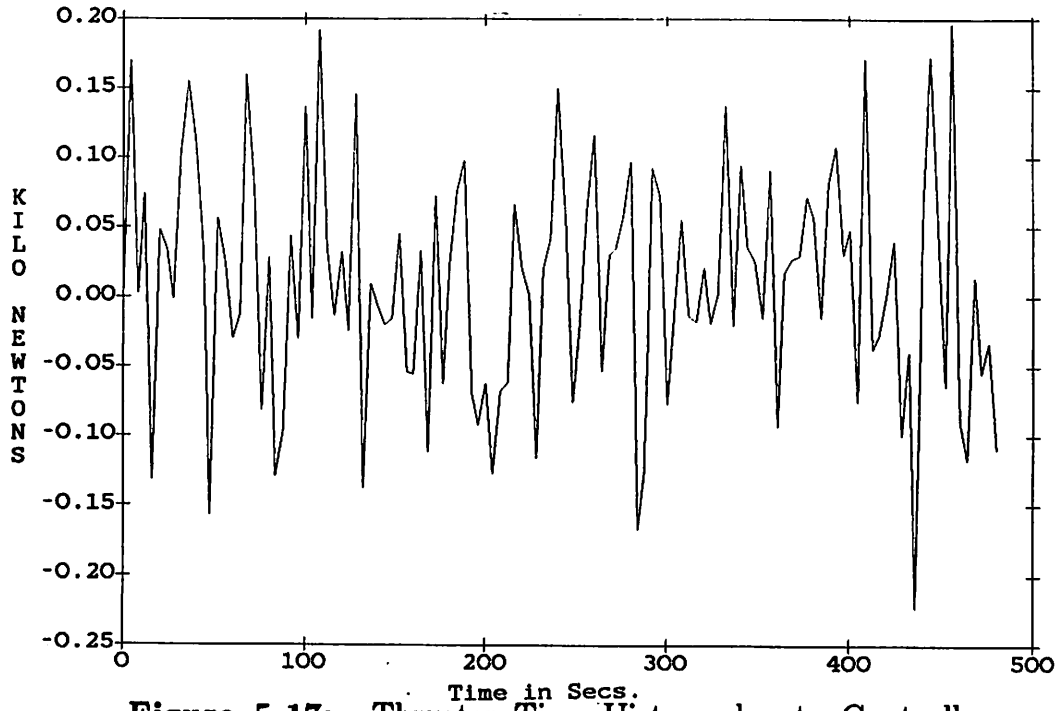

Figure 5-17: Thruster Time History due to Controller for the THLS and PAYLOAD.

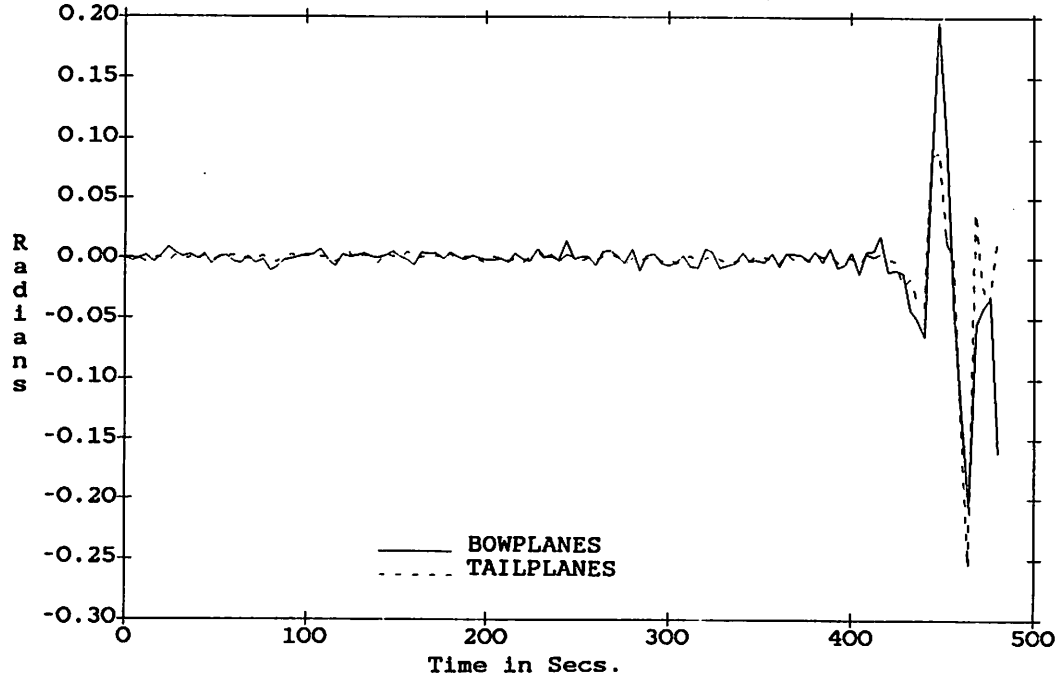

Figure 5-18: Control Deflections due to the Controller for the THLS and PAYLOAD.

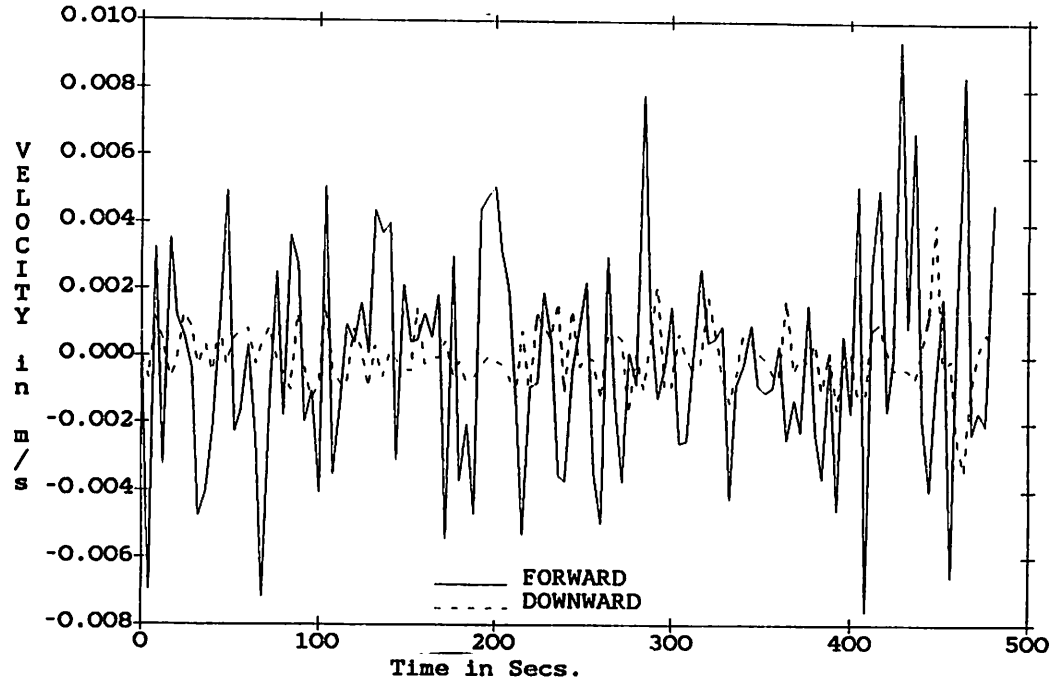

Figure 5-19: Perturbation Velocity of THLS and PAYLOAD.

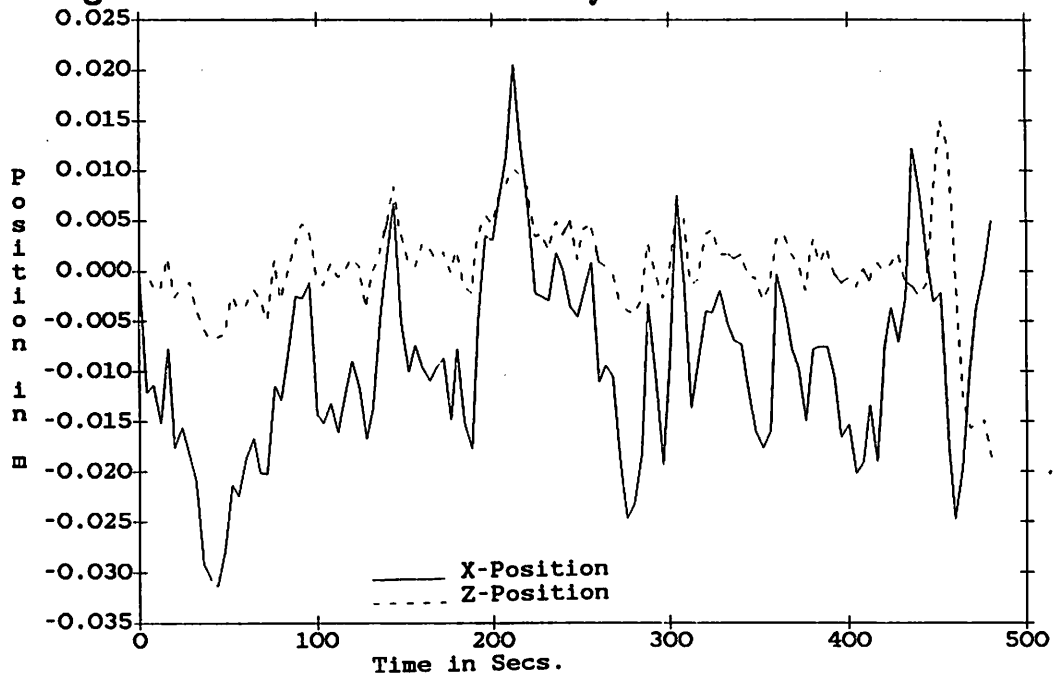

Figure 5-20: Perturbation Trajectory of THLS and PAYLOAD.

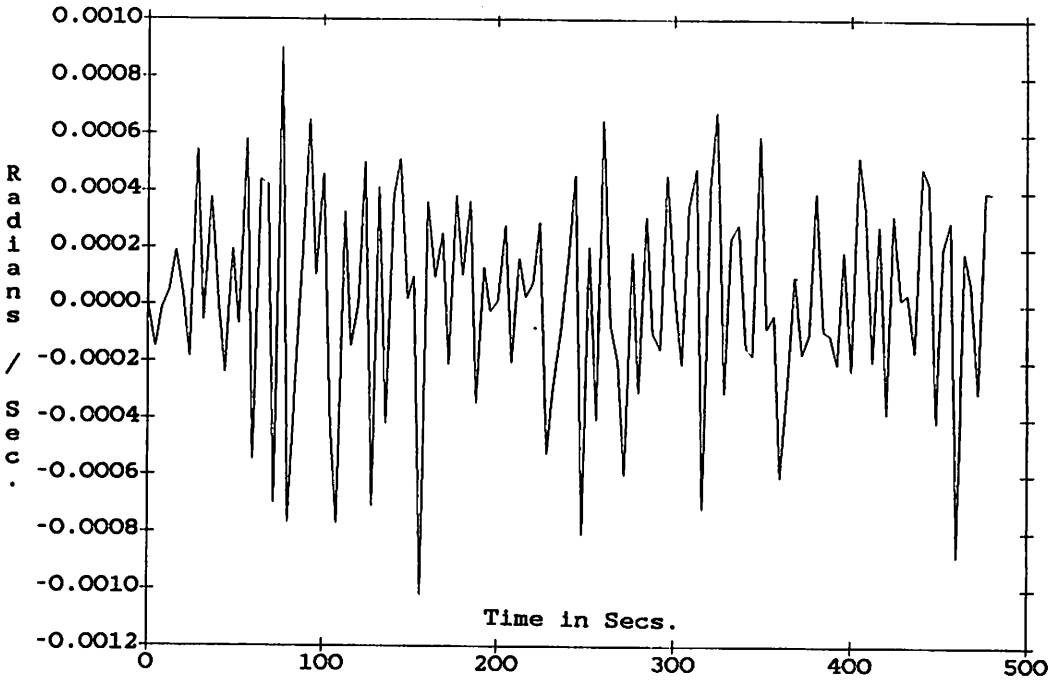

Figure 5-21: Perturbation Pitch Rate of THLS and PAYLOAD.

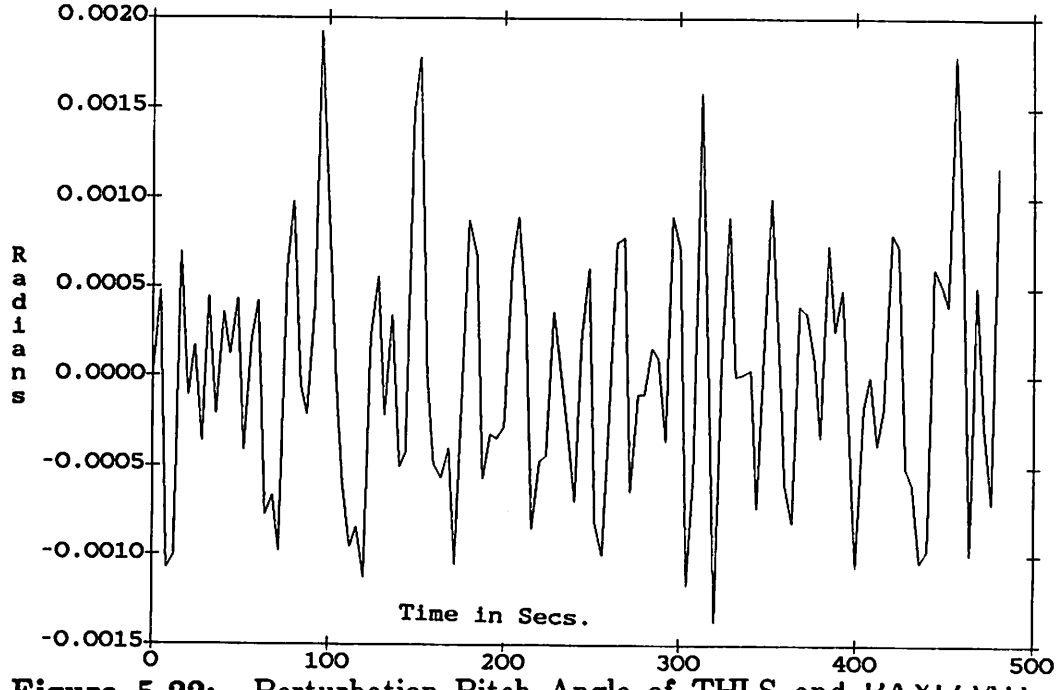

Figure 5-22: Perturbation Pitch Angle of THLS and PAYLOAD.

Chapter 6

Conclusion

6.1 Summary

This thesis covered the design process of a submersible, through the specific example of a Tethered Heavy Lift Submersible. After the design completed, the motion of the submersible was simulated to evaluate its performance and power requirements, both with and without payload. Finally, a controller was designed for the vehicle using LQG/LTR methodology and the simulations were repeated to evaluate the controller design.

- The materials available for use in pressure vessels, in the vehicle's frame and for buoyancy were presented. Presently the materials used for these three applications are titanium,aluminum and syntactic foam respectively. However, developments in sandwich foam core materials may provide better alternatives. In addition, the materials available for tether cable design were presented. The equipment that may be deployed on the submersible was investigated in terms of its possible weight and power requirements.
- In terms of equipment, two major types of equipment were considered : variable buoyancy systems and propulsion systems. The variable buoyancy system provides a flexible means of keeping the submersible neutrally buoyant despite its payload. There is however a certain amount of skepticism in the industry as to the effective performance of variable buoyancy systems. The problem

with propulsion is to be able to determine whether to use electrical thrusters or to use hydraulic thruster motors powered by an electrically driven pump. The consequences of this choice are illustrated, and it is found that the determing factor is the trade-off of decreased weight versus increased complexity and power required.

- The chapter on hydrodynamics provides methods for determining the added inertias, the lift, the drag and the pitching moment on various vehicle shapes. The methods for determining the lateral inertias, forces and coefficients are also covered. A few of these methods are not complete due to the lack of available information and some provide only rough estimates. Overall however, these methods should provide reasonable estimates of the hydrodynamics of the desired vehicle configuration.
- The design procedure is applied to the case of the Tethered Heavy Lift Submersible. The final iteration of the design procedure is carried out to determine the submersible's size, geometry and power requirements. The tether cable is also designed and a possible clump design is presented. The resulting system is of reasonable size and power requirements and may be airfreighted.
- The motion of the submersible is simulated in a shear flow with and without its 4,500 kg (wet) payload. The trajectory is between the clump which is around 300m off the sea floor and the worksite which is around 800m upstream. The simulation is two-dimensional in the vertical plane. The vehicle performed well and the overall dynamics of the vehicle with and without the payload were well

illustrated[5].

- The final chapter applies the Linear Quadratic Gaussian control methodolgy with Loop Transfer Recovery. This method employs singular values for loop shaping. The controller designed is non-linear through the use of gain scheduling. It is however, only two-dimensional since the purpose was to illustrate the control methodology. The controller improved the performance of the system considerably. The vehicle's response to disturbances was greatly attenuated.

6.2 Completion of Design Process

The present design is preliminary. In order to obtain a final design, the following steps need to be followed. If the preliminary design is satisfactory then a model is constructed in order to determine the vehicle's hydrodynamic characteristics with greater accuracy. The results of the model tests are then compared with the values predicted for the preliminary design. If the results are not desirable, then the design and the model should be altered accordingly and the model re-tested. If the results are acceptable then through curve fitting a more extensive and nonlinear model of the submersible is developed. The simulation model is then revised and the simulations are repeated. More stringent constraints may be introduced into the simulation to evaluate the

---

[5]Not included in the simulation model are the effects of partially filled buoyancy tanks. These may affect the dynamics of the submersible, however in our preliminary design it was felt that the number of buoyancy tanks should make this effect negligible. Clearly, these should be included in the simulation model if it is felt their contribution to the vehicle's dynamics is significant.

submersible's performance. This revised model is then used as the basis for the design of the non-linear controller, which is subsequently evaluated by simulations.

The design process is iterative and if at any time the design is unsatisfactory the previous step must be repeated. Thus having carried out the previous steps the final design may be carried out. This involves designing the different components of the submersible,then manufacturing and assembling them into a final prototype. It is hoped that by the time this stage is reached, any modifications to the design will be minor. In the design procedure the considerations of cost, production of required equipment and parts in the required delays has not been considered. These are important aspects of the design process, but will not be discussed in this thesis.

6.3 Considerations for Further Research

The two topics which seem to require more attention are the development of a sophisticted simulation program and a more extensive research on the hydrodynamics of submersible type shapes. More accurate results would reduce the amount of model testing required, although it would be impossible to eliminate it completely. As for the simulation program, the greater its sophistication the more usefull a tool it becomes. It can be used for designing the submersible, trying out different control strategies and also as a training tool. In the long term, once the simulation system is well developed and an adequate controller for the vehicle is designed, then the development of sophisticated automated navigation and sensing capabilities may be integrated into the vehicle. The cost of computational power has greatly

dropped, as has the cost of all electronic components. One may expect the significant cost and performance of the vehicle to depend on the physical design of the system and the software that controls it. The most significant cost in the long term may be in developing and maintaining the software for highly automated submersibles, if there is a need for such vehicles.

Appendix A

General Derivation of Acceleration Coefficients from Reference [37].

An alternate method for added mass coefficients to the one presented here may be found in reference [61]. The following six Lagrange equations are the momentum equations for the body-fluid system.

$$\frac{d}{dt}\frac{\partial T}{\partial u} = r\frac{\partial T}{\partial v} - q\frac{\partial T}{\partial w} - X$$

$$\frac{d}{dt}\frac{\partial T}{\partial v} = p\frac{\partial T}{\partial w} - r\frac{\partial T}{\partial u} - Y$$

$$\frac{d}{dt}\frac{\partial T}{\partial w} = q\frac{\partial T}{\partial w} - p\frac{\partial T}{\partial v} - Z$$

$$\frac{d}{dt}\frac{\partial T}{\partial p} = w\frac{\partial T}{\partial v} - v\frac{\partial T}{\partial w} + r\frac{\partial T}{\partial q} - q\frac{\partial T}{\partial r} - K$$

$$\frac{d}{dt}\frac{\partial T}{\partial q} = u\frac{\partial T}{\partial w} - w\frac{\partial T}{\partial u} + p\frac{\partial T}{\partial r} - r\frac{\partial T}{\partial p} - M$$

$$\frac{d}{dt}\frac{\partial T}{\partial r} = v\frac{\partial T}{\partial u} - u\frac{\partial T}{\partial v} + q\frac{\partial T}{\partial p} - p\frac{\partial T}{\partial q} - N$$

X = force in surge direction.
Y = force in sway direction.
Z = force in heave direction.

K = Rolling Moment.
M = Pitching Moment.
N = Yawing Moment.

u = surge velocity.
v = sway velocity.
w = heave velocity.

p = roll angular velocity.

q = pitch angular velocity.
r = yaw angular velocity.

T = total kinetic energy = $T_b + T_f$
T_b = body's kinetic energy.
T_f = fluid's kinetic energy.

From [37] the fluid's kinetic energy, T_f, is

$$2T_f = Au^2 + Bv^2 + Cw^2 + 2A'vw + 2B'wu + 2C'vu + Pp^2 + Qq^2 + Rr^2 + 2P'gr + 2Q'rp + 2R'pq + 2Lup + 2Mvp + 2Nwr + 2F(vr + wq) + 2G(wp + ur) + 2H(uq + vp) + 2F'(vr - wq) + 2G'(wp - ur) + 2H'(uq - vp)$$

let $F + F' = F_1$, $F - F' = F_2$, $G + G' = G_1$, $G - G' = G_2$,
$H + H' = H_1$, $H - H' = H_2$

thus A, B, C, A', B', C', P, Q, R, P', Q', R', L, M, N, F, G, H, F', G', H' are the acceleration coefficients or added mass terms.

A.1 X - Force, Surge

$$-X = \frac{d}{dt}\frac{\partial T_f}{\partial u} - r\frac{\partial T_f}{\partial v} + q\frac{\partial T_f}{\partial w}$$

$$\frac{d}{dt}\frac{\partial T_f}{\partial u} = A\dot{u} + B'\dot{w} + C'\dot{v} + L\dot{p} + G\dot{r} + G'\dot{r} + H\dot{q} + H'\dot{q}$$

$$-r\frac{\partial T_f}{\partial v} = -Brv - A'rw - C'ru - Mrq - Frr - F'rr - Hrp + H'rp$$

$$q\frac{\partial T_f}{\partial w} = Cqw + A'qv + B'qu + Nqr + Fqq - F'qq + Gqp + G'qp$$

$$X = -A\dot{u} - B'\dot{w} - C'\dot{v} - L\dot{p} - G_2\dot{r} - H_1\dot{q} + Brv + A'rw + C'ru + Mrq + F_1rr + H_2rp - Cqw - A'qv - B'qu - Nqr - F_2qq - G_1qp$$

$$A = -X_{\dot{u}}, \quad A' = X_{rw} = -X_{q\dot{v}}, \quad L = -X_{\dot{p}}, \quad F_1 = X_{rr}$$
$$F_2 = -X_{qq}$$

$$B = X_{r\dot{v}}, \quad B' = -X_{\dot{w}} = -X_{q\dot{u}}, \quad M = (X_{rq})_1,$$
$$G_1 = -X_{qp}, \quad G_2 = -X_{\dot{r}}$$

$$C = -X_{qw}, \quad C' = -X_{\dot{v}} = X_{ru}, \quad N = -(X_{qr})_2,$$
$$H_1 = -X_{\dot{q}}, \quad H_2 = X_{rp}$$

$$X_{rq} = M - N$$

A.2 Y - Force, Sway

$$-Y = \frac{d}{dt}\frac{\partial T_f}{\partial v} - p\frac{\partial T_f}{\partial w} + r\frac{\partial T_f}{\partial u}$$

$$\frac{d}{dt}\frac{\partial T_f}{\partial v} = B\dot{v} + A'\dot{w} + C'\dot{u} + M\dot{q} + F\dot{r} + F'\dot{r} + H\dot{p} - H'\dot{p}$$

$$- p\frac{\partial T_f}{\partial w} = -Cpw - A'pv - B'pu - Npr - Fpq + F'pq - Gpp - G'pp$$

$$r\frac{\partial T_f}{\partial u} = Aru + B'rw + C'rv + Lrp - Grr - G'rr + Hrq + H'rq$$

$$Y = -B\dot{v} - A'\dot{w} - C'\dot{u} - M\dot{q} - F_1\dot{r} - H_2\dot{p} + Cpw + A'pv + B'pw + Npr$$
$$+ F_2pq - G_1pp - Aru - B'rw - C'rv - Lrp - G_2rr - H_1rq$$

$$A = -Y_{\dot{v}}, \quad A' = -Y_{\dot{w}} = Y_{pv}, \quad M = -Y_{\dot{q}}, \quad F_1 = -Y_{\dot{r}},$$
$$F_2 = Y_{pq}$$

$$B = -Y_{\dot{v}}, \quad B' = -Y_{rw} = Y_{pu}, \quad N = (Y_{pr})_1,$$
$$G_1 = Y_{pp}, \quad G_2 = -Y_{rr}$$

$$C = Y_{pw}, \quad C' = -Y_{\dot{u}} = -Y_{rv}, \quad L = (-Y_{rp})_2,$$
$$H_1 = -Y_{rq}, \quad H_2 = -Y_{\dot{p}}$$

$$Y_{rp} = N - L$$

A.3 Z - Force, Heave

$$-Z = \frac{d}{dt}\frac{\partial T_f}{\partial w} - q\frac{\partial T_f}{\partial u} + p\frac{\partial T_f}{\partial v}$$

$$\frac{d}{dt}\frac{\partial T_f}{\partial w} = C\dot{w} + A'\dot{v} + B'\dot{u} + N\dot{r} + F'\dot{q} + G\dot{p} + G'\dot{p}$$

$$-q\frac{\partial T_f}{\partial u} = -Aqu - B'qw - C'qv - Lqp - Gqr + G'qr - Hqq - H'qq$$

$$p\frac{\partial T_f}{\partial v} = Bpv + A'pw + C'pu + Mpq + Fpr + F'pr + Hpp - H'pp$$

$$Z = -C\dot{w} - A'\dot{v} - B'\dot{u} - N\dot{r} - F_2\dot{q} - G_1\dot{p} + Aqu + B'qw + C'qv + Lqp + G_2qr + H_1qq - Bpv - A'pw - C'pu - Mpq - F_1pr - H_2pp$$

$$A = Z_{qu}, \quad A' = -Z_{\dot{v}} = -Z_{pw}, \quad L = (Z_{qp})_1,$$
$$F_1 = -Z_{pr}, \quad F_2 = -Z_{\dot{q}}$$

$$B = -Z_{pv}, \quad B' = Z_{qw} = -Z_{\dot{u}}, \quad M = (-Z_{pq})_2,$$
$$G_1 = -Z_{\dot{p}}, \quad G_2 = -Z_{qr}$$

$$C = -Z_{\dot{w}}, \quad C' = Z_{qv} = -Z_{pu}, \quad N = -Z_{\dot{r}}, \quad H_1 = Z_{qq},$$
$$H_2 = -Z_{pp}$$

Other resulting relations: $Z_{pq} = L - M$

A.4 K - Moment, Roll

$$K = -\frac{d}{dt}\frac{\partial T_f}{\partial p} + w\frac{\partial T_f}{\partial v} - v\frac{\partial T_f}{\partial w} + r\frac{\partial T_f}{\partial q} - q\frac{\partial T_f}{\partial r}$$

$$-\frac{d}{dt}\frac{\partial T_f}{\partial p} = -P\dot{p} - Q'\dot{r} - R'\dot{q} - L\dot{u} - G_1\dot{w} - H_2\dot{v}$$

$$w\frac{\partial T_f}{\partial v} = Bmw + A'ww + C'wu + Mwq + F_1wr + H_2wp$$

$$-v\frac{\partial T_f}{\partial w} = Cvw - A'vv - B'vu - Nvr - F_2vq - G_1vp$$

$$r\frac{\partial T_f}{\partial q} = Qrp + P'rr + R'rp + Mrv + F_2rw + H_1ru$$

$$-q\frac{\partial T_f}{\partial r} = Rqr - P'qq - Q'qp - Nqw - F_1qv - G_2qu$$

$$A' = K_{ww} = -K_{vv}, \qquad L = -K_u^{\cdot}, \qquad F_1 = (K_{wr})_1 = (-K_{qv})_1,$$

$$B = (K'_{wv})_1, \qquad B' = -K_{vu}, \qquad M = (K_{wq})_1 = (K_{rv})_1,$$
$$G_1 = K_{vp} = -K_w^{\cdot}$$

$$C = (-K_{vw})_2, \qquad C' = K_{wu}, \qquad N = (-K_{vr})_2 = (-K_{qw})_2,$$
$$H_1 = K_{ru}$$

$$F_2 = (-K_{vq})_2 = (K_{rw})_2, \qquad P = -K_p^{\cdot}$$
$$P' = K_{rr} = -K_{qq}$$

$$G_2 = -K_{qu}, \qquad Q = (K_{rq})_1, \qquad Q' = -K_r^{\cdot} = -K_{qp},$$

$$H_2 = -K_v^{\cdot} = K_{wp}, \qquad R = (-K_{qr})_2, \qquad R' = -K_q^{\cdot} = K_{rp},$$

Other resulting relations:
$$K_{wv} = B - C$$
$$K_{vr} = M - N$$
$$K_{qw} = M - N$$
$$K_{rw} = F_1 + F_2 = 2F$$
$$K_{vq} = -F_1 - F_2 = -2F$$
$$K_{qr} = Q - R$$

A.5 M - Moment, Pitch

$$M = -\frac{d}{dt}\frac{\partial T_f}{\partial q} + u\frac{\partial T_f}{\partial w} - w\frac{\partial T_f}{\partial u} + p\frac{\partial T_f}{\partial r} - r\frac{\partial T_f}{\partial p}$$

$$-\frac{d}{dt}\frac{\partial T_f}{\partial q} = -Q\dot{q} - P'\dot{r} - R'\dot{p} - M\dot{v} - F_2\dot{w} - H_1\dot{u}$$

$$u\frac{\partial T_f}{\partial w} = Cuw + A'uv + B'uu + Nur + F_2uq + G_1up$$

$$- w\frac{\partial T_f}{\partial u} = -Awu - B'ww - C'wv - Lwp - G_2wr - H_1wq$$

$$p\frac{\partial T_f}{\partial r} = Rpr + P'pq + Q'pp + Npw + F_1pv + G_2pu$$

$$- r\frac{\partial T_f}{\partial p} = -Prp - Q'rr - R'rq - Lru - G_1rw - H_2rv$$

$A = (-M_{wu})_1$, $A' = M_{uv}$, $L = (-M_{wp})_1 = (-M_{ru})_1$, $F_1 = M_{pv}$

$B' = M_{ww} = M_{uu}$, $M = -M_v^{\cdot}$, $G_1 = (M_{up})_1$

$C = (M_{uw})_2$, $C' = -M_{wv}$, $N = (M_{pw})_2 = (M_{ur})_2$, $H_1 = -M_u^{\cdot} = -M_{wq}$

$F_2 = -M_w^{\cdot} = M_{uq}$, $P = (-M_{rp})_1$, $P' = -M_r^{\cdot} = M_{pq}$,

$G_2 = (-M_{wr})_2 = (M_{pu})_2$, $Q = -M_q^{\cdot}$, $Q' = -M_{rr} = M_{pp}$

$H_2 = -M_{rv}$, $R = (M_{pr})_2$, $R' = -M_p^{\cdot} = M_{rq}$

Other resulting relations: $M_{wu} = C - A$
$M_{pw} = N - L$
$M_{ru} = N - L$
$M_{pu} = G_1 + G_2 = 2G$
$M_{rw} = -G_1 - G_2 = -2G$
$M_{rp} = R - P$

A.6 N - Moment, Yaw

$$N = \frac{d}{dt}\frac{\partial T_f}{\partial r} + v\frac{\partial T_f}{\partial u} - u\frac{\partial T_f}{\partial v} + q\frac{\partial T_f}{\partial p} - p\frac{\partial T_f}{\partial q}$$

$$\frac{d}{dt}\frac{\partial T_f}{\partial r} = -R\dot{r} - P'\dot{q} - Q'\dot{p} - N\dot{w} - F_2\dot{v} - G_2\dot{u}$$

$$v\frac{\partial T_f}{\partial u} = Avu + B'vw + C'vv + Lvp + G_2vr + H_1vq$$

$$- u\frac{\partial T_f}{\partial v} = -Buv - A'uw - C'uu - Muq - F_1ur - H_2up$$

$$q\frac{\partial T_f}{\partial p} = Pqp + Q'qr + P'qq + Lqu + G_1qw + H_2qv$$

$$- p\frac{\partial T_f}{\partial q} = -Qpq - P'pr - R'pp - Mpv - F_2pw - H_1pu$$

$A = (N_{vu})_1$, $A' = N_{uw}$, $L = (N_{vp})_1 = (N_{qu})_1$,
$F_1 = -N^{\bullet}_v = -N_{ur}$

$B = (-N_{uv})_2$, $B' = N_{vw}$, $M = (-N_{vw})_2 = (-N_{pv})_2$,
$G_1 = N_{qw}$

$C' = N_{vv} = -N_{uu}$, $N = -N^{\bullet}_w$, $H_1 = (N_{vq})_1 = (-N_{pu})_1$,

$F_2 = -N_{pw}$, $P = (N_{qp})_1$, $P' = -N^{\bullet}_q = -N_{pr}$

$G_2 = -N^{\bullet}_u = N_{vr}$, $Q = (-N_{pq})_2$, $Q' = -N^{\bullet}_p = N_{qr}$,
$H_2 = (-N_{up})_2 = (N_{qv})_2$, $R = -N^{\bullet}_r$, $R' = N_{qq} = N_{pp}$,

Other resulting relations: $N_{vu} = A - B$
$N_{vp} = L - M$
$N_{qu} = L - M$
$N_{vq} = H_1 + H_2 = 2H$
$N_{pu} = -H_1 - H_2 = -2H$
$N_{pq} = P - Q$

$$A = -X^{\bullet}_u = -Y_{ru} = Z_{qu} = (-M_{wu})_1 = (N_{vu})_1$$

$$B = -Y^{\bullet}_v = X_{rv} = -Z_{pv} = (K_{wv})_1 = (-N_{uv})_2$$

$$C = -Z^{\bullet}_w = -X_{qw} = Y_{pw} = (-K_{vw})_2 = (M_{uw})_2$$

$$A' = -Z^{\bullet}_v = Y^{\bullet}_w = X_{rw} = -X_{qv} = Y_{pv} = -Z_{pw} = K_{ww}$$
$$= -K_{vv} = M_{uv} = N_{uw}$$

$$B' = -X^{\bullet}_w = -Z^{\bullet}_u = -X_{qu} = -Y_{rw} = Y_{pu} = Z_{qw} = -K_{vu}$$
$$= -M_{ww} = M_{uu} = N_{vw}$$

$$C' = -X^{\bullet}_{v} = -Y^{\bullet}_{u} = X_{ru} = -Y_{rv} = Z_{qv} = -Z_{pu} = K_{wu}$$
$$= -M_{wv} = N_{vv} = -N_{uu}$$

$$L = -X^{\bullet}_{p} = -K^{\bullet}_{u} = (Z_{qp})_1 = (-Y_{rp})_1 = (-M_{wp})_1$$
$$= (-M_{ru})_1 = (N_{vp})_1 = (N_{qu})_1$$

$$M = -Y^{\bullet}_{q} = -M^{\bullet}_{v} = (X_{rq})_1 = (-Z_{pq})_2 = (K_{wq})_1$$
$$= (K_{rv})_1 = (-N_{uq})_2 = (-N_{pv})_1$$

$$N = -Z^{\bullet}_{r} = -N^{\bullet}_{w} = (-X_{qr})_2 = (Y_{rp})_2 = (-K_{vr})_2$$
$$= (-K_{qw})_2 = (M_{pw})_2 = (M_{ur})_2$$

$$F_1 = Y^{\bullet}_{r} = -N^{\bullet}_{v} = X_{rr} = -Z_{pr} = (K_{wr})_1$$
$$= (K_{qv})_1 = M_{pv} = -N_{ur}$$

$$G_1 = -Z^{\bullet}_{p} = -K^{\bullet}_{w} = -X_{qp} = Y_{pp} = K_{vp} = (M_{up})_1$$
$$= (-M_{rw})_1 = N_{qw}$$

$$H_1 = -X^{\bullet}_{q} = -M^{\bullet}_{u} = -Y_{rq} = Z_{qq} = K_{ru} = -M_{wq}$$
$$= (N_{vq})_1 = (-N_{pu})_1$$

$$F_2 = -Z^{\bullet}_{q} = -M^{\bullet}_{w} = -X_{qq} = Y_{pq} = (K_{vq})_2$$
$$= (K_{rw})_2 = M_{uq} = -N_{pw}$$

$$G_2 = -X^{\bullet}_{r} = -N^{\bullet}_{u} = -Y_{rr} = -Z_{qr} = -K_{qu} = (-M_{wr})_2$$
$$= (M_{pu})_2 = N_{vr}$$

$$H_2 = -Y^{\bullet}_{p} = -K^{\bullet}_{v} = X_{rp} = -Z_{pp} = K_{wp} = -M_{rv}$$
$$= (-N_{up})_2 = (N_{qv})_2$$

$$P = -K^{\bullet}_{p} = (-M_{rp})_1 = (N_{qp})_1$$

$$Q = -M^{\bullet}_{q} = (K_{rq})_1 = (-N_{pq})_2$$

$$R = -N_r^{\bullet} = (-K_{qr})_2 = (M_{pr})_2$$

$$P' = -M_r^{\bullet} = -N_q^{\bullet} = K_{rr} = -K_{qq} = M_{pq} = -N_{pr}$$

$$Q' = -K_r^{\bullet} = -N_p^{\bullet} = -K_{qp} = -M_{rr} = M_{pp} = N_{qr}$$

$$R' = -K_q^{\bullet} = -M_p^{\bullet} = K_{rp} = -M_{rq} = N_{qq} = -N_{pp}$$

When xz-plane symmetry exists, then the following coefficients are zero; A', C', P', R', L, M, N, G, G'.

When the yz-plane symmetry exists, then the following coefficients are zero; B', C', Q', R', L, M, N, F, F'.

When two planes of symmetry exist, all of the terms that are zero in the single plane cases are zero.

Appendix B

Acceleration Coefficients for an Ellipsoid with Three Unequal Axes

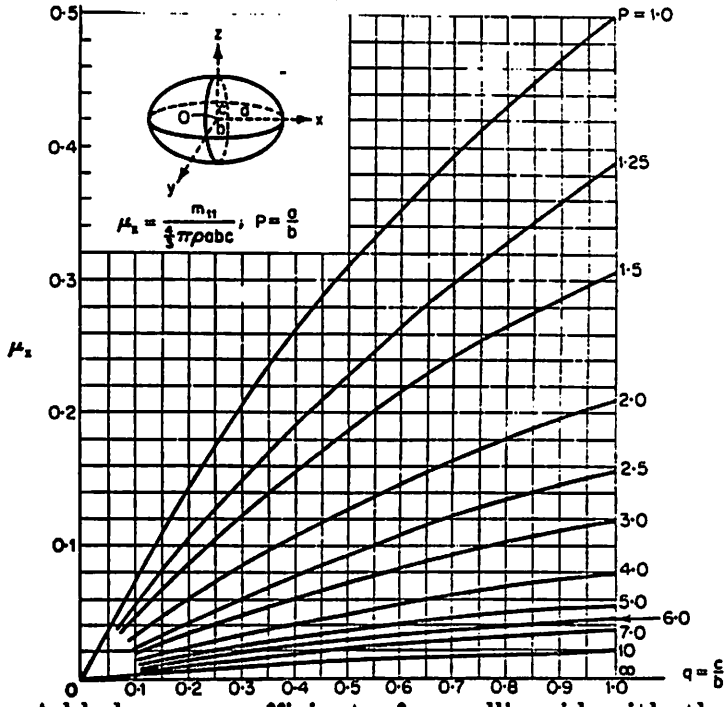

Figure B-1: Added-mass coefficient of an ellipsoid with three unequal axes, for acceleration along the longest axis.

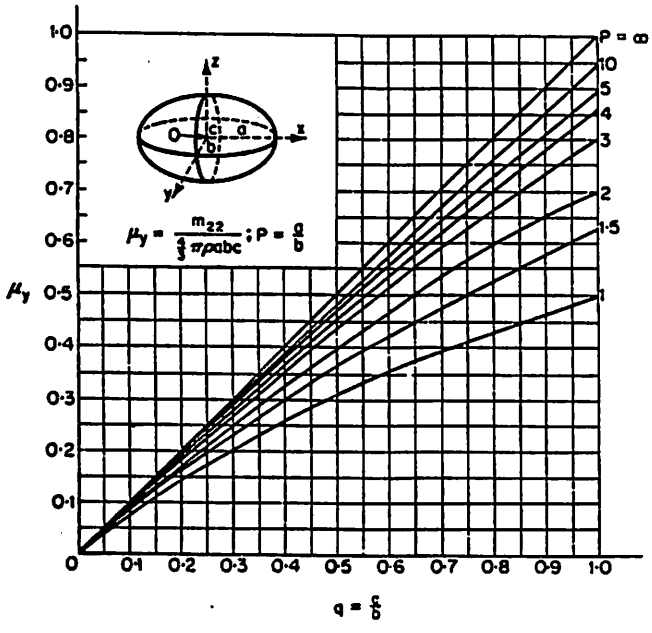

Figure B-2: Added-mass coefficient of an ellipsoid with three unequal axes, for acceleration along the intermediate axis.

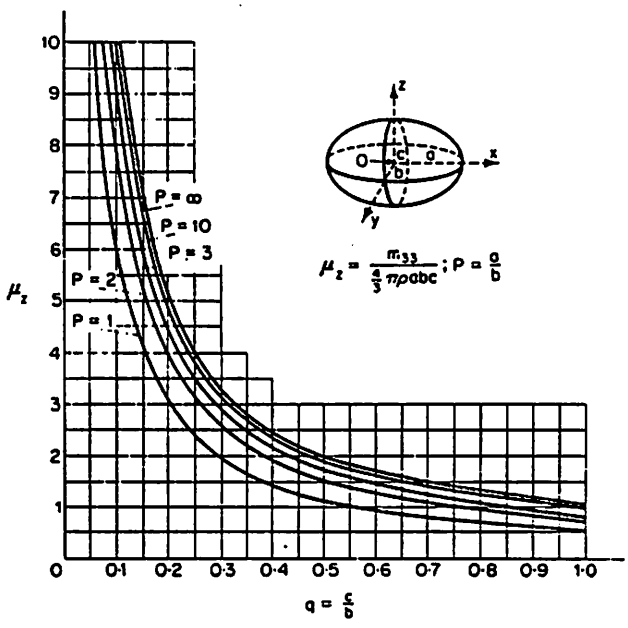

Figure B-3: Added-mass coefficient of an ellipsoid with three unequal axes, for acceleration along the shortest axis.

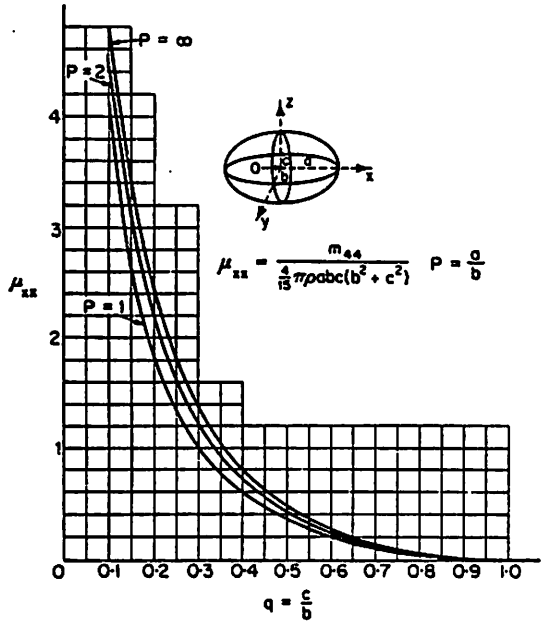

Figure B-4: Added moment of inertia coefficient of an ellipsoid, for rotation about the longest axis.

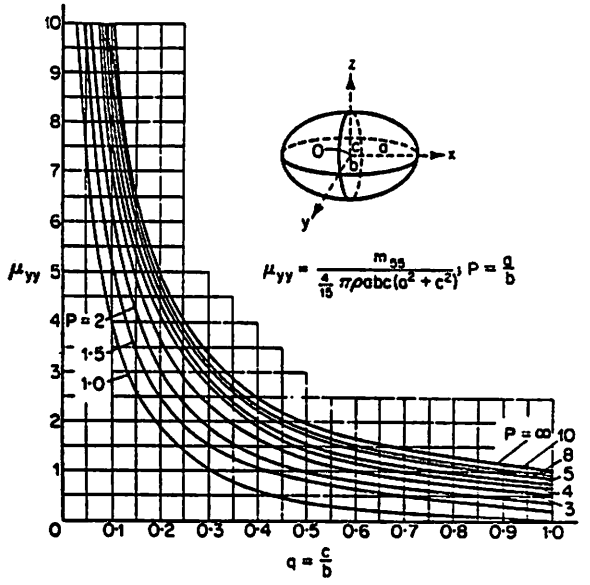

Figure B-5: Added moment of inertia coefficient of an ellipsoid, for rotation about the intermediate axis.

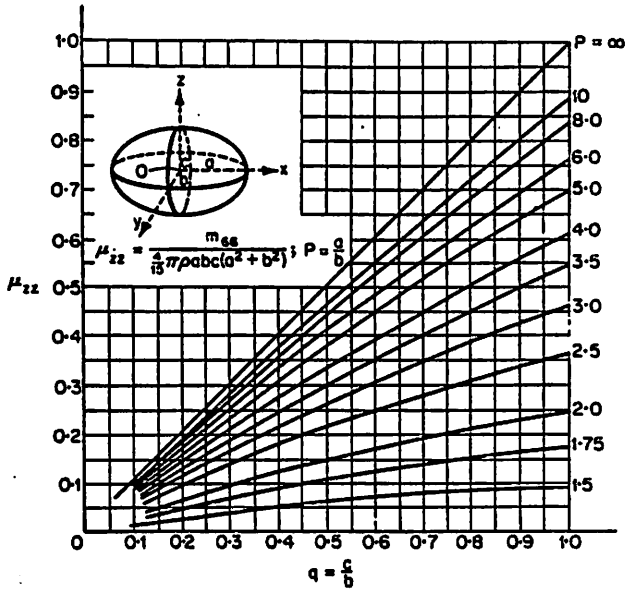

Figure B-6: Added moment of inertia coefficient of an ellipsoid, for rotation about the shortest axis.

Appendix C

Drag, Lift and Pitching Moment for Box Shaped Vehicles.

The following figures were obtained from reference [60] and is the result of experimental work done by H. Nakaguchi.

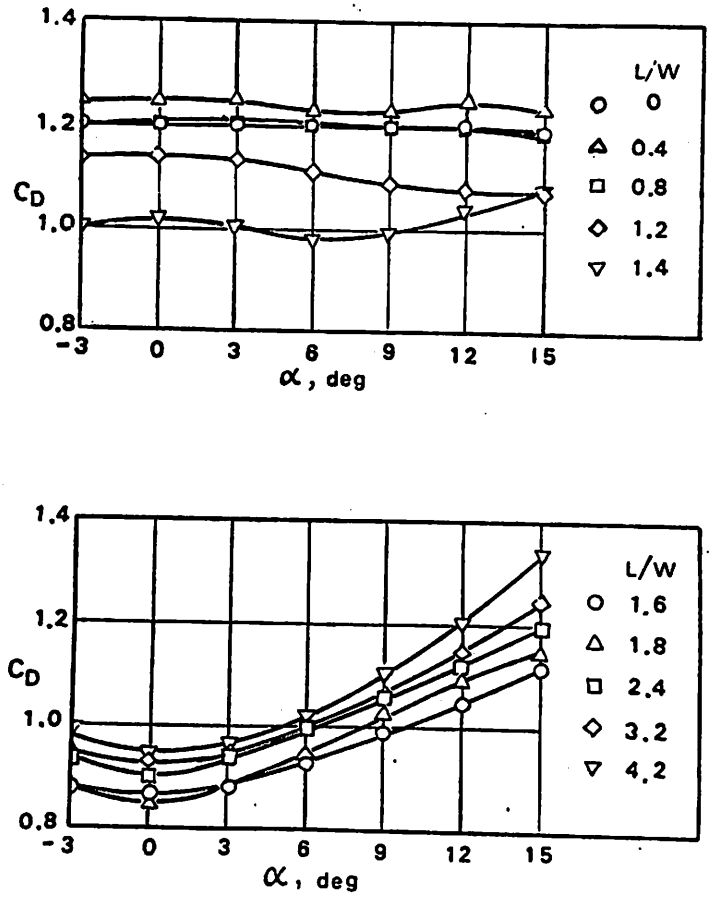

Figure C-1: Wind-axis drag coefficient vs. angle of incidence.

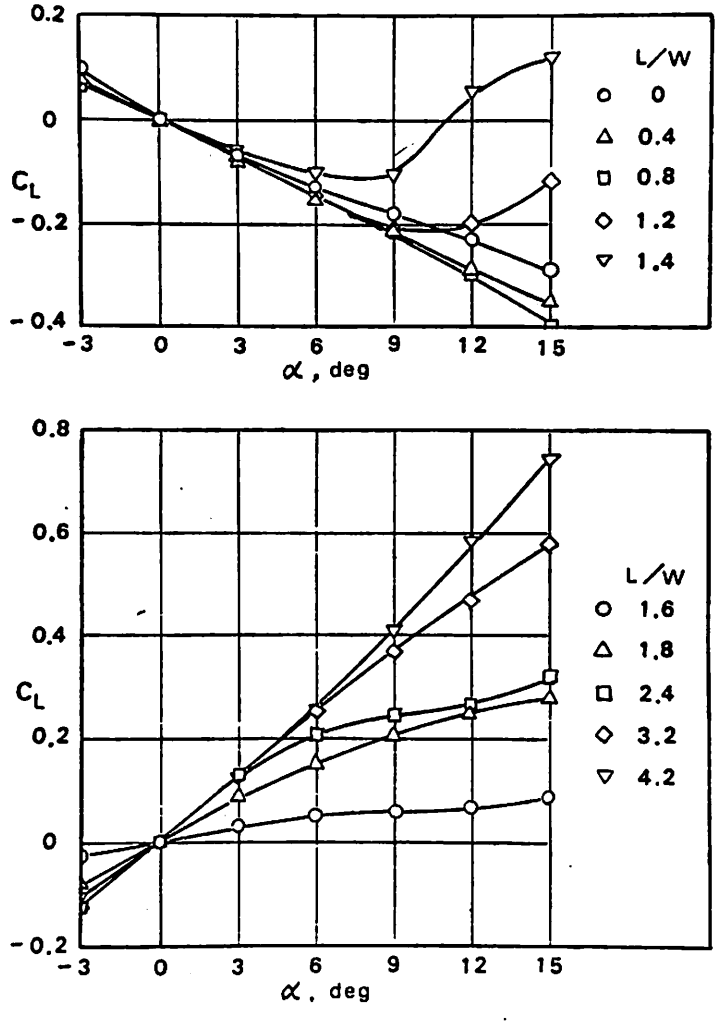

Figure C-2: Wind-axis lift coefficient vs. angle of incidence.

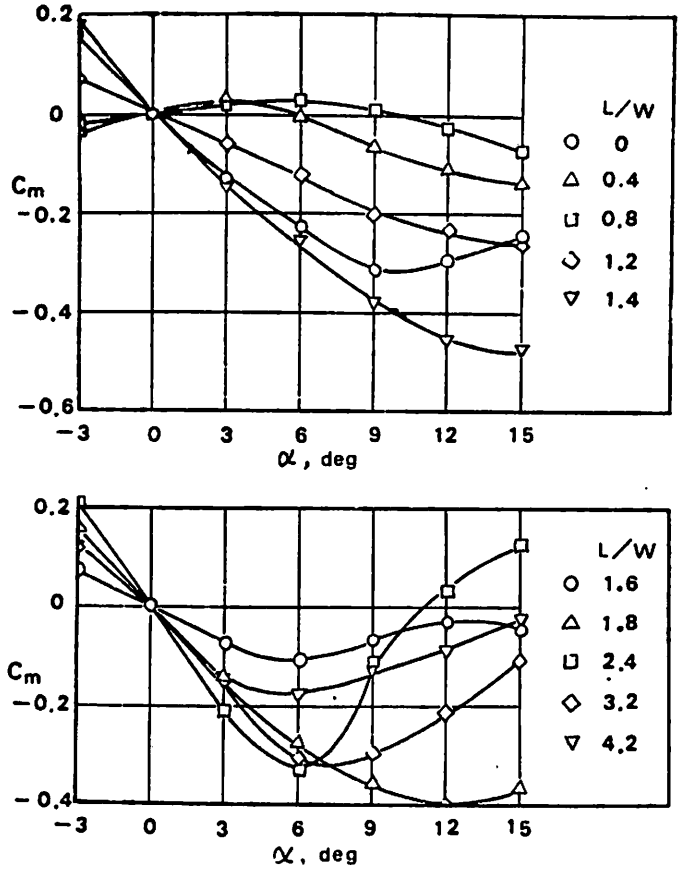

Figure C-3: Wind-axis pitching moment coefficient vs. angle of incidence.

Appendix D

Derivation of the Simulation Coefficients

In this appendix two different types of coefficients are derived, the steady state coefficients and the perturbation coefficients. For the steady state coefficients the gravitational and cable forces due to the vehicle's attitude are derived. For the perturbation coefficients the gravitational and cable forces due to the vehicle's attitude are derived, aswell as the circulation and viscous terms.

D.1 Steady State Gravitational Terms

The forces due to gravity are zero since the vehicle is neutrally buoyant. Furthermore, since the co-ordinate system is at the vehicle's geometric center the only ptiching moment is due to the moment arm to the center of gravity. The forces due to gravity are given as the vector $\mathbf{F}_G$ and the location of the center of gravity as $\mathbf{r}_G$.

$$\mathbf{F_G} = \begin{bmatrix} 0 \\ 0 \\ mg \end{bmatrix} \text{ and } \mathbf{r_G} = \begin{bmatrix} x_G \\ y_G \\ z_G \end{bmatrix} \tag{D.1}$$

If the vehicle is rotated by an angle θ (about the y-axis), the forces due to gravity become,

$$\mathbf{F_G} = \begin{bmatrix} -mg\ \sin\theta \\ 0 \\ mg\ \cos\theta \end{bmatrix} \tag{D.2}$$

The gravitational moments are given by $\mathbf{M_g} = \mathbf{r_G} \times \mathbf{F_G}$

$$\begin{aligned} M_g &= -mg \{ z_G \sin\theta + x_G \cos\theta \} \int \\ M_G &= -mg \{ z_G \sin\theta + x_G \cos\theta \} \end{aligned} \tag{D.3}$$

D.2 Steady-State Cable Terms

The cable exerts a tension T_C at a distance z_C above the center of the co-ordinate system (x_C and y_C are chosen as zero). The cable's inclination to the horizontal is the angle ψ and the vehicle's attitude is the angle θ (See figure D-1). The cable forces and moment are,

$$\begin{aligned} X_C &= -T_C \cos(\psi + \theta) \\ Y_C &= -T_C \sin(\psi + \theta) \end{aligned} \tag{D.4}$$

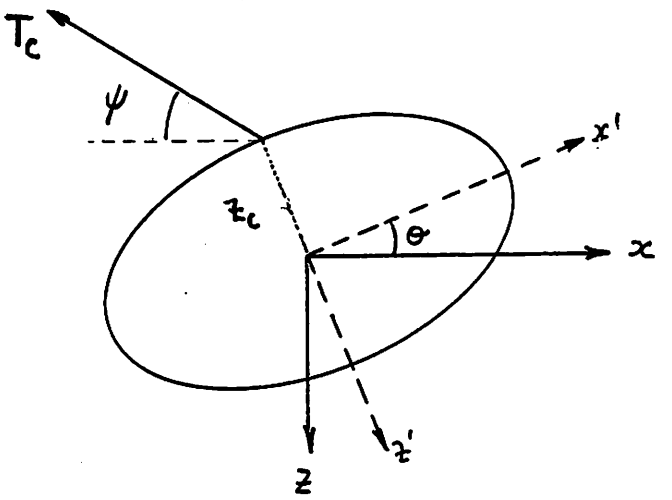

Figure D-1: Cable Forces and Moments on the Submersible.

$$M_C = z_C X_C$$

D.3 Perturbation Terms due to Gravity

These are derived from the steady-state terms by setting $\theta = \theta_o + \tilde{\theta}$. Then $\sin \theta \simeq \theta_o + \tilde{\theta}$ and $\cos \theta \simeq 1 - \theta_o\tilde{\theta}$. The result is,

$$\tilde{M}_G = mg\ (x_G\theta_o - z_G)\ \tilde{\theta} \qquad (D.5)$$

D.4 Lift and Circulation Perturbation Terms

In this section the perturbation terms for the forces X, Z and the moment M are derived. Note, that since the terms X_q, Z_q and M_q are linear, as is M_w, these are also the perturbation coefficients. Such that,

$$X_q = X_{\tilde{q}}\ ,\ Z_q = Z_{\tilde{q}},\ M_q = M_{\tilde{q}}\ ,\ M_w = M_{\tilde{w}}.$$

The terms $X_{\dot{u}}$, $X_{\dot{w}}$, $Z_{\dot{u}}$, $Z_{\dot{w}}$ are derived as follows (see figure D-2), first the terms due to variations in angle of incidence are derived.

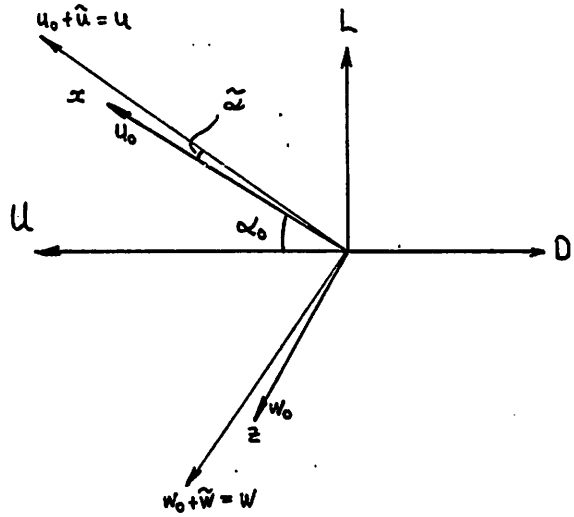

Figure D-2: Coordinate System Relative to Perturbations in the Current.

α = angle of attack of the vehicle.
$\alpha = \alpha_o + \tilde{\alpha}$ where $\sin \tilde{\alpha} \simeq \tilde{\alpha}$.

$$\tan \alpha_o = \frac{w_o}{u_o} \text{ and } \tan (\alpha_o + \tilde{\alpha}) = \frac{w_o + \tilde{w}}{u_o + \tilde{u}}$$

$$\tan (\alpha_o + \tilde{\alpha}) = \left(\frac{\tan\alpha_o + \tan\tilde{\alpha}}{1 - \tan\alpha_o \tan\tilde{\alpha}} \right) \simeq \left(\frac{\tan\alpha_o + \tilde{\alpha}}{1 - \tilde{\alpha} \tan\alpha_o} \right)$$

$$\tan (\alpha_o + \tilde{\alpha}) = \frac{w_o + \tilde{w}}{u_o + \tilde{u}} \simeq \frac{w_o/u_o + \tilde{\alpha}}{1 - \tilde{\alpha}\, w_o/u_o}$$

$$\tilde{\alpha} = \frac{u_o\tilde{w} - w_o\tilde{u}}{u_o^2 + w_o^2} = \frac{u_o\tilde{w} - w_o\tilde{u}}{U^2} \qquad (D.6)$$

$$\frac{\partial\, \tilde{\alpha}}{\partial\, \tilde{u}} = \frac{-\, w_o}{U^2} \text{ and } \frac{\partial\, \tilde{\alpha}}{\partial\, \tilde{u}} = \frac{u_o}{U^2}$$

The lift and drag forces are given as,

$$L = \frac{1}{2}\rho U^2 S\, C_{L_\alpha}\alpha = \frac{1}{2}\rho U^2 S\, C_{L_\alpha}(\alpha_o + \tilde{\alpha})$$

$$D = \frac{1}{2}\rho U^2 S\,(C_{D_o} + C_{D_2}\,\alpha^2) \qquad (D.7)$$

$$= \frac{1}{2}\rho U^2 S\,(C_{D_o} + C_{D_2}\,(\alpha_o^2 + 2\,\tilde{\alpha}\alpha_o\,))$$

The vehicle viscous/circulation forces are,

$$X = \quad L \sin\alpha - D\cos\alpha$$

$$Z = -L\cos\alpha - D\sin\alpha \qquad (D.8)$$

$$X = \frac{1}{2}\rho U^2 S\,\{\, C_{L_\alpha}(\alpha_o^2 + 2\alpha_o\tilde{\alpha}) - (C_{D_o} - C_{D_o}\alpha_o\tilde{\alpha}$$
$$+ C_{D_2}\,(\alpha_o^2 + (\,2\,\alpha_o - \alpha_o^3\,)\,\tilde{\alpha}\,)\,\}$$

$$Z = \frac{1}{2}\rho U^2 S\,\{\, -C_{L_\alpha}\,(\alpha_o + \tilde{\alpha} - \alpha_o^2\tilde{\alpha}) - (C_{D_o}\,(\alpha_o + \tilde{\alpha})$$
$$+ C_{D_2}\,(\alpha_o^3 + 3\alpha_o^2\,\tilde{\alpha}\,))\,\}$$

$$\frac{\partial X}{\partial\,\tilde{\alpha}} = \frac{1}{2}\rho U^2 S\,\{\, C_{L_\alpha}\,2\alpha_o + C_{D_o}\alpha_o - C_{D_2}\,(2\,\alpha_o - \alpha_o^3\,)\,\}$$

$$\frac{\partial Z}{\partial\,\tilde{\alpha}} = \frac{1}{2}\rho U^2 S\,\{\, -C_{L_\alpha}\,(1 - \alpha_o^2) - C_{D_o} - C_{D_2}\;3\alpha_o^2\,\}$$

The resulting derivatives are presented below. Note that the derivatives that are superscripted with a '*' are still incomplete and need to have added the component dependent on forward velocity variation.

$$X_{\tilde{u}}^{*} = -\frac{1}{2}\rho S \{ C_{L_\alpha} 2\alpha_o + C_{D_o}\alpha_o - C_{D_2} (2\alpha_o - \alpha_o^3) \} w_o$$

$$X_{\tilde{w}} = \frac{1}{2}\rho S \{ C_{L_\alpha} 2\alpha_o + C_{D_o}\alpha_o - C_{D_2} (2\alpha_o - \alpha_o^3) \} u_o$$

$$Z_{\tilde{u}}^{*} = -\frac{1}{2}\rho S \{ -C_{L_\alpha} (1 - \alpha_o^2) - C_{D_o} - C_{D_2} 3\alpha_o^2 \} w_o$$

$$Z_{\tilde{w}} = \frac{1}{2}\rho S \{ -C_{L_\alpha} (1 - \alpha_o^2) - C_{D_o} - C_{D_2} 3\alpha_o^2 \} u_o$$

Finally, the components of the derivatives due to variation in forward velocity need to be derived. The overall hydrodynamic velocity of the vehicle in a current is given by the term U. Where,

$$U^2 \doteq u_o^2 + 2u_o\tilde{u} + w_o^2 + 2w_o\tilde{w} + H.O.T.$$

The Pitching Moment is needed for the $M_{\tilde{u}}$ derivative and is given as,

$$M_{\tilde{u}} = \frac{1}{2}\rho U^2 S C_{M_\alpha} \alpha$$

Thus the derivative components due to forward velocity,

$$X_{\tilde{u}}^{v} = \rho u_o S C_{L_\alpha}\alpha_o^2 - C_{D_o} - C_{D_2}\alpha_o^2$$

$$Z_{\tilde{u}}^{v} = \rho u_o S - C_{L_\alpha}\alpha_o - C_{D_o} - C_{D_2}\alpha_o^3$$

Therefore,

$$X_{\tilde{u}} = X_{\tilde{u}}^{*} + X_{\tilde{u}}^{v}$$

$$Z_{\tilde{u}} = Z_{\tilde{u}}^{*} + Z_{\tilde{u}}^{v}$$

Appendix E

Tether Cable undamped and damped impedance responses.

The Undamped Cable Impedance Response Curves are courtesy of Antoine Bliek.

The Damped Cable Impedance Response Curves are courtesy of Hyunkyong Shin.

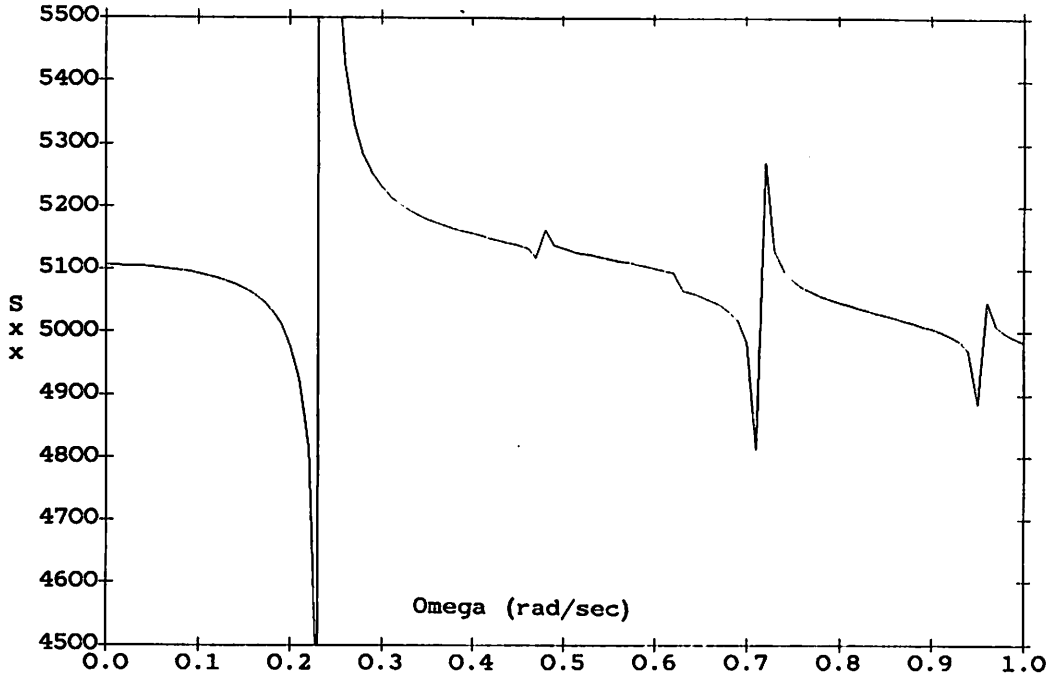

Figure E-1: Undamped Cable Impedance Response Sxx.

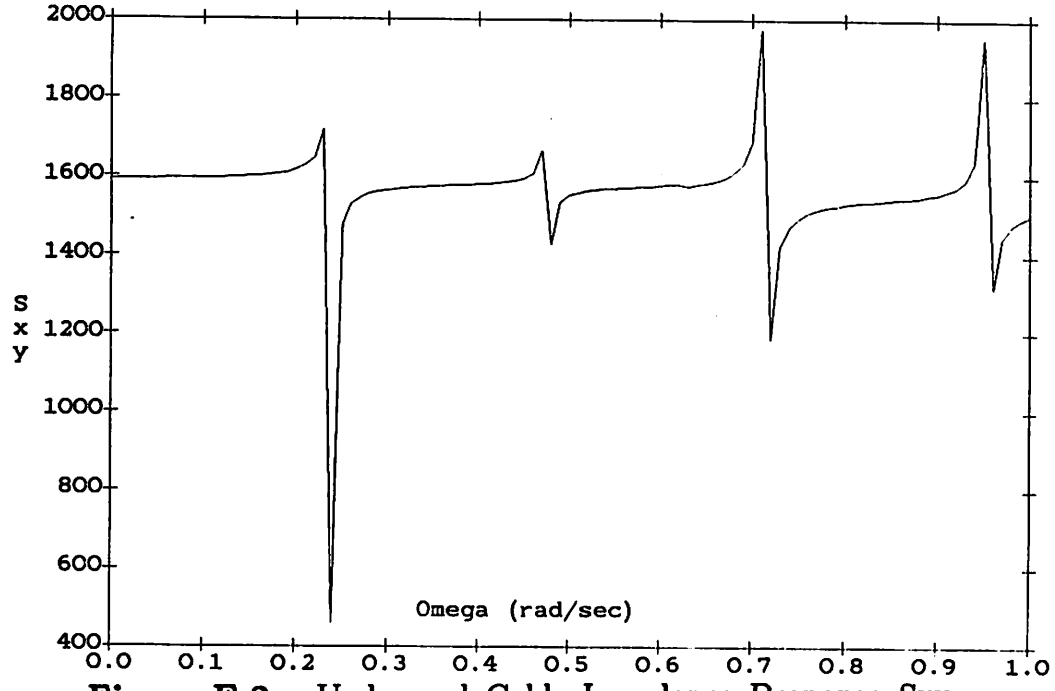

Figure E-2: Undamped Cable Impedance Response Sxy.

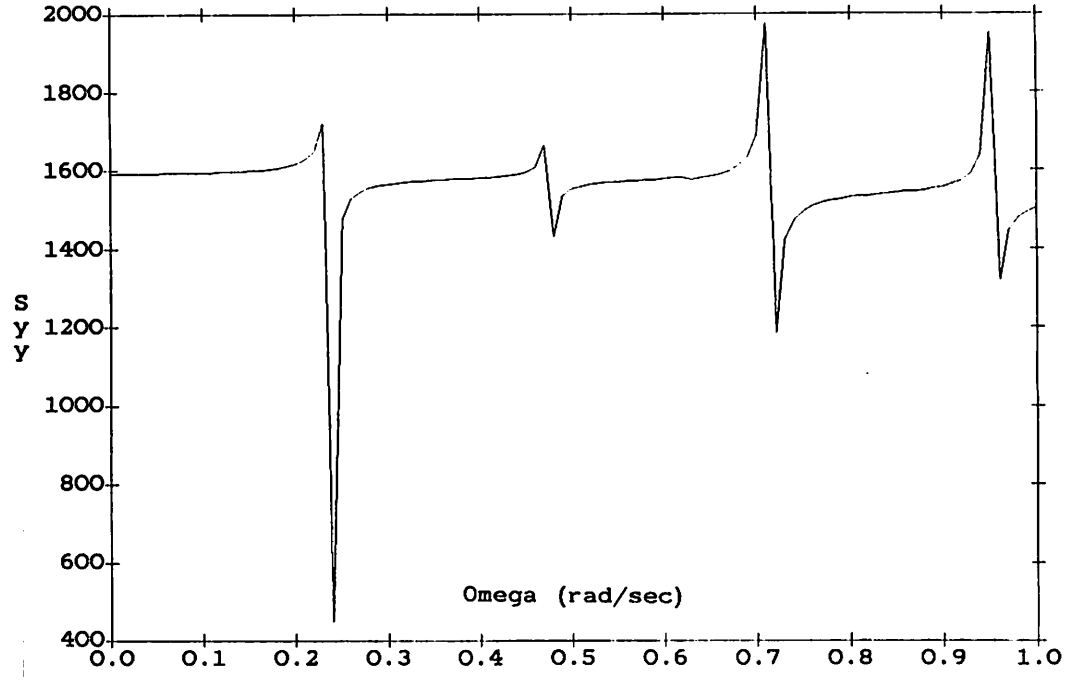

Figure E-3: Undamped Cable Impedance Response Syy.

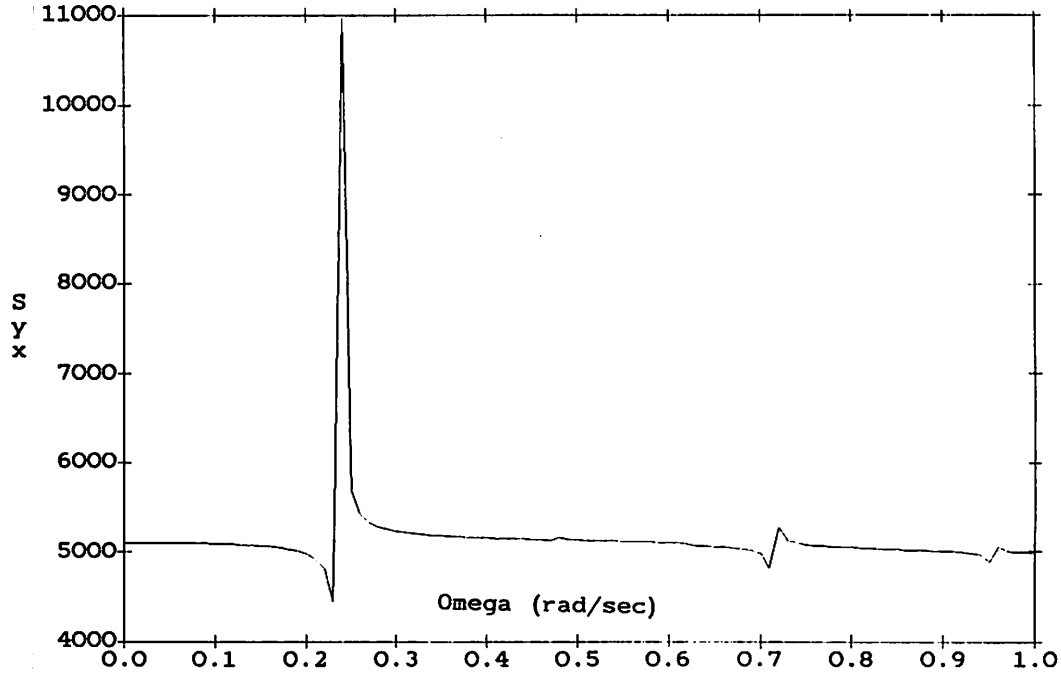

Figure E-4: Undamped Cable Impedance Response Syx.

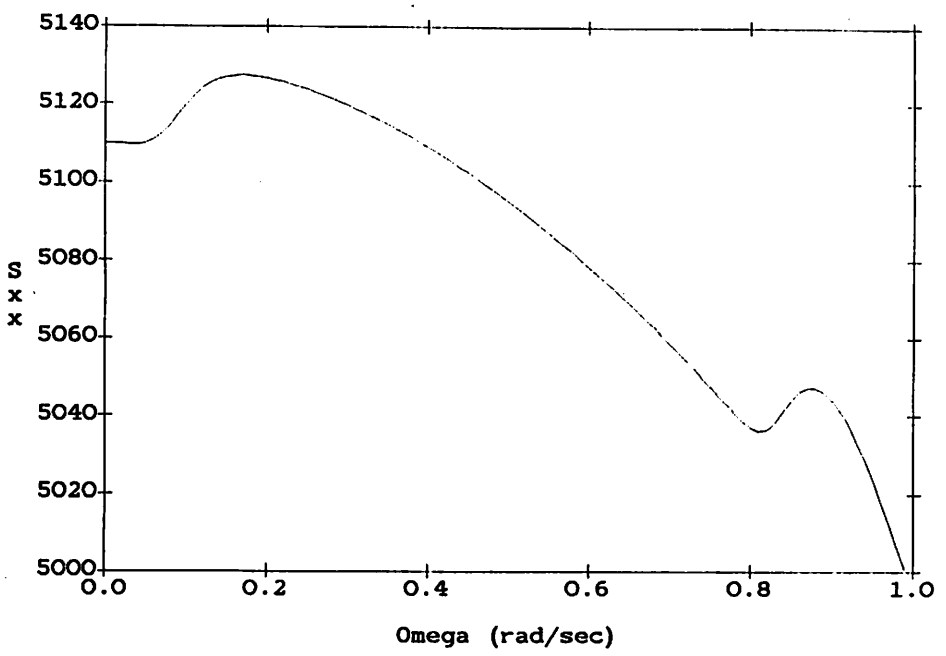

Figure E-5: Damped Cable Impedance Response Sxx, magnitude.

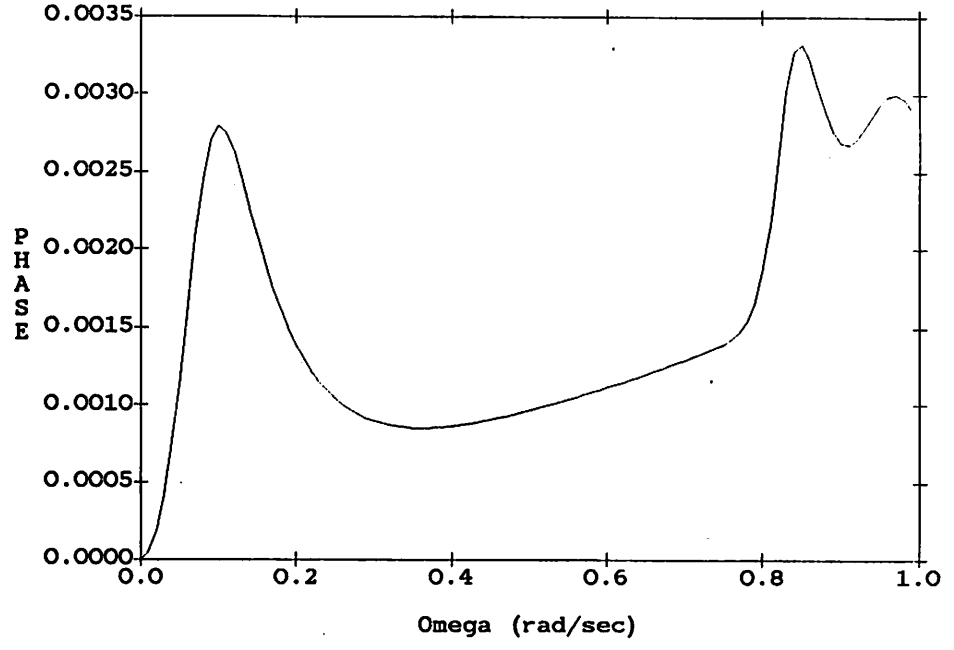

Figure E-6: Damped Cable Impedance Response Sxx, phase.

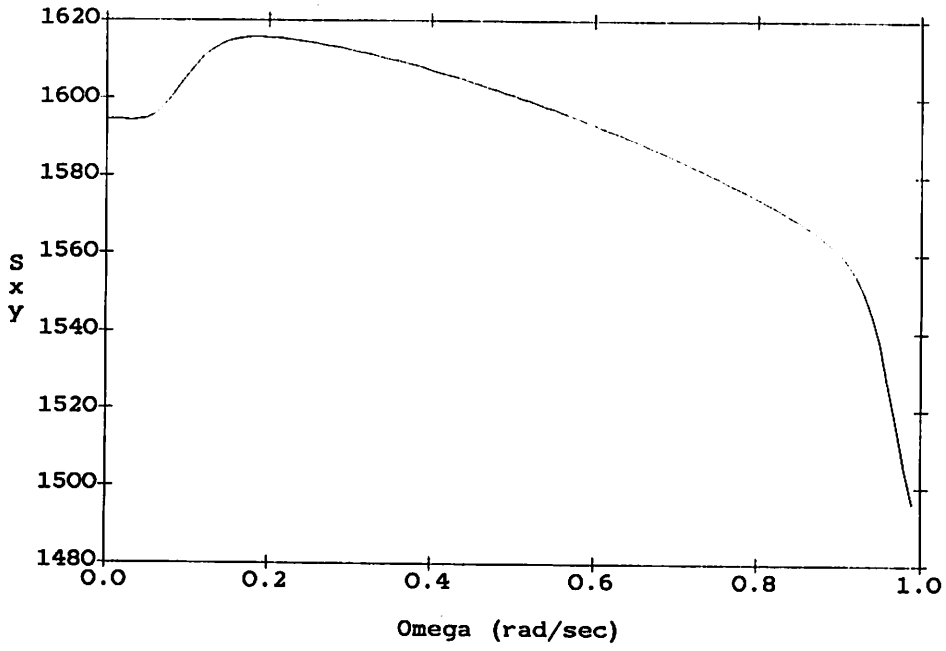

Figure E-7: Damped Cable Impedance Response Sxy, magnitude.

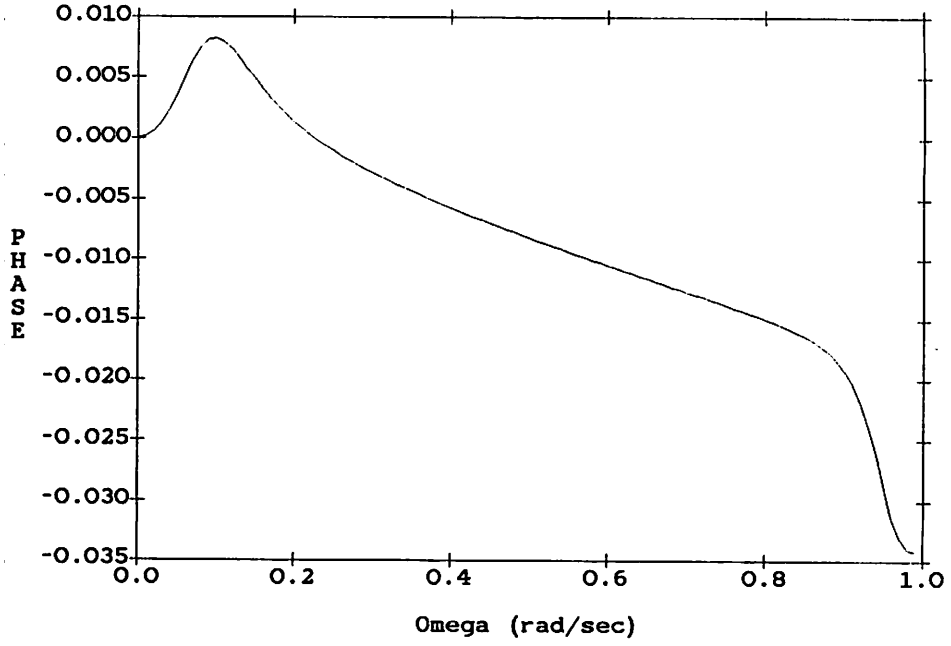

Figure E-8: Damped Cable Impedance Response Sxy, phase.

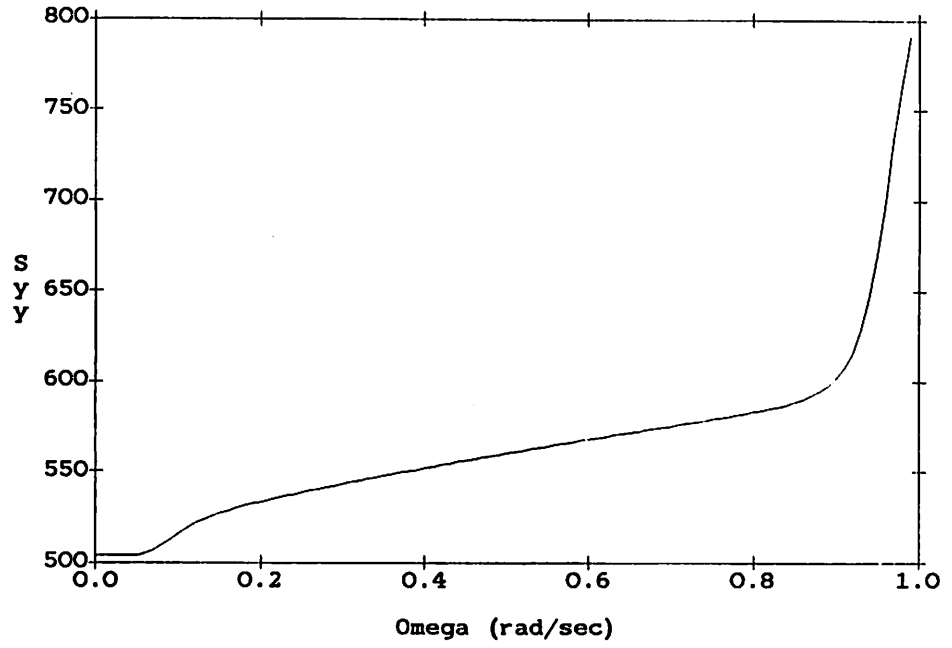

Figure E-9: Damped Cable Impedance Response Syy, magnitude.

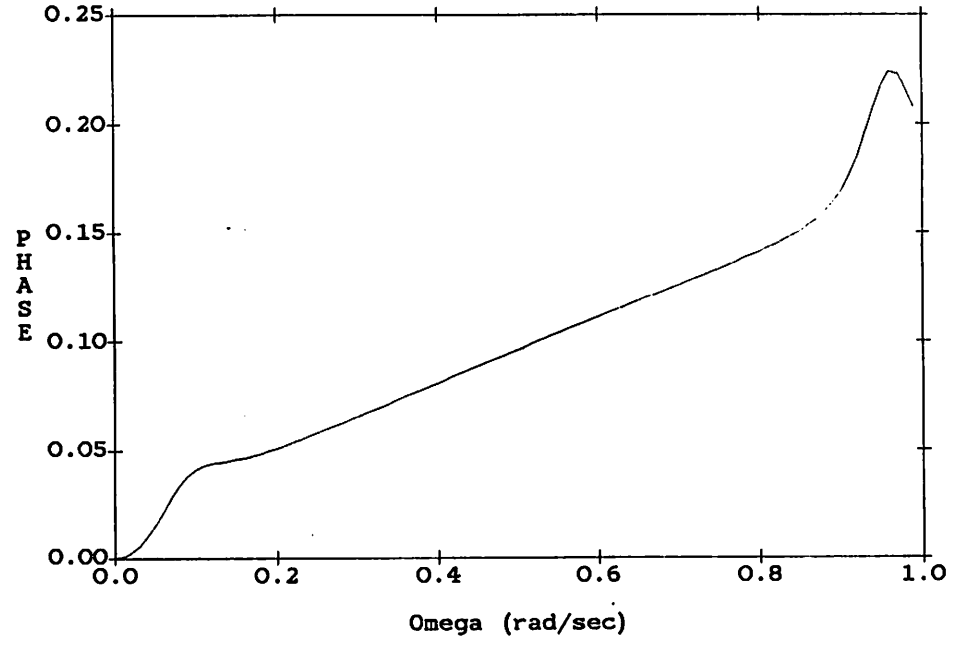

Figure E-10: Damped Cable Impedance Response Syy, phase.

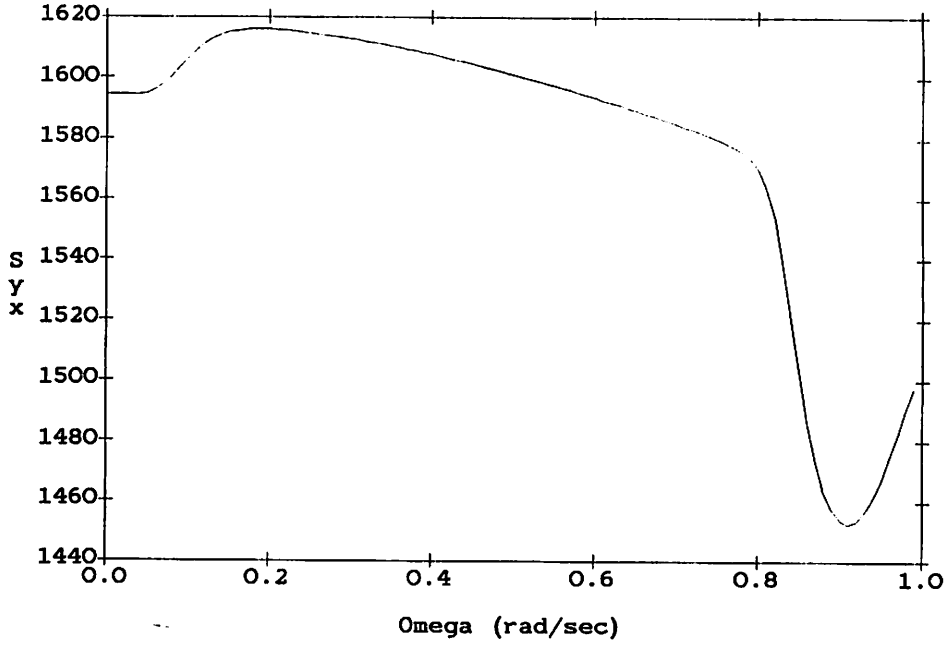

Figure E-11: Damped Cable Impedance Response Syx, magnitude.

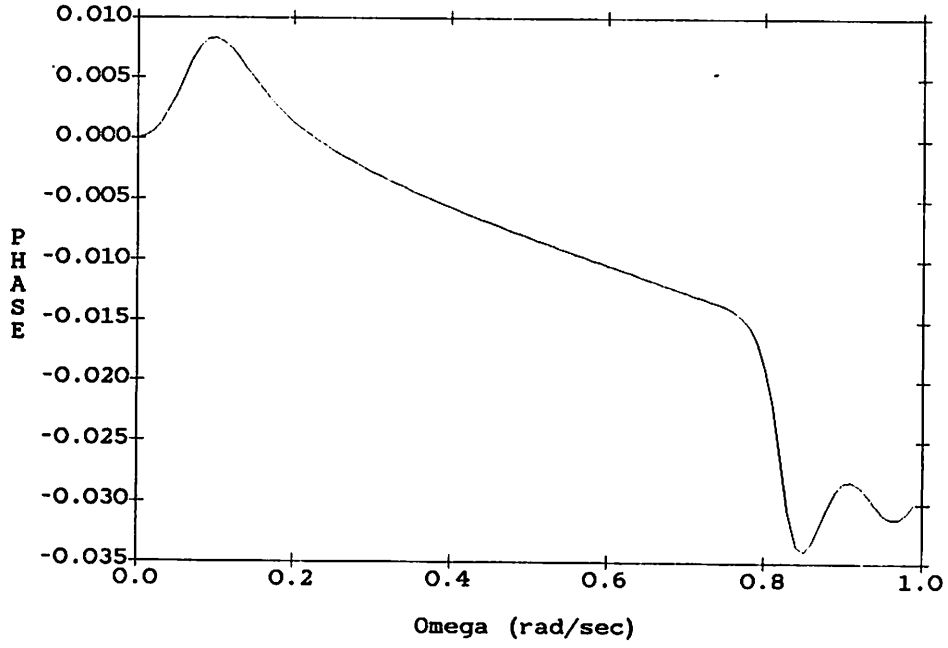

Figure E-12: Damped Cable Impedance Response Syx, phase.

Appendix F
Programs Used For Simulations

F.1 Program Description

The programs used to produce the results of chapters 5 and 6 are listed in the following pages. First, they will be briefly introduced and their use will be described. The following programs are included : *Hydro*, *Findcf*, *Gencfp*, *Genctr*, *Ctrlc*, and *Simulc*.

The program *Hydro* calculates the hydrodynamic and inertial coefficients for the longitudinal dynamics of a submersible and outputs them to a file. This program assumes that the submersible has bowplanes and tailplanes. The user may choose to add a payload in the form of a drum suspended below the vehicle, and/or choose between two tailplane configurations. The two possible tailplane configurations are an inverted 'T' tailplane or an 'H' tailplane. The values produced by this program are quite accurate for an unloaded elongated submersible. For excessively large payloads or short submersibles the accuracy of the values may degenerate.

In order to run a simulation with desired steady state values, it is necessary to be able to determine what the required control forces will be at any particular point of the simulation. The program *Findcf* allows the user to specify the steady state operating point for the vehicle and to iterate in the control forces untill the vehicle reaches the equilibrium value. This program requires the file 'COEFFS.DAT'.

The program *Gencfp* generates all the specific data required for a

simulation as well as the time histories for the control forces. Generally, before using this program all the specifics for the simulation should already be known. This program prompts for information from the user ,as does *Hydro*, and places all the information into a file.

The program *Genctr* produces a file named 'CTRVA.DAT' that contains the velocity and angle of attack at which the state equations for the vehicle dynamics are determined (specifically the A and B matrices). The state equations are placed in a file with the filename specified in 'CTRVA.DAT'. The program *Ctrlc* calculates the state equations according to the commands in the file 'CTRVA.DAT' and based on the coefficients in the file 'COEFFS.DAT'.

The state equation files must be processed with a control package such as CTRLC, HONEY-X, or MATRIX-X. In our case, the control package CTRLC of System Control Technology was used. (Not to be confused, the program named *Ctrlc* and the control package, they are very different !) Once the control gain matrices are found they must be ordered and stored in a file called 'GAINS.DAT'. The specific format for this file can be deduced from the read statements at the beginning of the program *Simulc*.

The program *Simulc* is the simulation program which includes the LQG/LTR controller. It carries out both the steady state simulation and the simulation of the disturbed/controlled dynamics. The program *Simulc* requires the file 'COEFKM.DAT' to generate the time varying state equations used by the LQG compensator, and the file 'COEFFP.DAT' for the vehicle. Thus a compensator designed for an unloaded vehicle can be evaluated for the loaded vehicle or for variations on the vehicle design. The program *Simulc* also requires the file 'CTRLFP.DAT' in order to carry out the simulation. The

program *Simulc* contains comment lines that should provide more specific information on the program.

NOTE : ***These programs were written in FORTRAN 77 on a DEC PRO/350 using Digital Equipment Corporation's compiler for the PDP 11. These programs should be transportable. It may be necessary though, to alter certain I/O statements. The remainder should not pose any problems.***

Program Example : HYDRO

```
*********************************************
*                                           *
*  This Program determines the hydrodynamic *
*  coefficients for a submersible with an   *
*  ellipsoidal body, equipped with bowplanes, *
*  tailplanes and kort nozzle shrouds over  *
*  the horizontal thrusters. In addition,   *
*  effects of a payload may be added.       *
*  NOTE : Only the longitudinal coefficients *
*  are determined.                          *
*                                           *
*********************************************

Name of submersible.
THLS :-
Enter the vehicle s length :
11.956
Enter the length vehicle s nosecone :
3.5
Enter the length vehicle s tailcone :
3.5
Enter the vehicle s heigth :
1.52
Enter the vehicle s width :
2.286
Enter vertical position of the vehicle s cg :
.1

*********************************************
*                                           *
*  The bowplane is assumed to be a completely *
*  movable surface, whereas the taiplane is *
*  assumed to have a flap along its full span.*
*                                           *
*                                           *
*  Note that distances aft of amidships are *
*  -ve and that distances fore are +ve.     *
*                                           *
*                                           *
*  Following distances measured at wing body *
*  intersections. These are the location of *
*  of the wing relative to the amidships.   *
*                                           *
*********************************************

Position of bowplane s mid-chord :
4.
Position of tailplane s mid-chord :-

Position of bowplane s mid-chord :
0.
Position of tailplane s mid-chord :
-5.
Position at shroud s middle :
-7.5

*********************************************
*                                           *
*  Following distances measured at wing body *
*  intersections. These are the location of *
*  of the wing relative to the centerline.  *
*  These are averages of position where the *
*  wing root meets the vehicle body.        *
*                                           *
*********************************************
```

```
Position of bowplane s root :
1.0267
Position of tailplane s root :
.71
Position of thruster centerline :
.75

**********************************************
*                                            *
*  Though these surfaces may be tapered they *
*  are assumed fore/aft symmetric.           *
*                                            *
**********************************************

Bowplane s chord at wing tip :
.6
Bowplane s chord at wing root :
.8
Bowplane s span (from centerline) :
2.
Tailplane s chord at wing tip :
1.2
Tailplane s chord at wing root :
1.4
Tailplane s span (from centerline) :
2.7
Enter the control surface chord ratio :
.35

**********************************************
*                                            *
*  The thicness of all the surfaces need to  *
*  be known.                                 *
*                                            *
**********************************************

Bowplane s Maximum thickness :
0.05
Bowplane s Average thickness :
0.03
Tailplane s Maximum thickness :
0.05
Tailplane s Average thickness :
0.03
Vertical Tailplane s Average thickness :
0.03
Shroud s Average thickness :
0.03
Vehicle has a single vertical tail ==> 1
Vehicle has an H tail ==> 2
2
Enter span of vertical tail :
2.2
Enter tail chord at tip :
1.
Enter shroud width :
0.4
Enter shroud radius :
0.3
Enter number of shrouds :
2
```

```
Enter number of ducts not in vehicle s wake :
6
Enter duct cross sectional area :
.265
Moment arm of Vertical Thruster :
5.
Enter Scaling Factor for the Horizontal Thrusters :
1000.
Is there a payload (Y/N) .
y

**********************************************
*                                            *
*  The Payload is assumed to be a cylinder in *
*  contact with the vehicle.                 *
*                                            *
**********************************************

Enter diameter of payload :
1.524
Enter length of the payload :
3.048
Enter the mass of the payload :
4500.
Enter the name of the data file :
coeffs.dat

**********************************************
*                                            *
*  All the required data has been supplied !  *
*                                            *
**********************************************
```

Program Example : GENCFP

```
 Enter the Name of the Simulation.
DIVE
 Enter the name of the data file
 Use at most six characters followed by .dat
ctrlfp.dat
 Enter starting time for simulation .
0.
 Enter time for simulation to end.
440.
 Enter time interval between successive values.
.05
 Enter error bound .
.001
************************************************
*                                              *
* Note : The origin of the coordinate system is *
*        at the clump. X is to the right and Z  *
*        is down.  The clump is 250 meters from *
*        the sea bottom. There is a sea current *
*        of 0.3 knots till Z=50m and then the   *
*        current drops using the 1/7th power law.*
*                                              *
************************************************

 Enter Direction of Trajectory, forward = -1 .
 backwards = 1.
-1
 Number of output values to skip.
80
 Enter x position of the vehicle :
1.E-7
 Enter z position of the vehicle :
0.
 Enter the cable tension :
5000.
Enter the X-force disturbance intensity :
3.5E+7
Enter the Z-force disturbance intensity :
3.5E+7
Enter the M-moment disturbance intensity :
3.5E+7
Enter the X-force disturbance bandwidth :
10.
Enter the Z-force disturbance bandwidth :
10.
Enter the M-moment disturbance bandwidth :
10.
Enter (int.) seed for disturbance generation :
315667
 Enter horizontal thruster scaling factor :
1000.
 Enter time interval for control file generation.
2.5
 Enter the values for the Bowplane.
 Present value for t =  0.0000000     is   0.0000000
 Enter Coefficient for t^0 :
0.
 Enter Coefficient for t^1 :
.001
 Enter Final Value of t for this function :
20.
 Enter the values for the Tailplane.
 Present value for t =  0.0000000     is   0.0000000
 Enter Coefficient for t^0 :
0.
 Enter Coefficient for t^1 :
.003
 Enter Final Value of t for this function :
20.
```

```
 Enter the values for the Thrusters.
 Present value for t =  0.0000000     is   0.0000000
 Enter Coefficient for t^0 :
7500.
 Enter Coefficient for t^1 :
250.
 Enter Final Value of t for this function :
10.
 Enter values for Fore Vert. Thrus.
 Present value for t =  0.0000000     is   0.0000000
 Enter Coefficient for t^0 :
-500.
 Enter Coefficient for t^1 :
0.
 Enter Final Value of t for this function :
10.
 Enter values for Aft Vert. Thrus.
 Present value for t =  0.0000000     is   0.0000000
 Enter Coefficient for t^0 :
500.
 Enter Coefficient for t^1 :
0.
 Enter Final Value of t for this function :
10.
 Enter the values for the Thrusters.
 Present value for t =   10.00000     is    10.00000
 Enter Coefficient for t^0 :
10000.
 Enter Coefficient for t^1 :
0.
 Enter Final Value of t for this function :
400.
 Enter values for Fore Vert. Thrus.
 Present value for t =   10.00000     is   -500.0000
 Enter Coefficient for t^0 :
-500.
 Enter Coefficient for t^1 :
200.
 Enter Final Value of t for this function :
12.5
 Enter values for Fore Vert. Thrus.
 Present value for t =   12.50000     is   0.0000000
 Enter Coefficient for t^0 :
0.
 Enter Coefficient for t^1 :
0.
 Enter Final Value of t for this function :
400.
 Enter the values for the Bowplane.
 Present value for t =   20.00000     is   0.2000000
 Enter Coefficient for t^0 :
.2
 Enter Coefficient for t^1 :
0.
 Enter Final Value of t for this function :
400.
```

```
      Program Hydro
c*****************************************************************
c                                                                *
c     Program to determine coefficients of submersible in        *
c     the longitudinal plane.                                    *
c                                                                *
c     The coefficients are written to a file named :             *
c     ====>  'COEFFS.DAT'                                        *
c                                                                *
c*****************************************************************
c
      Real Icoef(4),Subdim(6),Acoef(4),Ccoef(7,3),Cfder(3,3)
c
      Integer Tltyp,Shnum,Dctnum
      Real Lnbd,Lnbdnc,Lnbdtc,Hgbd,Wdbd,Cgz,Cschrt,Bpmdch,Tpmdch,
     + Shfex,Bpry,Tpry,Thcny,Bpchtp,Bpchrt,Bpsp,Tpchtp,Tpchrt,Tpsp,
     + Bpmxth,Bpavth,Tpmxth,Tpavth,Shavth,Vthg,Vtchrt,Vtchtp,Shwid,
     + Shrad,Pldd,Pldl,Pldm,Vtavth,Dctare,Vthder(2,3),Thscal
c
      Data Vthder/ 0.05,0.1,-2.1142857,-1.2666667,0.0,0.0/
c
      Character*20 Subnm,Datafl
      Character*2 Pldflg
      External Inerti,Aspect,Accel,Drag,Veloc,Datasv,Cf
c
c     Declaration of mensurations that are needed by the subroutines.
c     These values are always available.
c
      Real Bpefch,BpAR,BpefAR,Tpefch,TpAR,TpefAR,Bdmxa,Volbd,Laminv
     #     ,K2,K1
c
c     Declaration of common blocks to provide access to the
c     variables by the subroutines.
c
      Common /main/ Lnbd,Lnbdnc,Lnbdtc,Hgbd,Wdbd,Cgz,Cschrt,Bpmdch,
     %              Tpmdch,Shfex,Bpry,Tpry,Thcny,Bpchtp,Bpchrt,Bpsp,
     %              Tpchtp,Tpchrt,Tpsp,Bpmxth,Bpavth,Tpmxth,Tpavth,
     %              Shavth,Vthg,Vtchrt,Vtchtp,Shwid,Shrad,Pldd,Pldl,
     %              Pldm,Vtavth,Tltyp,Shnum,Dctnum,Dctare,Thscal
     %       /name/ Subnm,Datafl,Pldflg
c
      Common /aspct/ Bpefch,BpAR,BpefAR,Tpefch,TpAR,TpefAR,Bdmxa,
     %               Volbd,Laminv,K2,K1
c
c
c
      Print *,'*************************************************'
      Print *,'*                                               *'
      Print *,'*  This Program determines the hydrodynamic     *'
      Print *,'*  coefficients for a submersible with an        *'
      Print *,'*  ellipsoidal body, equipped with bowplanes,    *'
      Print *,'*  tailplanes and kort nozzle shrouds over       *'
      Print *,'*  the horizontal thrusters. In addition,        *'
      Print *,'*  effects of a payload may be added.            *'
      Print *,'*  NOTE : Only the longitudinal coefficients     *'
      Print *,'*  are determined.                               *'
      Print *,'*                                               *'
      Print *,'*************************************************'
      Print *,' '
      Print *,'Name of submersible.'
      Read(5,5) Subnm
5     Format(A20)
c
c     Obtain the geometric data.
c
      Print *,'Enter the vehicle s length : '
      Read (5,10) Lnbd
10    Format (E14.7)
      Print *,'Enter the length vehicle s nosecone : '
      Read (5,10) Lnbdnc
      Print *,'Enter the length vehicle s tailcone : '
      Read (5,10) Lnbdtc
      Print *,'Enter the vehicle s heigth : '
      Read (5,10) Hgbd
      Print *,'Enter the vehicle s width : '
      Read (5,10) Wdbd
      Print *,'Enter vertical position of the vehicle s cg : '
      Read (5,10) Cgz
c
      Print *,' '
      Print *,'*************************************************'
      Print *,'*                                               *'
      Print *,'*  The bowplane is assumed to be a completely   *'
      Print *,'*  movable surface, whereas the taiplane is     *'
      Print *,'*  assumed to have a flap along its full span.  *'
      Print *,'*                                               *'
      Print *,'*                                               *'
      Print *,'*  Note that distances aft of amidships are     *'
      Print *,'*  -ve and that distances fore are +ve.         *'
      Print *,'*                                               *'
      Print *,'*                                               *'
      Print *,'*  Following distances measured at wing body    *'
      Print *,'*  intersections. These are the location of     *'
      Print *,'*  of the wing relative to the amidships.       *'
      Print *,'*                                               *'
      Print *,'*************************************************'
      Print *,' '
      Print *,'Position of bowplane s mid-chord : '
      Read (5,10) Bpmdch
      Print *,'Position of tailplane s mid-chord : '
      Read (5,10) Tpmdch
      Print *,'Position at shroud s middle : '
      Read (5,10) Shmdx
c
      Print *,' '
      Print *,'*************************************************'
      Print *,'*                                               *'
      Print *,'*  Following distances measured at wing body    *'
      Print *,'*  intersections. These are the location of     *'
      Print *,'*  of the wing relative to the centerline.      *'
      Print *,'*  These are averages of position where the     *'
      Print *,'*  wing root meets the vehicle body.            *'
      Print *,'*                                               *'
      Print *,'*************************************************'
      Print *,' '
      Print *,'Position of bowplane s root : '
      Read (5,10) Bpry
      Print *,'Position of tailplane s root : '
      Read (5,10) Tpry
      Print *,'Position of thruster centerline : '
      Read (5,10) Thcny
c
      Print *,' '
      Print *,'*************************************************'
      Print *,'*                                               *'
      Print *,'*  Though these surfaces may be tapered they     *'
      Print *,'*  are assumed fore/aft symmetric.              *'
      Print *,'*                                               *'
```

```
      Print *,'************************************************'
      Print *,'  '
      Print *,'Bowplane s chord at wing tip : '
      Read (5,10) Bpchtp
      Print *,'Bowplane s chord at wing root : '
      Read (5,10) Bpchrt
      Print *,'Bowplane s span (from centerline) : '
      Read (5,10) Bpsp
      Print *,'Tailplane s chord at wing tip : '
      Read (5,10) Tpchtp
      Print *,'Tailplane s chord at wing root : '
      Read (5,10) Tpchrt
      Print *,'Tailplane s span (from centerline) : '
      Read (5,10) Tpsp
      Print *,'Enter the control surface chord ratio :'
      Read (5,10) Cschrt
c
      Print *,'  '
      Print *,'************************************************'
      Print *,'*                                              *'
      Print *,'*  The thickness of all the surfaces need to   *'
      Print *,'*  be known.                                   *'
      Print *,'*                                              *'
      Print *,'************************************************'
      Print *,'  '
c
      Print *,'Bowplane s Maximum thickness : '
      Read (5,10) Bpmxth
      Print *,'Bowplane s Average thickness : '
      Read (5,10) Bpavth
      Print *,'Tailplane s Maximum thickness : '
      Read (5,10) Tpmxth
      Print *,'Tailplane s Average thickness : '
      Read (5,10) Tpavth
      Print *,'Vertical Tailplane s Average thickness : '
      Read (5,10) Vtavth
      Print *,'Shroud s Average thickness : '
      Read (5,10) Shavth
c
c     Need to now whether vehicle has a single vertical tail
c     or an H tail to calculate the drag forces correctly.
c
 14   Print *,'Vehicle has a single vertical tail ==> 1'
      Print *,'Vehicle has an H tail ==> 2'
      Read (5,15) Tltyp
 15   Format (I2)
      if ((Tltyp .lt. 1).or.(Tltyp .gt. 2)) go to 14
c
      if (Tltyp .eq. 1) then
         Print *,'Enter height of vertical tail :'
         Read (5,10) Vthg
         Print *,'Enter tail chord at root : '
         Read (5,10) Vtchrt
         Print *,'Enter tail chord at tip : '
         Read (5,10) Vtchtp
      end if
c
      if (Tltyp .eq. 2) then
         Print *,'Enter span of vertical tail :'
         Read (5,10) Vthg
         Vtchrt = Tpchtp
         Print *,'Enter tail chord at tip : '
         Read (5,10) Vtchtp
      end if
```

```
c
c     Enter shroud dimensions.
c
      Print *,'Enter shroud width :'
      Read (5,10) Shwid
      Print *,'Enter shroud radius :'
      Read (5,10) Shrad
      Print *,'Enter number of shrouds :'
      Read (5,15) Shnum
c
c     Enter number of transveral ducts and their cross-sectional
c     areas.
c
      Print *,'Enter number of ducts not in vehicle s wake :'
      Read (5,15) Dctnum
      Print *,'Enter duct cross sectional area :'
      Read (5,10) Dctare
      Vthder(1,3) = Dctare
      Print *,'Moment arm of Vertical Thruster : '
      Read (5,10) Vthder(2,3)
      Print *,'Enter Scaling Factor for the Horizontal Thrusters : '
      Read (5,10) Thscal
c
c     Need to now whether vehicle has a payload.
c
      Print *,'Is there a payload (Y/N) .'
      Read (5,20) Pldflg
 20   Format (A2)
c
      If ((Pldflg .eq. 'y').OR.(Pldflg .eq. 'Y')) then
         Print *,'
         Print *,'************************************************'
         Print *,'*                                              *'
         Print *,'*  The Payload is assumed to be a cylinder in  *'
         Print *,'*  contact with the vehicle.                   *'
         Print *,'*                                              *'
         Print *,'************************************************'
         Print *,'  '
         Print *,'Enter diameter of payload : '
         Read (5,10) Pldd
         Print *,'Enter length of the payload : '
         Read (5,10) Pldl
         Print *,'Enter the mass of the payload : '
         Read (5,10) Pldm
      end if
c
c     Enter the name of the file that stores the data.
c
      Print *,'Enter the name of the data file :'
      Read (5,5) Datafl
c
      Print *,'  '
      Print *,'************************************************'
      Print *,'*                                              *'
      Print *,'*  All the required data has been supplied !   *'
      Print *,'*                                              *'
      Print *,'************************************************'
      Print *,'  '
c
c     Determine the vehicle s inertia terms.
c
      Call Inerti(Icoef)
c
c     Determine the aspect ratio of the control surfaces.
```

```
c
      Call Aspect(Subdim)
c
c     Determine the acceleration coefficients.
c
      Call Accel(Acoef,Icoef)
c
c     Determine the drag coefficient.
c
      Call Drag(Cf,Ccoef)
c
c     Determine the velocity related coefficients.
c
      Call Veloc(Ccoef,Cfder)
c
c     Save the coefficients in a data file.
c
      Call Datasv(Icoef,Subdim,Acoef,Ccoef,Cfder,Vthder)
c
c
c
      End
c*****************************************************************
c                                                               *
c     END OF MAIN PROGRAM HYDRO.                                *
c                                                               *
c*****************************************************************
      Subroutine Inerti(Icoef)
c
      Real Icoef(4)
c
      Integer Tltyp,Shnum,Dctnum
      Real Lnbd,Lnbdnc,Lnbdtc,Hgbd,Wdbd,Cgz,Cschrt,Bpmdch,Tpmdch,
     +  Shfex,Bpry,Tpry,Thcny,Bpchtp,Bpchrt,Bpsp,Tpchtp,Tpchrt,Tpsp,
     +  Bpmxth,Bpavth,Tpmxth,Tpavth,Shavth,Vthg,Vtchrt,Vtchtp,Shwid,
     +  Shrad,Pldd,Pldl,Pldm,Vtavth,Dctare,Thscal
      Character*20 Subnm,Datafl
      Character*2 Pldflg
      Parameter (Pi=3.1415297,Rho=1025.9)
c
      Real Bpefch,BpAR,BpefAR,Tpefch,TpAR,TpefAR,Laminv,K2,K1
c
c
c     Variables calculated in this procedure.
c
      Real Bdmxa,Lencen,Volnc,Voltc,Volcen,Volbd,Volsh,Volbps,
     #     Voltps,Volvt,Inc,Itc,Icen,Ibps,Itps,Ishs,Ivt
c
c     Declaration of common blocks to provide access to the
c     variables by the subroutines.
c
      Common /main/ Lnbd,Lnbdnc,Lnbdtc,Hgbd,Wdbd,Cgz,Cschrt,Bpmdch,
     %              Tpmdch,Shfex,Bpry,Tpry,Thcny,Bpchtp,Bpchrt,Bpsp,
     %              Tpchtp,Tpchrt,Tpsp,Bpmxth,Bpavth,Tpmxth,Tpavth,
     %              Shavth,Vthg,Vtchrt,Vtchtp,Shwid,Shrad,Pldd,Pldl,
     %              Pldm,Vtavth,Tltyp,Shnum,Dctnum,Dctare,Thscal
     %       /name/ Subnm,Datafl,Pldflg
c
      Common /aspct/ Bpefch,BpAR,BpefAR,Tpefch,TpAR,TpefAR,Bdmxa,
     %               Volbd,Laminv,K2,K1
c
c     Find the maximum cross-sectional area of the body and
c     the volumes tail cone, nose cone and central section.
c
      Bdmxa = Pi*Hgbd*Wdbd/4
      Lencen = (Lnbd - Lnbdnc - Lnbdtc)
      Volnc = Bdmxa*Lnbdnc*2/3
      Voltc = Bdmxa*Lnbdtc*2/3
      Volcen = Bdmxa*Lencen
      Volbd = Volnc + Volcen + Voltc
c
c     Find the volume of the shrouds.
c
      Volsh = 2*pi*Shrad*Shavth*Shwid*Shnum
c
c     Find the volume of the Surfaces.
c
      Volbps = (Bpsp - Bpry)*(Bpchtp + Bpchrt)*Bpavth
c
      Voltps = (Tpsp - Tpry)*(Tpchtp + Tpchrt)*Tpavth
c
      if (Tltyp .eq. 1) Volvt=Vthg*Vtavth*(Vtchrt+Vtchtp)/2
      if (Tltyp .eq. 2) Volvt=Vthg*Vtavth*(Vtchrt+Vtchtp)
c
c     Total Mass of Vehicle.
c
      Icoef(1) = Rho*(Volbd+Volsh+Volbps+Voltps)
c
c     In the case of a payload th center of gravity is different.
c
      If ((Pldflg .eq. 'y').OR.(Pldflg .eq. 'Y')) then
         Icoef(3)=(Pldm/Icoef(1))*((Pldd+Hgbd)/2 - Cgz)
      else
         Icoef(3)=Cgz
      end if
      Icoef(4) = - Hgbd / 2.0
c
c     Find the Inertia of the vehicle's body.
c
      Inc=Rho*Volnc*((Lnbdnc**2+(Hgbd/2)**2)/10+((Lnbd/2)-Lnbdnc)**2)
c
      Itc=Rho*Voltc*((Lnbdtc**2+(Hgbd/2)**2)/10+((Lnbd/2)-Lnbdtc)**2)
c
      Icen=Rho*Volcen*((Lencen**2)/12 + (Hgbd**2)/16)
c
c     Find the inertia of the vehicle's surfaces.
c
      Ibps=Rho*Volbps*((Bpchtp**2 + Bpchrt**2)/12 + Bpmdch**2)
c
      Itps=Rho*Voltps*((Tpchtp**2 + Tpchrt**2)/12 + Tpmdch**2)
c
      Ishs=Rho*Volsh*((Shrad**2)/2 + (Shwid**2)/12 + Shmdx**2)
c
      Ivt=Rho*Volvt*((((Vtchrt+Vtchtp)/2)**2 + Vthg**2)/12 +
     &  Tpmdch**2)
c
c     Vehicle's Total Moment of Inertia.
c
      Icoef(2)=Inc+Itc+Icen+Ibps+Itps+Ishs+Ivt+Icoef(1)*Icoef(3)**2
c
c     End of Procedure.
c
      Return
      End
c*****************************************************************
c                                                               *
c     END OF SUBROUTINE INERTI.                                 *
c                                                               *
```

```
c*****************************************************************
      Subroutine Aspect(Subdim)
c
      Real Subdim(6)
c
c     This procedure finds usefull geometric information that the
c     subroutines Accel, Drag and Veloc will need.
c
      Integer Tltyp,Shnum,Dctnum
      Real Lnbd,Lnbdnc,Lnbdtc,Hgbd,Wdbd,Cgz,Cschrt,Bpmdch,Tpmdch,
     + Shfex,Bpry,Tpry,Thcny,Bpchtp,Bpchrt,Bpsp,Tpchtp,Tpchrt,Tpsp,
     + Bpmxth,Bpavth,Tpmxth,Tpavth,Shavth,Vthg,Vtchrt,Vtchtp,Shwid,
     + Shrad,Pldd,Pld1,Pldm,Vtavth,Dctare,Thscal
      Character*20 Subnm,Datafl
      Character*2 Pldflg
      Parameter (Pi=3.1415297,Rho=1025.9)
c
c     Variables calculated in this procedure.
c
      Real Bpefch,BpAR,Bpbt,BpefAR,BpefAt,Tpefch,TpAR,Tpbt,TpefAR,
     #     TpefAt,Bdmxa,Volbd,Laminv,K2,K1
c
c     Declaration of common blocks to provide access to the
c     variables by the subroutines.
c
      Common /main/ Lnbd,Lnbdnc,Lnbdtc,Hgbd,Wdbd,Cgz,Cschrt,Bpmdch,
     %              Tpmdch,Shfex,Bpry,Tpry,Thcny,Bpchtp,Bpchrt,Bpsp,
     %              Tpchtp,Tpchrt,Tpsp,Bpmxth,Bpavth,Tpmxth,Tpavth,
     %              Shavth,Vthg,Vtchrt,Vtchtp,Shwid,Shrad,Pldd,Pld1,
     %              Pldm,Vtavth,Tltyp,Shnum,Dctnum,Dctare,Thscal
     %       /name/ Subnm,Datafl,Pldflg
c
      Common /aspct/ Bpefch,BpAR,BpefAR,Tpefch,TpAR,TpefAR,Bdmxa,
     %               Volbd,Laminv,K2,K1
c
c     First these values are determined for the bowplanes.
c
c     Calculate effective chord.
c
      Bpefch=((Bpchrt+Bpchtp)*0.5*(Bpsp-Bpry)+Bpchrt*Bpry)/Bpsp
c
c     Calculate aspect ratio, effective semi-span, effective
c     aspect ratio.
c
      BpAR = Bpsp/Bpefch
      Bpbt=Bpsp*(1 - (Bpry/Bpsp)**2)
      BpefAR=(BpAR+2)*Bpbt/Bpsp - 2
c
c     Calculate effective Bowplane Area.
c
      BpefAt=4*Bpbt*Bpbt/BpefAR
c
c     Next these values are determined for the tailplanes.
c
      if (Tltyp .eq. 2) go to 10
c
c     CASE OF SINGLE VERTICAL TAIL WITH TWO HORIZONTAL TAILPLANES.
c
c     Calculate effective chord.
c
      Tpefch=((Tpchrt+Tpchtp)*0.5*(Tpsp-Tpry)+Tpchrt*Tpry)/Tpsp
c
c     Calculate aspect ratio, effective semi-span, effective
c     aspect ratio.
c
      TpAR = Tpsp/Tpefch
      Tpbt=Tpsp*(1 - (Tpry/Tpsp)**2)
      TpefAR=(TpAR+2)*Tpbt/Tpsp - 2
c
c     Calculate effective tailplane Area.
c
      TpefAt=4*Tpbt*Tpbt/TpefAR
c
      Subdim(1) = Bdmxa
      Subdim(2) = BpefAt
      Subdim(3) = TpefAt
      Subdim(4) = Lnbd/4
      Subdim(5) = Bpmdch+Bpefch/4
      Subdim(6) = Tpmdch+Tpefch/4
c
      Return
c
c     CASE OF H TAILPLANE CONFIGURATION, HORIZONTAL TAILPLANE HAS
c     AN INFINITE ASPECT RATIO.  IN EFFECT THE HORIZONTAL SURFACE
c     BE CONSIDERED TWO DIMENSIONAL.
c
 10   Tpefch=(Tpchrt + Tpchtp)/2
      TpefAt = Tpefch*(Tpsp - Tpry)*2
c
c
      Subdim(1) = Bdmxa
      Subdim(2) = BpefAt
      Subdim(3) = TpefAt
      Subdim(4) = Lnbd/4
      Subdim(5) = Bpmdch+Bpefch/4
      Subdim(6) = Tpmdch+Tpefch/4
c
      Return
      End
c*****************************************************************
c                                                                *
c     END OF SUBROUTINE ASPECT.                                  *
c                                                                *
c*****************************************************************
      Subroutine Accel(Acoef,Icoef)
c
      Real Acoef(4),Icoef(4)
c
c     This subroutine determines the added mass coefficients of the
c     vehicle, including the control surfaces.
c
      Integer Tltyp,Shnum,Dctnum
      Real Lnbd,Lnbdnc,Lnbdtc,Hgbd,Wdbd,Cgz,Cschrt,Bpmdch,Tpmdch,
     + Shfex,Bpry,Tpry,Thcny,Bpchtp,Bpchrt,Bpsp,Tpchtp,Tpchrt,Tpsp,
     + Bpmxth,Bpavth,Tpmxth,Tpavth,Shavth,Vthg,Vtchrt,Vtchtp,Shwid,
     + Shrad,Pldd,Pld1,Pldm,Vtavth,Dctare,Thscal
      Character*20 Subnm,Datafl
      Character*2 Pldflg
      Parameter (Pi=3.1415297,Rho=1025.9)
c
      Real Bpefch,BpAR,BpefAR,Tpefch,TpAR,TpefAR,Bdmxa,Volbd,Laminv
c
c     Variables calculated in this procedure.
c
      Real Ex,temp1,temp2,Alpha0,Beta0,K1,K2,Kb,Zwbp,Zwtp,Zwsh,
     #     Mqbp,Mqtp,Mqsh
c
c     Declaration of common blocks to provide access to the
```

```
c       variables by the subroutines.
c
        Common /main/ Lnbd,Lnbdnc,Lnbdtc,Hgbd,Wdbd,Cgz,Cschrt,Bpmdch,
     x                Tpmdch,Shfex,Bpry,Tpry,Thcny,Bpchtp,Bpchrt,Bpsp,
     x                Tpchtp,Tpchrt,Tpsp,Bpmxth,Bpavth,Tpmxth,Tpavth,
     x                Shavth,Vthg,Vtchrt,Vtchtp,Shwid,Shrad,Pldd,Pld1,
     x                Pldm,Vtavth,Tltyp,Shnum,Dctnum,Dctare,Thscal
     x         /name/ Subnm,Datafl,Pldflg
c
        Common /aspct/ Bpefch,BpAR,BpefAR,Tpefch,TpAR,TpefAR,Bdmxa,
     x                 Volbd,Laminv,K2,K1
c
c       Set the height of the vehicle to its height plus the diameter
c       of its payload in the case of a payload.
c
        If ((Pldflg .eq. 'y').OR.(Pldflg .eq. 'Y')) then
           Hgbd = Hgbd + Pldd
        end if
c
c       Calculate eccentricity of vehicle assuming it is a prolate
c       ellipsoid of diameter equal to the width.
c
        Ex = Sqrt(1 - (Wdbd*Wdbd)/(Lnbd*Lnbd))
c
c       calculate lamb's inertia coefficients.
c
        temp1 = log((1 + Ex)/(1 - Ex))
        temp2 = (1 - Ex*Ex)*Ex**(-3.)
c
        Alpha0 = 2*temp2*(0.5*temp1 - Ex)
        Beta0 = Ex**(-2.) - 0.5*temp2*temp1
c
        temp1 = Beta0 - Alpha0
        temp2 = 2 - Ex*Ex
c
        K1 = Alpha0/(2 - Alpha0)
        K2 = Beta0/(2 - Beta0)
        Kb = temp1*Ex**4/((2*Ex*Ex - temp2*temp1)*temp2)
c
c       Set temp1 to be the correction factor C1.
c
        temp1 = Hgbd/Wdbd
        temp1 = (-0.52*temp1 + 1.51)*temp1
c
        Acoef(1) = temp1*K1*Rho*Volbd
c
c       The three following terms are the main contributions to
c       C accel term due to the bovplanes, tailplanes and the shroud.
c
        Zwbp = (1 + 1/BpAR)**(-.5)*(Bpsp-Bpry)*Bpefch**2.
        if (Tltyp .eq. 1) then
           Zwtp = (1 + 1/TpAR)**(-.5)*(Tpsp-Tpry)*Tpefch**2.
        else
           Zwtp = (Tpsp-Tpry)*Tpefch**2.
        end if
        Zwsh = 2*(1 + 1/(2*Shrad/Shwid))**(-.5)*Shwid*Shwid*Shrad
c
c       Complete value of accel term C is,
c
        Acoef(2) = (K2*Wdbd*Wdbd*Lnbd/3 + .5*(Zwbp+Zwtp+Zwsh))*Pi*Rho
c
c       Value of Accel Term F2 is
c
        Acoef(3) = - .5*((Zwbp*Bpmdch) + (Zwtp*Tpmdch)
     *                 + (Zwsh*Shmdx)) * Pi * Rho
c
c       The three following terms are the main contributions to
c       Q accel term due to the bovplanes, tailplanes and the shroud.
c
        Mqbp = (BpAR/9)**(.36)*(Bpsp**2)*(Bpefch**3)/24
        Mqbp = Mqbp + Zwbp*Bpmdch**2
        if (Tltyp .eq. 1) then
           Mqtp = (TpAR/9)**(.36)*(Tpsp**2)*(Tpefch**3)/24
        else
           Mqtp = Tpsp*(Tpefch**4)/4
        end if
        Mqtp = Mqtp + Zwtp*Tpmdch**2
        Mqsh = ((2*Shrad)/(9*Shwid))**(.36)*(Shwid**3.)/6
        Mqsh = Mqsh*Shrad**2 + Zwsh*Shmdx**2
c
c       Complete value of the Accel Term Q,
c       set temp1 to moment of inertia of the displaced fluid.
c
        temp1=Icoef(1)*(Lnbd**2 + Hgbd**2)/20
        Acoef(4) = (Kb*temp1) + (Mqbp+Mqtp+Mqsh)*Rho*Pi
        If ((Pldflg .eq. 'y').OR.(Pldflg .eq. 'Y')) then
           Acoef(4)=Acoef(4) + Acoef(1)*((Pldd/2)**2.)
        end if
c
c       In the case of the payload, the vehicle's height was altered.
c       It must nov be restored since the following coefficients are
c       not altered.
c
        If ((Pldflg .eq. 'y').OR.(Pldflg .eq. 'Y')) then
           Hgbd = Hgbd - Pldd
        end if
c
        Return
        End
c*****************************************************************
c                                                                *
c       END OF SUBROUTINE ACCEL.                                 *
c                                                                *
c*****************************************************************
        Subroutine Drag(Cf,Ccoef)
c
        Real Ccoef(7,3)
        External Cf
c
        Integer Tltyp,Shnum,Dctnum
        Real Lnbd,Lnbdnc,Lnbdtc,Hgbd,Wdbd,Cgz,Cschrt,Bpmdch,Tpmdch,
     +  Shfex,Bpry,Tpry,Thcny,Bpchtp,Bpchrt,Bpsp,Tpchtp,Tpchrt,Tpsp,
     +  Bpmxth,Bpavth,Tpmxth,Tpavth,Shavth,Vthg,Vtchrt,Vtchtp,Shwid,
     +  Shrad,Pldd,Pld1,Pldm,Vtavth,Dctare,Thscal
        Character*20 Subnm,Datafl
        Character*2 Pldflg
        Parameter (Pi=3.1415297,Rho=1025.9)
c
        Real Bpefch,BpAR,BpefAR,Tpefch,TpAR,TpefAR,Bdmxa,K2,K1
c
c       Variables calculated in this procedure.
c
        Real temp1,Cfbd,Cfbp,Cftp,Laminv,Cdbd,Cdbprt,Cfvt,Cdvt,
     #       Cdvgtp,Vtarea,Cdthr,Cdpld
c
c       Declaration of common blocks to provide access to the
c       variables by the subroutines.
c
```

```
      Common /main/ Lnbd,Lnbdnc,Lnbdtc,Hgbd,Wdbd,Cgz,Cschrt,Bpmdch,
     %              Tpmdch,Shfex,Bpry,Tpry,Thcny,Bpchtp,Bpchrt,Bpsp,
     %              Tpchtp,Tpchrt,Tpsp,Bpmxth,Bpavth,Tpmxth,Tpavth,
     %              Shavth,Vthg,Vtchrt,Vtchtp,Shwid,Shrad,Pldd,Pldl,
     %              Pldm,Vtavth,Tltyp,Shnum,Dctnum,Dctare,Thscal
     %       /name/ Subnm,Datafl,Pldflg
c
      Common /aspct/ Bpefch,BpAR,BpefAR,Tpefch,TpAR,TpefAR,Bdmxa,
     %               Volbd,Laminv,K2,K1
c
c     NOTE : The frictional drag coefficient calculated
c     corresponds to the value at a forward velocity of
c     1 knot.  If the vehicle is moving faster this drag
c     coefficient is higher than the required value.
c
      Cfbd = Cf(Lnbd)
      Cfbp = Cf(Bpefch)
      Cftp = Cf(Tpefch)
c
c     Calculate the drag coefficient for the body.
c
      Laminv = (sqrt(Wdbd*Hgbd))/Lnbd
      Cdbd = Cfbd * (3/Laminv + 4.5*Laminv**.5 + 21*Laminv**2)
c
c     obtain contribution due to bowplane body intersection.
c
      Cdbprt = (.85*((Bpmxth/Bpchrt)**3.) - .0003)*Bpchrt**2
c
c     find drag coefficient of vertical surfaces.
c
      temp1 = (Vtchrt + Vtchtp)/2
      Cfvt = Cf(temp1)
      Cdvt = 2*Cfvt*(1 + 2*Vtavth/temp1 + 60*(Vtavth/temp1)**4)
c
c     if the tail is not the H tail then,
c     (in this case root drag of the tailplanes is neglected
c     since they are in the vehicles wake.)
c
      if (Tltyp .eq. 1) then
         Cdwgtp = .075*(2*(Bpmxth**2 + Tpmxth**2) + Vtavth**2)
         Vtarea = (Vtchrt + Vtchtp)*Vthg
      end if
c
c     in the case of a vehicle with an H tail.
c
      if (Tltyp .eq. 2) then
         Cdwgtp = .3*Vtavth**2
         Vtarea = 4*(Vtchrt + Vtchtp)*Vthg
      end if
c
c     contribution from thruster duct openings.
c
      Cdthr = .14*Dctnum*Dctare
c
c     Payload contribution if there is one
c
      Cdpld=0.
      If ((Pldflg .eq. 'y').OR.(Pldflg .eq. 'Y')) then
         Cdpld = 1.1 * Pldd*Pldd * Pi / 4
         Ccoef(7,1) = Cdpld
         Ccoef(7,2) = (Hgbd + Pldd)/2
      end if
c
c     Complete drag of vehicle may be found.
c
      Ccoef(1,1) = (Cdbd*(Wdbd*Hgbd*Pi)/4 + Cdbprt + Cdvt * Vtarea
     &  + Cdvgtp + Cdthr + Cdpld)/((Wdbd*Hgbd*Pi)/4)
c
c     Calculate drag coefficient of the bowplanes
c
      Ccoef(1,2)=2*Cfbp*(1+(Bpmxth/Bpefch)*2+60*(Bpmxth/Bpefch)**4)
c
c     Calculate drag coefficient of the tailplanes
c
      Ccoef(1,3)=2*Cftp*(1+(Tpmxth/Tpefch)*2+60*(Tpmxth/Tpefch)**4)
c
c
      Return
      End
c*************************************************************
c                                                            *
c     END OF SUBROUTINE DRAG.                                *
c                                                            *
c*************************************************************
      Subroutine Veloc(Ccoef,Cfder)
c
      Real Ccoef(7,3),Cfder(3,3)
c
c     This subroutine finds all the velocity related coefficients
c     except for the non-induced drag.
c
      Integer Tltyp,Shnum,Dctnum
      Real Lnbd,Lnbdnc,Lnbdtc,Hgbd,Wdbd,Cgz,Cschrt,Bpmdch,Tpmdch,
     +  Shfex,Bpry,Tpry,Thcny,Bpchtp,Bpchrt,Bpsp,Tpchtp,Tpchrt,Tpsp,
     +  Bpmxth,Bpavth,Tpmxth,Tpavth,Shavth,Vthg,Vtchrt,Vtchtp,Shwid,
     +  Shrad,Pldd,Pldl,Pldm,Vtavth,Dctare,Thscal
      Character*20 Subnm,Datafl
      Character*2 Pldflg
      Parameter (Pi=3.1415297,Rho=1025.9)
c
      Real Bpefch,BpAR,BpefAR,Tpefch,TpAR,TpefAR,Bdmxa,Volbd,Laminv
     #     ,K2,K1
c
c     Variables calculated in this procedure.
c
      Real temp1,temp2,Massnd,Clabd,Gtp,Ktp,Lambda,Wkfctr,Ftp,Cmbd,
     #     Zq0,Mq0,Cflpcr,Cflpcm,Kbp
c
c     Declaration of common blocks to provide access to the
c     variables by the subroutines.
c
      Common /main/ Lnbd,Lnbdnc,Lnbdtc,Hgbd,Wdbd,Cgz,Cschrt,Bpmdch,
     %              Tpmdch,Shfex,Bpry,Tpry,Thcny,Bpchtp,Bpchrt,Bpsp,
     %              Tpchtp,Tpchrt,Tpsp,Bpmxth,Bpavth,Tpmxth,Tpavth,
     %              Shavth,Vthg,Vtchrt,Vtchtp,Shwid,Shrad,Pldd,Pldl,
     %              Pldm,Vtavth,Tltyp,Shnum,Dctnum,Dctare,Thscal
     %       /name/ Subnm,Datafl,Pldflg
c
      Common /aspct/ Bpefch,BpAR,BpefAR,Tpefch,TpAR,TpefAR,Bdmxa,
     %               Volbd,Laminv,K2,K1
c
c     Calculate lift coefficients of the vehicle.
c
      Lambda=1/Laminv
      Massnd=(Pi*Wdbd*Wdbd*Lnbd/3)/(Lnbd**3)
      Clabd=0.234*Massnd**(.79)
c
c     Gtp is the effect of the body's downwash on the tailplane's
```

```
c       lift slope coefficient and is needed later.
c
        Gtp = 1 - 1.6*Lambda*Lambda*Clabd/Pi
c
c       Kbp is the effect of the body's downwash on the bowplane's
c       rotational derivative.
c
        Kbp = (Bpmdch+Bpefch/4)/Lnbd - .16/12
c
c       Ktp is the effect of the body's downwash on the tailplane's
c       rotational derivative.
c
        Ktp=Abs(Tpmdch+Tpefch/4)/Lnbd - .16*Lambda*Lambda*Massnd/Pi
c
c       Normalize the lift slope with respect to the vehicle's
c       cross-sectional area.
c
        Clabd=Clabd*Lnbd*Lnbd/Bdmxa
c
c       Liftslope coefficient for the bowplane.
c
        temp1=tanh(2/BpAR)
        temp1=(1 + BpAR/2)*temp1/(1 + temp1)
        temp2=(Wgbd*Hgbd*Pi)/(4*Lnbd*Lnbd)
        temp2=0.9*Sqrt(7.176*Lambda*temp2*Ccoef(1,1))
c
        Fbp=2*Pi*temp1/(1 + 2/BpefAR)
c
c       Liftslope coefficient for the tailplane.
c
        Wkfctr=0.9*(1 - (0.375*Laminv*Lnbd*temp2)/(Tpsp-Tpry))
c
        if (Tltyp .eq. 1) then
           temp1=tanh(2/TpAR)
           temp1=(1 + TpAR/2)*temp1/(1 + temp1)
           Ftp=2*Pi*temp1*Wkfctr/(1 + 2/TpefAR)
        end if
c
        if (Tltyp .eq. 2) then
           Ftp=2*Pi*Wkfctr
        end if
c
c       Find the body's pitching moment.
c
        temp1 = 1.0
        temp2 = Wdbd/Hgbd
        if (temp2 .lt. 1.) then
           temp1=(-.153*temp2+.176)*Hgbd/Lnbd + temp2
        end if
        if (temp2 .gt. 1.) then
           temp1=(-.69*temp2+.715)*Hgbd/Lnbd + temp2
        end if
c
        Cmbd = .87*(K2-K1)*Massnd*temp1*Lnbd*Lnbd/Bdmxa
c
c       Find the force rotational derivative of the body.
c
        Zq0 = (0.1 - K1)*Massnd*Lnbd*Lnbd/Bdmxa
c
c       Find the moment rotational derivative of the body.
c
        Mq0 = 0.045*Massnd*Lnbd*Lnbd/Bdmxa
c
c       Now that all the velocity derivatives are known they can be
c       stored in the main coefficient array.
c
        Ccoef(3,1) = Clabd
        Ccoef(3,2) = Fbp
        Ccoef(3,3) = Ftp*Gtp
c
        Ccoef(4,1) = Cmbd/(Lnbd*0.25)
        Ccoef(4,2) = Ccoef(3,2)
        Ccoef(4,3) = Ccoef(3,3)
c
        Ccoef(5,1) = Zq0
        Ccoef(5,2) = Fbp*Kbp
        Ccoef(5,3) = Ftp*Ktp
c
        Ccoef(6,1) = Mq0
        Ccoef(6,2) = Ccoef(5,2)
        Ccoef(6,3) = Ccoef(5,3)
c
        Ccoef(2,1) = (Ccoef(3,1)**2.)/(Pi*Wdbd/Lnbd)
        Ccoef(2,2) = (Ccoef(3,2)**2.)/(Pi*BpefAR)
        if (Tltyp .eq. 1) then
           Ccoef(2,3) = (Ccoef(3,3)**2.)/(Pi*TpefAR)
        else
           Ccoef(2,3) = 0.0
        end if
c
c       Find the control force derivatives.
c
        Cfder(1,1) = - Ccoef(2,2)
        Cfder(2,1) = - Ccoef(3,2)
        Cfder(3,1) = Ccoef(4,2)/(Bpmdch+Bpefch/2)+Ccoef(3,2)
c
        Cflpcr=-2.*(sqrt(Cschrt*(1-Cschrt)) + asin(sqrt(Cschrt)))/Pi
        Cflpcm= 2.*sqrt(Cschrt*(1-Cschrt)**3.)
        Cfder(1,2) = Ccoef(2,3)*Cflpcr
        Cfder(2,2) = Ccoef(3,3)*Cflpcr
        Cfder(3,2) = Cflpcm*(Tpefch/4)/Abs(Tpmdch+Tpefch/4)+Cfder(2,2)
        Cfder(3,2) = Abs(Cfder(3,2))
c
        Cfder(1,3) = Thscal
        Cfder(2,3) = 0.0
        Cfder(3,3) = 0.0
c
        Return
        End
c*****************************************************************
c                                                                *
c       END OF SUBROUTINE VELO.                                  *
c                                                                *
c*****************************************************************
        Subroutine Datasv(Icoef,Subdim,Acoef,Ccoef,Cfder,Vthder)
c
        Real Icoef(4),Subdim(6),Acoef(4),Ccoef(7,3),Cfder(3,3),
     1       Vthder(2,3)
c
c       This subroutine saves the data onto the datafile 'datafl'
c       for use by the simulation programs.
c
        Parameter (Accn=4,Sdmax=6,Inrn=4,Ccfn=7)
        Character*20 Subnm,Datafl
        Character*2 Pldflg
c
c       Declaration of common blocks to provide access to the
c       variables by the subroutines.
```

```
c
      Common /name/ Subnm,Datafl,Pldflg
c
c
c
      Open(unit=3,file=Datafl,status='new')
      write (3,5) subnm
 5    format (' ',A20)
      write (3,25) (Acoef(i), i=1,Accn)
      write (3,30) (Subdim(i), i=1,3)
      write (3,30) (Subdim(i), i=4,Sdnum)
      write (3,25) (Icoef(i), i=1,Inrn)
      do 10 i=1,Ccfn
         write (3,30) (Ccoef(i,j), j=1,3)
10    continue
      do 20 i=1,3
         write (3,30) (Cfder(i,j), j=1,3)
20    continue
      do 21 i=1,2
         write (3,30) (Vthder(i,j), j=1,3)
21    continue
      Close(unit=3)
c
c
      Return
c
c     Format statements to ouput the data.
25    format (' ',3(E14.7,2X),E14.7)
30    format (' ',2(E14.7,2X),E14.7)
      End
c*********************************************************************
c                                                                    *
c     END OF SUBROUTINE DATASV.                                      *
c                                                                    *
c*********************************************************************
      Real Function Cf(x)
c
      Real x
c
      Cf=0.515*x/1.83E-6
c
      Cf=(log10(Cf) - 2)**(-2.)*.075
c
      Return
      End
c*********************************************************************
c                                                                    *
c     END OF FUNCTION CF.                                            *
c                                                                    *
c*********************************************************************
```

```
      Program Findcf
C*****************************************************************************
C                                                                             *
C     This program requires the following data files :                        *
C                                                                             *
C     COEFFS.DAT ==> inertial & hydrodynamic coefficients of the              *
C                    submersible. (input file)                                *
C                                                                             *
C*****************************************************************************
C
C     Declaration of variables.
C
      integer i,j,Ndim,Direct,ihlf,Accn,Sdnum,Inrn,Ccfn
      real Acoef(4),subdim(6),Icoef(4),Vcoef(8),Ccoef(7,3),
     1 Cfder(3,3),Ginv(6,6),D,L(6),M(6),y(6),dery(6),prmt(5),
     2 aux(16,6),Cbltsn,time0,Vthder(2,3),uc,utau,kinvis
      parameter (Accn=4,Sdnum=6,Inrn=4,Ccfn=7)
      parameter (utau=2.90677E-3, kinvis=1.83E-6)
      character*20 subnm
      character*40 Simnm
C
      common /coefs/ Acoef,Subdim,Icoef,Vcoef,Ccoef,Cfder,Cbltsn,
     1 Ginv,Direct,time0,Vthder
C
C     Declaration of subroutines.
C
      external Minv,Imtrx,Velder,Fnderi,Ctfder
C
C     Read the vehicle's coefficients from the data file.
C
      Open(unit=3,file='COEFFS.DAT',status='old')
      read (3,5) subnm
 5    format (A20)
      read (3,15) (Acoef(i), i=1,4)
      read (3,16) (Subdim(i), i=1,3)
      read (3,16) (Subdim(i), i=4,6)
      read (3,15) (Icoef(i), i=1,4)
      do 10 i=1,Ccfn
         read (3,16) (Ccoef(i,j), j=1,3)
 10   continue
      do 11 i=1,3
         read (3,16) (Cfder(i,j), j=1,3)
 11   continue
      do 12 i=1,2
         read (3,16) (Vthder(i,j), j=1,3)
 12   continue
 15   format (' ',3(E14.7,2X),E14.7)
 16   format (' ',2(E14.7,2X),E14.7)
      Close(unit=3)
C
C     Calculate the vehicle's inertial matrix.
C
      Call Imtrx(Ginv,Acoef,Icoef)
C
C     Invert the inertial matrix in order to obtain the derivatives
C     of u,w and q.
      Ndim = 6
      Call Minv(Ginv,Ndim,D,L,M)
C
C     Determine all the velocity derivatives that are required.
C
      call Velder(Ccoef,Vcoef,Subdim)
C
C     Determine all the control derivatives that are required.
C
      call Ctfder(Cfder,Subdim)
c
c     input general data concerning the vehicle
c
      type *, 'Enter the direction of the vehicle .'
      type *, '1 for up and -1 for down.'
      read(5,20) Direct
      print *,'Direct :',Direct
 20   format(I2)
      type *, 'Enter the horizontal velocity of the vehicle .'
      read(5,25) y(1)
      print *,'y(1) :',y(1)
 25   format(e14.7)
      type *, 'Enter the vehicle''s angle of attack'
      read(5,25) alpha
      print *,'alpha :',alpha
      type *, 'Enter the vehicle''s x position.'
      read(5,25) y(4)
      print *,'y(4) :',y(4)
      type *, 'Enter the vehicle''s z position.'
      read(5,25) y(5)
      print *,'y(5) :',y(5)
      type *, 'Enter the vehicle''s pitch angle.'
      read(5,25) y(6)
      print *,'y(6) :',y(6)
      y(2) = y(1)*tan(alpha)
      print *,'y(2) :',y(2)
      type *, 'Enter the cable tension. '
      read(5,25) Cbltsn
      print *,'Cbltsn :',Cbltsn
      y(3) = 0.0
c
      call Fnderi(y)
C
      End
C
C*****************************************************************************
C                                                                             *
C     End of Main Program Simul                                               *
C                                                                             *
C*****************************************************************************
      Subroutine Imtrx(A,Acoef,Icoef)
c
      Real A(6,6),Acoef(4),Icoef(4)
c
      Integer i,j
c
      do 10 i=1,6
         do 20 j=1,6
            A(i,j)=0.0
 20      continue
 10   continue
c
c     determine the values of the coefficients of the inertial matrix.
c
      A(1,1) = Icoef(1) + Acoef(1)
      A(1,3) = Icoef(1) * Icoef(3)
      A(3,1) = A(1,3)
      A(2,2) = Icoef(1) + Acoef(2)
      A(2,3) = Acoef(3)
      A(3,2) = Acoef(3)
      A(3,3) = Icoef(2) + Acoef(4)
      A(4,4) = 1
```

```
      A(5,5) = 1
      A(6,6) = 1
c
      return
      end
c
c*************************************************************************
c                                                                        *
c*************************************************************************
      Subroutine Velder(Ccf,Vcf,Sdm)
c
      Real Ccf(7,3),Vcf(8),Sdm(6)
      real Swdens
      Parameter (Swdens = 1025.9)
c
      Vcf(1)= - Swdens*(Ccf(1,1)*Sdm(1) + Ccf(1,2)*Sdm(2)
     1  + Ccf(1,3)*Sdm(3))
c
      Vcf(2)= 0.5*Swdens*((Ccf(3,1) - Ccf(2,1))*Sdm(1)*2
     1  + (Ccf(3,2) - Ccf(2,2))*Sdm(2)*2
     2  + (Ccf(3,3) - Ccf(2,3))*Sdm(3)*2)
c
      Vcf(3)= - Swdens*(Ccf(3,1)*Sdm(1) + Ccf(3,2)*Sdm(2)
     1  + Ccf(3,3)*Sdm(3))
c
      Vcf(4)= - 0.5*Swdens*((Ccf(3,1) + Ccf(1,1))*Sdm(1)
     1  + (Ccf(3,2) + Ccf(1,2))*Sdm(2)
     2  + (Ccf(3,3) + Ccf(1,3))*Sdm(3))
c
      Vcf(5)= - Swdens*(Ccf(5,1)*Sdm(1)*Abs(Sdm(4))
     1  + Ccf(5,2)*Sdm(2)*Abs(Sdm(5))
     2  + Ccf(5,3)*Sdm(3)*Abs(Sdm(6)))
c
      Vcf(6)= Swdens*(Ccf(4,1)*Sdm(1)*Sdm(4)
     1  + Ccf(4,2)*Sdm(2)*Sdm(5)
     2  + Ccf(4,3)*Sdm(3)*Sdm(6))
c
      Vcf(7)= Swdens*(Ccf(6,1)*Sdm(1)*Sdm(4)
     1  + Ccf(6,2)*Sdm(2)*Sdm(5)
     2  + Ccf(6,3)*Sdm(3)*Sdm(6))
c
c     Vcf(8) is the effect of a payload displacing the center of
c     geometry.  This results in a coefficient Mu due to the drag
c     of the payload not acting through the center of the co-
c     ordinate system.
c
      Vcf(8) = -0.5*Swdens*Ccf(7,1)*Ccf(7,2)
c
      Return
      End
c
c*************************************************************************
c                                                                        *
c*************************************************************************
      Subroutine Ctfder(Cfd,Sdm)
c
      Real Cfd(3,3),Sdm(6)
      Real Swdens
      Parameter (Swdens = 1025.9)
c
      Cfd(1,1)= 0.5*Swdens*Cfd(1,1)*Sdm(1)
c
      Cfd(1,2)= 0.5*Swdens*Cfd(1,2)*Sdm(2)
c
      Cfd(2,1)= 0.5*Swdens*Cfd(2,1)*Sdm(1)
c
      Cfd(2,2)= 0.5*Swdens*Cfd(2,2)*Sdm(2)
c
      Cfd(3,1)= 0.5*Swdens*Cfd(3,1)*Sdm(1)*Sdm(5)
c
      Cfd(3,2)= 0.5*Swdens*Cfd(3,2)*Sdm(2)*Sdm(6)
c
c
      Return
      End
c
c*************************************************************************
c                                                                        *
c*************************************************************************
      Subroutine Fnderi(y)
c
      Real y(6)
c
      integer i,j,Direct,Cont
      real Acf(4),subdim(6),Icf(4),Vcoef(8),Ccoef(7,3),
     1  Cfder(3,3),Ginv(6,6),prmt(5),Cbltsn,time0,Vthder(2,3)
c
      common /coefs/ Acf,Subdim,Icf,Vcoef,Ccoef,Cfder,Cbltsn,
     1  Ginv,Direct,time0,Vthder
c
      real Vder(8),t0,t1,eta0,etal,etav,delta0,deltal,deltav,
     1  thrus0,thrusl,thrusv,dlt,psi,cblang,Xcable,Zcable,Mcable,
     2  Mgrav,uc,ui,vi,mq,Relvel,alpha,Cfvder(3,3),Vtf0,Vta0,
     3  Vtfl,Vtal,Vtfv,Vtav,Velrt,Vff,Vfa,Mvt,utau,kinvis,
     4  dery(6)
c
      save t0,t1,eta0,etal,etav,delta0,deltal,deltav,thrus0,
     1  thrusl,thrusv,Vtf0,Vta0,Vtfl,Vtal,Vtfv,Vtav
c
c
      parameter (utau=2.90677E-3, kinvis=1.83E-6)
c
  5   Relvel = sqrt(y(1)*y(1) + y(2)*y(2))
c
      do 10 i=1,8
         Vder(i) = Vcoef(i)*Relvel
 10   continue
c
      do 12 i=1,3
         do 14 j=1,2
            Cfvder(i,j) = Cfder(i,j)*Relvel*Relvel
 14      continue
         Cfvder(i,3) = Cfder(i,3)
 12   continue
c
c     The velocity derivatives Xw and Zu need to be multiplied
c     by the angle of incidence.
c
      if (y(1) .eq. 0.) then
         alpha = asin(1.0)
      else
         alpha = atan(y(2)/y(1))
      end if
      Vder(2) = Vder(2)*alpha
      Vder(3) = Vder(3)*alpha
c
c     find eta,delta and thrust
c
```

```
      type *, 'Enter the value for eta'
      read(5,25) etav
      print *,'etav :',etav
25    format (E14.7)
      type *, 'Enter the value for delta'
      read(5,25) deltav
      print *,'deltav :',deltav
      type *, 'Enter the value for thrust'
      read(5,25) thrusv
      print *,'thrusv :',thrusv
      type *, 'Enter the value for fore vert. thrust'
      read(5,25) vtfv
      print *,'vtfv :',vtfv
      type *, 'Enter the value for aft vert. thrust'
      read(5,25) vtav
      print *,'vtav :',vtav
      if ((Vtav .eq. 0.0) .and. (Vtfv .eq. 0.0)) go to 40
c
c     find the resulting velocity of the jets in the vertical
c     thrusters and scale the resulting vertical forces and pitching
c     moment.  The scaling is done with respect to the forward velocity.
c
      if (Vtfv .eq. 0.0) go to 41
c
      Vff=Vtfv/(512.95*Vthder(1,3))
      Vff=sqrt(Abs(Vff))
      Velrt=Abs(Relvel/Vff)
c
      if (Velrt .gt. 0.6) Velrt = 0.6
c
      if (Velrt .gt. Vthder(1,1)) then
         Vtfv=Vtfv*(1 + (Velrt - Vthder(1,1))*Vthder(1,2))
      end if
41    if (Vtav .eq. 0.0) go to 42
      Vfa=Vtav/(512.95*Vthder(1,3))
      Vfa=sqrt(Abs(Vfa))
      Velrt=Abs(Relvel/Vfa)
c
      if (Velrt .gt. 0.6) Velrt = 0.6
c
      if (Velrt .gt. Vthder(1,1)) then
         Vtav=Vtav*(1 + (Velrt - Vthder(1,1))*Vthder(1,2))
      end if
c
42    if (Vtfv .eq. 0.0) go to 43
      Vff=sqrt(Abs(Vff*Vff/Vthder(1,3)))
      Velrt=Abs(Relvel/Vff)
c
      if (Velrt .gt. 0.6) Velrt = 0.6
c
      if (Velrt .gt. Vthder(2,1)) then
         Mvt=Vtfv*(1+(Velrt-Vthder(2,1))*Vthder(2,2))
      else
         Mvt=Vtfv
      end if
43    if (Vtfv .eq. 0.0) go to 40
      Vfa=sqrt(Abs(Vfa*Vfa/Vthder(1,3)))
      Velrt=Abs(Relvel/Vfa)
c
      if (Velrt .gt. 0.6) Velrt = 0.6
c
      if (Velrt .gt. Vthder(2,1)) then
         Mvt=Mvt-Vtav*(1+(Velrt-Vthder(2,1))*Vthder(2,2))
      else
         Mvt=Mvt-Vtav
      end if
      Mvt=Mvt*Vthder(2,3)
c
c     find the static cable forces and moments aswell as pitching
c     moment due to gravity.
c
40    if (y(4) .eq. 0.0) then
        if (y(5) .lt. 0.0) then
           psi = - asin(1.0)
        else
           psi = asin(1.0)
        end if
      else
         psi = atan(y(5)/y(4))
      end if
      if (Direct .lt. 0) then
         cblang = psi + y(6)
         Xcable = -Cbltsn*cos(cblang)
      else
         cblang = psi - y(6)
         Xcable = Cbltsn*cos(cblang)
      end if
      Zcable = -Cbltsn*sin(cblang)
      Mcable = Icf(4)*Xcable
      Mgrav = -Icf(1)*9.81*Icf(3)*sin(y(6))
c
c     determine the current velocity, and from the hydrodynamic
c     velocity determine the inertial velocity of the vehicle.
c
      if (y(5) .le. 50.) then
         uc = 0.1545
      else if (y(5) .lt. 250.) then
            uc = 8.7*utau*((250.-y(5))*utau/kinvis)**(1./7.)
         else
            uc = 0.0
      end if
      if (Direct .lt. 0) then
         ui = y(1) - uc*cos(y(6))
         wi = y(2) - uc*sin(y(6))
      else
         ui = y(1) + uc*cos(y(6))
         wi = y(2) + uc*sin(y(6))
      end if
c
      mq = Icf(1)*y(3)
c
      fun1 = - mq*wi - Acf(2)*y(2)*y(3) - Acf(3)*y(3)*y(3)
     1  + Vder(1)*y(1) + Vder(2)*y(2)
     2  + Cfvder(1,1)*Abs((2*alpha+etav)*etav)
     3  + Cfvder(1,2)*Abs((2*alpha+deltav)*deltav)
     4  + Cfvder(1,3)*thrusv + Xcable
c
      fun2 = - mq*ui - Acf(1)*y(1)*y(3) + Icf(1)*Icf(3)**y(3)*y(3)
     1  + Vder(3)*y(1) + Vder(4)*y(2) + Vder(5)*y(3)
     2  + Cfvder(2,1)*etav + Cfvder(2,2)*deltav + Cfvder(2,3)*thrusv
     3  + Zcable + Vtfv + Vtav
c
      fun3 = - mq*wi*Icf(3) - Acf(3)*y(1)*y(3) + Vder(8)*y(1)
     1  + (Acf(2) - Acf(1))*y(1)*y(2) + Vder(6)*y(2)
     2  + Vder(7)*y(3) + Cfvder(3,1)*etav + Cfvder(3,2)*deltav
     3  + Cfvder(3,3)*thrusv + Mcable + Mgrav + Mvt
      Write(5,*) 'fun1',fun1,'   fun2',fun2,'   fun3',fun3
c
```

```
      do 30 i=1,3
         dery(i)=Ginv(i,1)*fun1 + Ginv(i,2)*fun2 + Ginv(i,3)*fun3
 30   continue
c
      dery(4) = ui*cos(y(6)) + wi*sin(y(6))
      dery(5) = - ui*sin(y(6)) + wi*cos(y(6))
      dery(6) = y(3)
c
      if (Direct .gt. 0) then
         dery(4) = - dery(4)
      end if
c
      Write(5,*) 'dery  ',dery(1),dery(2),dery(3)
c
      type *, 'Continue ? Enter 0 '
      read(5,31) Cont
 31   format(I2)
      if (Cont .eq. 0) go to 5
c
      return
 80   prmt(5)=1
      return
 90   format(' ',5(E14.7,2X),E14.7)
      end
c
```

```
      Program Gencfp
C*****************************************************************************
C                                                                              *
C       This program produces the following data file :                        *
C                                                                              *
C       CTRLFP.DAT ==> control force time histories for the simulation         *
C                      (output file)                                           *
C                                                                              *
C*****************************************************************************
c
c
      Integer i,Direct,Cntstp
      Integer*4 Iseed(3)
      Real eta,delta,thrus,etac(5),deltac(5),thrusc(5),
     1 Timedt(4),t,teta,tdel,tthr,Cbltsn,Xpos,Zpos,interv,
     2 Vtf,Vta,Vtfc(5),Vtac(5),tVtf,tVta,Intens(1),
     3 Bandwd(3),Thscal
      Character*40 Simnm,Datafl
c
c
      Print *,' Enter the Name of the Simulation.'
      Read(5,5) Simnm
 5    Format(A40)
 6    Format(' ',A40,2X,I2,2X,I3)
c
c     Obtain the name of the data file.
c
      Print *,' Enter the name of the data file '
      Print *,' Use at most six characters followed by .dat'
      Read (5,5) Datafl
c
c     Open the data file.
c
      Open (unit=3,file=Datafl,status='new')
c
c     Obtain the starting, and finishing times asvell as the time
c     interval and the error bound.
c
      Print *,' Enter starting time for simulation .'
      Read (5,10) Timedt(1)
      Print *,' Enter time for simulation to end.'
      Read (5,10) Timedt(2)
      Print *,' Enter time interval between successive values.'
      Read (5,10) Timedt(3)
      Print *,' Enter error bound .'
      Read (5,10) Timedt(4)
      Print *,'*************************************************'
      Print *,'*                                               *'
      Print *,'* Note : The origin of the coordinate system is  *'
      Print *,'*        at the clump. X is to the right and Z   *'
      Print *,'*        is down.  The clump is 250 meters from  *'
      Print *,'*        the sea bottom. There is a sea current  *'
      Print *,'*        of 0.3 knots till Z=50m and then the    *'
      Print *,'*        current drops using the 1/7th power law.*'
      Print *,'*                                               *'
      Print *,'*************************************************'
      Print *,' '
      Print *,' Enter Direction of Trajectory, forward = -1 .'
      Print *,' backwards = 1.'
      Read (5,11) Direct
      Print *,' Number of output values to skip.'
      Read (5,13) Cntstp
      Cntstp = Cntstp - 1
      Print *,' Enter x position of the vehicle :'
      Read (5,10) Xpos
      Print *,' Enter z position of the vehicle :'
      Read (5,10) Zpos
      Print *,' Enter the cable tension :'
      Read (5,10) Cbltsn
c
c     Write data that initialises the simulation.
c
      Write (3,6) Simnm,Direct,Cntstp
      Write (3,45) Xpos,Zpos,Cbltsn
      Write (3,40) (Timedt(i), i=1,4)
 10   Format (E14.7)
 11   Format (I2)
 12   Format (I6)
 13   Format (I3)
c
c     Acquire the intensities of the disturbances.
c
      Print *,'Enter the X-force disturbance intensity :'
      Read (5,10) Intens(1)
      Print *,'Enter the Z-force disturbance intensity :'
      Read (5,10) Intens(2)
      Print *,'Enter the M-moment disturbance intensity :'
      Read (5,10) Intens(3)
      Write (3,45) (Intens(i), i=1,3)
c
c     Acquire the bandwidth of the coloured noise (or disturbances).
c
      Print *,'Enter the X-force disturbance bandwidth :'
      Read (5,10) Bandwd(1)
      Print *,'Enter the Z-force disturbance bandwidth :'
      Read (5,10) Bandwd(2)
      Print *,'Enter the M-moment disturbance bandwidth :'
      Read (5,10) Bandwd(3)
      Write (3,45) (Bandwd(i), i=1,3)
c
      Print *,'Enter (int.) seed for disturbance generation :'
      Read (5,12) Iseed(1)
      Iseed(2) = Iseed(1) * 1.1
      Iseed(3) = Iseed(1) * 1.2
      Write (3,46) (Iseed(i), i=1,3)
c
      Print *,' Enter horizontal thruster scaling factor :'
      Read (5,10) Thscal
c
      Print *,' Enter time interval for control file generation.'
      Read (5,10) interv
c
c     Ask for starting characteristics of the control forces.
c
      call defun(etac,1)
      call defun(deltac,2)
      call defun(thrusc,3)
      call defun(Vtfc,4)
      call defun(Vtac,5)
c
c     generate control forces.
c
      do 20 t=Timedt(1),Timedt(2),interv
         eta=etac(1)
         delta=deltac(1)
         thrus=thrusc(1)
         Vtf=Vtfc(1)
         Vta=Vtac(1)
```

```
            teta = t - etac(5)
            tdel = t - deltac(5)
            tthr = t - thrusc(5)
            tVtf = t - Vtfc(5)
            tVta = t - Vtac(5)
            eta= eta + etac(2)*teta
            delta= delta + deltac(2)*tdel
            thrus= thrus + thrusc(2)*tthr
            thrus=thrus/Thscal
            Vtf= Vtf + Vtfc(2)*tVtf
            Vta= Vta + Vtac(2)*tVta
            etac(3)= eta
            deltac(3)= delta
            thrusc(3)= thrus
            Vtfc(3)= Vtf
            Vtac(3)= Vta
c
            Write (3,40) t,eta,delta,thrus,Vtf,Vta
c
            if (t .ge. etac(4)) then
               call defun(etac,1)
               etac(5) = t
            end if
            if (t .ge. deltac(4)) then
               call defun(deltac,2)
               deltac(5) = t
            end if
            if (t .ge. thrusc(4)) then
               call defun(thrusc,3)
               thrusc(5) = t
            end if
            if (t .ge. Vtfc(4)) then
               call defun(Vtfc,4)
               Vtfc(5) = t
            end if
            if (t .ge. Vtac(4)) then
               call defun(Vtac,5)
               Vtac(5) = t
            end if
c
 20     continue
c
c       End of Main Program Geneef
c
        Close (unit=3)
 40     Format (' ',5(E14.7,2X),E14.7)
 45     Format (' ',2(E14.7,2X),E14.7)
 46     Format (' ',2(I6,2X),I6)
        End
c
c
        Subroutine Defun(A,x)
c
        Integer x
        Real A(5)
c
        if (x .eq. 1) Print *,' Enter the values for the Bowplane.'
        if (x .eq. 2) Print *,' Enter the values for the Tailplane.'
        if (x .eq. 3) Print *,' Enter the values for the Thrusters.'
        if (x .eq. 4) Print *,' Enter values for Fore Vert. Thrus.'
        if (x .eq. 5) Print *,' Enter values for Aft Vert. Thrus.'
c
       Print *,' Present value for t =',A(4),' is ',A(3)
c
        Print *,' Enter Coefficient for t^0 : '
        Read (5,5) A(1)
        Print *,' Enter Coefficient for t^1 : '
        Read (5,5) A(2)
        Print *,' Enter Final Value of t for this function : '
        Read (5,5) A(4)
c
c
        Return
c
  5     Format (E14.7)
c
        End
c
```

```
      Program Genctr
c-----------------------------------------------------------------------
c
c       This program generates the data file 'CTRVA.DAT' for use
c       by the program ctrlc to generate the state equations that
c       will be used by to obtain the controller design.
c
c-----------------------------------------------------------------------
      integer ans
      real Uo,alpha,pi
      parameter(pi=3.141592653)
      character*20 Filenm
c
      Open(unit=3,file='CTRVA.DAT',status='new')
 10   Type *,'Enter the name of the desired file'
      Read (5,20) Filenm
c
      Type *,'Enter the hydrodynamic velocity U :'
      Read (5,30) Uo
c
      Type *,'Enter the angle of attack :'
      Read (5,30) alpha
      alpha = alpha*pi/180.
c
      Write (3,40) Uo,alpha,Filenm
c
      Type *,'Last entry ? ==> if yes answer with :  1'
      Read (5,50) ans
      if (ans .ne. 1) go to 10
c
      close(unit=3)
c
 20   Format(A20)
 30   Format(E14.7)
 40   Format(' ',E14.7,2X,E14.7,2X,A20)
 50   Format(I3)
c
      end
c
```

```
      Program Ctrlc
C*********************************************************************
C                                                                     *
C                                                                     *
C       This program determines the state equations for the vehicle as *
C       a function of the hydrodynamic velocity and the angle of inci- *
C       -dance of the submersible.  The vehicle's inertial velocity is *
C       not known, neither is the current velocity.  This program     *
C       assumes that the current velocity is much smaller than the    *
C       vehicle's inertial velocity, and that the hydrodynamic and the *
C       inertial velocities are almost identical.  This is not always  *
C       true and should be kept in mind.                              *
C                                                                     *
C       This program requires the following data files :              *
C                                                                     *
C       COEFFS.DAT ==> inertial & hydrodynamic coefficients of the    *
C                      submersible. (input file)                      *
C                                                                     *
C       CTRVA.DAT  ==> is an input file that specifies the vehicle's  *
C                      hydrodynamic velocity, its angle of attack and *
C                      the destination file names.                    *
C                                                                     *
C*********************************************************************
C
C       Declaration of variables.
C
        integer i,j,Ndim,ihlf,Accn,Sdnum,Inrn,Ccfn
        real Acoef(4),subdim(6),Icoef(4),Vcoef(8),Ccoef(7,3),
     1  Cfder(3,3),Ginv(6,6),D,L(6),M(6),y(13),dery(13),prmt(5),
     2  aux(16,13),Pert(4,4),Uo,alpha,A(4,4),B(4,3)
        parameter (Accn=4,Sdnum=6,Inrn=4,Ccfn=7)
        character*20 subnm,Filenm
C
        common /coefs/ Acoef,Subdim,Icoef,Vcoef,Ccoef,Cfder,Ginv,
     1  Pert
C
C       Declaration of subroutines.
C
        external Minv,Imtrx,Velder,Fnstat,Outp,Ctfder
C
C       Read the vehicle's coefficients from the data file.
C
        Open(unit=3,file='COEFFS.DAT',status='old')
        read (3,5) subnm
   5    format (A20)
        read (3,15) (Acoef(i), i=1,4)
        read (3,16) (Subdim(i), i=1,3)
        read (3,16) (Subdim(i), i=4,6)
        read (3,15) (Icoef(i), i=1,4)
        do 10 i=1,Ccfn
           read (3,16) (Ccoef(i,j), j=1,3)
  10    continue
        do 11 i=1,3
           read (3,16) (Cfder(i,j), j=1,3)
  11    continue
C
  15    format (' ',3(E14.7,2X),E14.7)
  16    format (' ',2(E14.7,2X),E14.7)
        Close(unit=3)
C
C       Calculate the vehicle's inertial matrix.
C
        Call Imtrx(Ginv,Acoef,Icoef)
C
C       Invert the inertial matrix in order to obtain the derivatives
C       of u,v and q.
        Ndim = 6
        Call Minv(Ginv,Ndim,D,L,M)
C
C       Determine all the velocity derivatives that are required.
C
        call Velder(Ccoef,Vcoef,Subdim)
C
C       Determine all the control derivatives that are required.
C
        call Ctfder(Cfder,Subdim)
C
C       Initialise the matrix of perturbation terms.
C
        do 60 i=1,3
              Pert(1,i) = 0.0
              Pert(i,1) = 0.0
              A(1,i) = 0.0
              B(1,i) = 0.0
  60    continue
        Pert(1,4) = 1.
        Pert(4,1) = - Icoef(1)*Icoef(3)*9.81
        A(1,4) = 1.
C
C       Calculate the coefficients for the velocities and angles of
C.      incidence specified in the data file 'CTRVA.DAT' .
        Open(unit=3,file='CTRVA.DAT',status='old')
C
  70    Read(3,65,end=75) Uo,alpha,Filenm
        Call Fnstat(Uo,alpha,A,B)
        Call Outp(Filenm,A,B)
        Go To 70
  75    Close(unit=3)
              B(1,i) = 0.0
  65    Format(' ',E14.7,2X,E14.7,2X,A20)
        End
C
C*********************************************************************
C                                                                     *
C       End of Main Program Simul                                     *
C                                                                     *
C*********************************************************************
        Subroutine Imtrx(A,Acoef,Icoef)
c
        Real A(6,6),Acoef(4),Icoef(4)
c
        Integer i,j
c
        do 10 i=1,6
           do 20 j=1,6
              A(i,j)=0.0
  20       continue
  10    continue
c
c       determine the values of the coefficients of the inertial matrix.
c
        A(1,1) = Icoef(1) + Acoef(1)
        A(1,3) = Icoef(1) * Icoef(3)
        A(3,1) = A(1,3)
        A(2,2) = Icoef(1) + Acoef(2)
        A(2,3) = Acoef(3)
        A(3,2) = Acoef(3)
        A(3,3) = Icoef(2) + Acoef(4)
```

```
      A(4,4) = 1
      A(5,5) = 1
      A(6,6) = 1
c
      return
      end
c
c*****************************************************************
c                                                                *
c*****************************************************************
      Subroutine Velder(Ccf,Vcf,Sdm)
c
      Real Ccf(7,3),Vcf(8),Sdm(6)
      Real Swdens
      Parameter (Swdens = 1025.9)
c
      Vcf(1)= - Swdens*(Ccf(1,1)*Sdm(1) + Ccf(1,2)*Sdm(2)
     1  + Ccf(1,3)*Sdm(3))
c
      Vcf(2)= 0.5*Swdens*((Ccf(3,1) - Ccf(2,1))*Sdm(1)*2
     1  + (Ccf(3,2) - Ccf(2,2))*Sdm(2)*2
     2  + (Ccf(3,3) - Ccf(2,3))*Sdm(3)*2)
c
      Vcf(3)= - Swdens*(Ccf(3,1)*Sdm(1) + Ccf(3,2)*Sdm(2)
     1  + Ccf(3,3)*Sdm(3))
c
      Vcf(4)= - 0.5*Swdens*((Ccf(3,1) + Ccf(1,1))*Sdm(1)
     1  + (Ccf(3,2) + Ccf(1,2))*Sdm(2)
     2  + (Ccf(3,3) + Ccf(1,3))*Sdm(3))
c
      Vcf(5)= - Swdens*(Ccf(5,1)*Sdm(1)*Abs(Sdm(4))
     1  + Ccf(5,2)*Sdm(2)*Abs(Sdm(5))
     2  + Ccf(5,3)*Sdm(3)*Abs(Sdm(6)))
c
      Vcf(6)= Swdens*(Ccf(4,1)*Sdm(1)*Sdm(4)
     1  + Ccf(4,2)*Sdm(2)*Sdm(5)
     2  + Ccf(4,3)*Sdm(3)*Sdm(6))
c
      Vcf(7)= Swdens*(Ccf(6,1)*Sdm(1)*Sdm(4)
     1  + Ccf(6,2)*Sdm(2)*Sdm(5)
     2  + Ccf(6,3)*Sdm(3)*Sdm(6))
c
c     Vcf(8) is the effect of a payload displacing the center of
c     geometry.  This results in a coefficient Mu due to the drag
c     of the payload not acting through the center of the co-
c     ordinate system.
c
      Vcf(8) = -0.5*Swdens*Ccf(7,1)*Ccf(7,2)
c
      Return
      End
c
c*****************************************************************
c                                                                *
c*****************************************************************
      Subroutine Ctfder(Cfd,Sdm)
c
      Real Cfd(3,3),Sdm(6)
      Real Swdens
      Parameter (Swdens = 1025.9)
c
      Cfd(1,1)= 0.5*Swdens*Cfd(1,1)*Sdm(1)
c
      Cfd(1,2)= 0.5*Swdens*Cfd(1,2)*Sdm(2)
c
      Cfd(2,1)= 0.5*Swdens*Cfd(2,1)*Sdm(1)
c
      Cfd(2,2)= 0.5*Swdens*Cfd(2,2)*Sdm(2)
c
      Cfd(3,1)= 0.5*Swdens*Cfd(3,1)*Sdm(1)*Sdm(5)
c
      Cfd(3,2)= 0.5*Swdens*Cfd(3,2)*Sdm(2)*Sdm(6)
c
c
      Return
      End
c
c*****************************************************************
c                                                                *
c*****************************************************************
      Subroutine Fnstat(Uo,alpha,A,B)
c-----------------------------------------------------------------
c
c     This procedure generates the state equations for the vehicle
c     at a specific operating condition.
c
c-----------------------------------------------------------------
      Real Uo,alpha,A(4,4),B(4,3)
c
      integer i,j,k
      real Acf(4),subdim(6),Icf(4),Vcoef(8),Ccoef(7,3),
     1  Cfder(3,3),Ginv(6,6),Pert(4,4)
c
      common /coefs/ Acf,Subdim,Icf,Vcoef,Ccoef,Cfder,Ginv,
     1  Pert
c
      real Vder(8),Wo,ui,wi,mq,Relvel,Cfvder(3,3),Swdens,
     1  Tmp(4),Xalpha,Zalpha,Xvel,Zvel,Mvel,Vcf6
c
c
      parameter (Swdens=1025.9)
c
      Wo = Uo*tan(alpha)
      ui = Uo
      wi = Wo
      Qo = 0.0
      Relvel = sqrt(Uo*Uo + Wo*Wo)
c
      Vcf6 = Vcoef(6)
      do 10 i=1,8
         Vder(i) = Vcoef(i)*Relvel
 10   continue
c
      Cfder(1,1) = 0.0
      Cfder(1,2) = 0.0
      do 12 i=1,3
         do 14 j=1,2
            Cfvder(i,j) = Cfder(i,j)*Relvel*Relvel
 14      continue
         Cfvder(i,3) = Cfder(i,3)
 12   continue
c
      mq = Icf(1)*Qo
c
c-----------------------------------------------------------------
c
c     The following section determines the state equation terms .
c
```

```
c-----------------------------------------------------------------------|
c
        do 45 i=1,3
           Tmp(i) = 0.0
           do 46 j=1,3
              Tmp(i) = Tmp(i) + Ccoef(i,j) * Subdim(j)
 46        continue
 45     continue
c
        Xalpha=0.5*Swdens*((Tmp(3)*2+Tmp(1)-Tmp(2)*(2-alpha*alpha))
     *        *alpha)
        Zalpha=0.5*Swdens*(Tmp(3)*(alpha*alpha-1)-Tmp(1)-Tmp(2)*3
     *        *alpha*alpha)
c
c       Following terms are the derivatives due to changes in velocity only.
c
        Xvel = Swdens*(Tmp(3)*alpha*sin(alpha)
     -        - (Tmp(1)+Tmp(2)*alpha**2)*cos(alpha))
        Zvel = Swdens*(-Tmp(3)*alpha*cos(alpha)
     -        - (Tmp(1)+Tmp(2)*alpha**2)*sin(alpha))
        Mvel = 2*Vcf6*alpha
c
        Pert(2,2)= - Xalpha*Wo + Xvel*Uo
c
        Pert(2,3)= Xalpha*Uo-(Acf(2)+Icf(1))*Qo
c
        Pert(2,4)= -(Acf(2)*Wo+Icf(1)*wi+Acf(3)*2*Qo)
c
        Pert(3,2)= -Zalpha*Wo-mq+Acf(1)*Qo + Zvel*Uo
c
        Pert(3,3)= Zalpha*Uo
c
        Pert(3,4)= Vder(5)+Icf(1)*(ui+Icf(3)*2*Qo)
c
        Pert(4,2)= Vder(8)+(Acf(2)-Acf(1))*Wo+Acf(3)*Qo
     +              + Mvel*Uo
c
        Pert(4,3)= Vder(6)-mq+(Acf(2)-Acf(1))*Uo
c
        Pert(4,4)= Vder(7)-(Icf(1)*Icf(3)*wi)+Acf(3)*Uo
c
c       Now that the individual components have been determined they
c       are multiplied with the inverse of the inertia matrix Ginv and the
c       matrices A and B can be determined.
c
        do 50 i=2,4
           do 55 j=1,4
           k=i-1
           A(i,j)=Ginv(k,1)*Pert(2,j) + Ginv(k,2)*Pert(3,j)
     #           + Ginv(k,3)*Pert(4,j)
 55        continue
c
           do 60 j=1,3
              k=i-1
              B(i,j) = Ginv(k,1)*Cfvder(1,j) + Ginv(k,2)*Cfvder(2,j)
     #              + Ginv(k,3)*Cfvder(3,j)
 60        continue
 50     continue
c
        return
        end
c
c*************************************************************************
c                                                                        *
```

```
c*********************************************************************
        subroutine Outp(Filenm,A,B)
c
        real A(4,4),B(4,3)
        character*20 Filenm
c
        integer i,j
c
        Open(unit=4,file=Filenm,status='new')
        do 20 i=1,4
           write (unit=4,fmt=10) (A(i,j), j=1,4)
 20     continue
        do 25 i=1,4
           write (unit=4,fmt=15) (B(i,j), j=1,3)
 25     continue
c
        Close(unit=4)
        return
 10     format (' ',3(E14.7,2X),E14.7)
 15     format (' ',2(E14.7,2X),E14.7)
c
        end
c
```

```
      Program Simulc
C*****************************************************************************
C                                                                             *
C                                                                             *
C     This program uses a hamming predictor-corrector to numerically          *
C     integrate the equations of motion to produce the velocity, the          *
C     position and attitude of the submersible.                               *
C                                                                             *
C     This program requires the following data files :                        *
C                                                                             *
C     COEFFP.DAT ==> inertial & hydrodynamic coefficients of the              *
C                    submersible. (input file)                                *
C                                                                             *
C     COEFKM.DAT ==> inertial & hydrodynamic coefficients of the              *
C                    compensator model. (input file)                          *
C                                                                             *
C     CTRLFP.DAT ==> bowplane & tailplane deflection and thrust time          *
C                    history. This also includes the data required            *
C                    generate coloured noise. (input file)                    *
C                                                                             *
C     SIMULP.DAT ==> contains the hydrodynamic and inertial velocity          *
C                    vector time histories, aswell as the position            *
C                    and attitude time history. (output file)                 *
C                                                                             *
C     SIMPER.DAT ==> contains the perturbation velocity vector time           *
C                    histories, aswell as the time history of the             *
C                    attitude and disturbance forces. (output file)           *
C                                                                             *
C     INPUTS.DAT ==> contains the controller inputs to the plant              *
C                    with time. (output file)                                 *
C                                                                             *
C     GAINS.DAT  ==> contains the control and filter gains of the             *
C                    LQG/LTR controller preceded by two arrays of             *
C                    ordering of the gain matrices with respect to            *
C                    velocity and angle of attack.                            *
C                                                                             *
C*****************************************************************************
C
C     Declaration of variables.
C
      integer i,j,k,l,Ndim,Direct,ihlf,Accn,Sdnum,Inrn,Ccfn,Cntstp
      real Acoef(4),subdim(6),Icoef(4),Vcoef(8),Ccoef(7,3),
     1     Cfder(3,3),Ginv(6,6),Dinv,Linv(6),M(6),y(25),dery(25),
     2     prmt(5),aux(16,25),Cbltsn,time0,Vthder(2,3),uc,
     3     utau,kinvis,Pert(4,4),Intens(3),Bandwd(3),alpham(7),
     4     velocm(6),Gcoef(3,7,7,6),Hcoef(7,3,7,6)
C
      real Kmacf(4),Kmsdm(6),Kmicf(4),Kmvcf(8),Kmccf(7,3),
     1     Kmcfd(3,3),Kmginv(6,6),Kmpert(4,4)
C
      parameter (Accn=4,Sdnum=6,Inrn=4,Ccfn=7)
      parameter (utau=2.90677E-3, kinvis=1.83E-6)
      character*20 subnm,compnm
      character*40 Simnm
      character*9 dtbuf
      character*8 tmbuf
C
      common /coefs/ Acoef,Subdim,Icoef,Vcoef,Ccoef,Cfder,Cbltsn,
     1               Ginv,Direct,time0,Vthder,Pert,Intens,Bandwd
      common /output/ Cntstp
C
      common /compens/ Kmacf,Kmsdm,Kmicf,Kmvcf,Kmccf,Kmcfd,Kmginv,
     1                 Kmpert
C
      common /matr/ alpham,velocm,Gcoef,Hcoef
C
C     Declaration of subroutines.
C
      external Minv,Hpcg,Imtrx,Velder,Fnderi,Outp,Ctfder
C
C     Read the vehicle's coefficients from the data file.
C
      Open(unit=3,file='COEFFP.DAT',status='old')
      read (3,5) subnm
    5 format (A20)
      read (3,15) (Acoef(i), i=1,4)
      read (3,16) (Subdim(i), i=1,3)
      read (3,16) (Subdim(i), i=4,6)
      read (3,15) (Icoef(i), i=1,4)
      do 10 i=1,Ccfn
         read (3,16) (Ccoef(i,j), j=1,3)
   10 continue
      do 11 i=1,3
         read (3,16) (Cfder(i,j), j=1,3)
   11 continue
      do 12 i=1,2
         read (3,16) (Vthder(i,j), j=1,3)
   12 continue
      Close(unit=3)
   15 format (' ',3(E14.7,2X),E14.7)
   16 format (' ',2(E14.7,2X),E14.7)
C
C     Read the compensator's coefficients from the data file.
C
      Open(unit=3,file='COEFKM.DAT',status='old')
      read (3,5) compnm
      read (3,15) (Kmacf(i), i=1,4)
      read (3,16) (Kmsdm(i), i=1,3)
      read (3,16) (Kmsdm(i), i=4,6)
      read (3,15) (Kmicf(i), i=1,4)
      do 20 i=1,Ccfn
         read (3,16) (Kmccf(i,j), j=1,3)
   20 continue
      do 21 i=1,3
         read (3,16) (Kmcfd(i,j), j=1,3)
   21 continue
      Close(unit=3)
C
C     Obtain the control and filter gain matrices.
C
      Open(unit=3,file='GAINS.DAT',status='old')
      read(3,*) (alpham(i), i=1,7)
      read(3,*) (velocm(i), i=1,6)
      read(3,*) ((((Gcoef(i,j,k,l),l=1,6),k=1,7),j=1,7),i=1,3)
      read(3,*) ((((Hcoef(i,j,k,l),l=1,6),k=1,7),j=1,3),i=1,7)
      Close(unit=3)
C
C=============================================================================
C
C     Calculate the vehicle's inertial matrix.
C
      Call Imtrx(Ginv,Acoef,Icoef)
C
C     Invert the inertial matrix in order to obtain the derivatives
C     of u,v and q.
      Ndim = 6
      Call Minv(Ginv,Ndim,Dinv,Linv,M)
C
```

```
C       Determine all the velocity derivatives that are required.
C
        call Velder(Ccoef,Vcoef,Subdim)
C
C       Determine all the control derivatives that are required.
C
        call Ctfder(Cfder,Subdim)
C
C=======================================================================
C
C       Calculate the compensator's inertial matrix.
C
        Call Imtrx(Kmginv,Kmacf,Kmicf)
C
C       Invert the inertial matrix in order to obtain the derivatives
C       of u,w and q.
        Ndim = 6
        Call Minv(Kmginv,Ndim,Dinv,Linv,M)
C
C       Determine all the velocity derivatives that are required.
C
        call Velder(Kmccf,Kmvcf,Kmsdm)
C
C       Determine all the control derivatives that are required.
C
        call Ctfder(Kmcfd,Kmsdm)
C
C=======================================================================
C
C       Open the files that are to be used during the simulation.
C
        Open(unit=7,file='SIMPER.DAT',status='new',recl=256)
        Open(unit=8,file='CTRLFP.DAT',status='old')
        Open(unit=9,file='SIMULP.DAT',status='new',recl=256)
        Open(unit=10,file='INPUTS.DAT',status='new')
C
C       Label Simulation data file for record keeping.
C
        Write (7,*) subnm,'      ',Simnm
        Write (9,*) subnm,'      ',Simnm
        Write (10,*) subnm,'      ',Simnm
C
C       Enter date and time for run.
C
        call date(dtbuf)
        call time(tmbuf)
        write(7,*) 'Simulation simulc on ',dtbuf,' at ',tmbuf,'.'
        write(9,*) 'Simulation simulc on ',dtbuf,' at ',tmbuf,'.'
        write(10,*) 'Simulation simulc on ',dtbuf,' at ',tmbuf,'.'
C
C       Write header for the variables.
C
        write (unit=9,fmt=30) 'TIME','X position','Z position',
     *  'Attitude','Forward vel','Downward vel','Pitch rate'
 30     Format(' ',6(A14,2X),A14)
        write (unit=7,fmt=31) 'TIME','X disturbance','Z disturbance',
     *  'M disturbance','Attitude','Forward vel','Downward vel',
     *  'Pitch rate','X displacement','Z displacement','Xpos total',
     *  'Zpos total'
 31     Format(' ',11(A14,2X),A14)
        write (unit=10,fmt=30) 'TIME','Bowplane','Tailplane','Thrust'
 32     Format(' ',3(A14,2X),A14)
C
C       Obtain the name of the simulation and the current direction.
C
        Read(8,40) Simnm,Direct,Cntstp
 40     Format(' ',A40,2X,I2,2X,I3)
C
C       Read the location of the submersible and obtain the cable
C       tension for the simulation.
C
        Read(8,41) y(4),y(5),Cbltsn
 41     Format(' ',2(E14.7,2X),E14.7)
C
C       Obtain the time interval & increment for the simulation.
C
        Read(8,50) (prmt(i), i=1,4)
 50     Format(' ',3(E14.7,2X),E14.7)
        time0=prmt(1)
C
C       Obtain disturbance intensities
C
        Read(8,51) (Intens(i), i=1,3)
 51     Format(' ',2(E14.7,2X),E14.7)
C
C       Obtain disturbance bandwidths.
C
        Read(8,51) (Bandwd(i), i=1,3)
C
C       Initialise weighting function for the numerical integration.
C
        dery(1)= 0.3
        dery(2)= 0.15
        dery(3)= 0.15
        dery(4)= 0.15
        dery(5)= 0.05
        do 56 i=6,25
           dery(i)= 0.01
           y(i)=0.0
 56     continue
C
        y(2)=0.0
        y(3)=0.0
c
c       determine the current velocity, and from the hydrodynamic
c       velocity determine the inertial velocity of the vehicle.
c
        if (y(5) .le. 50.) then
           uc = 0.1545
        else if (y(5) .lt. 250.) then
              uc = 8.7*utau*((250.-y(5))*utau/kinvis)**(1./7.)
           else
              uc = 0.0
        end if
C
C       Initialise the y vector as a function of the direction the
C       submersible is traveling as a function of the current.
C
        if (Direct .lt. 0) then
           y(1)= uc
        else
           y(1)= - uc
        end if
C
C       Initialise the matrix of perturbation terms.
C
        do 60 i=1,3
              Pert(1,i) = 0.0
```

```
            Pert(i,1) = 0.0
            Kmpert(1,i) = 0.0
            Kmpert(i,1) = 0.0
 60     continue
        Pert(1,4) = 1.
        Pert(4,1) = - Icoef(1)*Icoef(3)*9.81
        Kmpert(1,4) = 1.
        Kmpert(4,1) = - Kmicf(1)*Kmicf(3)*9.81
C
C       Now that the inverse of the inertia matrix is available, the
C       numerical integration using Hamming's modified predictor
C       corrector is used.
C
        Ndim = 25
        Call Hpcg(prmt,y,dery,ndim,ihlf,Fnderi,outp,aux)
C
C       Close all data files
C
        Close(unit=7)
        Close(unit=8)
        Close(unit=9)
        Close(unit=10)
C
        End
C
C*************************************************************************
C                                                                        *
C       End of Main Program Simulc                                       *
C                                                                        *
C*************************************************************************
        Subroutine Imtrx(A,Acoef,Icoef)
c
        Real A(6,6),Acoef(4),Icoef(4)
c
        Integer i,j
c
        do 10 i=1,6
           do 20 j=1,6
              A(i,j)=0.0
 20        continue
 10     continue
c
c       determine the values of the coefficients of the inertial matrix.
c
        A(1,1) = Icoef(1) + Acoef(1)
        A(1,3) = Icoef(1) * Icoef(3)
        A(3,1) = A(1,3)
        A(2,2) = Icoef(1) + Acoef(2)
        A(2,3) = Acoef(3)
        A(3,2) = Acoef(3)
        A(3,3) = Icoef(2) + Acoef(4)
        A(4,4) = 1
        A(5,5) = 1
        A(6,6) = 1
c
        return
        end
c
c*************************************************************************
c                                                                        *
c*************************************************************************
        Subroutine Velder(Ccf,Vcf,Sdm)
c
        Real Ccf(7,3),Vcf(8),Sdm(6)
        real Swdens
        Parameter (Swdens = 1025.9)
c
        Vcf(1)= - Swdens*(Ccf(1,1)*Sdm(1) + Ccf(1,2)*Sdm(2)
     1  + Ccf(1,3)*Sdm(3))
c
        Vcf(2)= 0.5*Swdens*((Ccf(3,1) - Ccf(2,1))*Sdm(1)*2
     1  + (Ccf(3,2) - Ccf(2,2))*Sdm(2)*2
     2  + (Ccf(3,3) - Ccf(2,3))*Sdm(3)*2)
c
        Vcf(3)= - Swdens*(Ccf(3,1)*Sdm(1) + Ccf(3,2)*Sdm(2)
     1  + Ccf(3,3)*Sdm(3))
c
        Vcf(4)= - 0.5*Swdens*((Ccf(3,1) + Ccf(1,1))*Sdm(1)
     1  + (Ccf(3,2) + Ccf(1,2))*Sdm(2)
     2  + (Ccf(3,3) + Ccf(1,3))*Sdm(3))
c
        Vcf(5)= - Swdens*(Ccf(5,1)*Sdm(1)*Abs(Sdm(4))
     1  + Ccf(5,2)*Sdm(2)*Abs(Sdm(5))
     2  + Ccf(5,3)*Sdm(3)*Abs(Sdm(6)))
c
        Vcf(6)= Swdens*(Ccf(4,1)*Sdm(1)*Sdm(4)
     1  + Ccf(4,2)*Sdm(2)*Sdm(5)
     2  + Ccf(4,3)*Sdm(3)*Sdm(6))
c
        Vcf(7)= Swdens*(Ccf(6,1)*Sdm(1)*Sdm(4)
     1  + Ccf(6,2)*Sdm(2)*Sdm(5)
     2  + Ccf(6,3)*Sdm(3)*Sdm(6))
c
c       Vcf(8) is the effect of a payload displacing the center of
c       geometry.  This results in a coefficient Mu due to the drag
c       of the payload not acting through the center of the co-
c       ordinate system.
c
        Vcf(8) = -0.5*Swdens*Ccf(7,1)*Ccf(7,2)
c
        Return
        End
c
c*************************************************************************
c                                                                        *
c*************************************************************************
        Subroutine Ctfder(Cfd,Sdm)
c
        Real Cfd(3,3),Sdm(6)
        Real Swdens
        Parameter (Swdens = 1025.9)
c
        Cfd(1,1)= 0.5*Swdens*Cfd(1,1)*Sdm(1)
c
        Cfd(1,2)= 0.5*Swdens*Cfd(1,2)*Sdm(2)
c
        Cfd(2,1)= 0.5*Swdens*Cfd(2,1)*Sdm(1)
c
        Cfd(2,2)= 0.5*Swdens*Cfd(2,2)*Sdm(2)
c
        Cfd(3,1)= 0.5*Swdens*Cfd(3,1)*Sdm(1)*Sdm(5)
c
        Cfd(3,2)= 0.5*Swdens*Cfd(3,2)*Sdm(2)*Sdm(6)
c
c
        Return
        End
c
```

```
c*****************************************************************************
c                                                                             *
c*****************************************************************************
      Subroutine Fnderi(t,y,dery)
c-----------------------------------------------------------------------------
c
c       This procedure generates the disturbance forces and filters
c       them, aswell as producing the hydrodynamic force relations.
c       Both the steady state and perturbation forces are determined.
c       The vector y is defined as follows :
c               y(1)  ---> hydrodynamic velocity u .
c               y(2)  ---> hydrodynamic velocity w .
c               y(3)  ---> pitch rate q .
c               y(4)  ---> position x in clump coords .
c               y(5)  ---> position z in clump coords .
c               y(6)  ---> pitch angle theta .
c               y(7)  ---> pertubation pitch angle theta" .
c               y(8)  ---> pertubation velocity u" .
c               y(9)  ---> pertubation velocity w" .
c               y(10) ---> pertubation pitch rate q" .
c               y(11) ---> low-pass filter X disturbance force .
c               y(12) ---> low-pass filter Z disturbance force .
c               y(13) ---> low-pass filter M disturbance moment .
c               y(14) ---> displaced x position in clump coords .
c               y(15) ---> displaced z position in clump coords .
c
c       Inputs to the Plant :
c
c               y(16) ---> bowplane deflection eta .
c               y(17) ---> tailplane deflection delta .
c               y(18) ---> horizontal thrust .
c
c       States of the Compensator in sequence.
c
c               y(19) ---> bowplane deflection eta .
c               y(20) ---> tailplane deflection delta .
c               y(21) ---> horizontal thrust .
c               y(22) ---> compensator pitch angle theta" .
c               y(23) ---> compensator velocity u" .
c               y(24) ---> compensator velocity w" .
c               y(25) ---> compensator pitch rate q" .
c
c-----------------------------------------------------------------------------
      Real t,y(25),dery(25)
c
      integer i,j,k,Direct
      integer*4 Iseed(3)
      real Acf(4),subdim(6),Icf(4),Vcoef(8),Ccoef(7,3),
     1 Cfder(3,3),Ginv(6,6),prmt(5),Cbltsn,time0,Vthder(2,3),
     2 Pert(4,4),Intens(3),Bandwd(3)
c
      real Kmacf(4),Kmsdm(6),Kmicf(4),Kmvcf(8),Kmccf(7,3),
     1     Kmcfd(3,3),Kmginv(6,6),Kmpert(4,4),Kmvder(8),
     2     Kmcfvd(3,3)
c
      common /coefs/ Acf,Subdim,Icf,Vcoef,Ccoef,Cfder,Cbltsn,
     1 Ginv,Direct,time0,Vthder,Pert,Intens,Bandwd
c
      common /compens/ Kmacf,Kmsdm,Kmicf,Kmvcf,Kmccf,Kmcfd,Kmginv,
     1                 Kmpert
c
      real Vder(8),t0,t1,eta0,eta1,etav,delta0,delta1,deltav,
     1 thrus0,thrus1,thrusv,dlt,psi,cblang,Xcable,Zcable,Mcable,
     2 Mgrav,uc,ui,wi,mq,Relvel,alpha,Cfvder(3,3),Vtf0,Vta0,
     3 Vtf1,Vta1,Vtfv,Vtav,Velrt,Vff,Vfa,Mvt,utau,kinvis,Swdens,
     4 Tmp(4),Xalpha,Zalpha,Hy(7),Bu(3),u(3),G(3,7),H(7,3),Xvel,
     5 Zvel,Mvel,tprev,rndm(3),Vcf6,Kmvcf6
c
      save t0,t1,eta0,eta1,etav,delta0,delta1,deltav,thrus0,
     1 thrus1,thrusv,Vtf0,Vta0,Vtf1,Vta1,Vtfv,Vtav,Iseed,tprev,
     2 rndm
c
c
      parameter (utau=2.90677E-3, kinvis=1.83E-6,Swdens=1025.9)
c
      Relvel = sqrt(y(1)*y(1) + y(2)*y(2))
c
      Vcf6 = Vcoef(6)
      Kmvcf6 = Kmvcf(6)
      do 10 i=1,8
         Vder(i) = Vcoef(i)*Relvel
         Kmvder(i) = Kmvcf(i)*Relvel
 10   continue
c
      do 12 i=1,3
         do 14 j=1,2
            Cfvder(i,j) = Cfder(i,j)*Relvel*Relvel
            Kmcfvd(i,j) = Kmcfd(i,j)*Relvel*Relvel
 14      continue
         Cfvder(i,3) = Cfder(i,3)
         Kmcfvd(i,3) = Kmcfd(i,3)
 12   continue
c
c     The velocity derivatives Xv and Zu need to be multiplied
c     by the angle of incidence.
c
      if (y(1) .eq. 0.) then
         alpha = asin(1.0)
      else
         alpha = atan(y(2)/y(1))
      end if
      Vder(2) = Vder(2)*alpha
      Vder(3) = Vder(3)*alpha
      Kmvder(2) = Kmvder(2)*alpha
      Kmvder(3) = Kmvder(3)*alpha
c
c     find eta,delta and thrust
c
      if (t .eq. time0) then
         read(unit=8,fmt=95,end=80) Iseed(1),Iseed(2),Iseed(3)
         read(unit=8,fmt=90,end=80) t0,eta0,delta0,thrus0,Vtf0,Vta0
         read(unit=8,fmt=90,end=80) t1,eta1,delta1,thrus1,Vtf1,Vta1
      end if
c
 20   if (t .gt. t1) then
         eta0 = eta1
         delta0 = delta1
         thrus0 = thrus1
         Vtf0 = Vtf1
         Vta0 = Vta1
         t0 = t1
         read(unit=8,fmt=90,end=80) t1,eta1,delta1,thrus1,Vtf1,Vta1
      end if
c
      if (t .gt. t1) go to 20
c
      dlt = (t - t0)/(t1 - t0)
c
```

```
      etav = eta0 + (eta1 - eta0)*dlt
      deltav = delta0 + (delta1 - delta0)*dlt
      thrusv = thrus0 + (thrus1 - thrus0)*dlt
      Vtfv = Vtf0 + (Vtf1 - Vtf0)*dlt
      Vtav = Vta0 + (Vta1 - Vta0)*dlt
      Mvt = 0.0
      if ((Vtav .eq. 0.0) .and. (Vtfv .eq. 0.0)) go to 40
c
c     find the resulting velocity of the jets in the vertical
c     thrusters and scale the resulting vertical forces and pitching
c     moment.  The scaling is done with respect to the forward velocity.
c
      if (Vtfv .eq. 0.0) go to 41
c
      Vff=Vtfv/(512.95*Vthder(1,3))
      Vff=sqrt(Abs(Vff))
      Velrt=Abs(Relvel/Vff)
c
      if (Velrt .gt. 0.6) Velrt = 0.6
c
      if (Velrt .gt. Vthder(1,1)) then
         Vtfv=Vtfv*(1 + (Velrt - Vthder(1,1))*Vthder(1,2))
      end if
 41   if (Vtav .eq. 0.0) go to 42
      Vfa=Vtav/(512.95*Vthder(1,3))
      Vfa=sqrt(Abs(Vfa))
      Velrt=Abs(Relvel/Vfa)
c
      if (Velrt .gt. 0.6) Velrt = 0.6
c
      if (Velrt .gt. Vthder(1,1)) then
         Vtav=Vtav*(1 + (Velrt - Vthder(1,1))*Vthder(1,2))
      end if
c
 42   if (Vtfv .eq. 0.0) go to 43
      Vff=sqrt(Abs(Vff*Vff/Vthder(1,3)))
      Velrt=Abs(Relvel/Vff)
c
      if (Velrt .gt. 0.6) Velrt = 0.6
c
      if (Velrt .gt. Vthder(2,1)) then
         Mvt=Vtfv*(1+(Velrt-Vthder(2,1))*Vthder(2,2))
      else
         Mvt=Vtfv
      end if
 43   if (Vtfv .eq. 0.0) go to 40
      Vfa=sqrt(Abs(Vfa*Vfa/Vthder(1,3)))
      Velrt=Abs(Relvel/Vfa)
c
      if (Velrt .gt. 0.6) Velrt = 0.6
c
      if (Velrt .gt. Vthder(2,1)) then
         Mvt=Mvt-Vtav*(1+(Velrt-Vthder(2,1))*Vthder(2,2))
      else
         Mvt=Mvt-Vtav
      end if
      Mvt=Mvt*Vthder(2,3)
c
c     find the static cable forces and moments aswell as pitching
c     moment due to gravity.
c
 40   if ((y(4) .eq. 0.0) .and. (y(14) .eq.0)) then
         if ((y(5) .lt. 0.0) .and. (y(15) .lt. 0.0)) then
            psi = - asin(1.0)
         else
            psi = asin(1.0)
         end if
      else
         psi = atan((y(5)+y(15))/(y(4)+y(14)))
      end if
      if (Direct .lt. 0) then
         cblang = psi + y(6)
         Xcable = -Cbltsn*cos(cblang)
      else
         cblang = psi - y(6)
         Xcable = Cbltsn*cos(cblang)
      end if
      Zcable = -Cbltsn*sin(cblang)
      Mcable = Icf(4)*Xcable
      Mgrav = -Icf(1)*9.81*Icf(3)*sin(y(6))
c
c     determine the current velocity, and from the hydrodynamic
c     velocity determine the inertial velocity of the vehicle.
c
      if (y(5) .le. 50.) then
         uc = 0.1545
      else if (y(5) .lt. 250.) then
            uc = 8.7*utau*((250.-y(5))*utau/kinvis)**(1./7.)
         else
            uc = 0.0
      end if
      if (Direct .lt. 0) then
         ui = y(1) - uc*cos(y(6))
         vi = y(2) - uc*sin(y(6))
      else
         ui = y(1) + uc*cos(y(6))
         vi = y(2) + uc*sin(y(6))
      end if
c
      mq = Icf(1)*y(3)
c
      fun1 = - mq*wi - Acf(2)*y(2)*y(3) - Acf(3)*y(3)*y(3)
     1  + Vder(1)*y(1) + Vder(2)*y(2)
     2  + Cfvder(1,1)*Abs((2*alpha+etav)*etav)
     3  + Cfvder(1,2)*Abs((2*alpha+deltav)*deltav)
     4  + Cfvder(1,3)*thrusv + Xcable
c
      fun2 = - mq*ui - Acf(1)*y(1)*y(3) + Icf(1)*Icf(3)**y(3)*y(3)
     1  + Vder(3)*y(1) + Vder(4)*y(2) + Vder(5)*y(3)
     2  + Cfvder(2,1)*etav + Cfvder(2,2)*deltav + Cfvder(2,3)*thrusv
     3  + Zcable + Vtfv + Vtav
c
      fun3 = - mq*wi*Icf(3) - Acf(3)*y(1)*y(3) + Vder(8)*y(1)
     1  + (Acf(2) - Acf(1))*y(1)*y(2) + Vder(6)*y(2)
     2  + Vder(7)*y(3) + Cfvder(3,1)*etav + Cfvder(3,2)*deltav
     3  + Cfvder(3,3)*thrusv + Mcable + Mgrav + Mvt
c
c
      do 70 i=1,3
         dery(i)=Ginv(i,1)*fun1 + Ginv(i,2)*fun2 + Ginv(i,3)*fun3
 70   continue
c
      dery(4) = ui*cos(y(6)) + vi*sin(y(6))
      dery(5) = - ui*sin(y(6)) + vi*cos(y(6))
      dery(6) = y(3)
c
      if (Direct .gt. 0) then
         dery(4) = - dery(4)
```

```
      end if
c
c
c-----------------------------------------------------------------------|
c                                                                       |
c     The following section determines the perturbation terms used      |
c     calculate the perturbation forces.  These in turn determine       |
c     the perturbation derivatives and are returned to dory(*) for      |
c     numerical integration by the SSP routine HPCG.                    |
c                                                                       |
c-----------------------------------------------------------------------|
c
      do 45 i=1,3
         Tmp(i) = 0.0
         do 46 j=1,3
            Tmp(i) = Tmp(i) + Ccoef(i,j) * Subdim(j)
 46      continue
 45   continue
c
      Xalpha=0.5*Swdens*((Tmp(3)*2+Tmp(1)-Tmp(2)*(2-alpha*alpha))
     *        *alpha)
      Zalpha=0.5*Swdens*(Tmp(3)*(alpha*alpha-1)-Tmp(1)-Tmp(2)*3
     *        *alpha*alpha)
c
c     Following terms are the derivatives due to changes in velocity only.
c
      Xvel = Swdens*(Tmp(3)*alpha*sin(alpha)
     -        - (Tmp(1)+Tmp(2)*alpha**2)*cos(alpha))
      Zvel = Swdens*(-Tmp(3)*alpha*cos(alpha)
     -        - (Tmp(1)+Tmp(2)*alpha**2)*sin(alpha))
      Mvel = 2*Vcf6*alpha
c
      Pert(2,2)= - Xalpha*y(2) + Xvel*y(1)
c
      Pert(2,3)= Xalpha*y(1) - (Acf(2)+Icf(1))*y(3)
c
      Pert(2,4)= -(Acf(2)*y(2)+Icf(1)*wi+Acf(3)*2*y(3))
c
      Pert(3,2)= -Zalpha*y(2)-mq+Acf(1)*y(3) + Zvel*y(1)
c
      Pert(3,3)= Zalpha*y(1)
c
      Pert(3,4)= Vder(5)+Icf(1)*(ui+Icf(3)*2*y(3))
c
      Pert(4,2)= Vder(8)+(Acf(2)-Acf(1))*y(2)+Acf(3)*y(3)
     +           + Mvel*y(1)
c
      Pert(4,3)= Vder(6)-mq+(Acf(2)-Acf(1))*y(1)
c
      Pert(4,4)= Vder(7)-(Icf(1)*Icf(3)*wi)+Acf(3)*y(1)
c
c-----------------------------------------------------------------------|
c                                                                       |
c     The following section determines the perturbation terms used      |
c     calculate the terms for the compensator state equation.           |
c                                                                       |
c-----------------------------------------------------------------------|
c
      do 47 i=1,3
         Tmp(i) = 0.0
         do 48 j=1,3
            Tmp(i) = Tmp(i) + Kmccf(i,j) * Kmsdm(j)
 48      continue
 47   continue
```

```
c
      Xalpha=0.5*Swdens*((Tmp(3)*2+Tmp(1)-Tmp(2)*(2-alpha*alpha))
     *        *alpha)
      Zalpha=0.5*Swdens*(Tmp(3)*(alpha*alpha-1)-Tmp(1)-Tmp(2)*3
     *        *alpha*alpha)
c
c     Following terms are the derivatives due to changes in velocity only.
c
      Xvel = Swdens*(Tmp(3)*alpha*sin(alpha)
     -        - (Tmp(1)+Tmp(2)*alpha**2)*cos(alpha))
      Zvel = Swdens*(-Tmp(3)*alpha*cos(alpha)
     -        - (Tmp(1)+Tmp(2)*alpha**2)*sin(alpha))
      Mvel = 2*Kmvcf6*alpha
c
      Kmpert(2,2)= - Xalpha*y(2) + Xvel*y(1)
c
      Kmpert(2,3)= Xalpha*y(1) - (Kmacf(2)+Kmicf(1))*y(3)
c
      Kmpert(2,4)= -(Kmacf(2)*y(2)+Kmicf(1)*wi+Kmacf(3)*2*y(3))
c
      Kmpert(3,2)= -Zalpha*y(2)-Kmicf(1)*y(3)+Kmacf(1)*y(3)
     +           + Zvel*y(1)
c
      Kmpert(3,3)= Zalpha*y(1)
c
      Kmpert(3,4)= Kmvder(5)+Kmicf(1)*(ui+Kmicf(3)*2*y(3))
c
      Kmpert(4,2)= Kmvder(8)+(Kmacf(2)-Kmacf(1))*y(2)
     +           + Kmacf(3)*y(3) + Mvel*y(1)
c
      Kmpert(4,3)= Kmvder(6)-Kmicf(1)*y(3)+(Kmacf(2)-Kmacf(1))*y(1)
c
      Kmpert(4,4)= Kmvder(7)-(Kmicf(1)*Kmicf(3)*wi)+Kmacf(3)*y(1)
c
c-----------------------------------------------------------------------|
c                                                                       |
c     Generate the disturbance forces and pass them to the HPCG.        |
c                                                                       |
c-----------------------------------------------------------------------|
      if (t .ne. tprev) then
         rndm(1) = (Ran(Iseed(1))-0.5)*sqrt(12*Intens(1))
         rndm(2) = (Ran(Iseed(2))-0.5)*sqrt(12*Intens(2))
         rndm(3) = (Ran(Iseed(3))-0.5)*sqrt(12*Intens(3))
      end if
      dery(11)= - Bandwd(1)*y(11) + rndm(1)
      dery(12)= - Bandwd(2)*y(12) + rndm(2)
      dery(13)= - Bandwd(3)*y(13) + rndm(3)
      tprev = t
c
c-----------------------------------------------------------------------|
c                                                                       |
c     The following section provides the control loop to compensate     |
c     for the disturbances to which the system has been subjected.      |
c                                                                       |
c-----------------------------------------------------------------------|
c
c     obtain the filter and control gain matrices.
c
      call calmat(alpha,y(1),G,H)
c
c     find the input vector u and then the value Bu for the plant
c
 97   do 100 i=1,3
         u(i)=0.0
```

```
            do 99 j=1,7
               k=j+18
               u(i) = u(i) - G(i,j)*y(k)
 99         continue
            k=i+15
            dery(k)=u(i)
            k=i+18
            dery(k)=u(i)
 100     continue
c
         do 105 i=1,3
            Bu(i)=0.0
            do 105 j=1,3
               k = j + 15
               Bu(i) = Bu(i) + Cfvder(i,j)*y(k)
 105     continue
c
c        Now that the individual components have been determined they
c        are multiplied with the state vector.  To these the disturbance
c        forces and moments are added.
c
         do 150 i=2,4
            Tmp(i) = 0.0
            do 151 j=1,4
               k = j+6
               Tmp(i) = Tmp(i) + Pert(i,j)*y(k)
 151        continue
            k = i+9
            Tmp(i) = Tmp(i) + y(k)
 150     continue
c
         dery(7) = y(10)
         do 155 i=1,3
            j = i+7
            dery(j) = Ginv(i,1)*(Tmp(2) + Bu(1))
     +              + Ginv(i,2)*(Tmp(3) + Bu(2))
     +              + Ginv(i,3)*(Tmp(4) + Bu(3))
 155     continue
c-----------------------------------------------------------------------|
c                                                                       |
c-----------------------------------------------------------------------|
         do 160 i=1,7
            Hy(i) = 0.0
            do 160 j=1,3
               k=j+6
               l=j+21
               Hy(i) = Hy(i) + (y(k) - y(l)) * H(i,j)
 160     continue
c
         dery(22)=y(25)
         do 165 i=23,25
            dery(i) = 0.0
            k=i-22
            m=i-21
            do 170 j=1,3
               l=j+18
               dery(i)=dery(i) + Kmcfvd(k,j)*y(l)
 170        continue
            do 175 j=1,4
               l=j+21
               dery(i)=dery(i) + Kmpert(m,j)*y(l)
 175        continue
 165     continue
c
```

```
         do 180 i=1,3
            tmp(i) = Kmginv(i,1)*dery(23)
     +             + Kmginv(i,2)*dery(24)
     +             + Kmginv(i,3)*dery(25)
 180     continue
         do 185 i=1,3
            j=i+22
            dery(j) = tmp(i)
 185     continue
c
         do 190 i=19,25
            j=i-18
            dery(i) = dery(i) + Hy(j)
 190     continue
c
c-----------------------------------------------------------------------|
c                                                                       |
c                                                                       |
c-----------------------------------------------------------------------|
c
         dery(14) = y(8)*cos(y(6)) + y(9)*sin(y(6))
         dery(15) = - y(8)*sin(y(6)) + y(9)*cos(y(6))
         if (Direct .ge. 0) dery(14) = - dery(14)
         return
 80      prmt(5)=1
         return
 90      format(' ',5(E14.7,2X),E14.7)
 95      format(' ',2(I6,2X),I6)
         end
c
c***********************************************************************
c                                                                      *
c***********************************************************************
         subroutine outp(t,y,dery,ihlf,ndim,prmt)
c
         integer ihlf,ndim
         real t,y(ndim),dery(ndim),prmt(5)
c
         integer count,Cntstp
         real xtot,ztot
         save count
         common /output/ Cntstp
c
         if (t .eq. 0.) count = Cntstp
         if (count .eq. Cntstp) then
            count = 0
         else
            count=count+1
            go to 20
         end if
c
         xtot = y(4) + y(14)
         ztot = y(5) + y(15)
         write (unit=9,fmt=10) t,y(4),y(5),y(6),dery(4),dery(5),dery(6)
     :                            ,y(1),y(2)
         write (unit=7,fmt=15) t,y(11),y(12),y(13),y(7),y(8),y(9),y(10)
     :                            ,y(14),y(15),xtot,ztot
         write (unit=10,fmt=*) t,y(16),y(17),y(18)
c
20       return
10       format (' ',8(E14.7,2X),E14.7)
15       format (' ',11(E14.7,2X),E14.7)
c
         end
```

```
c
c***********************************************************************
c                                                                      *
c                                                                      *
c                                                                      *
c----------------------------------------------------------------------|
      subroutine calmat(alpha,Uo,G,H)
c
c
      real alpha,Uo,G(3,7),H(7,3)
c
      integer i,j,k,l,amin,amax,vmin,vmax
      real alpham(7),velocm(6),Gcoef(3,7,7,6),Hcoef(7,3,7,6),
     *     delta,Gct(3,7,2),Hct(7,3,2),talpha,tuo
c
      common /matr/ alpham,velocm,Gcoef,Hcoef
c
      talpha = alpha
      tuo = Uo
      if (alpha .le. alpham(1)) then
         amin = 1
         amax = 1
         talpha = alpham(1)
         go to 14
      end if
      if (alpha .ge. alpham(7)) then
         amin = 7
         amax = 7
         talpha = alpham(7)
         go to 14
      end if
c
      do 10 i=1,7
         if ((alpham(i) .le. alpha) .and.
     *       (alpham(i+1) .gt. alpha)) then
             amin = i
             amax = i + 1
         end if
 10   continue
c
 14   if (Uo .le. velocm(1)) then
         umin = 1
         umax = 1
         tuo = velocm(1)
         go to 20
      end if
      if (Uo .ge. velocm(6)) then
         umin = 6
         umax = 6
         tuo = velocm(6)
         go to 20
      end if
c
      do 15 i=1,6
         if ((velocm(i) .le. Uo) .and.
     *       (velocm(i+1) .gt. Uo)) then
             umin = i
             umax = i + 1
         end if
 15   continue
c
 20   if (amax .eq. amin) then
         delta = 0.0
      else
         delta = (talpha - alpham(amin))/(alpham(amax) - alpham(amin))
      endif
c
      do 40 i=1,7
         do 40 j=1,3
            Gct(j,i,1)=(Gcoef(j,i,amax,umin) - Gcoef(j,i,amin,umin))
     *                 *delta + Gcoef(j,i,amin,umin)
            Hct(i,j,1)=(Hcoef(i,j,amax,umin) - Hcoef(i,j,amin,umin))
     *                 *delta + Hcoef(i,j,amin,umin)
            Gct(j,i,2)=(Gcoef(j,i,amax,umax) - Gcoef(j,i,amin,umax))
     *                 *delta + Gcoef(j,i,amin,umax)
            Hct(i,j,2)=(Hcoef(i,j,amax,umax) - Hcoef(i,j,amin,umax))
     *                 *delta + Hcoef(i,j,amin,umax)
 40   continue
c
      if (umax .eq. umin) then
         delta = 0.0
      else
         delta = (tuo - velocm(umin))/(velocm(umax) - velocm(umin))
      endif
c
      do 50 i=1,7
         do 50 j=1,3
            G(j,i)=(Gct(j,i,2) - Gct(j,i,1))*delta + Gct(j,i,1)
            H(i,j)=(Hct(i,j,2) - Hct(i,j,1))*delta + Hct(i,j,1)
 50   continue
c
      return
      end
c
c----------------------------------------------------------------------|
c                                                                      |
c                                                                      |
c                                                                      |
c----------------------------------------------------------------------|
c
c
c     ..................................................................
c
c       subroutine hpcg
c
c       purpose
c          to solve a system of first order ordinary general
c          differential equations with given initial values.
c
c       usage
c          call hpcg (prmt,y,dery,ndim,ihlf,fct,outp,aux)
c          parameters fct and outp require an external statement.
c
c       description of parameters
c          prmt   - an input and output vector with dimension greater
c                   or equal to 5, which specifies the parameters of
c                   the interval and of accuracy and which serves for
c                   communication between output subroutine (furnished
c                   by the user) and subroutine hpcg. except prmt(5)
c                   the components are not destroyed by subroutine
c                   hpcg and they are
c          prmt(1)- lower bound of the interval (input),
c          prmt(2)- upper bound of the interval (input),
c          prmt(3)- initial increment of the independent variable
c                   (input),
c          prmt(4)- upper error bound (input). if absolute error is
c                   greater than prmt(4), increment gets halved.
c                   if increment is less than prmt(3) and absolute
c                   error less than prmt(4)/50, increment gets doubled.
```

```
c                the user may change prmt(4) by means of his
c                output subroutine.
c        prmt(5) - no input parameter. subroutine hpcg initializes
c                prmt(5)=0. if the user wants to terminate
c                subroutine hpcg at any output point, he has to
c                change prmt(5) to non-zero by means of subroutine
c                outp. further components of vector prmt are
c                feasible if its dimension is defined greater
c                than 5. however subroutine hpcg does not require
c                and change them. nevertheless they may be useful
c                for handing result values to the main program
c                (calling hpcg) which are obtained by special
c                manipulations with output data in subroutine outp.
c        y       - input vector of initial values.  (destroyed)
c                lateron y is the resulting vector of dependent
c                variables computed at intermediate points x.
c        dery    - input vector of error weights.  (destroyed)
c                the sum of its components must be equal to 1.
c                lateron dery is the vector of derivatives, which
c                belong to function values y at a point x.
c        ndim    - an input value, which specifies the number of
c                equations in the system.
c        ihlf    - an output value, which specifies the number of
c                bisections of the initial increment. if ihlf gets
c                greater than 10, subroutine hpcg returns with
c                error message ihlf=11 into main program.
c                error message ihlf=12 or ihlf=13 appears in case
c                prmt(3)=0 or in case sign(prmt(3)).ne.sign(prmt(2)-
c                prmt(1)) respectively.
c        fct     - the name of an external subroutine used. it
c                computes the right hand sides dery of the system
c                to given values of x and y. its parameter list
c                must be x,y,dery. the subroutine should not
c                destroy x and y.
c        outp    - the name of an external output subroutine used.
c                its parameter list must be x,y,dery,ihlf,ndim,prmt.
c                none of these parameters (except, if necessary,
c                prmt(4),prmt(5),...) should be changed by
c                subroutine outp. if prmt(5) is changed to non-zero,
c                subroutine hpcg is terminated.
c        aux     - an auxiliary storage array with 16 rows and ndim
c                columns.
c
c     remarks
c        the procedure terminates and returns to calling program, if
c        (1) more than 10 bisections of the initial increment are
c            necessary to get satisfactory accuracy (error message
c            ihlf=11),
c        (2) initial increment is equal to 0 or has wrong sign
c            (error messages ihlf=12 or ihlf=13),
c        (3) the whole integration interval is worked through,
c        (4) subroutine outp has changed prmt(5) to non-zero.
c
c     subroutines and function subprograms required
c        the external subroutines fct(x,y,dery) and
c        outp(x,y,dery,ihlf,ndim,prmt) must be furnished by the user.
c
c     method
c        evaluation is done by means of hammings modified predictor-
c        corrector method. it is a fourth order method, using 4
c        preceeding points for computation of a new vector y of the
c        dependent variables.
c        fourth order runge-kutta method suggested by ralston is
c        used for adjustment of the initial increment and for
c        computation of starting values.
c        subroutine hpcg automatically adjusts the increment during
c        the whole computation by halving or doubling.
c        to get full flexibility in output, an output subroutine
c        must be coded by the user.
c        for reference, see
c        (1)  ralston/wilf, mathematical methods for digital
c             computers, wiley, new york/london, 1960, pp.95-109.
c        (2)  ralston, runge-kutta methods with minimum error bounds,
c             mtac, vol.16, iss.80 (1962), pp.431-437.
c
c     ..................................................................
c
      subroutine hpcg(prmt,y,dery,ndim,ihlf,fct,outp,aux)
c
c
      dimension prmt(5),y(ndim),dery(ndim),aux(16,ndim)
c**above card modified by ipc, june 1971, to make accessible to watfiv*
      n=1
      ihlf=0
      x=prmt(1)
      h=prmt(3)
      prmt(5)=0.
      do 1 i=1,ndim
      aux(16,i)=0.
      aux(15,i)=dery(i)
    1 aux(4,i)=y(i)
      if(h*(prmt(2)-x))3,2,4
c
c     error returns
    2 ihlf=12
      goto 4
    3 ihlf=13
c
c     computation of dery for starting values
    4 call fct(x,y,dery)
c
c     recording of starting values
      call outp(x,y,dery,ihlf,ndim,prmt)
      if(prmt(5))6,5,6
    5 if(ihlf)7,7,6
    6 return
    7 do 8 i=1,ndim
    8 aux(11,i)=dery(i)
c
c     the following part of subroutine hpcg computes by means of
c     runge-kutta method starting values for the not self-starting
c     predictor-corrector method.
      do 20 i=1,ndim
         aux(1,i)=h*dery(i)
 20      y(i)=aux(4,i)+(0.5*aux(1,i))
      x = x + (0.5*h)
      call fct(x,y,dery)
      do 21 i=1,ndim
         aux(2,i)=h*dery(i)
 21      y(i)=aux(4,i)+(0.5*aux(2,i))
      call fct(x,y,dery)
      do 22 i=1,ndim
         aux(3,i)=h*dery(i)
 22      y(i)=aux(4,i)+aux(3,i)
      x = x + (0.5*h)
      call fct(x,y,dery)
      do 23 i=1,ndim
         aux(5,i)=aux(4,i)+(aux(1,i)+2*(aux(2,i)+aux(3,i))
```

```
     +              +h*dery(i))/6
 23     y(i)=aux(5,i)
        call fct(x,y,dery)
        call outp(x,y,dery,ihlf,ndim,prmt)
c
        do 30 i=1,ndim
           aux(12,i)=dery(i)
           aux(1,i)=h*dery(i)
 30        y(i)=aux(5,i)+(0.5*aux(1,i))
        x = x + (0.5*h)
        call fct(x,y,dery)
        do 31 i=1,ndim
           aux(2,i)=h*dery(i)
 31        y(i)=aux(5,i)+(0.5*aux(2,i))
        call fct(x,y,dery)
        do 32 i=1,ndim
           aux(3,i)=h*dery(i)
 32        y(i)=aux(5,i)+aux(3,i)
        x = x + (0.5*h)
        call fct(x,y,dery)
        do 33 i=1,ndim
           aux(6,i)=aux(5,i)+(aux(1,i)+2*(aux(2,i)+aux(3,i))
     +              +h*dery(i))/6
 33        y(i)=aux(6,i)
        call fct(x,y,dery)
        call outp(x,y,dery,ihlf,ndim,prmt)
c
        do 40 i=1,ndim
           aux(13,i)=dery(i)
           aux(1,i)=h*dery(i)
 40        y(i)=aux(6,i)+(0.5*aux(1,i))
        x = x + (0.5*h)
        call fct(x,y,dery)
        do 41 i=1,ndim
           aux(2,i)=h*dery(i)
 41        y(i)=aux(6,i)+(0.5*aux(2,i))
        call fct(x,y,dery)
        do 42 i=1,ndim
           aux(3,i)=h*dery(i)
 42        y(i)=aux(6,i)+aux(3,i)
        x = x + (0.5*h)
        call fct(x,y,dery)
        do 43 i=1,ndim
           aux(7,i)=aux(6,i)+(aux(1,i)+2*(aux(2,i)+aux(3,i))
     +              +h*dery(i))/6
 43        y(i)=aux(7,i)
        call fct(x,y,dery)
        call outp(x,y,dery,ihlf,ndim,prmt)
        do 44 i=1,ndim
 44        aux(13,i)=dery(i)
        n=4
c
c
c       possible break-point for linkage
c
c       starting values are computed.
c       now start hammings modified predictor-corrector method.
  200 istep=3
  201 if(n-8)204,202,204
c
c       n=8 causes the rows of aux to change their storage locations
  202 do 203 n=2,7
        do 203 i=1,ndim
        aux(n-1,i)=aux(n,i)
```

```
  202 do 203 n=2,7
        do 203 i=1,ndim
        aux(n-1,i)=aux(n,i)
  203 aux(n+6,i)=aux(n+7,i)
        n=7
c
c       n less than 8 causes n+1 to get n
  204 n=n+1
c
c       computation of next vector y
        do 205 i=1,ndim
        aux(n-1,i)=y(i)
  205 aux(n+6,i)=dery(i)
        x=x+h
  206 istep=istep+1
        do 207 i=1,ndim
       Odelt=aux(n-4,i)+1.333333*h*(aux(n+6,i)+aux(n+6,i)-aux(n+5,i)+
       laux(n+4,i)+aux(n+4,i))
        y(i)=delt-.9256198*aux(16,i)
  207 aux(16,i)=delt
c       predictor is now generated in row 16 of aux, modified predictor
c       is generated in y. delt means an auxiliary storage.
c
        call fct(x,y,dery)
c       derivative of modified predictor is generated in dery
c
        do 208 i=1,ndim
       Odelt=.125*(9.*aux(n-1,i)-aux(n-3,i)+3.*h*(dery(i)+aux(n+6,i)+
       laux(n+6,i)-aux(n+5,i)))
        aux(16,i)=aux(16,i)-delt
  208 y(i)=delt+.07438017*aux(16,i)
c
c       test whether h must be halved or doubled
        delt=0.
        do 209 i=1,ndim
  209 delt=delt+aux(15,i)*abs(aux(16,i))
c
c       h must not be halved. that means y(i) are good.
  210 call fct(x,y,dery)
        call outp(x,y,dery,ihlf,ndim,prmt)
        if(prmt(5))212,211,212
  211 if(ihlf-11)213,212,212
  212 return
  213 if(h*(x-prmt(2)))214,212,212
  214 if(abs(x-prmt(2))-.1*abs(h))212,215,215
  215 goto 201
        end
c*************************************************************************
c                                                                        *
c*************************************************************************
```

References

[1] Abkowitz, Martin.
Stability and Motion Control of Ocean Vehicles.
MIT Press, 1969.

[2] Adamchak, Evans, Harvey, J. and John, C.
Ocean Engineering Structures.
MIT Press, 1969.

[3] Amzallag, Albert-Maurice.
Design and Control of a Tethered Heavy Lift Submersible.
Master's thesis, Massachusetts Institue of Technology, February, 1985

[4] Askenas, Irving, Graham, Dunstan and McRuer, Duane.
Aircraft Dynamics and Automatic Control.
Princeton University Press, 1973.

[5] Athans, M.
Multivariable Control System Design using the LQG/LTR Methodology.
1984.
Class Notes.

[6] Babister, A.W.
Aircraft Dynamic Stability and Response.
Pergamon, 1980.

[7] Barnes, C. C.
Power Cables: Their Design and Installation.
Chapman and Hall Ltd, Second Edition, 1966.

[8] Berju, K. K., Daniels, E. L. and Strohlein, E. M.
Engineering the Storage Battery as an Underwater Power Supply.
In *IEEE Proceedings Ocean.*, pages 279. 1973.

[9] Bernstein, Harold.
Pressure Hulls for Deep-Submergence Vehicles.
J. Hydronautics 1, no. 1, July, 1967.

[10] Billet, A. B.
A Responsive Compact Hydraulic System for a Remotely Operated Vehicle.
In *SAE proceedings 554, Aerospace Fluid Power and Control Systems..* October, 1983.

[11] Bishop, R.E.D. and Clayton, B.R.
Mechanics of Marine Vehicles.
E. & F.N. Spon Ltd, London, 1982.

[12] Brinser, Harry M., Pieroni, Charles A. and Smith, Raymond A.
Undersea optic fiber cable design of a physical testing program.
In *IEEE Proceedings OCEAN*, pages 186. 1979.

[13] Busby, R. F.
Engineering aspects of manned and remotely controlled vehicles.
Phil. Trans. R. Soc. Lond. A. 290 :135-152, 1978.

[14] Busby, R. F.
Remotely Operated Vehicles..
Technical Report, National Oceanic and Atmospheric Administration, August, 1979.

[15] Chen, C. T.
Linear Systems.
Holt Rinehart Winston, 1970.

[16] Clay, Peter and Jackson, Doug.
Syntactic Foam Sphere Improves Oceanographic Mooring Performance.
Sea Technology 23, no. 9, September, 1981.

[17] Collins, Charles, L.
ARMS: A proven, Remotely Operated Manipulator System Ready now to support offshore drilling in depths to 13,000 ft.
In *IEEE Proceedings Ocean.*, pages 1165. 1981.

[18] Comstock, John P.
Principles of Naval Architecture.
SNAME, 1967.

[19] Congwer, Calvin A.
President of Innerspace Corporation.
Letter and Thruster Data.

[20] Couch, Harold T.
Lift, Power and Propulsion Alternatives for Deep Ocean Submersibles.
In *Third International Symposium on Unmanned Untethered Submersible Technology.*, pages 150. University of New Hampshire, June, 6 - 9, 1983.

[21] Cowen, S. J.
Fiber optic video transmission system employing pulse frequency modulation.
In *IEEE Proceedings OCEAN*, pages 253. 1979.

[22] D Azzo, J. J. and Houpis, C. H.
Linear Control System Analysis and Design.
McGrawHill, Second Edition, 1981.

[23] Daubin, Scott, C.
Deep Ocean Work Boat (DOWB), an Advanced Deep Submergence Vehicle.
J. Hydronautics 2, no. 1, January, 1968.

[24] Elliott, Thomas John, Jr.
Preliminary Design Considerations of Pressure Vessels for a Deep Diving Submersible.
Master's thesis, Massachusetts Institue of Technology, September, 1974.

[25] Fickel, Monty George.
Bottom and Surface Proximity Effects on the Added Mass of Rankine Ovoids.
Master's thesis, Naval Postgraduate School, December, 1973.

[26] Finck, R.D. and Hoak, D.E.
USAF Stability and Control Datcom..
Technical Report MJIS Report N76 - 73204, Air Force Dynamic Lab, January, 1975.

[27] Forman, Will.
Glass Submersibles.
J. Hydronautics 3, no. 1, January, 1969.

[28] *Sea-mersible Motors and Thrusters Catalog.*
Franklin Electric, Bufton, Indiana, 1983.

[29] *Application Data.*
General Electric Co., Wire and Cable Dept., 1982.
Published by TECH DOC, Inacom Service.

[30] Goodier, J. N. and Timoshenko, S. P.
Theory of Elasticity.
McGrawHill, Third Edition, 1970.

[31] Goodman, M. W., Penzias, W.
Man Beneath the Sea.
Wiley Interscience, 1973.

[32] Hammett, D.; Vice President, SEDCO Inc.
What is Industry's Deepwater Capability?
Ocean Industry , November, 1980.

[33] Hightower, John D., Rosencrantz, Donald M. and Wilkins, George A.
Lightweight Cables for Deep Tethered Cables.
In *IEEE Proceedings OCEAN*, pages 138. 1975.

[34] Hoerner, S.F.
Fluid-Dynamic Drag.
Hoerner Fluid Dynamics, 1965.

[35] Hoerner, S.F. and Borst, H.V.
Fluid-Dynamic Lift.
Hoerner Fluid Dynamics, 1975.

[36] Holm, Carl H., McAllister, R.F. and Myers, John J.
Handbook of Ocean and Underwater Engineering.
McGrawHill, 1969.

[37] Horn, M. H., Riewald, P. G. and Zweben, C. H.
Strength and Durability Characteristics of Ropes and Cables from KEVLAR Aramid Fibers.
In *IEEE Proceedings OCEAN, Paper 24E.* 1977.

[38] Humphrey's, D.E. and Watkinson, K.W.
Prediction of Acceleration Hydrodynamic Coefficients for Underwater Vehicles from Geometric Parameters..
Technical Report Technical Report 327 - 78, Naval Coastal System Center, February, 1978.

[39] Johnson, J.L. and Landweber, L.
Prediction of Dynamic Stability Derivatives of an Elongated body of Revolution.
Technical Report Report no. C - 359, DTMB, May, 1951.

[40] *Underwater Manipulators*
SAL JUNGER MARINE, Manufacturers pamphlet, UWM, 1, 6/50; 2,B/80, 1982.

[41] Kailath.
Linear Systems.
Prentice Hall Inc., 1982.

[42] Kallas, Danos H. and Sorkin, George.
Hydrospace Materials.
J. Hydronautics 5, no. 3, July, 1971.

[43] Kerczek, Christian von and Wilson, Michael B.
An inventory of some Force Producers for use in Marine Vehicle Control.
Technical Report 79/097, DTNSRDC, 1979.

[44] Kesnick, Israel and Makander, Aleksander.
Syntactic Foams for Deep Sea Engineering Aoolications.
In *ASCE Conference, Civil Engineering in the Oceans..* 1967.

[45] Kottler, Carl F., Jr.
Underwater Systems Within the Scientific, Technological and Economic Framework.
J. Hydronautics 3, no. 1, January, 1969.

[46] Krenzke, Martin, A., Reynolds and Thomas, E.
Structural Research on Submarine Pressure Hulls at the David Taylor Model Basin.
J. Hydronautics 1, no. 1, July, 1967.

[47] Kwakernaak, H., and Sivan, R.
Linear Optimal Control Systems.
Wiley Interscience, 1972.

[48] Lamb, Horace.
Hydrodynamics.
Dover Publications, New York, 1945.

[49] Lambeck, Raymond P.
Hydraulic Pumps and Motors: Selection and Application for Hydraulic Power Control Systems.
Marcel Dekker, Inc., 1983.

[50] Lee, G. C.; McDermott Inc.
Recent Advances in Design and Construction of Deepwater Platforms.
Ocean Industry , November, 1980.

[51] Lewis, R.; Perry Oceanographic Inc.
Article from 'Oil & Gas Journal'.

[52] Lively, Kenneth A.
Multivariable Control System Design for a Submarine.
Master's thesis, Massachusetts Institue of Technology, May, 1984.

[53] Lund, Thomas J. and McCartney, Joseph F.
Application of Lithium, Thionyl Chloride to Marine Requirements.
In *IEEE Proceedings Ocean*, pages 177. 1979.

[54] Mandel, P. and Rodenbusch, George.
Small Submersible Design in Relation to Existing and Future Technology.
January, 24, 1975.
MIT Internal Paper.

[55] Masubushi, Koichi.
Materials for Ocean Engineering.
MIT Press, 1970.

[56] Masubushi, Koichi.
Future Trends of Materials and Welding Technology for Marine Structures.
In *SNAME.* Philadelphia, PA., June, 2-5, 1976.

[57] McAllister, D.
Electric Cables Handbook.
Granada Publishing, 1982.

[58] Miller, Stephen.
Flotation Technology Applied to Demands of Offshore Oil Industry.
Sea Technology 23, no. 9, September, 1981.

[59] Mills, Graham.
A choice of options on offer.
The Oilman , January, 1984.

[60] Milne-Thomas, L.M.
Theoretical Hydrodynamics.
Macmillan, New York: 5th edition, 19.

[61] Nakaguchi, H.
Recent Japanese Research on Three-Dimensional Bluff-Body Flows Relevant to Road-Vehicle Aerodynamics.
In *Symposium on 'Aerodynamic Drag Mechanisms of Bluff & Road Vehicles.'*. G M Labs, 1976.

[62] Newman, J.N.
Marine Hydrodynamics.
MIT Press, 1977.

[63] Newman, J.N.
Marine Hydrodynamics.
Class notes.

[64] Nickell, E. H.
Weight Considerations for Deep Submersibles.
In *SNAME, Paper at its Spring Meeting.*. Beverly Hills, CA., May, 21 - 24, 1969.

[65] Nielkanjh, J. and Shen-D'Ge'.
Structures/Materials Synthesis for Safety of Oceanic Deep-Submergence Bottom-Fixed Manned Habitat.
J. Hydronautics 2, no.3, July, 1968.

[66] Nielsen, Jack N.
Missile Aerodynamics.
McGraw Hill, 1960.

[67] Ogata, K.
Modern Control Engineering.
Prentice Hall Inc., 1981.

[68] Oosterveld, M.W.C.
Wake Adapted Ducted Propellers..
Technical Report Publication no. 345, NSMB, Wageningen, Netherlands, 1972.

[69] Rushfelt, Paul.
Telephone conversation with Paul Rushfelt of Perry Offshore.

[70] Schlichting, Herman and Truckenbrodt, Erich.
Aerodynamics of the Airplane.
McGraw Hill, 1979.

[71] Sheehan, Matt F.
Hamilton Standard Precision Buoyancy Control Unit.
In *Third International Symposium on Unmanned Untethered Submersible Technology.*, pages 52. University of New Hampshire, June, 6 - 9, 1983.

[72] Sheehan, Matt F.
Telephone conversation.

[73] Sheridan, Thomas B., William L., Verplank.
Human and computer control of undersea teleoperators..
Technical Report, Office of Naval Research, July, 1978.

[74] Staff Report.
Glass Microspheres Essential Ingredients of Flotation Foam.
Sea Technology 17, no. 4, April, 1976.

[75] Stanley, Robert.
Analysis of the Lateral Force Coefficient for Ship Maneuvering and Dynamic Stability Equations.
Master's thesis, Massachusetts Institue of Technology, June, 22, 1976.

[76] Stein, G.
Multivariable Feedback Design : Concepts for Classical Modern Synthesis.
IEEE Transactions on Automatic Control AC-26, February, 1981.

[77] Stein, G.
LQG-Based Multivariable Design : Frequency Domain Interpretation.
AGARD-LS-117.

[78] Stowell, Dan T. and Tsiyi, Kiyoshi.
Development of a Manned Transparent Capsule for Panoramic Observation.
J. Hydronautics 3, no. 1, January, 1969.

[79] Talkington, Howard R.
Undersea Work Systems.
Marcel Dekker Inc., 1981.

[80] Tamer, Roger.
Deepwater drilling expected to increase.
Offshore 44, no. 8, June, 1984.

[81] Taylor, D. M.
Industry Outlook.
Ocean Industry , October, 1981.

[82] Teers, M. L.
An Unmanned Tethered Vehicle for Deepwater Production Riser Maintenance. OTC 3576.
In *Offshore Technology Conference.* 1979.

[83] Wadsworth III, Joseph F.
A Compendium of Tension Member Properties for Input to Cable Structure Analysis Programs..
Technical Report CR 82.017, Naval Civil Engineering Laboratory, April, 1982.

[84] Wendel, K.
Hydrodynamic Masses and Hydrodynamic Moments of Inertia..
Technical Report Translation no. 260, DTMB, 19.

[85] Yee-Tak Yu.
Virtual Masses of Rectangular Plates and Parallelepipeds in Water.
Journal of Applied Physics 16, November, 1945.

[86] Yumori, I. Roy.
Ocean Testing of Motion Compensation Crane and KEVLAR Tether Cable Dynamics for an unmanned deep submersible using real time spectral analysis.
In *IEEE Proceedings OCEAN*, pages 764. 1979.

[87] Zahm, A.F.
Flow and Force Equations for a Body Revolving in a Fluid..
Technical Report Report no. 323, NACA, .

[88]
Article from 'Ocean Industry'.

[89]
Manipulator Bell Rescues Submersibles in 1,700 Ft of Water.
Article from 'Offshore Industry.

[90]
Diving Bell Crew on Thristle Field Rescued in Wet Transfer Operation.
Article from 'Offshore Industry'.

[91]
Article from 'Offshore Engineer'.

[92]
Article from 'Oil & Gas'.

[93]
How ROVs are competing with divers.
Article from 'Ocean Industry'.